/
Article / Book Information

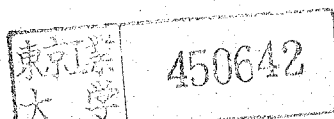|	
( )	
Title(English)	Nuclear Magnetic Resonance Study of the Kinetics of Ligand Exchange Reactions in the Equatorial Positions of Uranyl Complexes
( )	
Author(English)	Yasuhisa Ikeda
( )	: , : , : 1281 , :1981 3 26 , : , :
Citation(English)	Degree:Doctor of Engineering, Conferring organization: , Report number: 1281 , Conferred date:1981/3/26, Degree Type:Course doctor, Examiner:
( )	
Type(English)	Doctoral Thesis
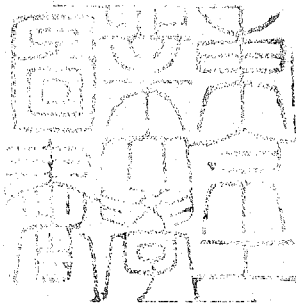
NUCLEAR MAGNETIC RESONANCE STUDY OF THE

KINETICS OF LIGAND EXCHANGE REACTIONS IN THE

EQUATORIAL POSITIONS OF URANYL COMPLEXES

by

YASUHISA IKEDA

Thesis supervisor: Professor Hiroshi Fukutomi

NUCLEAR MAGNETIC RESONANCE STUDY OF THE

KINETICS OF LIGAND EXCHANGE REACTIONS IN THE

EQUATORIAL POSITIONS OF URANYL COMPLEXES

by

YASUHISA IKEDA

Thesis supervisor: Professor Hiroshi Fukutomi

CONTENTS

ACKNOWLEDGMENT

CHAPTER I

INTRODUCTION

A. Historical Background

The study on the solvent exchange reactions and complex formation reactions of metal ions presents the information which is considered to be the most basic data for an understanding of the reactivity of metal ions in solvents. Therefore, a large number of solvent exchange and complex formation reactions of metal ions have been investigated by various methods, e.g., NMR line-broadening, ultrasonic absorption, temperature-jump, and stopped-flow methods. Particularly, the solvent exchange reactions in various metal ions have been studied by the NMR line-broadening method. The first quantitative theory for this method was established by Gutowsky et al.[1] and further developed by McConell[2]. Swift and Connick used this theory for the purpose of obtaining the water exchange rate in some paramagnetic transition metal ions, e.g. Mn^{2+}, Fe^{2+}, Co^{2+}, Ni^{2+}, and Cu^{2+} [3]. Thereafter, many authors have reported the solvent exchange reactions in various metal ions as listed in Table 1 [4-9]. Eigen et al. have studied the complex formation reactions of many metal ions with various anions by using the ultrasonic absorption method and proposed the following mechanism for the complex formation reactions in aqueous solution.

$$M(H_2O)_m^{p+} + L^{q-} \xrightleftharpoons{K_{os}} M(H_2O)_m^{p+}\text{---}L^{q-} \xrightarrow{k_{H_2O}} M(H_2O)_n L^{(p-q)+} + (m-n)H_2O$$
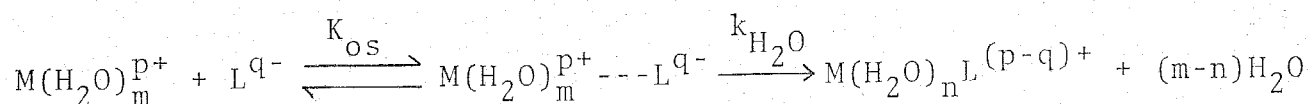
In this mechanism, the values of k_{H_2O}, which is the rate constant corresponding to the dissociation process of water molecules from the first coordination sphere of the metal ions, are independent

of metal ions, Thus far, the values of k_{H_2O} for many metal ions
have been obtained from the rate measurements of the complex
formation reactions[5]. These values are mostly in good agreement
with the rate constants of water exchange in metal ions measured
by NMR and other methods. This consistence indicates that the
rate-determining step of the complex formation and the water
exchange reactions is the dissociation process of water molecules
from the first coordination sphere of the metal ions. On the
basis of the rate constants of water exchange, the reactivity of
the metal ions has been widely discussed, and it is proposed
that the differences of reactivity among many metal ions are due
to differences in the ionic radius, charge, crystal field
stabilization energy, and coordination number of metal ions[5,11].

In spite of a large number of the kinetic studies for metal
ions in aqueous solutions, little is known concerning the kinetic
data for the metal ions in nonaqueous solvents. It is still not
obvious whether the mechanism of complex formation reactions in
nonaqueous solvents is similar to the reactions in aqueous solutions
and the reactivity of metal ions in nonaqueous solvents has not
been discussed systematically.

Benetto and Caldin[12,13] have made an extensive study of
solvent effects on the kinetics and activation parameters of Ni(II)
and Co(II) reactions with bipyridyl. Their results were inter-
preted as indicating that the factors other than the solvent
exchange rate, i.e. the rearrangement of solvent outside the first
coordination sphere of metal ions, must be taken into account
to explain the kinetics.

Table 1. Kinetic parameters for the solvent exchange reactions in various solvated metal ions

Metal Ion	Solvent	$k_{ex}(25\ °C)$ / sec^{-1}	$\Delta H^{\ddagger}$ / $kJ\ mol^{-1}$	$\Delta S^{\ddagger}$ / $JK^{-1}mol^{-1}$
Be^{2+}	H_2O	2.1×10^2	34.9	-63
	DMF	3.1×10^2	61.0	11
Mg^{2+}	H_2O	5.3×10^5	42.6	8.4
	CH_3OH	4.7×10^3	69.8	59
	C_2H_5OH	2.8×10^6	74.0	125
Al^{3+}	H_2O	1.7×10^{-1}	113	117
	DMF	4	74.0	20
	DMSO	$2.9 \times 10^{-1}(40°C)$	84	16
Sc^{3+}	TMP	6.66×10	29.8	-110.9
Ti^{3+}	H_2O	1.0×10^5	26	-63
	CH_3OH	1.9×10^5	14	-100
Ti^{4+}	DMF	3.0×10	117	
V^{2+}	H_2O	9.6×10	68.9	23.1
V^{3+}	H_2O	1×10^3	37.8	63
		1.6×10^3	25.9	-96
VO^{2+}	H_2O	5×10^2(eq.)	57.5	-2.5
		8×10^2(eq.)	55.9	-8.4
		10^{11}(ax.)		
	CH_3OH	3.3×10^2	50.4	-5.5
	DMF	2.0×10^2(eq.)	55	-17
		4.6×10^4(ax.)	64	58
	DMA	4.7×10^3(eq.)	42	-33
	CH_3CN	2.9×10^3	29.6	-84
Cr^{3+}	H_2O	4.3×10^{-7}	110	1.3
	DMF	5.5×10^{-8}	97.1	-58
	DMSO	$5.5 \times 10^{-5}(75°C)$	23.1	-12
Mn^{2+}	H_2O	3.1×10^7	34.0	12.2
		2.3×10^7	32.8	5.9
	CH_3OH	9.5×10^5	28.0	
		3.7×10^5	26	-50
	DMF	2.4×10^6	37	3
	DMSO	6.3×10^6	31	-10
	CH_3CN	1.2×10^7	30.3	-15

Table 1.   Continued
          Kinetic parameters for the solvent exchange reactions
          in various solvated metal ions

Metal Ion	Solvent	k_{ex} (25 °C) $\overline{\text{sec}^{-1}}$	$\Delta H^{\ddagger}$ $\overline{\text{kJ mol}^{-1}}$	$\Delta S^{\ddagger}$ $\overline{\text{JK}^{-1}\text{mol}^{-1}}$
Mn^{2+}	NH_3	3.6×10^7	33.4	21
	HMPA	1.0×10^7	51	43
	NBL	2.6×10^4	39	−25
Fe^{2+}	H_2O	3.2×10^6	32.3	−13
	CH_3OH	5.0×10^4	44.4	13
	CH_3CN	5.5×10^5	40.7	1.3
	DMF	1.7×10^6	48.9	38
	DMSO	1.0×10^6	47.2	29
Fe^{3+}	H_2O	$(0.8-2.0) \times 10^4$		
		1.5×10^2		
	CH_3OH	5.1×10^3	42.2	−34
	DMF	6.1×10	42.2	−69
	DMSO	5.0×10	39	−46
Co^{2+}	H_2O	2.4×10^6	43.7	21
		2.2×10^6	43.3	21.4
		1.1×10^6	33.6	−17.2
	CH_3OH	1.8×10^4	57.7	30
	DMF	3.9×10^5	56.8	53
	DMSO	3.1×10^5	51.0	41
	CH_3CN	3.5×10^5	47.7	22
	NH_3	7.2×10^6	46.8	43
Ni^{2+}	H_2O	2.7×10^4	48.7	2.5
		3.0×10^4	45.4	
		3.6×10^4	51.7	15.1
	CH_3OH	1.0×10^3	66.0	33
	C_2H_5OH	1.1×10^4	45	33
	DMF	3.8×10^3	62.7	−17
	DMSO	3.2×10^3	54.3	33
	CH_3CN	2.0×10^3	68.4	5.8
	NH_3	1.0×10^5	46	50
	DMMP	2.4×10^4	31.4	8
Cu^{2+}	H_2O	1.0×10^4 (eq.)	46	−12
		2×10^8 (ax.)	21	−12
	CH_3OH	7.4×10^7	25	−11

Table 1. Continued

Kinetic parameters for the solvent exchange reactions in various solvated metal ions

Metal Ion	Solvent	k_{ex}(25 °C) $\overline{\text{sec}^{-1}}$	$\Delta H^{\ddagger}$ $\overline{\text{kJ mol}^{-1}}$	$\Delta S^{\ddagger}$ $\overline{\text{JK}^{-1}\text{mol}^{-1}}$
Zn^{2+}	H_2O	1.8×10^3	26	-92
Ga^{2+}	H_2O	1.7×10^7	61	-35
	DMF	9×10^8		
Rh^{3+}	H_2O	3×10^{-8}	137	59
In^{3+}	H_2O	4.0×10^4	19	-97
Gd^{3+}	H_2O	6.3×10^7	12	18
		9×10^8	3.2	-7
Tb^{3+}	H_2O	$(2.1-7.8) \times 10^7$		
Dy^{3+}	H_2O	$(1.4-3.2) \times 10^7$		
		6.3×10^7		
Ho^{3+}	H_2O	$(0.9-6.1) \times 10^7$		
Er^{3+}	H_2O	$(0.54-13.5) \times 10^7$		
Tm^{3+}	H_2O	$(0.33-0.64) \times 10^7$		
ReO_4^-	H_2O	8.10×10^8		
	CH_3OH	2.6×10^8		
U^{4+}	H_2O	$1-100$		
NpO_2^+	CH_3OH	3.5×10^5	31.5	-34

eq. : Equatorial position. ax. : Axial position.

Recently, it is proposed that a correlation exists in between the solvent basicity and the activation enthalpy for the solvent exchange reactions and the complex formation reactions in nonaqueou solvents[14,15]. However, it is doubtful that the correlation is generally applicable to the solvent exchange and complex formation reactions in nonaqueous solvents.

The kinetics for the oxocations including a uranyl ion has not been well studied except a vanadium(IV) ion (VO^{2+}), and the reactivity of these oxocations in solution has been little known.

In paralell with the study of the solvent exchange reactions, extensive data on the coordination number of metal ions in solutions, have also been obtained by the NMR method[16]. The outline of this method is as follows. If the solvent exchange can be slowed by the addition of such an inert solvent as acetone, followed by cooling the sample, separate NMR signals can be observed for solvent molecules in the first coordination sphere of a metal ions, and in the bulk. The area measurements of the separate signals, combined with a knowledge of the metal ion concentration, yields the coordination number of the metal ion.

Besides the NMR area integration method, the coordination number of the metal ions have also been determined by the NMR chemical shift method, X-ray diffraction method, isotope dilution method, and ion exchange separation and chemical analysis method and so on[4,17]. The coordination number obtained so far are listed in Table 2.

With respect to a uranium(VI) ion, which is known to exist in solutions as an oxo ion, UO_2^{2+}, the study on the kinetics and

Table 2. Solvation numbers of various metal ions

Cation	Solvent	CN[a]	Method[b]
Li^+	H_2O	4	X-ray
$Be(ClO_4)_2$	H_2O	3.7–3.9	^{17}O NMR
	DMF	4.0–4.2	PMR
$BeCl_2$	H_2O	4.0–4.5	PMR
	H_2O	4.0–4.3	^{17}O NMR
Na^+	H_2O	4	X-ray
$Mg(ClO_4)_2$	H_2O	6	PMR
	CH_3OH	6	PMR
	C_2H_5OH	5.9 ± 0.4	PMR
	NH_3	5.9 ± 0.1	PMR
$Al(ClO_4)_3$	H_2O	6.0	PMR
	DMF	6.0	PMR
	DMSO	5.8–6.0	PMR
$Al(NO_3)_3$	H_2O	6.0	^{18}O ID
		6.0	PMR
$AlCl_3$	H_2O	6.0	PMR
		5.8–6.1	^{17}O NMR
	DMF	6.0	PMR
AlI_3	DMF	6.0	PMR
	NH_3	6.0	^{14}N NMR
K^+	H_2O	4	X-ray
KF,KI	H_2O	3.5	NMR
Ca^{2+}	H_2O	6	X-ray
$CaCl_2$	H_2O	6	NMR
$Ca(ClO_4)_2$	H_2O	6	NMR
$Ca(NO_3)_2$	H_2O	6	NMR

9

Table 2. Continued

Solvation numbers of various metal ions

Cation	Solvent	CN	Method
$Sc(NO_3)_3$	H_2O	5.1	PMR
$VOSO_4$	H_2O	4 (eq.)	PMR
		1 (ax.)	PMR
$Cr(ClO_4)_3$	H_2O	6.2 ± 0.2	^{18}O ID
		6	^{17}O NMR
	DMSO	6	Ion ex.
	pyridine	6	Ion ex.
	N-oxide	6	Ion ex.
	CH_3OH	6	Ion ex.
$Cr(NO_3)_3$	NH_3	6.0 ± 0.2	^{15}N ID
Mn^{2+}	H_2O	6	X-ray
Fe^{2+}	H_2O	6	X-ray
$Fe(ClO_4)_2$	H_2O	6	NMR
$Co(ClO_4)_2$	H_2O	5.9 ± 0.3	PMR
	CH_3OH	5.8	PMR
	DMF	6.0	PMR
	CH_3CN	5.7 ± 0.3	PMR
$CoCl_2$	H_2O	6	X-ray
$CoBr_2$	H_2O	6	X-ray
Co^{2+}	DMSO	6	PMR
$Ni(ClO_4)_2$	H_2O	4 or 6	^{17}O NMR
	CH_3OH	4.8 ± 0.7	PMR
$Ni(NO_3)_2$	H_2O	6.0 ± 0.2	PMR
Ni^{2+}	H_2O	6	X-ray
Cu^{2+}	H_2O	6	PMR,X-ray

Table 2. Continued

Solvation numbers of various metal ions

Cation	Solvent	CN	Method
Zn^{2+}	H_2O	6	PMR,X-ray
$Zn(ClO_4)_2$	CH_3OH	6	PMR
$Zn(NO_3)_2$	CH_3OH	6	PMR
$Ga(ClO_4)_2$	H_2O	6	^{17}O NMR,PMR
	DMF	5.9 ± 0.1	PMR
$Ga(NO_3)_2$	H_2O	5.9 ± 0.1	PMR
$GaCl_2$	H_2O	5.7	PMR
$Y(NO_3)_3$	H_2O	2.4	PMR
Ag^+	H_2O	2	X-ray
Cd^{2+}	H_2O	6	X-ray
$Cd(NO_3)_2$	H_2O	4.6	PMR
$InCl_3$	H_2O	5.8	PMR
$SnCl_4$	H_2O	6	PMR
$SnBr_4$	H_2O	6	PMR
Er^{3+}	H_2O	6	X-ray
$(CH_3)_3Pt(ClO_4)_2$	H_2O	3	^{17}O NMR
$(NH_3)_2Pt(ClO_4)_2$	H_2O	1.8 ± 1.3	^{17}O NMR
	CH_3CN	2.0 ± 0.1	PMR
$Hg(NO_3)_2$	H_2O	4.9	NMR
$Pb(NO_3)_2$	H_2O	5.7	NMR
$Th(NO_3)_4$	H_2O	2.9	PMR

[a] CN = Number of solvent molecules bound in the cation solvation shell.

[b] Method: PMR, ^1H NMR; ^{15}N ID, ^{15}N isotope dilution; ^{18}O ID, ^{18}O isotope dilution; Ion ex., ion exchange and chemical analysis.

the coordination number in the equatorial plane of uranyl ion

has not been appreciably performed in spite of a large number

of studies on the photochemical redox reactions of uranyl ion, the

redox reactions between other metal ions and uranyl ion, the

solvent extraction of uranyl ion[18-20].

The hydration number of the uranyl ion has been estimated

to be 5 or 6 from indirect methods such as gravimetric, thermo-

chemical, and spectroscopic studies[21-23]. Fratiello et al.

recently determined the hydration number of uranyl ion in solution

to be 4, i.e. $UO_2(H_2O)_4^{2+}$, by NMR area method[24-26]. More recently,

Alcock et al. studied the crystal structure of solid uranyl di-

perchlorate heptahydrate by the single crystal X-ray method and

indicated the hydration number to be 5 [27]. Furthermore, from

the coordination number studies of uranyl complex ions by NMR

area method, it has become apparent that the four- or five-

coordinated complexes in the equatorial plane of uranyl ion

exist in solution, e.g. $UO_2(HMPA)_4^{2+}$ (HMPA = hexamethylphosphor-

amide) [28,29], $UO_2L_5^{2+}$ (L = N,N-dimethylacetamide(DMA), trimethyl

phosphate(TMP), triethyl phosphate(TEP), tetramethylurea(TMU),

and N-methylacetamide(NMA)[30-33].

For these complexes, the ligand exchange reactions have also

been studied and the mechanism for these reactions has been

proposed to be D or I_d mechanism[34] except the exchange of HMPA

in $UO_2(HMPA)_4^{2+}$, where the exchange proceeds through both the

D and A mechanisms[34]. Besides these ligand exchange reactions,

it is known that the oxygen atoms which occupy the axial positions

are extremely inert except in the case of irradiation with light

of an appropriate wavelength[35-38]. There is also a kinetic
study of the reaction of UO_2^{2+} ion with $ClCH_2COO^-$, SO_4^{2-}, CH_3COO^-,
and SCN^- by the temperature-jump method[39]. Recently Ekstrom
and Johnson[40] reported the kinetics of the reaction between
UO_2^{2+} ion and 4-(2-pyridylazo)resorcinol and estimated the rate
constant for the water exchange reaction to be greater than 10^5
$M^{-1} sec^{-1}$ at room temperature. More recently, Hynes and Regan[41,42]
studied the reaction of uranyl ion with β-diketone and obtained
almost the same value for the water exchange rate constant as
that of Ekstrom and Johnson.

The data obtained so far are listed in Table 3.

Table 3. Kinetic parameters for the various substitution reactions in uranyl complexes

System	Method	Temp./°C	k/sec^{-1}	$\Delta H^{\ddagger}$/kJ mol^{-1}	$\Delta S^{\ddagger}$/JK^{-1} mol^{-1}	Ref.
$UO_2(H_2O)_4^{2+}$ – –yl oxygen in water	^{17}O NMR	25	1.5×10^{-7}			36
	Label	25	4.8×10^{-8}			35
$UO_2(H_2O)_4^{2+}$ – SCN$^-$ in water	T-jump	20	$2.90 \times 10^2/M^{-1}$			39
– SO$_4^{2-}$ in water	T-jump	20	$1.80 \times 10^2/M^{-1}$			39
– ClCH$_2$COO$^-$ in water	T-jump	20	$1.1 \times 10^2/M^{-1}$			39
– CH$_3$COO$^-$ in water	T-jump	20	$1.05 \times 10^3/M^{-1}$			39
$UO_2(H_2O)_4^{2+}$ – Hacac^a in water	Stopped-flow	25	$5.33 \times 10^3/M^{-1}$			42
in water-methanol	Stopped-flow	25	$4.93 \times 10^3/M^{-1}$			42
$UO_2(H_2O)_4^{2+}$ – Htta^b in water	Stopped-flow	25	$1 \times 10^4/M^{-1}$			41
in water-methanol	Stopped-flow	25	$1 \times 10^3/M^{-1}$			42
$UO_2(H_2O)_4^{2+}$ – Htftbd^c in water	Stopped-flow	25	$1.3 \times 10^3/M^{-1}$			42
in water-methanol	Stopped-flow	25	$1 \times 10^3/M^{-1}$			42
$UO_2(H_2O)_4^{2+}$ – PAR^d in water	Stopped-flow	25	$3.5 \times 10^4/M^{-1}$	34.3	-43.7	40
$UO_2(DMA)_5^{2+}$ – DMA^e in CD$_2$Cl$_2$	PMR	25	1.10×10^3	42.8	-43.7	30
$UO_2(TMP)_5^{2+}$ – TMP^f in CD$_2$Cl$_2$	PMR	25	4.88×10^2	25.2	-109.6	31
$UO_2(TEP)_5^{2+}$ – TEP^g in CD$_2$Cl$_2$	PMR	25	4.97×10^2	43.7	-47.5	31
$UO_2(TMU)_5^{2+}$ – TMU^h in CD$_2$Cl$_2$	PMR	25	1.88×10^3	80	85	32
$UO_2(NMA)_5^{2+}$ – NMA^i in CD$_2$Cl$_2$	PMR	25	2.74×10^3	67	45	33
$UO_2(HMPA)_5^{2+}$ – HMPA^j in CD$_2$Cl$_2$	PMR	25	2.58×10	13.9	-172.2	29
	PMR	25	$4.52 \times 10^2/M^{-1}$	22.3	-120.1	29

^{a}Hacac = acetylacetone. ^{b}Htta = thenoyltrifluoroacetone. ^{c}Htftbd = 4,4,4-trifluoro-1-(2-thienyl)butane-1,3-dione ^{d}PAR = 4-(2-pyridylazo) resorcinol. ^{e}DMA = N,N-dimethylacetoamide. ^{f}TMP = trimethyl phosphate. ^{g}TEP = triethyl phosphate. ^{h}TMU = tetramethylurea. ^{i}NMA = N-methylacetamide. ^{j}HMPA = hexamethylphosphoramide.

B. Introduction

Although some kinetic data have become available with respect to the reactivity of ligands which coordinate to the equatorial plane of uranyl ion, the kinetics of the water exchange reaction in the equatorial plane of uranyl ion, which seems to give the most fundamental information about the properties of uranyl ion in solution, has not been studied. Furthermore, the coordination number in the equatorial plane of uranyl ion is somewhat uncertain. The coordination number in the equatorial plane ranges from 4 or 5 for oxygen donor unidentate ligands to 6 for oxygen donor bidentate ligands[43,44)

The purpose of this study is

(i)   to determine the rate constant and the mechanism of the water exchange reaction in the equatorial plane;

(ii)   to examine the ligand effect on the ligand exchange reactions in uranyl complexes;

(iii) to find out the relationships between the coordination number of the equatorial plane of uranyl ion and the properties of coordinated ligands;

(iv)   to measure the exchange rate of the bidentate ligands in uranyl-bidentate complexes, and to make the mechanism clear.

The present research was initiated by determining the hydration number of uranyl ion and then studied the water exchange reaction in the equatorial plane of uranyl ion by the NMR line-broadening method. The ligand exchange reactions in UO_2^{2+}-DMSO

and UO_2^{2+}-DMF, where DMSO and DMF are dimethyl sulfoxide and
N,N-dimethylformamide, respectively, were studied to examine
the ligand effect on the ligand exchange reactions in uranyl
complexes. Moreover, the exchange reactions of DMSO in UO_2-
(acac)$_2$DMSO and UO_2(dbm)$_2$DMSO (acac = acetylacetonate, dbm =
dibenzoylmethanate), and of DMF in UO_2(acac)$_2$DMF were studied
in order to examine the steric effect on the ligand exchange
reactions. The exchange reactions of methyl groups of coordinated
acac in UO_2(acac)$_2$L (L = DMSO, DMF and DEF where DEF = N,N-
diethylformamide) were also studied to examine the stereochemical
rigidity of the uranyl complex.

Finally, the exchange reaction of acac in UO_2(acac)$_2$DMSO
was investigated and compared with the exchange reactions of
unidentate ligands in uranyl complexes.

On the basis of these results, the detailed discussion
is given about the properties of uranyl complexes in solutions.

REFERENCES

1. H.S. Gutowsky, D.M. McCall, and C.P. Slichter, J. Chem. Phys., <u>21</u>, 279(1953)

2. H.M. McConnell, J. Chem. Phys., <u>28</u>, 430(1958).

3. T.J. Swift and R.T. Connick, J. Chem. Phys., <u>37</u>, 307(1962).

4. 大滝 仁志, 田中 元治, 舟橋 重信「溶液反応の化学」付表13. 東京大学出版会 (1977).

5. E. Martell, Coordination Chemistry, American Chemical Society, Washington, D.C. (1978).

6. N.S. Angerman and R.B. Jordan, Inorg. Chem., <u>8</u>, 65(1969).

7. D.L. Pisaniello and S.F. Lincoln, Inorg. Chim. Acta., <u>36</u>, 85(1979).

8. J.C. Sheppard and J.L. Burdett, Inorg. Chem., <u>5</u>, 921(1966).

9. C. Kienner, G. Folcher, P. Rigny, and J. Virlet, Can. J. Chem., <u>54</u>, 303(1976).

10. M. Eigen, Ber, Bunsenges. Physik. Chem., <u>67</u>, 753(1963).

11. F. Basolo and R.G. Pearson, Mechanisms of Inorganic Reactions. 2nd Ed., John Wiley and Sons, Inc., New York (1967).

12. H.P. Benetto and E.F. Caldin, J. Chem. Soc. (A), 2198(1971).

13. E.F. Caldin and H.P. Benetto, J. Solution Chem., <u>2</u>, 217(1973).

14. F. Pickert, H. Hoffmann, and T. Janjic, Ber. Bunsenges. Physik. Chem., <u>78</u>, 712(1974).

15. S. Funahashi and R.B. Jordan., Inorg. Chem., <u>16</u> 1301(1977).

16. J.O. Edwards, Inorganic Reaction Mechanisms. Part II. p 57, John Wiley and Sons, Inc. New York. London. Sydney. Toronto.(1972

17. S.F. Lincoln, Coord. Chem. Rev., 6, 309(1971).

18. T.W. Newton and F.B. Baker, Adv. Chem. Ser., <u>67</u>, 268(1967).

19. H.D. Burrows and T.J. Kemp, Chem. Soc. Rev., $\underline{3}$, 139(1974).

20. H. Irving and D.N. Edgington, J. Inorg. Nucl. Chem., $\underline{15}$, 158 (1960).

21. J.D. Edwards and J.A. Stitar, Sience, $\underline{142}$, 1651(1963).

22. I.I. Lipilian and O. Ya. Samoilov, Dokl. Akad. Nauk. SSSR., $\underline{98}$, 99(1954).

23. S.P. McGlynn and J.K. Smith, J. Mol. Spectrosc, $\underline{6}$, 164(1961).

24. A. Fratiello, V. Kubo, R.E. Lee, S. Perk, and R.E. Schuster, J. Inorg. Nucl. Chem., $\underline{32}$, 3114(1970).

25. A. Fratiello, V. Kubo, and R.E. Schuster, Inorg. Chem., $\underline{10}$, 744(1971).

26. A. Fratiello, V. Kubo, R.E. Lee, and R.E. Schuster, J. Phys. Chem., $\underline{74}$, 3726(1970).

27. N.W. Alcock and S. Esperås, J.C.S. Dalton, 893(1977).

28. A. Fratiello, G.A. Vidlich, C. Cheng, and V. Kubo, J. Solution Chem., $\underline{1}$, 433(1972).

29. G.J. Honan, S.F. Lincoln, and E.H. Williams, Inorg. Chem., $\underline{17}$, 1855(1978).

30. R.P. Bowen, S.F. Lincoln, and E.H. Williams, Inorg. Chem., $\underline{15}$, 2126(1976).

31. J. Crea, R. Digiusto, S.F. Lincoln, and E.H. Williams, Inorg. Chem., $\underline{16}$, 2825(1977).

32. G.J. Honan, S.F. Lincoln, and E.H. Williams, J.C.S. Dalton, 320(1979).

33. G.H. Honan, S.F. Lincoln, and E.H. Williams, J.C.S. Dalton, 1220(1979).

34. G.H. Langford and H.B. Gray, Ligand Substitution Processes, Benjamin, London(1974).

35. G. Gordon and H. Taube, J. Inorg. Nucl. Chem., 16, 272(1961).

36. S.W. Rabideau, J. Phys. Chem., 71, 2747(1967).

37. Y. Kato and H. Fukutomi, J. Inorg. Nucl. Chem., 38, 1323(1976).

38. K. Okuyama, Y. Ishikawa, Y. Kato, and H. Fukutomi, Bull. Res. Lab. Nucl. Reactor, 3, 39(1978).

39. P. Hurwitz and K. Kustin, J. Phys. Chem., 71, 324(1967).

40. A. Ekstrom and D.A. Johnson, J. Inorg. Nucl. Chem., 36, 2549 (1974).

41. M.T. Hynes and B.D. O Regan, D.C.S. Dalton, 1200(1976).

42. M.T. Hynes and B.D. O Regan, J.C.S. Dalton, 1502(1980).

43. I.I. Chernyae, Complex Compounds of Uranium(Translated from Russian), Israel Program for Scientific Translations, Jerusalem(1966).

44. H.T. Evans, Science, 141, 154(1963).

CHAPTER II

THEORY OF NMR LINE-BROADENING METHOD

A. General Theory

The first quantitative theory for study of chemical exchange reaction by the NMR method was developed by Gutowsky et al.[1], and more general treatments of the problem have been developed by some authors[2-4]. They quatify the concepts for the case of two-site exchange reaction, which may be represented as

$$A \; \underset{\tau_B^{-1}}{\overset{\tau_A^{-1}}{\rightleftharpoons}} \; B \tag{1}$$

where A and B are different nuclear sites which are distinguished with chemical shifts $\nu_A = (\omega_{0A}/2\pi)$ and $\nu_B = (\omega_{0B}/2\pi)$, and τ_A and τ_B are the mean lifetimes in the sites A and B, respectively, and related with the exchange rate by the following equation (2).

$$-d[A]/dt = [A]/\tau_A \quad \text{and} \quad -d[B]/dt = [B]/\tau_B \tag{2}$$

A transfer of a nuclear spin from A to B causes dephasing at site B and an increase in magnetization of site B. Similarly transfer of a nuclear spin from site B to site A causes dephasing at site A and increases the magnetization of site A.

The Bloch equations[5] for sites A and B may, therefore, be modified to the following equations (3) and (4),

$$dG_A/dt = -[i(\omega_{0A} - \omega) + 1/T_{2A}]G_A + i\gamma H_1 M_z^A - G_A/\tau_A + G_B/\tau_B \tag{3}$$

$$dG_B/dt = -[i(\omega_{0B} - \omega) + 1/T_{2B}]G_B + i\gamma H_1 M_z^B - G_B/\tau_B + G_A/\tau_A \tag{4}$$

where G_A and G_B are the magnetizations of nuclei in sites A and B, respectively, and ω, γ, and H_1 are the observed frequency, the gyromagnetic ratio and the radio-frequency field, respectively, and T_{2A} and T_{2B} are the transverse relaxation times in the sites A and B in the absence of exchange, respectively.

Since the system is supposed to be in equiliblium, the ratio of the mean lifetimes in the sites A and B should be equal to that of the corresponding fractional populations P.

$$\tau_A / \tau_B = P_A / P_B \tag{5}$$

where $P_A = [A]/([A] + [B])$ and $P_B = 1 - P_A$. In addition, a new variable can be defined by Eq. (5), that is,

$$\tau = \tau_A P_B = \tau_B P_A \tag{6}$$

If ω is swept slowly enough through the resonance frequency, the magnetization might become stationary. It is also assumed that saturation is avoided by choosing a low H_1 field. Under these conditions, the following equation can be applied.

$$dG_A/dt = dG_B/dt = 0, \quad M_z^A = M_0^A = P_A M_0, \quad M_z^B = M_0^B = P_B M_0 \tag{7}$$

From Eq. (7), the modified Bloch equations become linear equations in G_A and G_B

$$-[i(\omega_{0A} - \omega) + 1/T_{2A} + 1/\tau_A]G_A + G_B/\tau_B = -iP_A\gamma H_1 M_0 \tag{8a}$$

$$-[i(\omega_{0B} - \omega) + 1/T_{2B} + 1/\tau_B]G_B + G_A/\tau_A = -iP_B\gamma H_1 M_0 \qquad (8b)$$

and can be easily solved. If one defines

$$\alpha_A = 1/T_{2A} - i(\omega_{0A} - \omega) \qquad (9a)$$

$$\alpha_B = 1/T_{2B} - i(\omega_{0B} - \omega) \qquad (9b)$$

the total transverse magnetization $G = G_A + G_B$ is given by

$$G = \frac{-i\gamma H_1 M_0 [(\tau_A + \tau_B) + \tau_A \tau_B (\alpha_A P_B + \alpha_B P_A)]}{(1 + \alpha_A \tau_A)(1 + \alpha_B \tau_B) - 1} \qquad (10)$$

To obtain the spectrum in the absorption mode, it is only necessary to extract the imaginary part(v) of the complex quantity. The imaginary part is derived from Eq. (10)

$$v = -i\gamma H_1 M_0 (AC + BD)/(C^2 + D^2) \qquad (11)$$

where

$$A = 1/\tau_A + 1/\tau_B + P_B/T_{2A} + P_A/T_{2B}$$

$$B = \omega_A P_B + \omega_B P_A$$

$$C = 1/(T_{2A}\tau_B) + 1/(T_{2B}\tau_A) + 1/(T_{2A}T_{2B}) - \omega_A \omega_B$$

$$D = \omega_A (1/T_{2B} + 1/\tau_B) + \omega_B (1/T_{2A} + 1/\tau_A)$$

$$\omega_A = \omega_{0A} - \omega, \qquad \omega_B = \omega_{0B} - \omega$$

From Eq. (11), one can derive the equation corresponding to some conditions in exchange reactions. One of the conditions is limit of very slow exchange, i.e. τ_A^{-1}, $\tau_B^{-1} \ll |\omega_{0A} - \omega_{0B}|$, T_{2A}^{-1}, T_{2B}^{-1}. Under this condition, Eq. (11) reduces to Eq. (12)

$$v = \frac{-\gamma H_1 M_0 P_A T_{2A}^{-1}}{T_{2A}^{-2} + (\omega_{0A} - \omega)^2} + \frac{-\gamma H_1 M_0 P_B T_{2B}^{-1}}{T_{2B}^{-2} + (\omega_{0B} - \omega)^2} \tag{12}$$

and only two separate signals with relative intensities P_A and P_B are observed at ω_{0A} and ω_{0B}. The spectrum in this case is given in Fig. 1a.

When the exchange rate increases and corresponds to the conditions, τ_A^{-1}, $\tau_B^{-1} \ll |\omega_{0A} - \omega_{0B}|$, τ_A^{-1} is comparable to T_{2a}^{-1}, and also τ_B^{-1} is comparable to T_{2B}^{-1}, Eq. (11) yields the following equation for v.

$$v = \frac{-\gamma H_1 M_0 P_A (T_{2A}^{-1} + \tau_A^{-1})}{(T_{2A}^{-1} + \tau_A^{-1})^2 + (\omega_{0A} - \omega)^2} + \frac{-\gamma H_1 M_0 P_B (T_{2B}^{-1} + \tau_B^{-1})}{(T_{2B}^{-1} + \tau_B^{-1})^2 + (\omega_{0B} - \omega)^2} \tag{13}$$

Again, the signals of the Lorentzian lineshape are observed at ω_{0A} and ω_{0B}. The only difference between Eqs. (12) and (13) is in the full linewidth at half height intensity of each signal.

The observed transverse relaxation times of each signal are given by Eq. (14).

$$1/T_{2Aobs} = 1/T_{2A} + 1/\tau_A \text{ and } 1/T_{2Bobs} = 1/T_{2B} + 1/\tau_B \qquad (14)$$

The linewidths are increased by a mean lifetime facor or chemical exchange factor, τ_A or τ_B, because the observed linewidth in sec^{-1}, defined as the full linewidth at half height, is given by $\Delta\nu = (\pi T_{2obs})^{-1}$. Therefore, τ_A and τ_B are simply calculated from the linewidth of each signal and the exchange rate constants are obtained. The spectrum in this case is shown in Fig. 1b.

In the fast exchange limit, τ_A^{-1}, $\tau_B^{-1} > |\omega_{0A} - \omega_{0B}|$, the signal is centered at the weighted average position and the half linewidth at half height intensity is given by

$$1/T_2 = P_A/T_{2A} + P_B/T_{2B} + P_A^2 P_B^2 (\omega_{0A} - \omega_{0B})^2 (\tau_A + \tau_B) \qquad (15)$$

If one can estimate precisely the difference of chemical shift, $\omega_{0A} - \omega_{0B}$, in this equation, one can obtain the exchange rate constants by using this equation and Eq. (6). The spectrum in this case is indicated in Fig. 1d.

The last limit which yields a relatively simple form for Eq. (11) is the very fast exchange limit, τ_A^{-1}, $\tau_B^{-1} \gg |\omega_{0A} - \omega_{0B}|$, T_{2A}^{-1}, T_{2B}^{-1}. Under this condition, ν is expressed by Eq. (16).

$$v = \frac{-\gamma H_1 M_0 (P_A T_{2B}^{-1} + P_B T_{2B}^{-1})}{(P_A T_{2A}^{-1} + P_B T_{2B}^{-1})^2 + (P_A \omega_{0A} + P_B \omega_{0B} - \omega)^2} \tag{16}$$

A sigle Lorentzian signal is observed at $(P_A \omega_{0A} + P_B \omega_{0B})$ and whose linewidth is $1/T_{2obs} = P_A T_{2A}^{-1} + P_B T_{2B}^{-1}$. The spectrum in this case is shown in Fig. 1e.

The lineshapes of NMR signals change with the exchange rate as mentioned above. If such spectrum as Fig. 1b is observed the τ_A and τ_B values can be easily obtained from the linewidths of each signal by using Eq. (14). From Eq. (14), τ_A and τ_B are given by Eqs. (17a) and (17b)

$$1/\tau_A = 1/T_{2Aobs} - 1/T_{2A} \tag{17a}$$

$$1/\tau_B = 1/T_{2Bobs} - 1/T_{2B} \tag{17b}$$

where $1/T_{2Aobs}$ and $1/T_{2Bobs}$ are equal to the observed linewidths, and $1/T_{2A}$ and $1/T_{2B}$ are the linewidths in the absence of exchange which are given by Eq. (12). For other cases, e.g. Fig. 1c and Fig. 1d, it is difficult to obtain directly the τ_A and τ_B values from the linewidths of spectra and hence the computed and experimentally obtained spectra should be matched to obtain τ_A and τ_B values by using a computer. If the τ_A and τ_B are obtained, the first order rate constant is obtained from Eq. (2).

B. Application to the Present Study

In the present study, the exchange reaction is expressed by Eq. (19)

$$UO_2L_n^{m+} + L^* \underset{\tau_F^{-1}}{\overset{\tau_c^{-1}}{\rightleftharpoons}} UO_2L_{n-1}L^{*m+} + L \qquad (19)$$
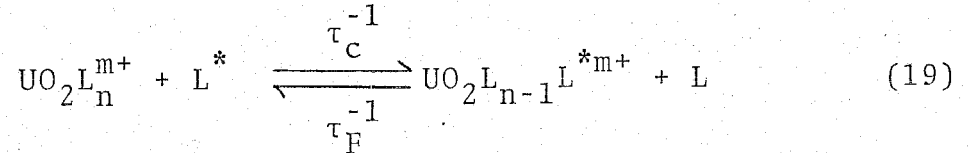
where L represents a exchanging ligand, subscripts c and F represent the coordinated and free sites, respectively, and τ_c and τ_F are the mean lifetimes at each site. According to Eq. (2), τ_c is related to the exchange rate by Eq. (20)

$$-[UO_2L_n^{m+}]/dt = n[UO_2L_n^{m+}]/\tau_c \qquad (20)$$

and hence the first-order exchange rate constant, k_{ex}, is given by Eq. (21)

$$k_{ex} = 1/\tau_c = \text{rate}/(n[UO_2L_n^{m+}])$$

$$= (kT/h)\exp(-\Delta H^{\ddagger}/RT)\exp(\Delta S^{\ddagger}/R) \qquad (21)$$

If the spectra are measured at various temperatures and the corresponding best-fit τ_c-values are calculated, the first-order rate constants can be obtained from Eq. (21). Then, the activation parameters, $\Delta H^{\ddagger}$ and $\Delta S^{\ddagger}$, can be calculated from the plots of $\ln k_{ex}$ vs. $1/T$.

In order to calculate the best-fit τ_c-values by a computer, the following equation was derived from Eqs. (6) and (10), where

the subscripts A and B were changed to c and F, respectively.

$$G = \frac{-i\gamma H_1 M_0 [P_c + P_F + \tau(P_F \alpha_c + P_c \alpha_F)]}{P_c \alpha_c + P_F \alpha_F + \alpha_c \alpha_F \tau} \qquad (22)$$

where

$$\tau = P_c \tau_F = P_F \tau_c \qquad (6')$$

$$\alpha_c = 1/T_{2c} - i(\omega_{0c} - \omega) \qquad (9a')$$

$$\alpha_F = 1/T_{2F} - i(\omega_{0F} - \omega) \qquad (9b')$$

Equation (22) is the function of τ, P_c, P_F, T_{2c}, T_{2F}, ω_{0c}, and ω_{0F}. The values of P_c and P_F are calculated from the concentrations of $UO_2 L_n^{m+}$ L

$$P_c = n[UO_2 L_n^{m+}]/(n[UO_2 L_n^{m+}] + [L]) \qquad (23)$$

$$P_F = 1 - P_c \qquad (24)$$

and the values of $1/T_2$ and ω_0 with the subscripts of c and F are equal to the linewidths and chemical shifts of two sites in the absence of exchange, respectively.

The theoretical spectra can be calculated from Eq. (22) by using these known parameters and appropriate τ-values, and compared with the experimental spectra. Both spectra are compared with respect to the following values, i.e. linewidths

at one-fourth, one-half and three-fourths maximum intensity, and, below coalescence, the difference of chemical shift between the two signal maxima and the ratios of maximum intensity to the intensity at the central minimum. In this manner the best-fit τ-values are determined. From Eq. (6'), τ_c and k_{ex} are obtained. The program used in the calculation is similar to that proposed by Binsch[6]. All computations were carried out on a Hitach M-200 computer in the Tokyo Institute of Technology.
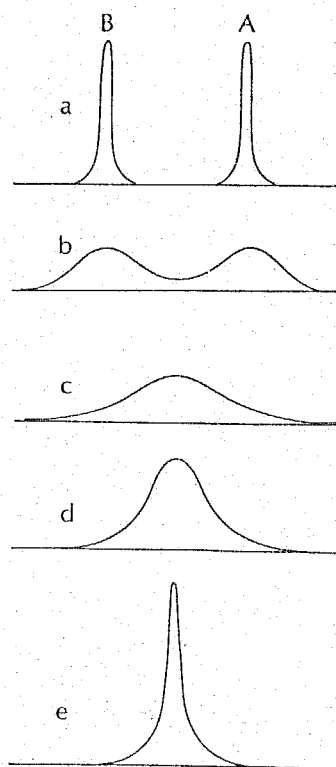
Fig. 1. Lineshapes of NMR signals as a function of exchange rate in the two site exchange reaction.

REFERENCES

1. H.S. Gutowsky, D.M. McCall, and C.P. Slichter, J. Chem. Phys., $\underline{21}$, 279(1953).

2. J.A. Pople, W.G. Schneider, and H.J. Bernstein, High-Resolution Nuclear Magnetic Resonance. MaGraw Hill, New York, N.Y.(1959).

3. G.N. La Mar, W.D. Horrocks, and R.H. Holm, NMR of Paramagnetic Molecules. Academic Press, New York(1973).

4. L.M. Jackman and F.A. Cotton, Dynamic Nuclear Magnetic Resonance Spectroscopy. Academic Press, New York(1975).

5. F. Bloch, Phys. Rev., $\underline{70}$, 460(1946).

6. E.L. Eliel and N.L. Allinger, Top. Stereochem., $\underline{3}$, 97(1968).

CHAPTER III

KINETIC STUDY OF THE LIGAND EXCHANGE REACTIONS
IN URANYL COMPLEXES WITH UNIDENTATE LIGANDS BY
NMR

i.   INTRODUCTION

Only limited kinetic data have been available with respect
to the reactivity of ligands which coordiante in the equatorial
plane of uranyl ion[1-7]. Particularly, the water exchange
reaction in uranyl aqua ion, which seems to give the most basic
information about the properties of uranyl ion in solution, has
not been studied, while the rate constant of water exchange has
been estimated from the complex formation reaction to be 10^2 M^{-1}
sec^{-1} or 10^5 M^{-1} sec^{-1} [1,3].

The hydration number of uranyl ion and the exchange rate
of water in uranyl aqua complex, which were determined by the
NMR method, will be presented in this chapter. The ligand exchange
reactions in UO_2^{2+}-DMSO and UO_2^{2+}-DMF complexes were also studied
to examine the ligand effect on the ligand exchange reactions in the
uranyl complexes. DMSO and DMF molecules have a large basicity
than that of water and hence it is expected that the structure
and the reactivity of the complexes coordinated by DMSO and DMF
in solution are different from those of uranyl aqua complex.
Furthermore, DMSO and DMF has been extensively used in the study
of the solvent exchange reactions in various metal ions. The
obtained kinetic data can be compared with those in various metal
ions.

On the basis of these results, a detailed discussion is
given on the relationship in the mechanism of ligand exchange
reaction, the structure of the uranyl complexes, and the basicity
and the size of ligands.

ii. EXPERIMENTAL

A. Synthesis of Complexes

Uranyl perchlorate stock solutions were prepared by dissolving U_3O_8 in an appropriate amount of perchloric acid. The U_3O_8 was prepared by heating $UO_2(NO_3)_2 6H_2O$ about 920 °C. Concentrations of uranyl ion in stock solutions were determined gravimetrically and acid concentrations were determined by passing stock solutions through a Dowex 50W-X12 cation exchange resin column, followed by titration of the resultant acid solutions with standardized $Ba(OH)_2$.

The preparation of the $[UO_2(DMSO)_5](ClO_4)_2$ complex was made in an atmosphere of nitrogen by refluxing hydrated uranyl per-chlorate with triethyl orthoformate at 50-60 °C for 1 hour. Then dimethyl sulfoxide was added at room temperature and the resulting light yellow crystals were filtered off, washed with ethyl ether, and dried in vacuo for 2 days. Anal. Calcd for $[UO_2(DMSO)_5](ClO_4)_2$: C, 13.94; H, 3.52; S, 18.65. Found: C, 13.84; H, 3.49; S, 18.40.

The preparation of the $[UO_2(DMF)_5](ClO_4)_2$ complex was performed by the same method as the synthesis of the $[UO_2(DMSO)_5](ClO_4)_2$ complex. Anal. Calcd for $[UO_2(DMF)_5](ClO_4)_2$: C, 21.59; H, 4.22; N, 8.39. Found: C, 21.65; H, 4.20; N, 8.50.

Elemental analysis of the complexes was carried out in the Institute of Physical and Chemical Research.

B. Other Materials

Perchloric acid ($HClO_4$), hydrochloric acid (HCl), and hydro-

bromic acid (HBr) (Wako Pure Chemical Ind. Ltd.) are of reagent grade. Analytical grade acetone (Wako Pure Chemical Ind. Ltd.) was used. Acetone-d_6 (CD$_3$COCD$_3$, Merk 99.8 %), which was dried over 3A molecular sieves (Wako Pure Chemical Ind. Ltd.), was used as the diluent in the exchange reaction of DMSO in UO$_2^{2+}$-DMSO complex. Dichloraomethane-d_2 (CD$_2$Cl$_2$, Merk 99 %), which was dried over 4A molecular sieves, was used in the exchange reaction of DMF in UO$_2^{2+}$-DMF complex. Dimethyl sulfoxide (Wako Pure Chemical Ind. Ltd.) was distilled in vacuo, followed by the distillation with 3A molecular sieves, and dried over 3A molecular sieves before use. N,N-Dimethylformamide (Wako Pure Chemical Ind. Ltd.) was purified and dried by vaccum distillation from barium oxide. The distillate was stored over 3A molecular sieves and then distilled under vaccum and stored over 3A molecular sieves. Triethyl orthoformate (Wako Pure Chemical Ind. Ltd.) was of reagent grade and used without further purification.

The reasons why CH$_3$COCH$_3$, CD$_3$COCD$_3$, and CD$_2$Cl$_2$ were used as the diluents are as follows. Acetone(mp: -95.4 °C) dissolve water and uranyl perchlorate and can be cooled down below -90 °C. Furthermore, CD$_3$COCD$_3$, which has a smaller basicity than that of water according to Gutmann's donor number concepts[8,9], does not coordinate to uranyl ion under the present experimental conditions. Acetone-d_6 is thought to have the same properties as those of CH$_3$COCH$_3$, and sufficient solubility of the [UO$_2$(DMSO)$_5$](ClO$_4$)$_2$ complex makes it possible to observe the methyl proton signal of DMSO. Dichloromethane-d_2 was used by the same reason as that of acetone-d_6. Acetone-d_6 and dichloromethane-d_2 was used as an NMR lock reagent.

C. Preparation of Samples

Sample solutions containing a diluent were prepared by weighting sample substances in a 1 or 5 cm^3 volumetric flask and some of each solution was placed in an NMR tube and sealed. All procedures except the preparation of samples for the water exchange reactions were done in a glove box filled with dried nitrogen. Proper precautions were taken to minimize the probability of photochemical redox reactions.

D. Measurements of NMR and IR Spectra

The measurements of ^{1}H NMR spectra were carried out at 100 MHz on a JEOL JNM-MH 100 NMR spectrometer and JEOL JNM-FX 100 FT-NMR spectrometer equipped with a JNM-VT-3B temperature controller. For the water exchange reaction, the spectra of the water protons in the bulk phase water measured at least three times. For the exchange of DMSO in UO_2^{2+}-DMSO complex, the spectra of methyl proton signals of coordinated and free DMSO were measured a minimum of three times. Similarly, the spectra of formyl proton signals of coordinated and free DMF were measured for the exchange reaction of DMF in UO_2^{2+}-DMF complex.

Infrared spectra of the $[UO_2(DMF)_5](ClO_4)_2$ complex in CD_2Cl_2 were recorded in the range 4000-200 cm^{-1} by using a Jasco DS-701G IR spectrometer.

E. Kinetic Analysis

Kinetic analysis of all the exchange reactions, except the water exchange reaction in uranyl aqua ion, were done by the same method as described in Chapter II.

In the case of the water exchange reaction in uranyl aqua ion, the first-order exchange rate constants, k_{ex}, were obtained from the linewidths of bulk water signals. If the relaxation process is controlled by a chemical exchange process between the coordinated and bulk water molecules, the following equation is derived from the Eq. (17) in Chapter II.

$$1/T_2 - 1/T_{2F} = 1/\tau_F$$

where T_2 and T_{2F} are the transverse relaxation times of bulk water protons in the presence of uranyl ion and the absence of uranyl ion, respectively. The mean lifetime τ_F is related to the first-order rate constant by the following equation

$$k_{ex} = P_F/(P_C \tau_F) = (kT/h)\exp(-\Delta H^{\ddagger}/RT)\exp(\Delta S^{\ddagger}/R)$$

where P_C and P_F are mole fractions of coordinated and free water molecules, respectively. These mole fractions are expressed by the equation

$$P_C = 1 - P_F = n[UO_2^{2+}]/[\text{total } H_2O]$$

where n is the number of hydrated water molecules. Hence if the plot of log $(1/T_2 - 1/T_{2F})$ vs. $1/T$ give a straight line with a negative slope, the k_{ex} values are obtained from the linewidths of bulk water proton signals in the temperature range.

For the exchange of DMSO in the UO_2^{2+}-DMSO complex, the methyl

proton signals of coordinated and free DMSO molecules were measured. The formyl proton signals of coordinated and free DMF molecules for the exchange of DMF in the UO_2^{2+}-DMF complex were measured.

The values of P_c, P_F, T_{2c}, T_{2F}, ω_{0c}, and ω_{0F} are necessary to obtain the best-fit τ-values by using Eq. (22) in Chapter II. The values of P_c and P_F were obtained from the following equation

$$P_c = 1 - P_F = n[UO_2L_n^{2+}]/(n[UO_2L_n^{2+}] + [L])$$

where L is DMSO and DMF, and n is the number of L bound per UO_2^{2+} ion.

The linewidths of methyl proton signals of DMSO in CD_3COCD_3 and of formyl proton signals of DMF in CD_2Cl_2 were used as the values of T_{2c} and T_{2F} in each exchange reaction. The chemical shifts of methyl proton signals of coordianted and free DMSO molecules at -80 °C were used as the values of ω_{0c} and ω_{0F}, respectively. Similarly, the chemical shifts of formyl proton signals of coordianted and free DMF molecules at -80 °C were used as the values of ω_{0c} and ω_{0F}.

iii. RESULTS AND DISCUSSION

1. KINETIC STUDY OF THE EXCHANGE OF WATER MOLECULES IN URANYL AQUA COMPLEXES BY NMR

A. Structure of the Uranyl Aqua Complex in Acetone-d_6- Water Mixed Solvents

From the study of the crystal structure of solid uranyl diperchlorate heptahydrate [10], it is found that the hydration number of uranyl ion is five, where perchlorate ions bind to coordinated water by hydrogen bonds.

Fratiello et al. [11,12] determined the hydration number of uranyl ion to be four in water-acetone mixed solvents by the NMR method. They suggested also that the effects of solvation of acetone and of the hydrolysis of uranyl ion are negligible, because the signal of coordinated aceotne was not observed and the measured hydration number did not depend on the concentrations of perchloric acid. Furthermore, it appeares that ClO_4^- ion is not present in the first coordination sphere of uranyl ion in the presence of excess water from IR data [13].

In view of these previous works, we have followed Fratiello's experiments and obtained the same value for the hydration number of the uranyl ion. A typical spectrum of a solution containing uranyl ion, water and acetone-d_6, from which the hydration number is determined, is shown in Fig. 1. In this figure, the symbols of F_{H_2O} and C_{H_2O} represent the proton signals of bulk and coordinated water. The obtained hydration numbers are listed in Table 1.

$[UO_2^{2+}] = 0.140$ M

$[UO_2^{2+}]$: $[H_2O]$: $[H^+]$: $[CD_3COCD_3]$

$= 1 : 17.5 : 0.15 : 91.5$

100 Hz

F_{H_2O}

C_{H_2O}
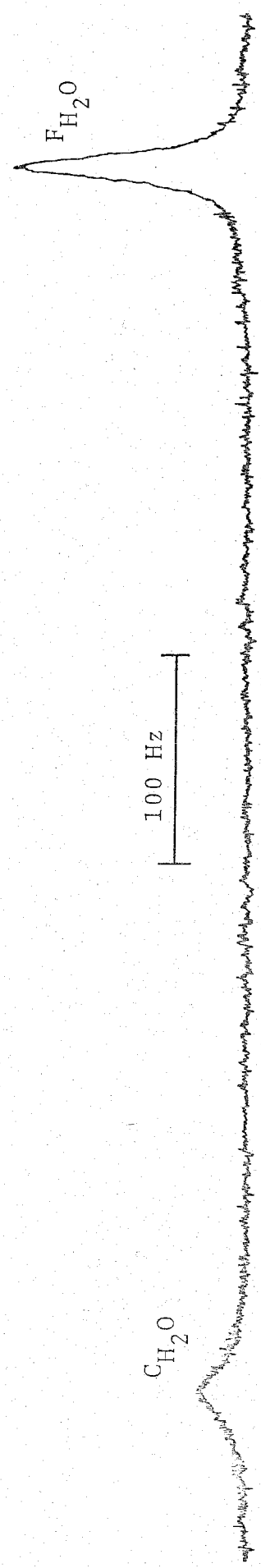
Fig. 1. The ^{1}H NMR spectrum of a solution consisting of $UO_2(ClO_4)_2$, $HClO_4$, H_2O, and CD_3COCD_3 at -90 °C.

B. Exchange Reaction of H_2O in $UO_2(H_2O)_4^{2+}$ in Acetone-d_6-
   Water Mixed Solvents

In the NMR measurement of water, where the ratio of $[H_2O]/$
$[D_2O]$ was 1/10, no line broadening was observed on addition of
uranyl ion at room temperature. This suggests that the water
exchange between the water molecules coordinated to uranyl ion
and the bulk water may be too fast on the NMR time scale in this
temperature region. However, in the presence of uranyl ion at
temperature below 0 °C the linewidth of the water proron signal
broadened as the temperature was decreased, and below -50 °C,
two sets of water signals were observed as shown in Fig. 2.
The signal observed in higher field(F_{H_2O}) is assigned to the
protons of bulk water molecules, and the downfield signal(C_{H_2O})
attributes to the water molecules in the first coordination sphere
of the uranyl ion. The linewidth of the water signal(R_{H_2O}) in
the absence of uranyl ion broadened slightly as the tempearture
decreased. Table 2 shows the observed linewidths and the values
of $(1/T_2 - 1/T_{2F})$, where T_2 and T_{2F} are the transverse relaxation
time of the bulk water protons in the presence and absence of
uranyl ion at various temperatures, respectively. A semilogarithmic
plot of $(1/T_2 - 1/T_{2F})$ against the reciprocal temperature is shown
in Fig. 3. This plot is linear with a negative slope over the
temperature range from -60 to -80 °C. The relaxation process may
be controlled by a chemical exchange process between the first
coordination sphere and the bulk water molecules; hence the
following equation is applicable in the temperature range from -60
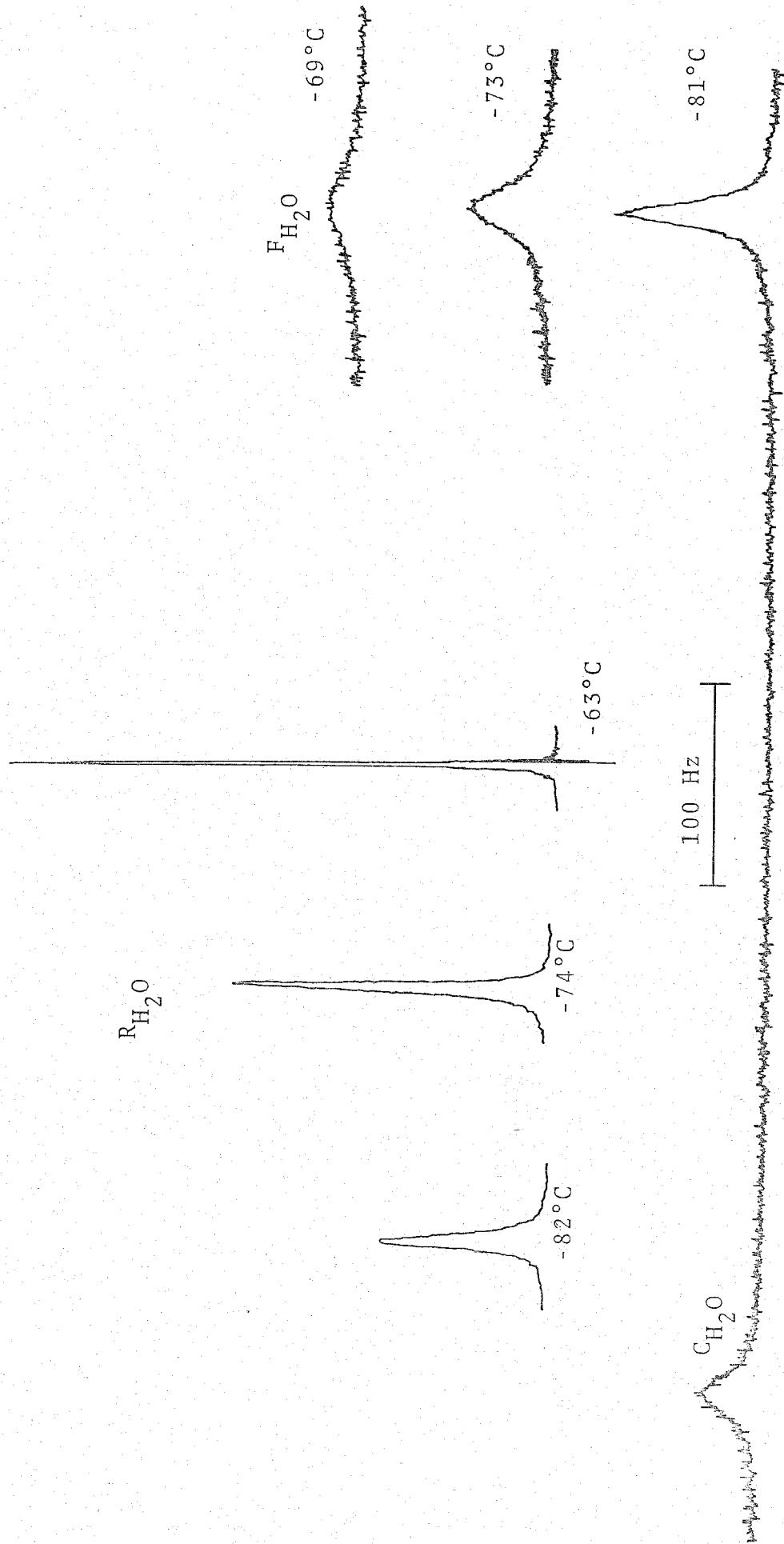to -80 °C.

Fig. 2. Temperature dependence of ^{1}H NMR spectra of bulk water in the presence of uranyl ion and of water in the absence of uranyl ion in CD_3COCD_3.
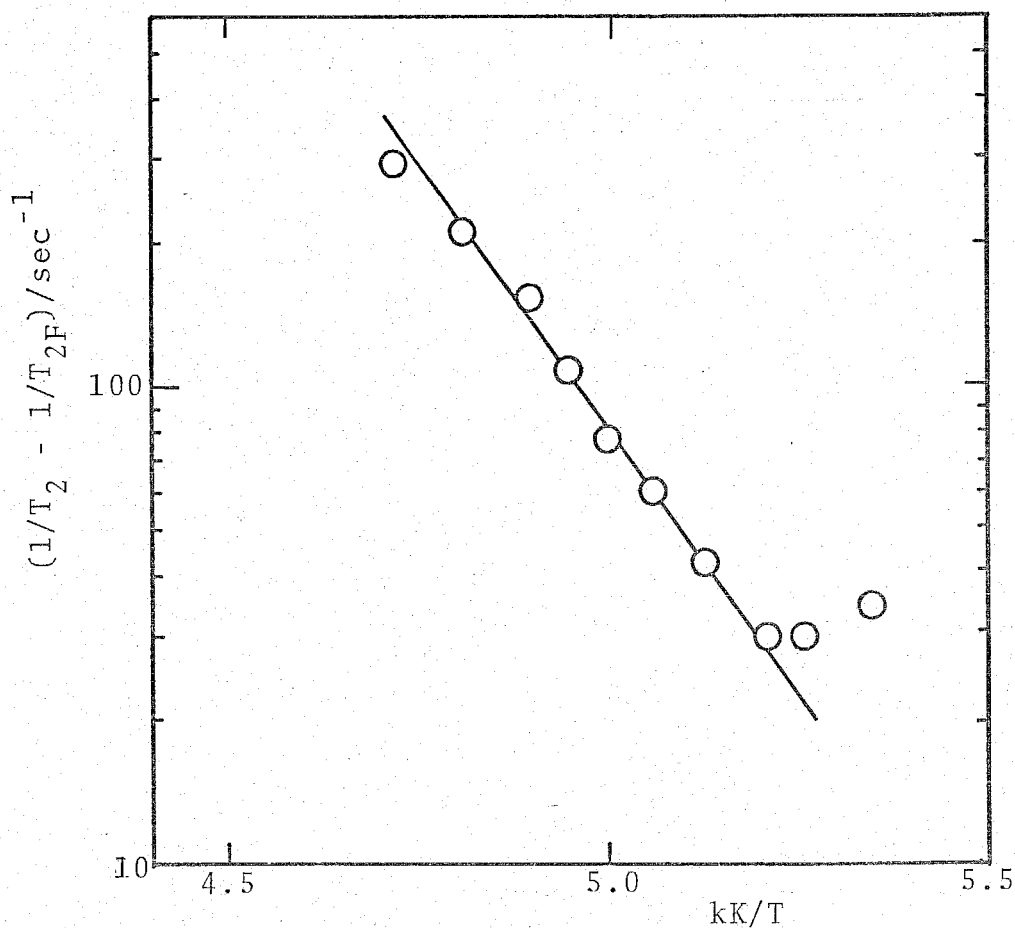
Fig. 3. A semilogarithmic plot of $(1/T_2 - 1/T_{2F})$ against the reciprocal temperature for the excahange of water in uranyl aqua complex. $[UO_2^{2+}] = 0.139$ M, $[UO_2^{2+}]$: $[H^+]$: $[H_2O]$: $[CD_3COCD_3] = 1 : 0.15 : 13.0 : 93.6$.
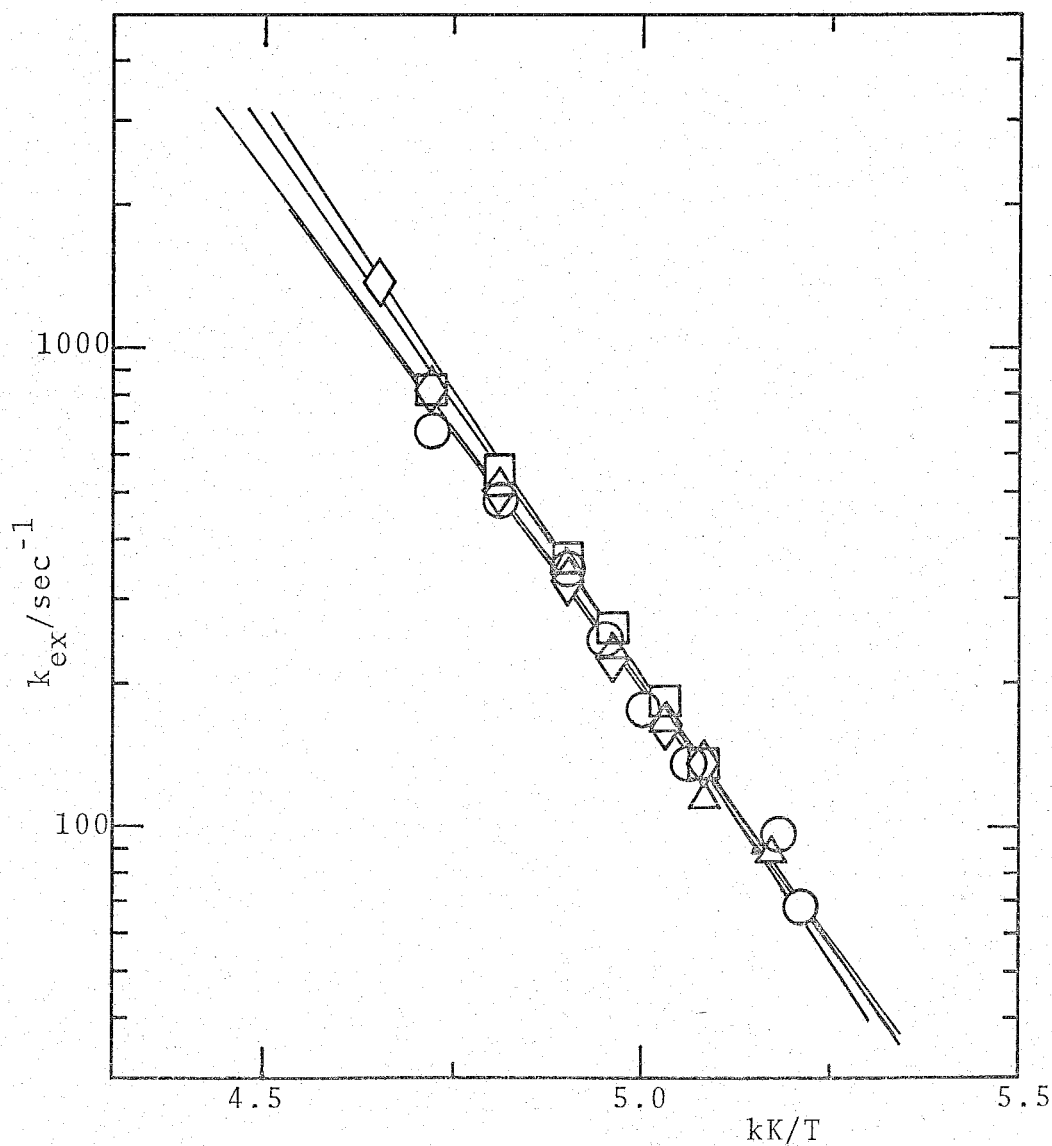
Fig. 4. Semilogarithmic plots of k_{ex} against the reciprocal temperature for the exchange of water in uranyl aqua complex. The symbols of $\bigcirc$, $\triangle$, $\square$, and $\diamondsuit$ correspond to (i), (ii), (iii), and (iv) in Table 1.

Table 1. Solution compositions and kinetic parameters for the exchange of H_2O in $UO_2(H_2O)_4^{2+}$

Solution	$[UO_2^{2+}]$ M	$[H_2O]$ M	$[CD_3COCD_3]$ M	CN^a	$\Delta H^{\ddagger}$ kJ mol^{-1}	$\Delta S^{\ddagger}$ JK^{-1}mol^{-1}	$k_{ex}(-69°C)$ 10^2 sec^{-1}
i	0.139	1.80	13.0	4.1 ± 0.2	39.9 ± 1.3	0.8 ± 7.6	3.41 ± 0.03
ii	0.140	2.42	12.8	3.9 ± 0.3	44.1 ± 2.5	22.7 ± 13.4	3.51 ± 0.11
iii	0.140	2.92	12.8	4.1 ± 0.1	42.0 ± 0.8	12.2 ± 3.8	3.57 ± 0.01
iv	0.140	3.50	12.5	4.2 ± 0.3	39.5 ± 1.7	-0.8 ± 9.7	3.27 ± 0.00

a CN = number of H_2O molecues bound per UO_2^{2+}.

Table 2. Linewidths and rate constants for the exchange of H_2O at various temperatures in uranyl aqua complex

Temp. °C	Line-width[a] Hz	Line-width[b] Hz	$1/T_2 - 1/T_{2F}$ $10 \ sec^{-1}$	k_{ex} $10^2 \ sec^{-1}$
-61.0	94.6 ± 0.0	1.16	29.4 ± 0.0	6.61 ± 0.00
-65.0	68.7 ± 4.1	1.69	21.1 ± 1.3	4.74 ± 0.29
-69.0	50.1 ± 0.4	1.91	15.1 ± 0.1	3.41 ± 0.03
-71.0	36.3 ± 0.6	2.07	10.8 ± 0.2	2.42 ± 0.04
-73.0	26.8 ± 0.2	2.26	7.71 ± 0.07	1.74 ± 0.01
-75.5	21.6 ± 0.3	2.55	5.99 ± 0.10	1.35 ± 0.02
-78.0	16.5 ± 0.0	2.99	4.25 ± 0.00	0.96 ± 0.00
-81.0	13.5 ± 0.0	3.98	2.99 ± 0.00	0.67 ± 0.00
-83.0	14.6 ± 0.2	5.03	3.00 ± 0.05	c
-86.0	17.4 ± 0.3	6.58	3.40 ± 0.00	c

[a] The full linewidth($\Delta \nu$) at a half height of the water proton signal in the presence of uranyl ion. $1/T_2 = \pi \Delta \nu$

[b] The full linewidth($\Delta \nu_F$) at a half height of the water proton signal in the absence of uranyl ion. $1/T_{2F} = \pi \Delta \nu_F$.

[c] The linewidth is independent of the chemical exchange in this region.

$[UO_2^{2+}] = 0.139$ M and $[UO_2^{2+}]$: $[H_2O]$: $[CD_3COCD_3] = 1 : 13.0 : 93.6$

$$1/T_2 - 1/T_{2F} = 1/\tau_F = P_c/(P_F\tau_c) \tag{1}$$

$$k_{ex} = 1/\tau_c = (kT/h) \exp(-\Delta H^{\ddagger}/RT)\exp(\Delta S^{\ddagger}/R)$$

$$= rate/4[UO_2(H_2O)_4^{2+}] \tag{2}$$

The observed exchage rate constants, k_{ex}, are shown in Table 2. The NMR measurements were made in solutions with various water concentrations listed in Table 1. The logarithms of the observed k_{ex} values are plotted against the reciprocal temperature in Fig. 4. The activation parameters obtained from the plots are listed in Table 1. It is found that k_{ex} is independent of the bulk water concentration.

C. Exchange Reactions of Water Molecules in Various Uranyl Aqua Complexes

In order to gain a better understanding of the water exchange process, additional experiments were carried out using other substituting species including DMSO molecule, chloride and bromide ion. In the case of the DMSO experiments, the mole ratio of UO_2^{2+} to DMSO to H_2O was 1 : 1 : 12. Under these conditions the main species is considered to be $[UO_2(H_2O)_3DMSO^{2+}]$ [11], which has also confirmrd by our measurements of the area of the NMR signals of both the coordinated(C_{H_2O}) and the bulk water(F_{H_2O}) as shown in Fig. 5. In the chloro and bromo complexes, the mole ratios of UO_2^{2+} to Cl^- to H_2O and of UO_2^{2+} to Br^- to H_2O were 1 : 1 : 30 and 1 : 1 : 18, respectively. Figures 6 and 7 show the spectra of solutions containing UO_2^{2+}, HCl, H_2O and CH_3COCH_3, UO_2^{2+}, HBr, H_2O and CH_3COCH_3 at

$$[UO_2^{2+}] = 0.150 \text{ M}$$

$$[UO_2^{2+}] : [DMSO] : [H_2O] : [CH_3COCH_3]$$

$$= 1 : 1.0 : 12.0 : 84.6$$
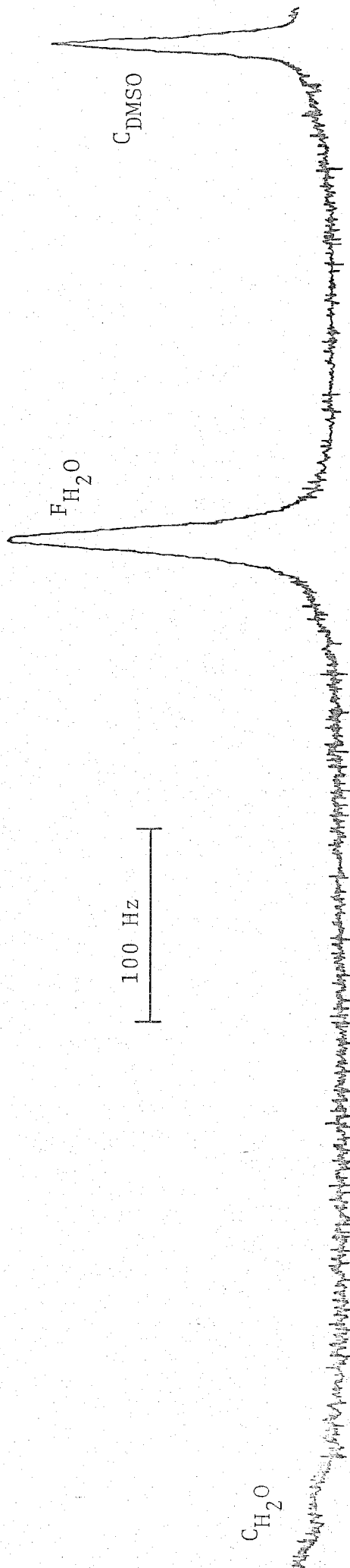
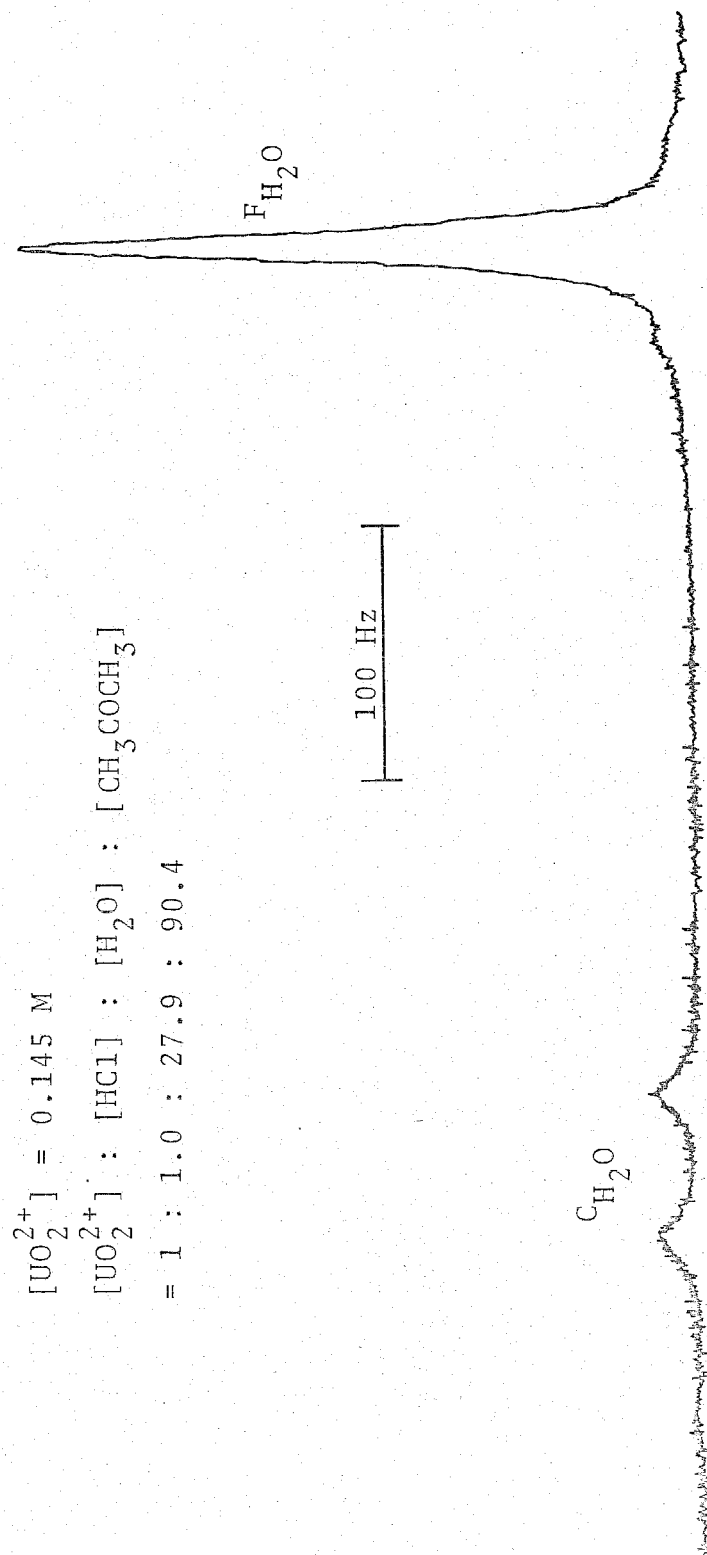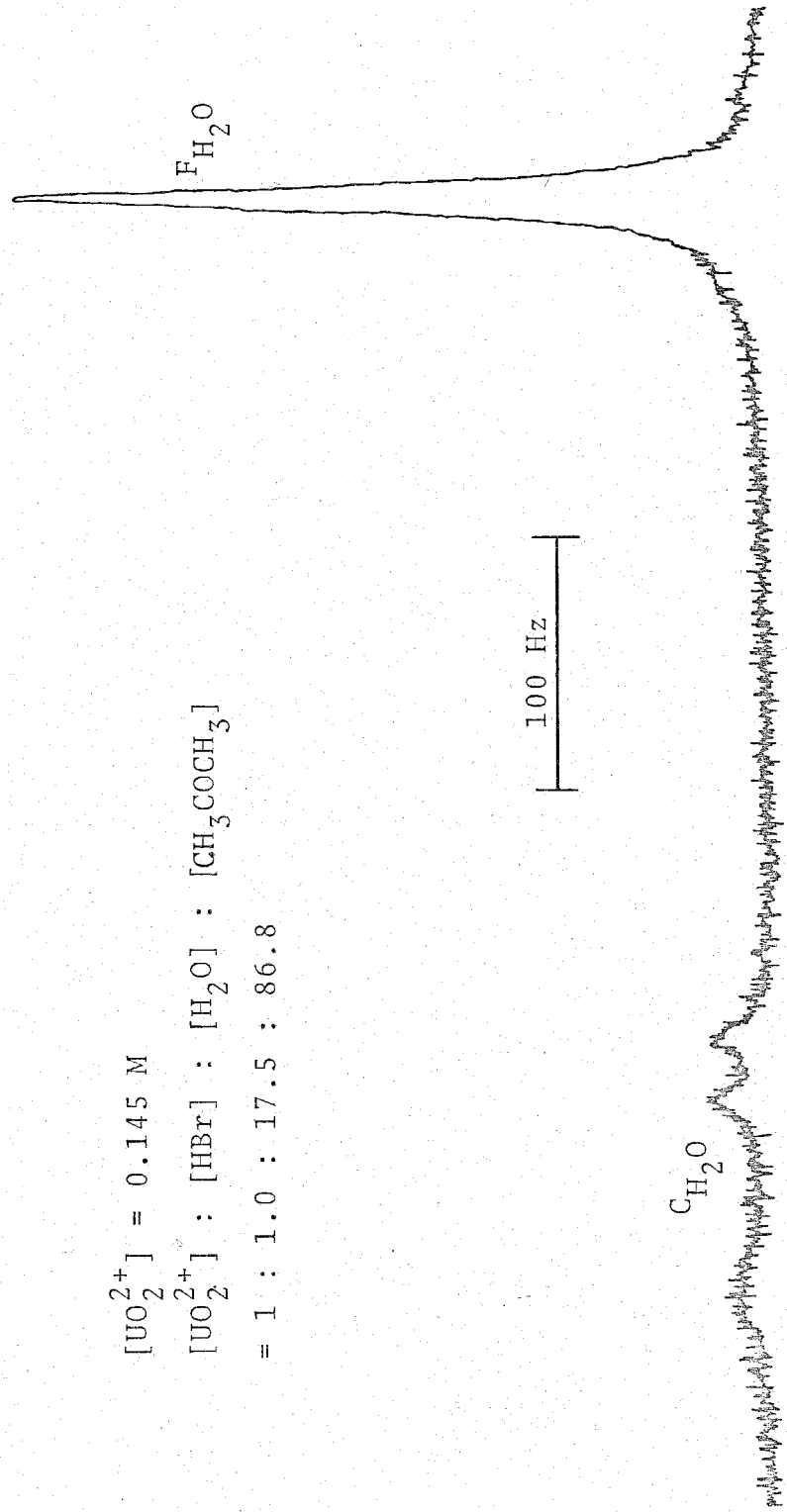Fig. 5. The ^1H NMR spectrum of a solution consisting of $UO_2(ClO_4)_2$, DMSO, H_2O, and CH_3COCH_3 at -90 °C.

46

$[UO_2^{2+}] = 0.145$ M

$[UO_2^{2+}] : [HCl] : [H_2O] : [CH_3COCH_3]$

$= 1 : 1.0 : 27.9 : 90.4$

Fig. 6. The ^1H NMR spectrum of solution consisting of $UO_2(ClO_4)_2$, HCl, H_2O and CH_3COCH_3 at -90 °C.

48

$[UO_2^{2+}] = 0.145$ M

$[UO_2^{2+}] : [HBr] : [H_2O] : [CH_3COCH_3]$

$= 1 : 1.0 : 17.5 : 86.8$

F_{H_2O}

C_{H_2O}

100 Hz

Fig. 7. The ^{1}H NMR specrtum of solution consisting of $UO_2(ClO_4)_2$, HBr, H_2O and

GH_3COCH_3 at -90 °C.
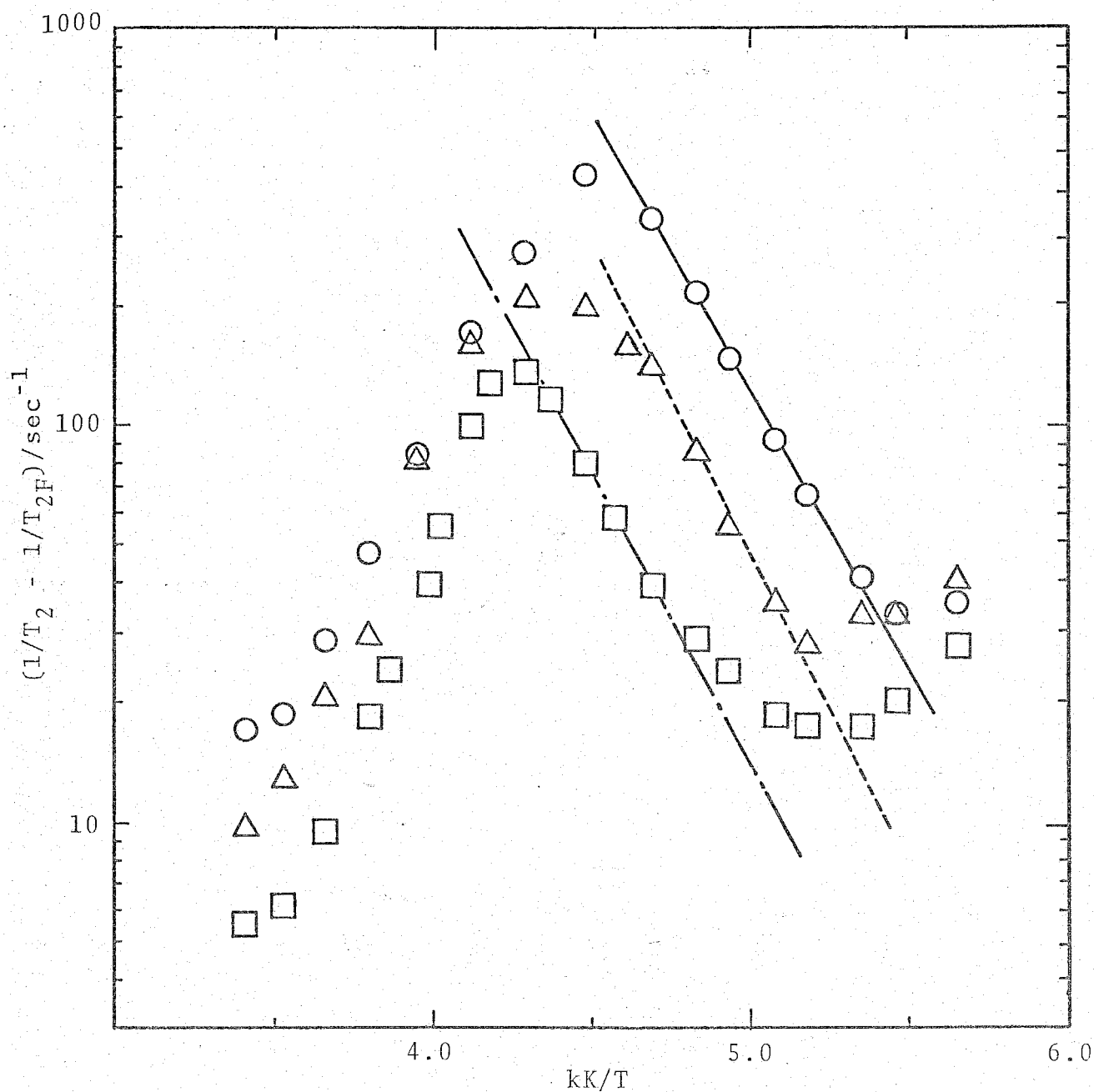
g. 8. A semilogarithmic plot of $(1/T_2 - 1/T_{2F})$ against the reciprocal temperature for the exchange of water in uranyl mono DMSO, mono chloro, and mono bromo complexes: ◯, $[UO_2^{2+}] = 0.150$ M, $[UO_2^{2+}]$: [DMSO] : $[H^+]$: $[H_2O]$: $[CH_3COCH_3] = 1 : 1.0 : 12.0 :$ 84.6; ▢, $[UO_2^{2+}] = 0.145$ M, $[UO_2^{2+}]$: [HCl] : $[H_2O]$: $[CH_3COCH_3]$ = 1 : 1.0 : 27.9 : 90.4; △, $[UO_2^{2+}] = 0.145$ M, $[UO_2^{2+}]$: [HBr] :

Table 3. Kinetic parameters for the exchange of H_2O in various uranyl complexes

Complex	$\Delta H^{\ddagger}$ $kJ\ mol^{-1}$	$\Delta S^{\ddagger}$ $JK^{-1}mol^{-1}$	$k_{ex}(-70°C)$ $10^2\ sec^{-1}$	$k_{ex}(25°C)^b$ $10^4\ sec^{-1}$
$UO_2(H_2O)_4^{2+}$	41.6 ± 2.1	8.8 ± 10.9	2.99 ± 0.19^a	98.0
$UO_2(H_2O)_3DMSO^{2+}$	24.8 ± 0.4	-68.0 ± 2.5	4.55 ± 0.02	8.42
$UO_2(H_2O)_3Cl^{+}$	25.6 ± 0.0	-73.9 ± 0.8	1.63 ± 0.17^a	2.97
$UO_2(H_2O)_3Br^{+}$	28.1 ± 1.7	-56.7 ± 7.6	2.65 ± 0.00	8.49

a Calculated values from $\Delta H^{\ddagger}$ and $\Delta S^{\ddagger}$ at -70°C. b Calculated values from $\Delta H^{\ddagger}$ and $\Delta S^{\ddagger}$ at 25°C.

-90 °C, respectively. Although there is some uncertainty in the measurement of the NMR signal areas for these complexes, it seems most probable that under the conditions reported here, the main species are the monochloro and monobromo complexes, in these systems

In the same way as for the aqua complex, the logarithms of $(1/T_2 - 1/T_{2F})$ values were plotted against the reciprocal temperature for these complexes as shown in Fig. 8. It can be seen that the region where the relaxation process is controlled by only chemical exchange is very similar to that obtained for the aqua complex. The rate constants which were obtained by the same way as for the water exchange in the aqua complexes, and the resulting activation parameters are shown in Table 3.

D. Mechanism

The rate constants of the water exchange reaction in the uranyl aqua complex are independent of the bulk water concentrations. This fact suggests that the water exchange in uranyl aqua complex proceeds through either the dissociative(D) or the dissociative interchange(I_d) mechanism[14].

The D mechanism is represented by Eq. (3)

$$UO_2(H_2O)_4^{2+} + H_2O^* \xrightarrow[slow]{k_d} UO_2(H_2O)_3^{2+} + H_2O + H_2O^*$$

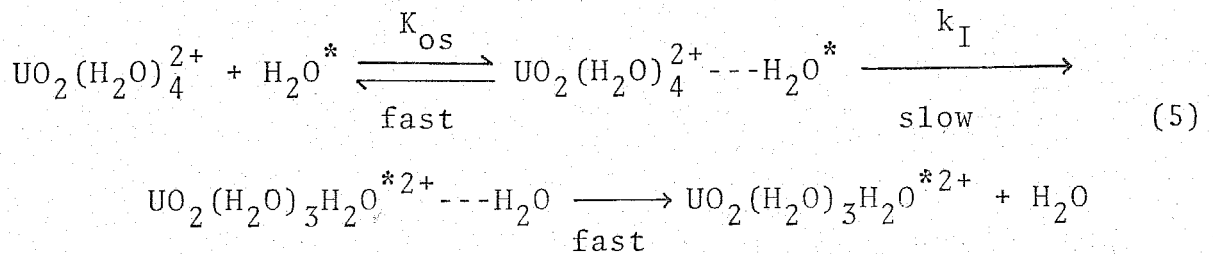$$\xrightarrow{fast} UO_2(H_2O)_3 H_2O^{*2+} + H_2O \tag{3}$$
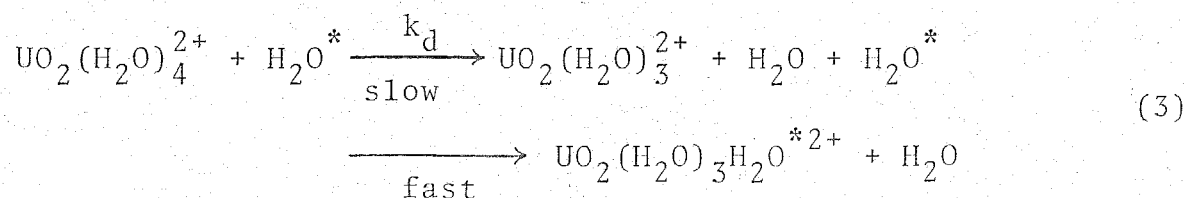
where the asterisk is a typographical distinction only. In this mechanism, the rate-determining step is the dissociation of water

from the first coordination sphere leading to the formation of a trigonal-bipyramidal intermediate. The first-order rate constant, k_{ex}, is given by Eq. (4).

$$k_{ex} = k_d \tag{4}$$

In the I_d mechanism the rate-determining step is also primarily governed by the dissociation of the coordinated water molecule. The reaction scheme is shown by Eq. (5).

$$UO_2(H_2O)_4^{2+} + H_2O^* \underset{fast}{\overset{K_{os}}{\rightleftharpoons}} UO_2(H_2O)_4^{2+}---H_2O^* \overset{k_I}{\underset{slow}{\longrightarrow}} \tag{5}$$

$$UO_2(H_2O)_3H_2O^{*2+}---H_2O \underset{fast}{\longrightarrow} UO_2(H_2O)_3H_2O^{*2+} + H_2O$$

where the exchange of H_2O occurs within an outer-sphere complex $UO_2(H_2O)_4^{2+}---H_2O^*$ in which the entering H_2O^* is in the second coordination sphere immediately adjacent to $UO_2(H_2O)_4^{2+}$ and k_I is the corresponding rate constnat, and $K_{os} = [UO_2(H_2O)_4^{2+}---H_2O^*]/([UO_2(H_2O)_4^{2+}][H_2O])$.

From this mechanism, k_{ex} is expressed by Eq. (6).

$$k_{ex} = k_I K_{os}[H_2O]/(1 + K_{os}[H_2O]) \tag{6}$$

which simplifies to $k_{ex} = k_I$ when $K_{os}[H_2O] \gg 1$, i.e. the exchange rate becomes independent of bulk water concentrations as observed in this experiment. Both D and I_d mechanisms can explain the results of the water exchange reaction in the uranyl aqua ion. However, the D mechanism seems to be unlikely because the axial

oxygen atoms in the uranyl ion are extremely inert and hence are unaffected during the water exchange reaction. The structure of the intermediate in the D mechanism is most probably a trigonal-bipyramidal species and the D_{3h} symmetry of this structure is unfavorable with respect to bond formation between the uranyl d- or f-orbitals and the sigma orbitals of the equatorial ligands. Thus, the trigonal-bipyramidal uranyl intermediate is not likely.

As mentioned above, the rate constant of the water exchange reaction is independent of the water concentration. If the condition, $K_{os}[H_2O] \gg 1$, is satisfied, the I_d mechanism would appear to be reasonable. This condition can be fulfilled in these solutions because the mole ratios of UO_2^{2+} to H_2O to CD_3COCD_3 are in the range from 1 : 13 : 94 to 1 : 25 : 89 and the basicity of H_2O is thought to be larger than that of CD_3COCD_3 on the basis of the Gutmann's donor number(DN)[8,9] and hence the second coordination sphere of the uranyl ion should be saturated with water. Therefore, it may be more plausible that the water exchange in uranyl aqua ion proceeds through the I_d mechanism.

This mechanism explains the observation that the value of $\Delta H^{\ddagger}$ for the aqua complex is considerably larger than those for the DMSO, chloro-, and bromo-complexes. Since strong basic ligands such as DMSO or the negatively charged ligands, e.g. Cl^- and Br^- in the coordination sphere may serve to weaken the bonds between the uranyl ion and the coordinated water molecules, the values of $\Delta H^{\ddagger}$ could be reduced for the mono-substituted complexes.

This mechanism can also explain the large negative values of $\Delta S^{\ddagger}$ observed in the mono-substituted complexes. For these

complexes, the water molecules entering the inner sphere will be hindered by the relatively strong inner sphere ligands as compared with water and, therefore, the probability of the intermediate complex formation will be reduced. As a result, the exchange rate for the mono-substituted complexes becomes slower than that for the aqua complex at room temperature in spite of the smaller values of $\Delta H^{\ddagger}$.

Ekstrom and Johnson[3] studied the kinetics of the reaction between the uranyl ion and 4-(2-pyridylazo)resocinol(PAR). The activation enthalpy of this reaction was 34.2 kJ mol^{-1}. Although this value is slightly smaller than that reported here for the water exchange process of the uranyl aqua complex, the activation energy for ligand substitution appeares to correspond to the energy of bond rupture between the uranyl ion and the water molecules. It is of interest to note that they estimated the rate constant for the water exchange process to be greater than 10^5 M^{-1} sec^{-1} at room temperature. And also Hynes and Regan[15] studied the kinetics of the reaction between the uranyl ion and thenoyltri-fluoroacetone and obtained almost the same value as that of Ekstrom and Johnson. These values are in very good agreement with the experimental results reported here.

2. KINETIC STUDY OF THE EXCHANGE OF DIMETHYL SULFOXIDE
   IN URANYL PENTAKIS(DIMETHYL SULFOXIDE) ION BY NMR

A. Structure of $[UO_2(DMSO)_5](ClO_4)_2$ in CD_3COCD_3

Figure 9 shows the ^1H NMR spectra of the solution containing $[UO_2(DMSO)_5](ClO_4)_2$, DMSO and CD_3COCD_3 at -49 °C. In comparison with the spectrum of pure DMSO, the signals of (a) and (b) were assigned to the methyl protons of coordinated and free DMSO, respectively. The number of coordinated DMSO molecules was deter-mined by area integrations of the coordinated and free DMSO signals and the results are listed in Table 4.

The absence of any significant variation of the number of coordinated DMSO molecules over these concentration ranges in Table 4 indicates that neither CD_3COCD_3 nor perchlorate ion enters into the first coordination sphere of uranyl ion, and the absence of any splitting of the coordinated DMSO signal indicates that the five coordinated DMSO molecules occupy the equivalent equa-torial positions of the uranyl ion. This result is different from that of Fratiello et al.[11], in which the coordination number was determined to be four. However, uranyl ion seems unlikely to be fully coordinated by DMSO under their experimental conditions, in which DMSO was added to $UO_2(ClO_4)_2$ in acetone-water mixed solvents. It is well known that $UO_2L_5^{2+}$ (L = ligand) has a pentagonal bipyra-midal structure in the solid state or in CD_2Cl_2[4-7,10]. Therefore, it can be assumed that $UO_2(DMSO)_5^{2+}$ ion has a similar structure in CD_3COCD_3.
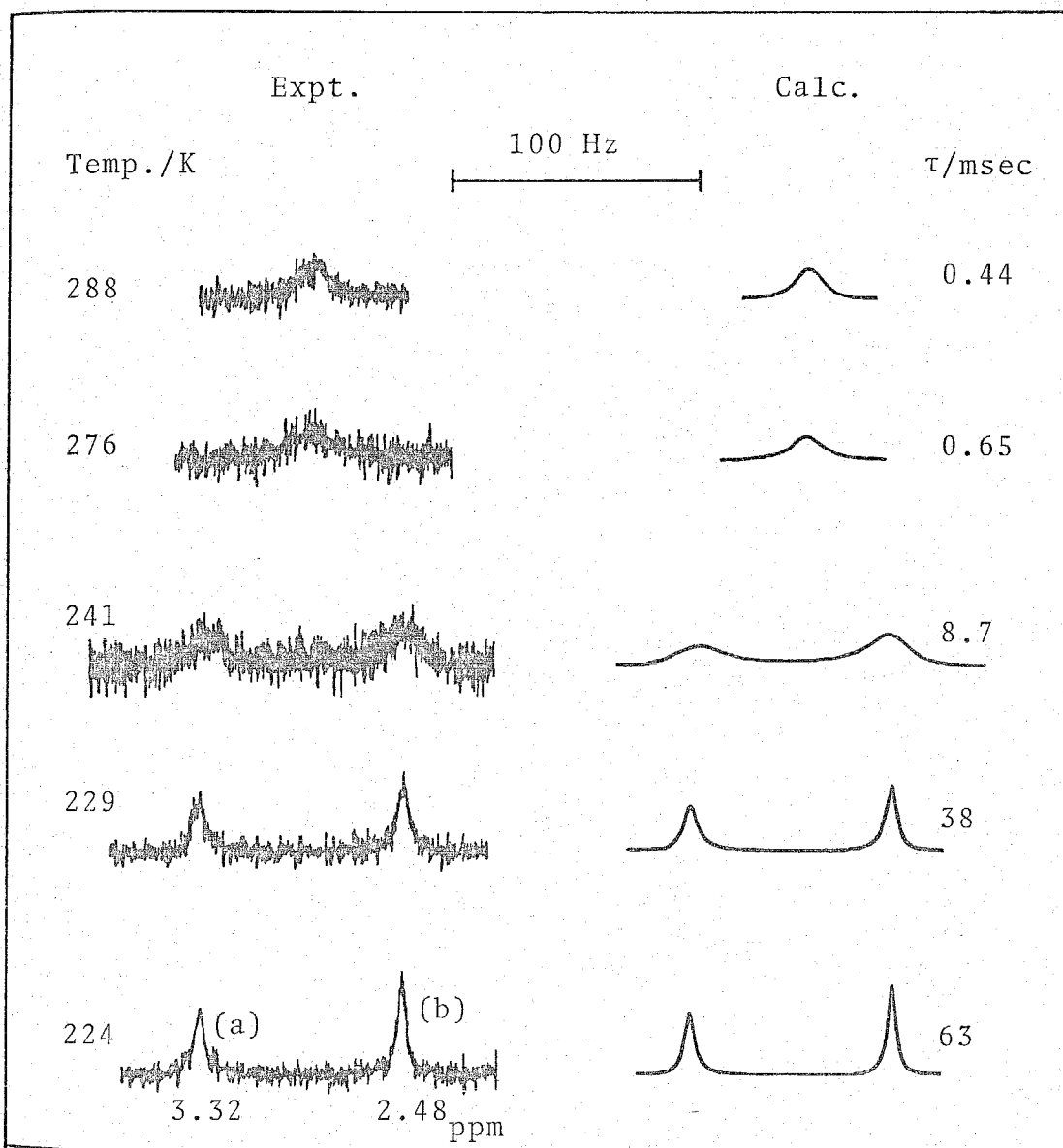
Fig. 9. Experimental (left-hand side) and best-fit calculated
^{1}H NMR lineshapes of a solution consisting of $UO_2(DMSO)_5^{2+}$
(0.0112 M), DMSO(0.0730 M), and CD_3COCD_3(13.5 M)
Temperatures and best-fit τ-values are shown at left- and right-
hand sides of the figure, respectively. The signals of (a)
and (b) correspond to the methyl protons of coordinated and
free DMSO, respectively.

Table 4. Solution compositions and coordination numbers for the exchange of DMSO in $UO_2(DMSO)_5^{2+}$.

Solution	$[UO_2(DMSO)_5^{2+}]^a$ 10^{-2} M	$[DMSO]^b$ M	$[CD_3COCD_3]$ M	CN^c
i	1.11	0.0730	13.5	5.1 ± 0.2
ii	1.08	0.105	13.4	5.0 ± 0.1
iii	1.01	0.123	13.4	5.1 ± 0.0
iv	1.14	0.215	13.2	5.1 ± 0.1
v	1.16	0.381	13.1	5.2 ± 0.3

[a] Added as $[UO_2(DMSO)_5](ClO_4)_2$. [b] Added as DMSO. [c] CN = number of DMSO molecules bound per UO_2^{2+}.

B. Exchange Reaction of DMSO in $UO_2(DMSO)_5^{2+}$ Ion in CD_3COCD_3

The change in the lineshape of methyl proton signals of the coordinated and free DMSO with temperature is shown at the left side of Fig. 9. As is seen from Fig. 9 it is found that a coalescence of the coordinated and free DMSO signals occurs with the rise of temperature. This phenomenon indicates that the DMSO exchange occurs between the coordinated and free sites. Therefore, we determined the best-fit τ-values at each temperature by the method described in Chapter II. The obtained τ-values are shown on the right side of Fig. 9. The first-order exchange rate constant, k_{ex}, which is represented by Eq. (7), was calculated by using Eq. (21) in Chapter II.

$$k_{ex} = rate/5[UO_2(DMSO)_5^{2+}]$$

$$= (kT/h)\exp(-\Delta H^{\ddagger}/RT)\exp(\Delta S^{\ddagger}/R) \qquad (7)$$

The same measurements were carried out for the solutions with different compositions listed in Table 4. The semilogarithmic plots of k_{ex} against the reciprocal temperature are shown in Fig. 10 and it is apparent that k_{ex} depends on the DMSO concentration. The plots of k_{ex} vs. [DMSO] give the straight lines as shown in Fig. 11 and k_{ex} can be expressed by Eq. (8)

$$k_{ex} = k_1 + k_2[DMSO] \qquad (8)$$

The values of k_1 and k_2 are obtained from the intercepts and the slopes in Fig. 11, respectively, and the results are listed
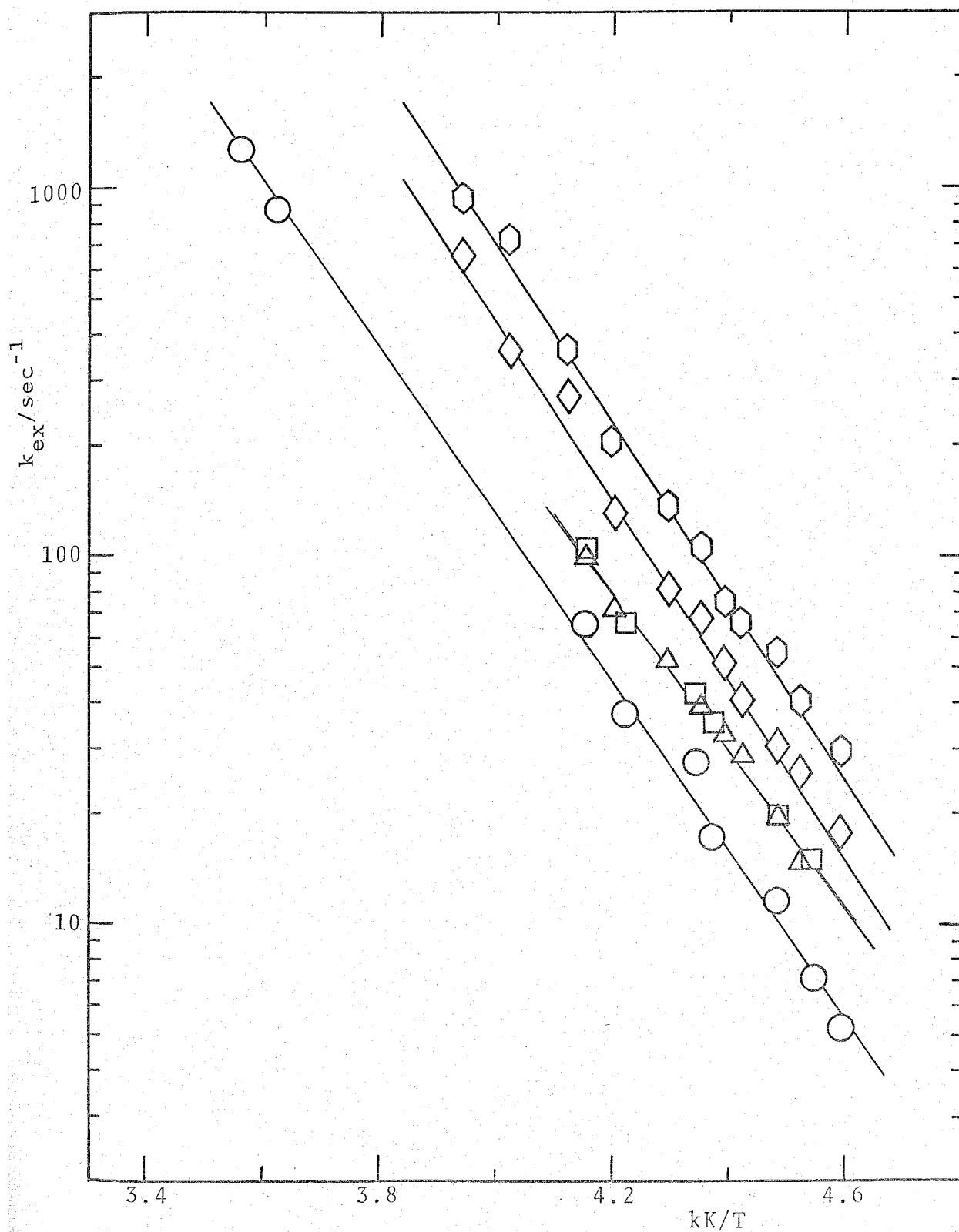
Fig. 10. Semilogarithmic plots of k_{ex} against the reciprocal temperature for the exchange of DMSO in $UO_2(DMSO)_5^{2+}$. The symbols of ◯, △, ▢, ◇, and ⬡ correspond to (i), (ii), (iii), (iv), and (v) in Table 4.
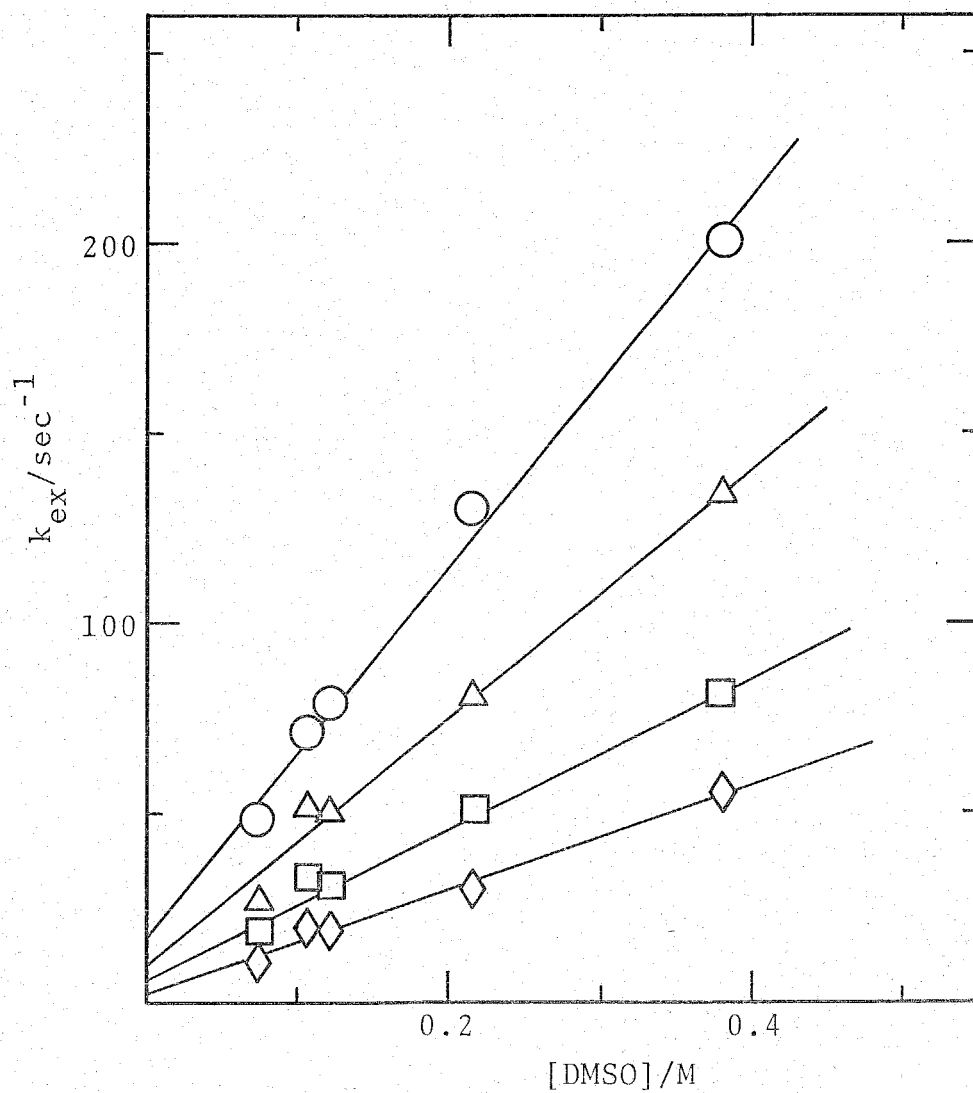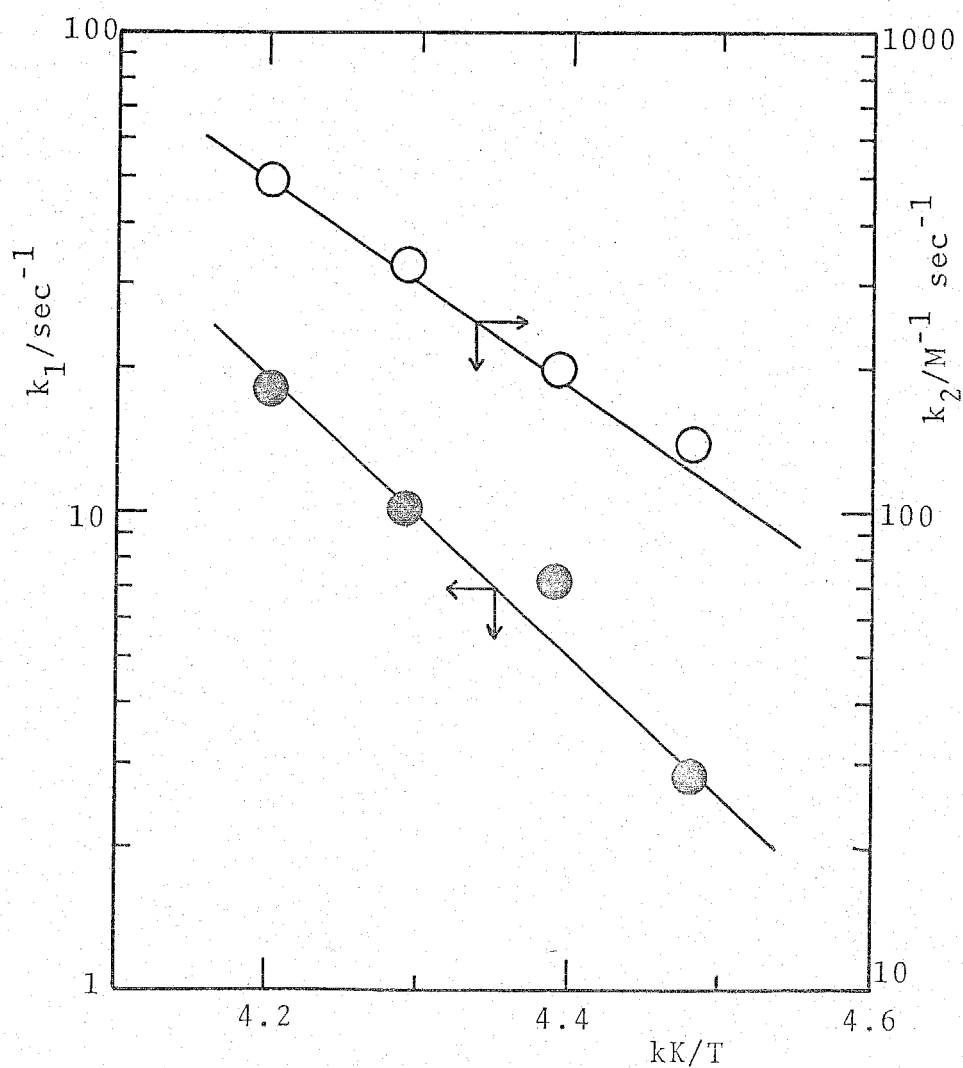
Fig. 11. Plots of k_{ex} vs. [DMSO] for the exchange of DMSO in $UO_2(DMSO)_5^{2+}$. $\bigcirc$: -35 °C; $\triangle$: -40 °C; $\square$: -45 °C; $\diamondsuit$: -50 °C.

Fig. 12. Semilogarithmic plots of k_1 and k_2 against the reciprocal temperature for the exchange of DMSO in $UO_2(DMSO)_5^{2+}$.

in Table 5. The semilogarithmic plots of k_1 and k_2 against the reciprocal temperature in Fig. 12 yield the activation parameters for k_1 and k_2 paths and the results are tabulated in Table 6.

Table 5. The values of k_1 and k_2 at various temperatures for the exchange of DMSO in $UO_2(DMSO)_5^{2+}$

Temp. °C	k_1 sec^{-1}	k_2 $10^2 \ M^{-1}sec^{-1}$
-35	18.0 ± 4.7	4.88 ± 0.22
-40	10.2 ± 4.8	3.27 ± 0.23
-45	7.06 ± 3.82	1.97 ± 0.18
-50	2.79 ± 1.60	1.38 ± 0.08

Table 6. Kinetic parameters of k_1 and k_2 paths for the exchange of DMSO in $UO_2(DMSO)_5^{2+}$

	$\Delta H^{\ddagger}$ $kJ \ mol^{-1}$	$\Delta S^{\ddagger}$ $JK^{-1}mol^{-1}$	$k(25 \ °C)^*$ $10^3 \ sec^{-1}$
k_1 path	53.8 ± 2.4	6.3 ± 14.5	5.53
k_2 path	39.1 ± 1.7	-28.1 ± 5.0	32.2 /M^{-1}

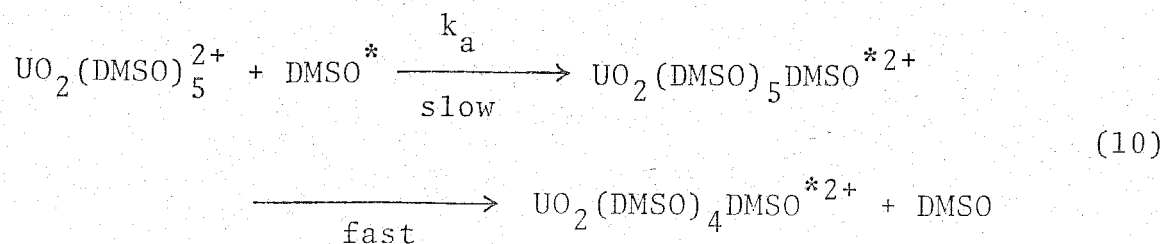* Calculated values from $\Delta H^{\ddagger}$ and $\Delta S^{\ddagger}$ at 25 °C.

C. Mechanism

It is found that the exchange reaction of DMSO in $UO_2(DMSO)_5^{2+}$ proceeds through two paths, that is k_1 and k_2 paths. The k_1 path, where the exchange rate is independent of the free DMSO concentrations, seems to be consistent with the D mechanism. On the other hand, the k_2 path exhibits a first-order dependence on the free DMSO concentration and seems to proceed through the I_d or associative(A) mechanism[14].
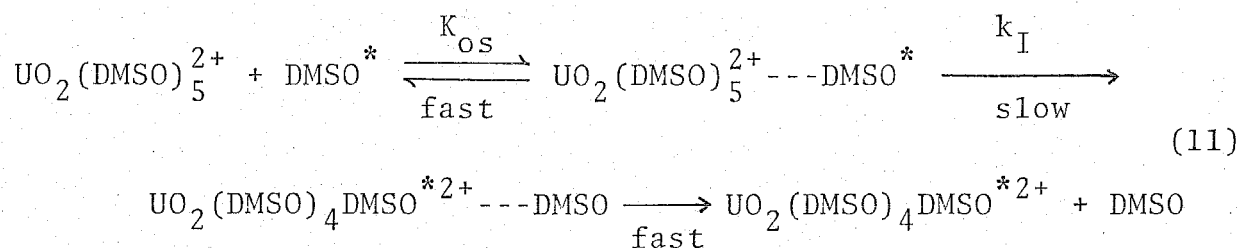
The D mechanism is expressed by Eq. (9)

$$UO_2(DMSO)_5^{2+} + DMSO^* \xrightarrow[slow]{k_d} UO_2(DMSO)_4^{2+} + DMSO + DMSO^*$$

$$\xrightarrow[fast]{} UO_2(DMSO)_4 DMSO^{*2+} + DMSO \tag{9}$$
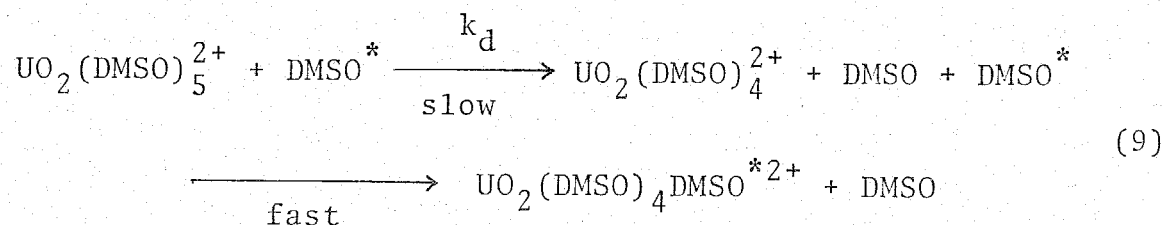
In this mechanism, the rate-determining step is the dissociation of DMSO from the first coordination sphere of uranyl ion and hence a four-coordinated intermediate in the equatorial plane is formed.

The A mechanism is represented by Eq. (10)

$$UO_2(DMSO)_5^{2+} + DMSO^* \xrightarrow[slow]{k_a} UO_2(DMSO)_5 DMSO^{*2+}$$

$$\xrightarrow[fast]{} UO_2(DMSO)_4 DMSO^{*2+} + DMSO \tag{10}$$

The rate-determining step is the coordination of DMSO to $UO_2(DMSO)_5^{2+}$ ion leading to the formation of a six-coordinated intermediate in the equatorial plane.

Another mechanism, I_d is given by Eq. (11)

$$UO_2(DMSO)_5^{2+} + DMSO^* \; \underset{fast}{\overset{K_{os}}{\rightleftharpoons}} \; UO_2(DMSO)_5^{2+}\text{---}DMSO^* \; \xrightarrow[slow]{k_I}$$

(11)

$$UO_2(DMSO)_4DMSO^{*2+}\text{---}DMSO \; \xrightarrow{fast} \; UO_2(DMSO)_4DMSO^{*2+} + DMSO$$

where $K_{os} = [UO_2(DMSO)_5^{2+}\text{---}DMSO]/([UO_2(DMSO)_5^{2+}][DMSO])$. As was described previously, the bond breaking between UO_2^{2+} and DMSO in the first coordination sphere mainly contributes to the activation energy. The DMSO exchange occurs within an outer-sphere complex and k_I is the corresponding rate constant.

If the k_1 and k_2 paths proceed through the D and A mechanisms, respectively, k_{ex} is given by Eq. (12) from Eqs. (9) and (10)

$$k_{ex} = k_d + k_a[DMSO]$$

(12)

where k_d and k_a correspond to k_1 and k_2 in Eq. (8), respectively. On the other hand, if the k_1 and k_2 paths occur through the D and I_d mechanism, the following equation is derived from Eqs. (9) and (11)

$$k_{ex} = (k_d + k_I K_{os}[DMSO])/(1 + K_{os}[DMSO])$$

(13)

When $K_{os}[DMSO] \ll 1$, Eq. (13) is simplified to

$$k_{ex} = k_d + k_I K_{os}[DMSO]$$

(14)

where k_d and $k_I K_{os}$ correspond to k_1 and k_2 in Eq. (8), respectively.

Hence both Eqs. (12) and (14) are consistent with the experimental results.

In both mechanisms, the D mechanism should have a four-coordinated intermediate in the equatorial plane. The formation of such a four-coordinated intermediate may be supported by the following fact, i.e. the existence of the four-coordinated uranyl complexes is well establised, e.g. $UO_2(H_2O)_4^{2+}$ in solution[11,12], $UO_2(HMPA)_4^{2+}$ (HMPA = hexamethylphosphoramide) in solution and solid state[16,17], and $UO_2Cl_2(pph_3)_2$ (pph_3 = triphenylphosphine oxide) in solid state[18]. Therefore, it is reasonable to assume that the k_1 path proceeds through the D mechanism.

Next we deal in analogous way with the k_2 path which is assumed to proceed through the I_d or A mechanism. If the k_2 path occurs through the I_d mechanism, it is required that the value of K_{os} is much smaller than 1.0 M^{-1} to satisfy the condition $K_{os}[DMSO] \ll 1$. This value seems to be reasonable because DMSO molecules are uncharged. In the A mechanism which is another possibility for the k_2 path, a six-coordianted intermediate in the equatorial plane should be formed. It is likely that the UO_2^{2+} ion forms the six-coordianted intermediate with DMSO in the equatorial plane because it has been well known that the UO_2^{2+} ion forms six-coordianted complexes in the equatorial plane with small ligands, e.g. $UO_2(CH_3COO)_3^-$ and $UO_2(CO_3)_3^{4-}$[19]. It might be difficult to distinguish unequivocally whether the k_2 path occurs through the A or I_d mechanism from the present kinetic results.

It has been generally known that if the exchange reaction proceeds through the A mechanism, the exchange rate is subjected to some steric effect. We studied the exchange of DMSO in UO_2-$(acac)_2DMSO$ (acac = acetylacetonato) in CD_3COCD_3 as described in Chapter IV. In this exchange reaction, the exchange rate was independent of the free DMSO concentrations and the rate constant was smaller than that of the exchange of DMSO in $UO_2(DMSO)_5^{2+}$. These facts can be interpreted by considering that acac is a bulky chelating ligand and may hinder the approach of incoming DMSO to the first coordiantion sphere of UO_2^{2+}.

From these results the A mechanism is most likely for the k_2 path of the DMSO exchange in $UO_2(DMSO)_5^{2+}$.

Recently, Lincoln et al.[20] also reported the DMSO exchange in $UO_2(DMSO)_5^{2+}$ in CD_3COCD_3 and the mechanism to be the D or I_d because the exchange rate of DMSO was independent of the free DMSO concentrations, which is a different conclusion from the present results. They performed the experiments in very limited concentration ranges of DMSO and hence it is probable that they could not observe the dependence of the DMSO exchange rate on the free DMSO concentrations.

3. KINETIC STUDY OF THE EXCHANGE OF N,N-DIMETHYLFORMAMIDE
   IN URANYL PENTAXIS(N,N-DIMETHYLFORMAMIDE) ION BY NMR

A. Structure of $[UO_2(DMF)_5](ClO_4)_2$ in CD_2Cl_2

Figure 13 shows the ^1H spectrum of a solution containing $[UO_2(DMF)_5](ClO_4)_2$, DMF, and CD_2Cl_2 at -80 °C. In comparison with the spectrum of pure DMF, the signals (a) and (b) are assigned to the methyl protons of free and coordinated DMF, respectively. And also the signals (c) and (d) are attributed to the formyl protons of free and coordianted DMF, respectively. The number of coordianted DMF molecules was determined by area integrations of the methyl and formyl proton signals of free and coordinated DMF, respectively and the results are listed in Table 7.

The absence of any significant variation of the number of coordianted DMF molecules over the concentration range in Table 7 indicates that neither CD_2Cl_2 nor perchlorate ion enters into the first coordination sphere of uranyl ion. The signal of methyl protons of coordinated DMF should essentially be a doublet. However, the observed methyl proton signal of coordinated DMF is a singlet, while that of the free DMF is a doublet and the formyl proton signals of both free and coordinated DMF are singlets. This phenomenon has not been observed in other DMF complexes, e.g. $Al(DMF)_6^{3+}$, $Ga(DMF)_6^{3+}$, and $Be(DMF)_4^{2+}$ [21-23]. This may be due to the rotation on the C-N bond in coordinated DMF molecules, which is assumed to be too fast on the NMR time scale in this temperature range, or to the equalization of chemical shifts of both methyl groups of co-ordianted DMF molecules caused by the magnetic anisotropy of the uranyl
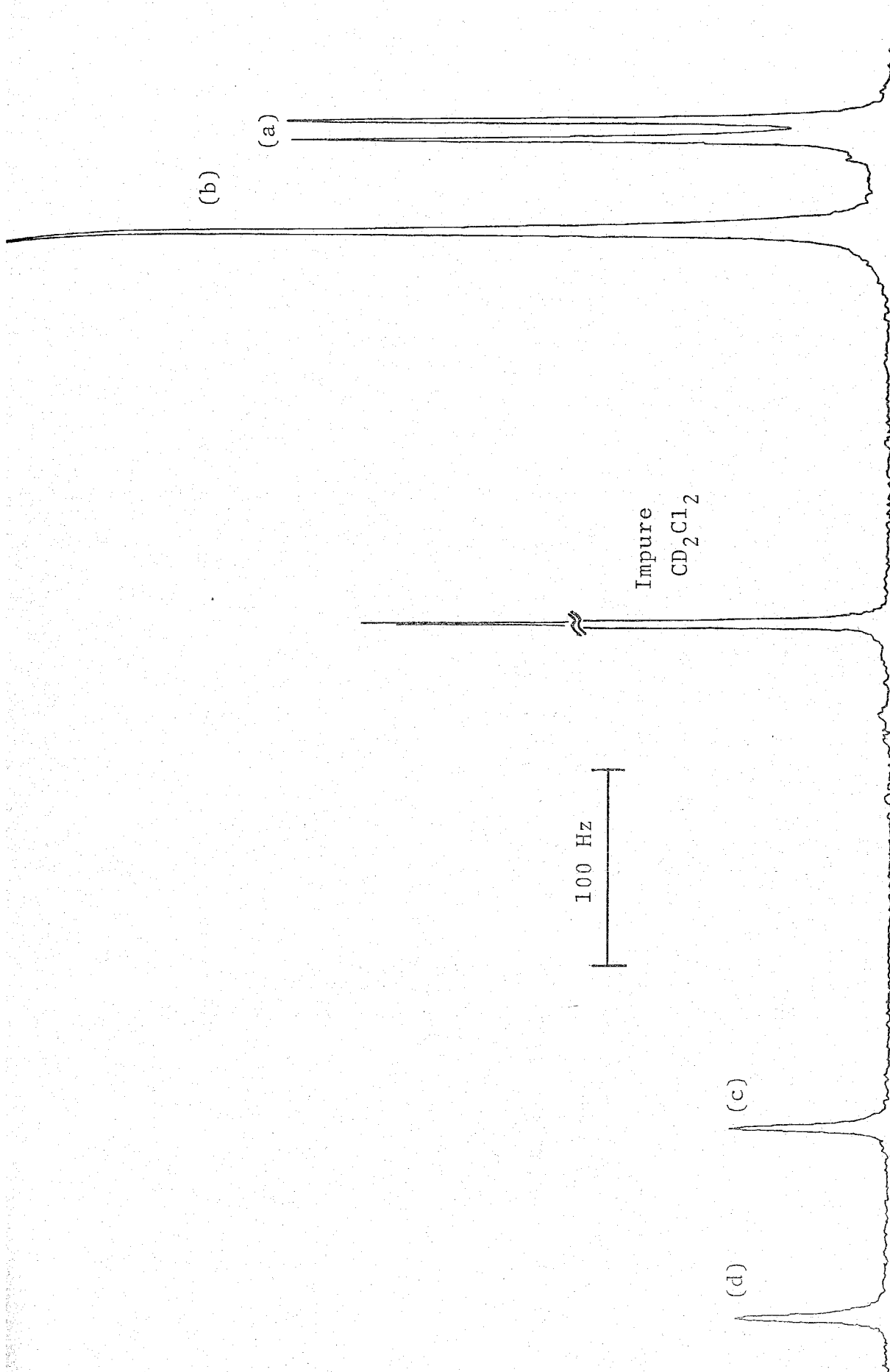
Fig. 13. The ^1H NMR spectrum of a solution consisting of $UO_2(DMF)_5^{2+}$ (0.00611 M), DMF(0.0304 M), and CD_2Cl_2(16.1 M) at -80 °C.

ion. The former is not likely because the IR spectrum of this complex in CD_2Cl_2 give the value of 1642 cm^{-1} for the C-O stretching of DMF, which is 33 cm^{-1} lower than that observed in pure DMF (1675 cm^{-1}). This fact suggests that the DMF molecules coordinate to uranyl ion through oxygen, since the C-O stretching, so called Amide I, is shifted to a lower side when DMF is coordinated through oxygen[24-26]. Such coordination tends to increase the double bond character of the C-N group, and hence makes more difficult the rotation along the C-N bond.

On the other hand, it is more likely that the magnetic anisotropy of the uranyl ion may introduce the degeneration of the doublet of the methyl groups of coordinated DMF. Pople et al.[27] gave the equation for the chemical shift($\Delta\delta$) caused by the anisotropic field

$$\Delta\delta = \Delta\chi_{atomic}(1 - 3\cos^2\gamma)/3R^3 \qquad (15)$$

where $\Delta\chi_{atomic} = \chi_{atomic}$(parallel to axis) - χ_{atomic}(perpendicular to axis), in which the axis is taken to be the O=U=O axis, R is the distance of the proton from the uranuim atom, and γ is the angle between a straight line connecting the proton and uranium atom and the O=U=O axis. The value of $\Delta\chi_{atomic}$ is obtained by Eisenstein et al.[28] to be -2.74 x 10^{-28}. From this equation, it is expected that the chemical shifts of both methyl groups of coordinated DMF become identical at the particular values of γ and R. In fact, Lincoln et al.[29] estimated the values of $\Delta\delta$ for both methyl groups of coordinated DMF by using Eq. (15) and found out that the calculated values were consistent with the experimental ones.

They insisted, hence, that the magnetic anisotropy is a contri-
buting factor to the equivalent chemical shift of the methyl
groups of bound DMF. Since the DMF methyl proton signal of
$UO_2(acac)_2DMF$ in CD_3COCD_3 and CD_2Cl_2 is a doublet as shown in
Figs. 18 and 19 in Chapter IV in spite of the coordination of DMF
in the same equatorial plane of uranyl ion, the values of γ and
R appeared to be possibly different from those mentioned above.

Furthermore, the absence of any splitting of the coordinated
DMF formyl proton signal indicates that the five molecules of
coordinated DMF have the equivalent equatorial positions of the
uranyl ion. These results confirm that $UO_2(DMF)_5^{2+}$ ion in CD_2Cl_2
has a pentagonal bipyramidal structure.

Table 7. Solution compositions and coordination numbers for
the exchange of DMF in $UO_2(DMF)_5^{2+}$

Solution	$[UO_2(DMF)_5^{2+}]$ [a] 10^{-3} M	$[DMF]$ [b] M	$[CD_2Cl_2]$ M	CN [c]
i	3.60	0.0123	16.2	5.2 ± 0.1
ii	6.11	0.0304	16.1	5.1 ± 0.3
iii	6.47	0.0739	16.1	5.1 ± 0.1
iv	5.75	0.130	15.2	4.8 ± 0.2
v	29.0	0.588	14.5	5.0 ± 0.1

[a] Added as $[UO_2(DMF)_5](ClO_4)_2$. [b] Added as DMF. [c] CN =
number of DMF molecules bound per UO_2^{2+} ion.

B.   Exchange Reaction of DMF in $UO_2(DMF)_5^{2+}$ Ion in CD_2Cl_2

A typical temperature dependence of lineshape for the coordinated and free DMF is shown at the left side of Fig. 14. This figure shows that the DMF exchange reaction occurs between the coordinated and free DMF. The best-fit τ-values were determined by the same method described in Chapter II and are shown on right side of Fig. 14 together with the corresponding lineshapes. From these τ-values, the first-order rate constants, k_{ex}, were calculated by using Eq.(21) in Chapter II and k_{ex} is given by Eq.(16)

$$k_{ex} = rate/5[UO_2(DMF)_5^{2+}]$$

$$= (kT/h)\exp(-\Delta H^{\ddagger}/RT)\exp(\Delta S^{\ddagger}/R) \qquad (16)$$

The same measurements were carried out for the solutions with different compositions listed in Table 7. The logarithms of obtained k_{ex} are plotted against the reciprocal temperature in Fig. (15), which shows that k_{ex} depends on the free DMF concentrations. The plots of k_{ex} against the DMF concentration do not yield a simple linear relationship, as seen in Fig. 16, but the intercepts and the limiting values at high concentration region.
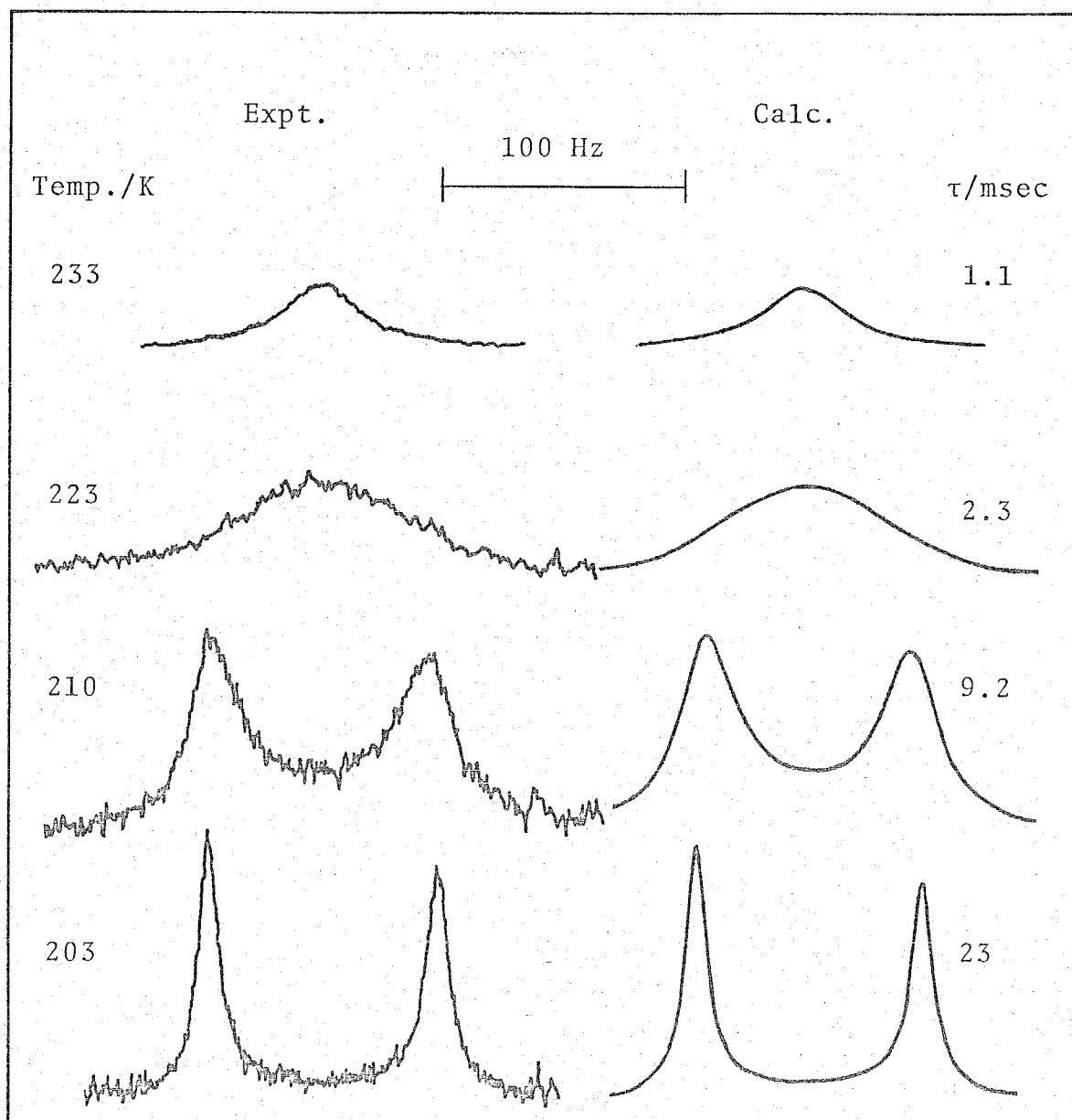
Fig. 14. Experimental(left-hand side) and best-fit calculated
^{1}H NMR lineshapes of a solution consisting of $UO_2(DMF)_5^{2+}$
(0.00611 M), DMF(0.0304 M), and CD_2Cl_2(16.1 M)
Temperatures and best-fit τ-values are shown at left-
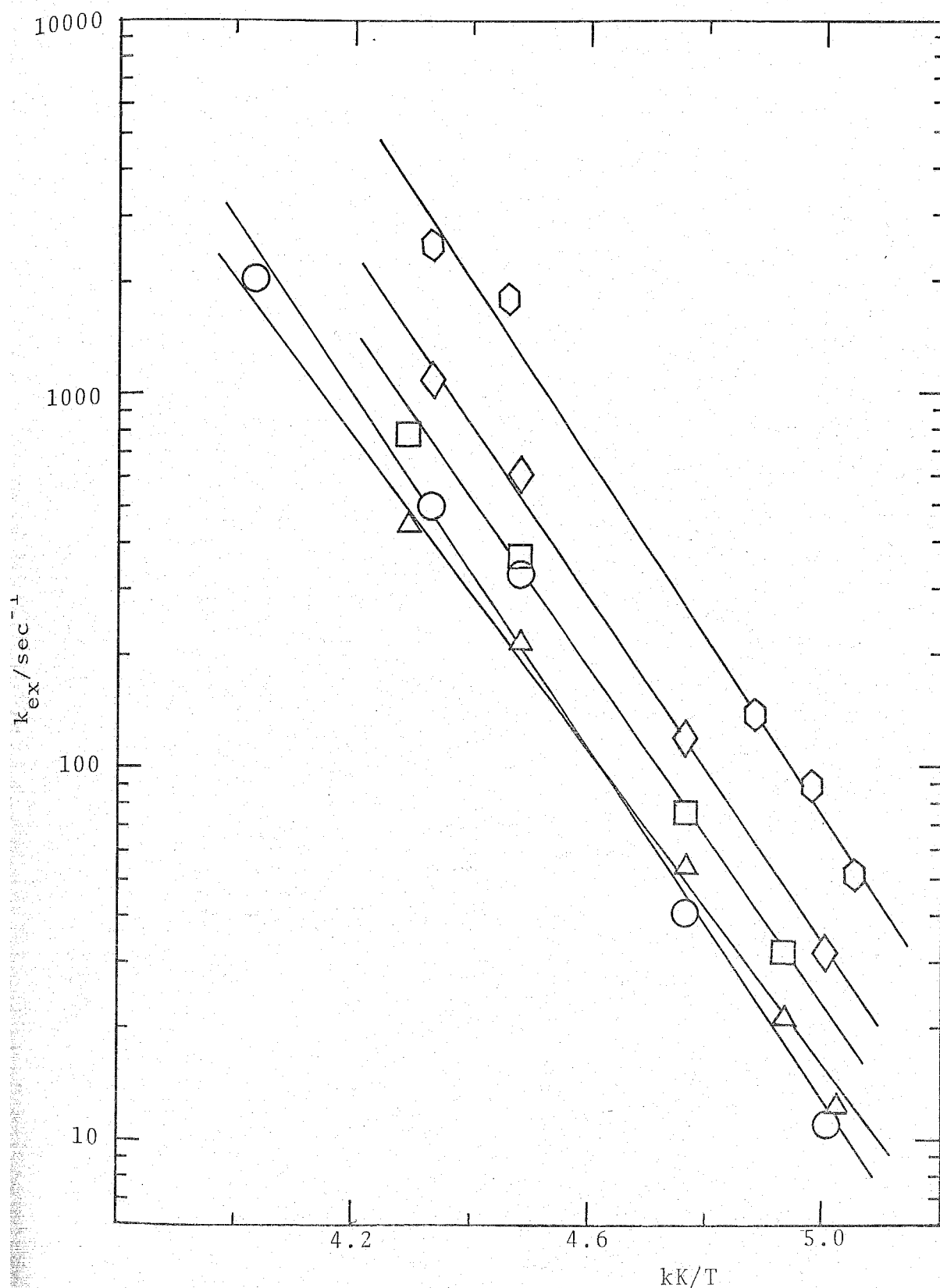and right-hand sides of the figure, respectively.

Fig. 15. Semilogarithmic plots of k_{ex} against the reciprocal temperature for the exchange of DMF in $UO_2(DMF)_5^{2+}$ The symbols of ○, △, □, ◇, and ⬡ correspond to (i), (ii), (iii), (iv), and (v) in Table 7.
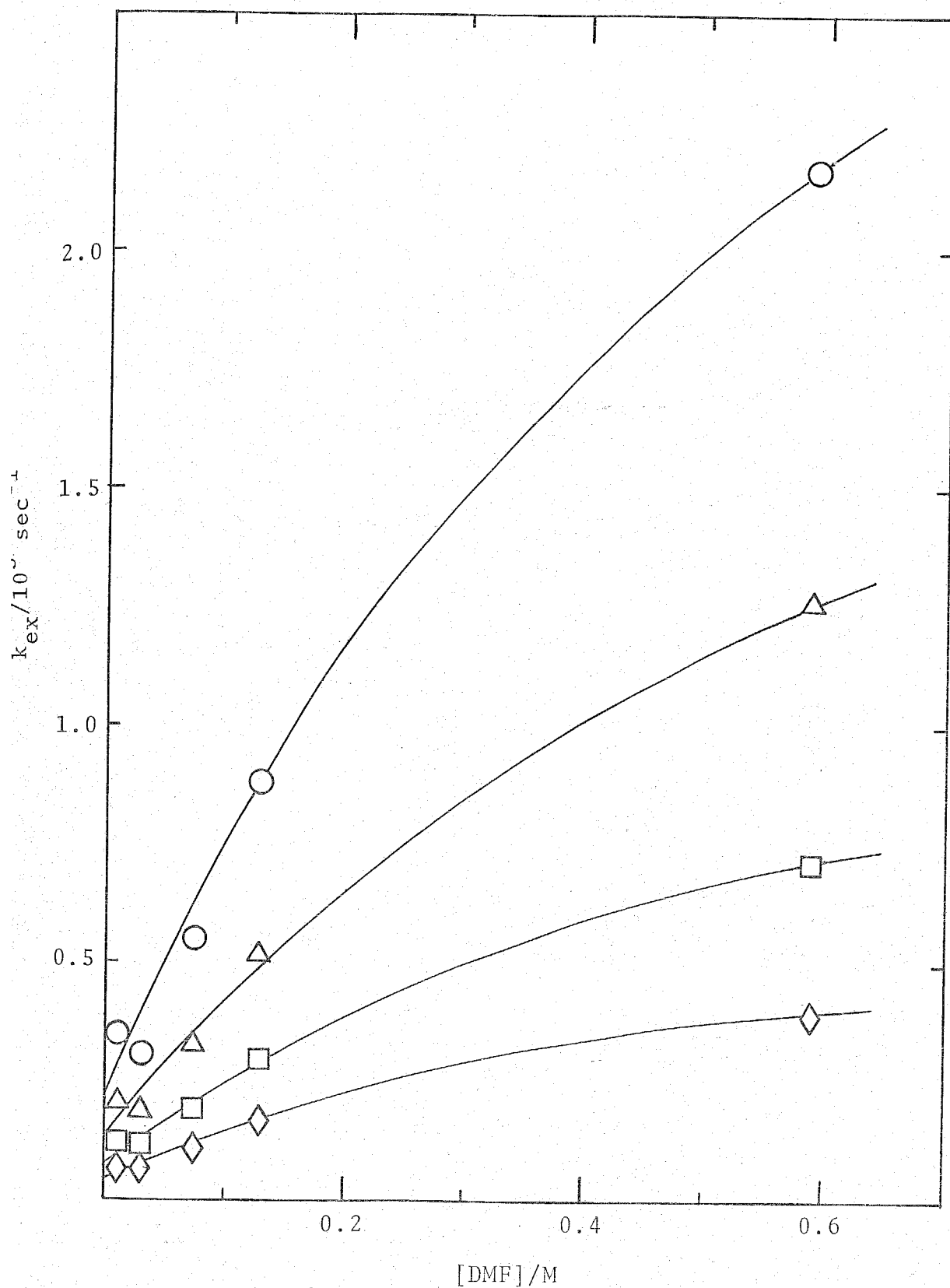
Fig. 16. Plots of k_{ex} vs. [DMF] for the exchange of DMF in $UO_2(DMF)_5^{2+}$. $\bigcirc$: -45 °C; $\triangle$: -50 °C; $\square$: -55 °C; $\Diamond$: -60 °C. The solid lines are the least-squares fit lines.

C. Mechanism

Figure 16 suggests that the DMF exchange reaction in UO_2-$(DMF)_5^{2+}$ proceeds through two paths, that is, one is the path which is independent of the free DMF concentrations, and another is the path which depends on free DMF in its low concentration region and becomes independent of free DMF in high DMF concentration region.

This can be given by Eqs. (17-a) and (17-b), in which the DMF exchange reaction is assumed to proceed through the D and I_d mechanisms.

$$UO_2(DMF)_5^{2+} + DMF^* \xrightarrow[slow]{k_d} UO_2(DMF)_4^{2+} + DMF + DMF^*$$

$$\hspace{6cm} (17\text{-}a)$$

$$\xrightarrow{fast} UO_2(DMF)_4DMF^{*2+} + DMF$$

$$UO_2(DMF)_5^{2+} + DMF^* \underset{fast}{\overset{K_{os}}{\rightleftharpoons}} UO_2(DMF)_5^{2+}\text{---}DMF^* \xrightarrow[slow]{k_I}$$

$$\hspace{6cm} (17\text{-}b)$$

$$UO_2(DMF)_4DMF^{*2+}\text{---}DMF \xrightarrow{fast} UO_2(DMF)_4DMF^{*2+} + DMF$$
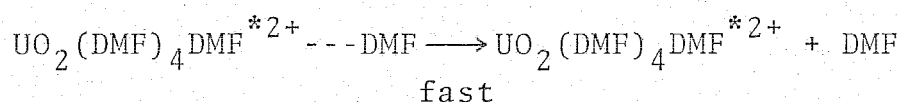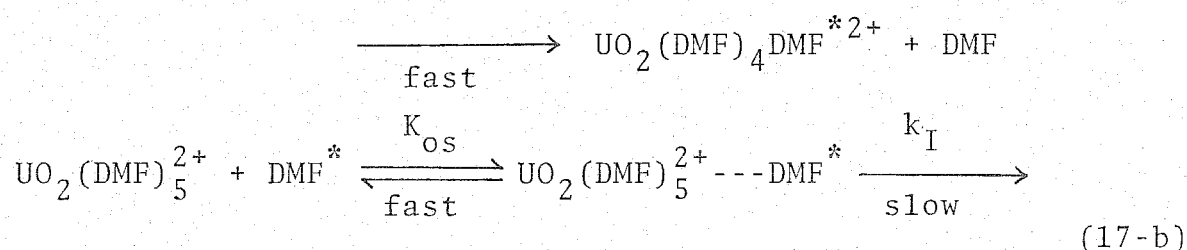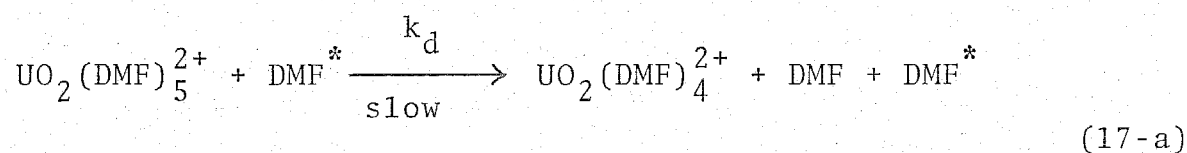
where detailed descriptions for these mechanisms are given on pages 63-64. These mechanisms lead to the following equation for k_{ex}

$$k_{ex} = (k_d + k_I K_{os}[DMF])/(1 + K_{os}[DMF]) \hspace{1cm} (18)$$

This expression can be simplified to $k_{ex} = k_d + k_I K_{os}[DMF]$ when $K_{os}[DMF] \ll 1$. This corresponds to the dependence of k_{ex} on the DMF concentration in the low concentration region. If the values

of K_{os}[DMF] are much larger than unity, Eq. (18) becomes $k_{ex} \approx k_I$, which agrees with the fact that the DMF exchange rate becomes independent of the DMF concentrations in the high concentration region.

The values of k_d, k_I and K_{os} were calculated by using non-linear least-squares method and are listed in Table 8. The solid lines in Fig. 16 are the best-fit lines obtained from the calculated values of k_d, k_I and K_{os}, and indicate that the experimental data are in fair agreement with the calculated values. From Fig. 17, in which logarithms of k_d and k_I are plotted against the reciprocal temperature, the activation parameters for k_d and k_I paths were obtained and are listed in Table 9.

Despite the fact that the values of K_{os} are larger than that expected from the Fuoss equation[30], these values are fairly reasonable by considering the large basicity and the relatively large dipole moment of DMF(3.86 D)[31]. It is seen from Table 9 that k_I path contributes predominantly to the DMF exchange reaction, and the positive activation entropy suggests that the k_I path proceeds through the I_d mechanism.

These results are different from those of Lincoln et al.[31]. In their experiments, the first-order rate constants are obtained from the lineshapes of the DMF methyl proton signals and the concentration range of free DMF(0.00213 - 0.04323 M) is lower than that of the present experiments(0.0123 - 0.588 M). They suggested that the rate of DMF exchange is independent of free DMF concentrations, and that this exchange reaction proceeds
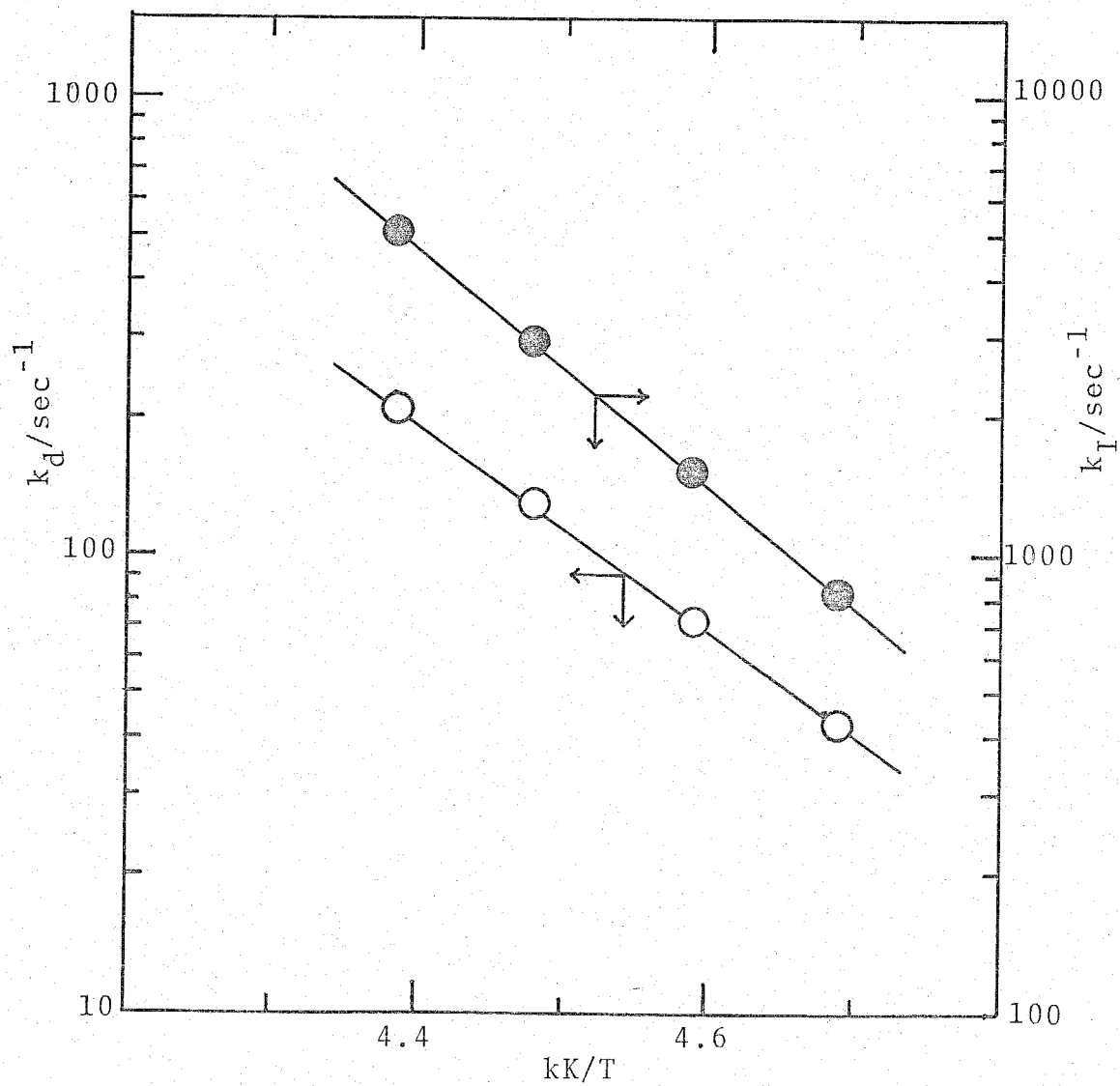
Fig. 17. Semilogarithmic plots of k_d and k_I against the reciprocal temperature for the exchange of DMF in $UO_2(DMF)_5^{2+}$.

Table 8. The values of k_d, k_I, and K_{os} at various temperatures for the exchange of DMF in $UO_2(DMF)_5^{2+}$

Temp. $^\circ C$	$\dfrac{k_d}{10^2 \ sec^{-1}}$	$\dfrac{k_I}{10^3 \ sec^{-1}}$	$\dfrac{K_{os}}{M^{-1}}$
-45	2.10 ± 0.39	5.08 ± 0.12	1.15 ± 0.14
-50	1.30 ± 0.21	2.94 ± 0.07	1.15 ± 0.08
-55	0.72 ± 0.10	1.51 ± 0.03	1.36 ± 0.04
-60	0.43 ± 0.05	0.83 ± 0.01	1.36 ± 0.02

Table 9. Kinetic parameters for k_d and k_I paths in the exchange of DMF in $UO_2(DMF)_5^{2+}$

	$\dfrac{\Delta H^{\ddagger}}{kJ \ mol^{-1}}$	$\dfrac{\Delta S^{\ddagger}}{JK^{-1}mol^{-1}}$	$\dfrac{k(25 \ ^\circ C)^a}{10^4 \ sec^{-1}}$
k_d path	42.0 ± 2.1	-15.1 ± 3.3	4.70
k_I path	48.3 ± 0.9	38.6 ± 2.6	234

[a] Calculated values from $\Delta H^{\ddagger}$ and $\Delta S^{\ddagger}$ at 25 $^\circ C$.

through the D mechanism. However, if the exchange reaction proceeds through only the D mechanism, the exchange rate might become fast by the steric effect. In order to examine this steric effect, the exchange reaction of DMF in $UO_2(acac)_2DMF$ has been studied as shown in Chapter IV. From Table 14 in Chapter IV, it is found that the DMF exchange rate constant in $UO_2(acac)_2DMF$ is smaller than that of DMF in $UO_2(DMF)_5^{2+}$.

A recent study[32] on the substitution reactions of $UO_2(DMF)_5^{2+}$ with SCN^- and N_3^- in DMF revealed that the substitution reactions proceed through the I_a mechanism and that the rate constant, k_I, for interchange path(sec^{-1}) and the activation parameters, $\Delta H^{\ddagger}$ (kJ mol^{-1}) and $\Delta S^{\ddagger}$(JK^{-1} mol^{-1}) at 25 °C are 1.5 x 10^2, 56.7, -14.3 for SCN^- and 1.5 x 10^3, 50.4, -19.7 for N_3^-, respectively.

Although the solvent used in their experiments is different from the present ones, the rate constants are much smaller than those of the DMF exchange in $UO_2(DMF)_5^{2+}$.

These facts may support that the the exchange reaction of DMF in $UO_2(DMF)_5^{2+}$ proceeds through not only the D mechanism but also the I_d mechanism.

iv. SUMMARY

The results of the ligand exchange reaction in uranyl complexes, which have been measured up to the present, are shown in Table 10. In these complexes, ligands coordinate to the uranyl ion through oxygen. All complexes except $UO_2(H_2O)_4^{2+}$ [11] and $UO_2(HMPA)_4^{2+}$ [16], have the pentagonal bipyramidal structures. The structure of the uranyl aqua complex in solution is different from that in the solid state, while the UO_2^{2+}-HMPA complex has the same structure in solution and in the solid state. It has been also known that UO_2^{2+} ion formes six-coordinated complexes in the equatorial plane with small ligands, e.g. $UO_2(CH_3COO)_3^-$ and $UO_2(CO_3)_3^{4-}$ in the solid state [19].

It is interesting to point out that UO_2^{2+} ion has various coordination numbers, depending on the ligands. It might be reasonable to assume that the difference in the coordination numbers of uranyl complexes is attributed to the basicity and size of ligands. The ligand having large basicity can strongly coordinate to UO_2^{2+} ion, and the ligand size affects the bulkiness in the equatorial plane. The Gutmann's donor number(DN)[8,9] and molar volume(V_{mol}), which are used as the measure of the basicity and the size of ligands, respectively, are also listed in Table 10. By comparison of these values with the coordination number in the equatorial plane, it is found that the assumption is almost varid as mentioned below. The complexes coordinated with ligands, which have relatively large donor numbers and smaller molar volumes than HMPA, are the five coordinated species in the equatorial plane. On the other hand, HMPA has a large

donor number and a large molar volume, and hence the equatorial plane becomes bulky. As a result, five HMPA molecules can not coordinate to the equatorial plane of the UO_2^{2+} ion. In the case of H_2O, the molar volume is small and the steric hindrance in the equatorial plane could be small. However the donor number of H_2O is so small that the coordination number stays 4 in the equatorial plane.

This assumption can explain also the difference in the mechanisms because the basicity and size of ligands contribute to the structure of intermediates in the reactions. The H_2O exchange reaction in $UO_2(H_2O)_4^{2+}$ does not proceed through the A mechanism in spite of the possibility of the formation of a five-coordinated intermediate in the equatorial plane by considering the structure in the solid state, while the HMPA exchange in $UO_2(HMPA)_4^{2+}$ proceeds through the A mechanism. As mentioned above, HMPA has a large donor number and hence can form a five-coordinated inter-mediate in the equatorial plane despite the large molar volume, whereas the donor number of H_2O seems to be too small to form such a intermediate. Among the five-coordinated complexes in Table 10, only $UO_2(DMSO)_5^{2+}$ has the reaction path through the A mechanism, in which the six-coordinated intermediate is formed. This fact can be also accounted for by the large donor number and the small molar volume of DMSO. Ligands, other than DMSO, have the large molar volumes and the small donor numbers compared with DMSO and tend to have the D or I_d mechanism, in which the dissociation of these bulky ligands moderate a crowded structure in the equatorial plane.

As mentioned above, it is suggested that the structure of

uranyl complexes in solution and the mechanism of ligand exchange reactions in uranyl complexes closely relate to the basicity and size of ligands.

A correlation between the activation enthalpy for the solvent exchange reaction and the solvent basicity has been proposed recently[33,34]. Funahashi and Jordan have proposed that the following equation holds between $\Delta H^{\ddagger}$ and DN.

$$\Delta H^{\ddagger} = aDN - bDN^2 \qquad (19)$$

where a and b are empirical fitting constants depending on metal ions. This relation is based on the idea that if the mechanism is dissociative, $\Delta H^{\ddagger}$ is propotional to the solvent basicity and metal acidity, and the metal acidity may vary linearly with the coordinated solvent basicity. They have found that Eq. (19) holds for the solvent exchange reactions in Ni(II), Co(II), Fe(II) and Mn(II).

We tried to test the applicability of Eq. (19) to the ligand exchange reactions in uranyl complexes, but a good agreement was not obtained, and the following equation rather than Eq. (19) seems to applicable to these ligand exchange reactions as shown in Fig. 18.

$$\Delta H^{\ddagger} = aDN$$

Such a relationship has also been found by Chattopadhyay et al.[55]. However, some authors have pointed out that these simple relations are incidental and cannot be applied generally to the ligand

exchagne reactions [36,37].

On the other hand, Benetto and Caldin[38] have proposed that if the solvent exchange reaction proceeds through the same mechanism, the plots of $\Delta H^{\ddagger}$ and $\Delta S^{\ddagger}$ yield the linear relationship and this isokinetic relationship is due to the rearrangement of solvent or diluent arround the metal ion, followed by the simultaneous formation of the transition state. This interpretation for the activation parameters is different from those of Hoffman[33] and Funahashi[34]. Lincoln et al.[6] have reported that this iso-kinetic relationship is applicable to the ligand exchange reactions in $UO_2L_5^{2+}$ in Table 10 and the surface charge density of these uranyl complexes lies between that in AlL_6^{3+} and ML_6^{2+} (M = Ni, Co, Mn, Fe, V and Mg).

If the interpretation by Benetto et al. is valid, this result indicates that the difference in the activation parameters for the exchange reactions in uranyl complexes is due to the re-arrangement of outer solvents of the first coordination sphere of uranyl complexes.

Table 10. Kinetic parameters for the exchange reactions in various uranyl complexes

Complex	Solvent	Mechanism	$\Delta H^{\ddagger}$ kJ mol^{-1}	$\Delta S^{\ddagger}$ JK^{-1}mol^{-1}	$k_{ex}(25°C)^{a}$ sec^{-1}	DN^{b}	V_{mol}^{c} cm^{3}	Ref.
UO$_2$(H$_2$O)$_4^{2+}$	CD$_3$COCD$_3$ + H$_2$O	I$_d$	41.6 ± 2.1	8.8 ± 10.9	9.8 × 10^5	18.0	18.1	d
UO$_2$(HMPA)$_4^{2+}$	CD$_2$Cl$_2$	D	13.9 ± 2.9	-172.2 ± 10.9	2.58 × 10	38.8	174.5	39
		A	22.3 ± 2.9	-120.1 ± 8.8	4.52 × 10^2/M^{-1}			
UO$_2$(DMSO)$_5^{2+}$	CD$_3$COCD$_3$	D	53.8 ± 2.4	6.3 ± 14.5	5.53 × 10^3	29.8	71.3	d
		A	39.1 ± 1.7	-28.1 ± 5.0	3.22 × 10^4/M^{-1}			
UO$_2$(DMF)$_5^{2+}$	CD$_2$Cl$_2$	D	42.0 ± 2.1	-15.1 ± 3.3	4.70 × 10^4	26.6	77.4	d
		I$_d$	48.3 ± 0.9	38.6 ± 2.6	2.34 × 10^6			
UO$_2$(DMA)$_5^{2+}$	CD$_2$Cl$_2$	D	42.8 ± 0.8	-43.7 ± 2.9	1.10 × 10^3	27.8	93.0	4
UO$_2$(TMP)$_5^{2+}$	CD$_2$Cl$_2$	D or I$_d$	25.2 ± 1.3	-109.6 ± 9.7	4.88 × 10^2	23.0	117.0	5
UO$_2$(TEP)$_5^{2+}$	CD$_2$Cl$_2$	D or I$_d$	43.7 ± 1.7	-47.5 ± 5.9	4.97 × 10^2		169.9	5
UO$_2$(TMU)$_5^{2+}$	CD$_2$Cl$_2$	D	80 ± 2	85 ± 7	1.88 × 10^3		119.9	6
UO$_2$(NMA)$_5^{2+}$	CD$_2$Cl$_2$	D	67 ± 1	45 ± 6	2.74 × 10^3		77.0	7
	CD$_3$CN	D	55.6 ± 0.6	8.0 ± 2.3	3.38 × 10^3			

a. Calculated values from $\Delta H^{\ddagger}$ and $\Delta S^{\ddagger}$ at 25 °C.   b DN = Gutmann's donor number.   c V_{mol} = molar volume.

d. ⌐ℸℸ
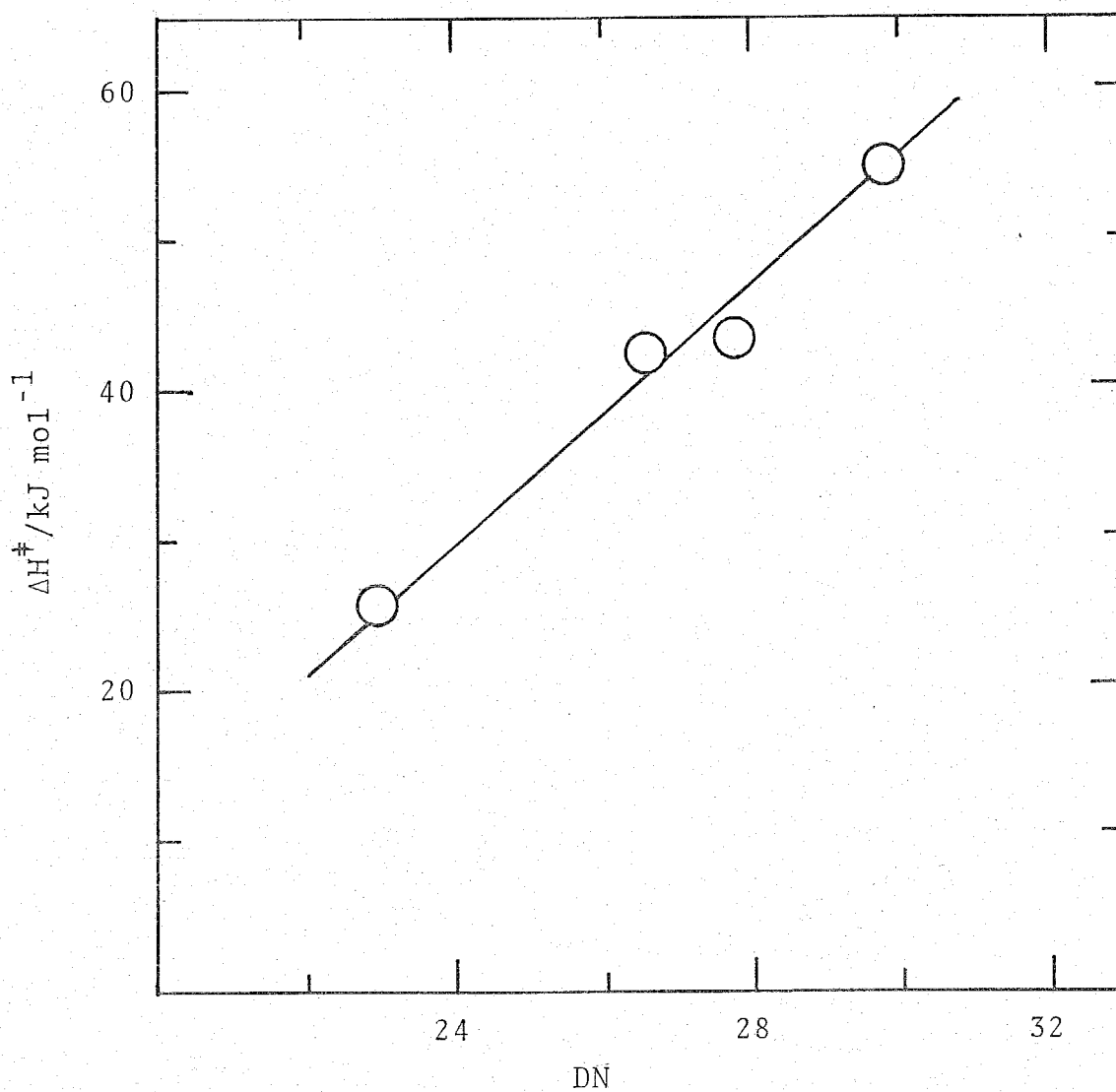
Fig. 18. A plot of $\Delta H^{\ddagger}$ vs. DN for the ligand exchange in various uranyl complexes.

REFERENCES

1. P. Hurwitz and K. Kustin, J. Phys. Chem., 71, 324(1967).

2. M.P. Whiiaker, E.M. Eyring, and E. Dibble, J. Phys. Chem., 69, 2319(1965).

3. A. Ekstrom and D.A. Johnson, J. Inorg. Nucl. Chem., 36, 2549 (1974).

4. R.P. Bowen, S.F. Lincoln, and E.H. Williams, Inorg. Chem., 15, 2126(1976).

5. J. Crea, R. Digiusto, S.F. Lincoln, and E.H. Williams, Inorg. Chem., 16, 2825(1977).

6. G.J. Honan, S.F. Lincoln, and E.H. Williams, J.C.S. Dalton, 320(1979).

7. G.J. Honan, S.F. Lincoln, and E.H. Williams, J.C.S. Dalton, 1220(1979).

8. V. Gutmann and R. Schmid, Coord. Chem. Rev., 12, 263(1974).

9. V. Gutmann, Coordination Chemistry in Non-Aqueous Solutions, Springer-Verlag, Wien.New York(1968).

0. N.W. Alcock and S. Esperās, J.C.S. Dalton, 893(1977).

1. A. Fratiello, V. Kubo, and R.E. Lee, and R.E. Schuster, J. Phys. Chem., 74, 3726(1970).

2. A. Fratiello, V. Kubo, and R.E. Schuster, Inorg. Chem., 10, 744,(1971).

3. V.M. Vdovenko, L.G. Mashirov, and D.N. Suglobov, Radiokimiya., 6, 299(1964); 9, 37(1967).

4. G.H. Langford and H.B. Gray, Ligand Substitution Processes, Benjamin, London(1974).

15. M.J. Hynes and B.D. O Regan, J.C.S. Dalton, 1200(1976).

16. A. Fratiello, G.A. Vidlich, C. Cheng, and V. Kubo, J. Solution Chem., 1, 433(1972).

17. L.R. Nassimbeni and A.L. Rodgers, Cryst. Struct. Commun., 5, 301(1976).

18. G. Bombieri, J.P. Day, and W.I. Azeez, J.C.S. Dalton, 1978(1978).

19. I.I. Chernyaev, Complex Compounds of Uranium(Translated from Russian), Israel Program for Scientific Translations, Jerusalem(1966).

20. G.J. Honan, S.F. Lincoln, and E.H. Williams, J. Solution Chem., 7, 433(1978).

21. W.G. Movius and N.A. Matwiyoff, Inorg. Chem., 6, 847(1967).

22. W.G. Movius and N.A. Matwiyoff, Inorg. Chem., 8, 925(1969).

23. N.A. Matwiyoff and W.G. Movius, J. Am. Chem. Soc., 89, 6077(1967).

24. W. Gerrard, M.F. Lappert, H. Pyszora, and J.W. Wallis, J. Chem. Soc., 2144(1960).

25. C.D. Schmulbach and R.S. Drago, J. Am. Chem. Soc., 82, 4484 (1960).

26. S.J. Kuhn and J.S. McIntyre, Can. J. Chem., 43, 375(1965).

27. J.A. Pople, W.G. Schneider, and H.G. Bernstein, High Resolution Nuclear Magnetic Resonance, McGraw Hill, New York, N.Y.(1959).

28. T.H. Siddall III and C.A. Prohaska, J. Am. Chem. Soc., 84, 3467(1962).

29. R.P. Bowen, G.H. Honan, S.F. Lincoln, T.M. Spotswood, and E.H. Williams, Inorg. Chim. Acta., 33, 235(1979).

30. R.M. Fuoss, J. Am. Chem. Soc., $\underline{80}$, 5059(1958).

31. T.R. Griffiths and D.C. Pugh, Coord. Chem. Rev., $\underline{29}$, 129(1979).

32. H. Doine, Y. Ikeda, and H. Fukutomi, to be published.

33. F. Dickert, H. Hoffmann, and T. Janjic, Ber. Bunsenges. Phys. Chem., $\underline{78}$, 712(1974).

34. S. Funahashi and R.B. Jordan., Inorg. Chem., $\underline{16}$, 1301(1977).

35. a) P.K. Chattopadhyay and B. Kratochvil, Inorg. Chem., $\underline{15}$, 3104(1976); b) P.K. Chattopadhyay and B. Kratochvil, Can. J. Chem., $\underline{55}$, 1609(1977).

36. L.L. Rusnak, E.S. Yang, and R.B. Jordan, Inorg. Chem., $\underline{17}$, 1810(1978).

37. J.F. Coetzee and C.G. Karakatsanis, Inorg. Chem., $\underline{15}$, 3112(1976).

38. a) H.P. Benetto and E.F. Caldin, J. Chem. Soc. (A), 2198(1971); b) E.F. Caldin and H.P. Benetto, J. Solution. Chem., $\underline{2}$, 217 (1973).

39. G.J. Honan, S.F. Lincoln, and E.H. Williams, Inorg. Chem., $\underline{17}$, 1855(1978).

CHAPTER IV

KINETIC STUDY OF THE SOLVENT EXCHANGE REACTIONS
IN THE SOLVATED URANYL β-DIKETONATO COMPLEXES
BY NMR

i. INTRODUCTION

In the previous chapter, kinetic results were described for the exchange reactions of DMSO in $UO_2(DMSO)_5^{2+}$ in CD_3COCD_3 and of DMF in $UO_2(DMF)_5^{2+}$ in CD_2Cl_2.

It is difficult to determine unequivocally the mechanism of the exchange reactions of DMSO and DMF from usual kinetic results. Particularly, it was not evident whether the mechanism for the k_2 path of the exchange of DMSO in $UO_2(DMSO)_5^{2+}$ was either I_d or A mechanism.

Therefore, the exchange reactions of DMSO in $UO_2(acac)_2$-DMSO and $UO_2(dbm)_2DMSO$ (acac = acetylacetonate, dbm = dibenzoyl-methanate) are studied in order to examine the steric effect on the DMSO exchange rate. It is expected that if the k_2 path of the DMSO exchange in $UO_2(DMSO)_5^{2+}$ proceeds through the A mechanism, the rate for the exchange of DMSO in $UO_2(acac)_2DMSO$ and $UO_2(dbm)_2DMSO$ will become slower than that in $UO_2(DMSO)_5^{2+}$ owing to the steric effect of bulky chelating ligands, acac and dbm.

The exchange reaction of DMF in $UO_2(acac)_2DMF$ was also studied for the purpose of the comparison with the DMSO exchange in $UO_2(acac)_2DMSO$ and the DMF exchange in $UO_2(DMF)_5^{2+}$.

This type of complex, $UO_2(\beta\text{-diketonato})_2L$ (L= donor solvents), has been studied extensively in the view of the extraction of uranyl ion[1-7], where β-diketones are the extractants and the donor solvents, e.g. DMSO, DMF and TMP, yield the synergistic effect. The structure of $UO_2(acac)_2H_2O$ in the solid state has known

to be pentagonal bipyramidal as shown in Fig. 1[8,9], but the structure of this type of complex in solution has not been determined in detail. Therefore, the study on the structure of $UO_2(acac)_2L$ (L = DMSO and DMF) and $UO_2(dbm)_2DMSO$ in CD_3COCD_3 and CD_2Cl_2 by using NMR and IR spectometers will be described at the beginning of each section in this chapter, followed by kinetic results.
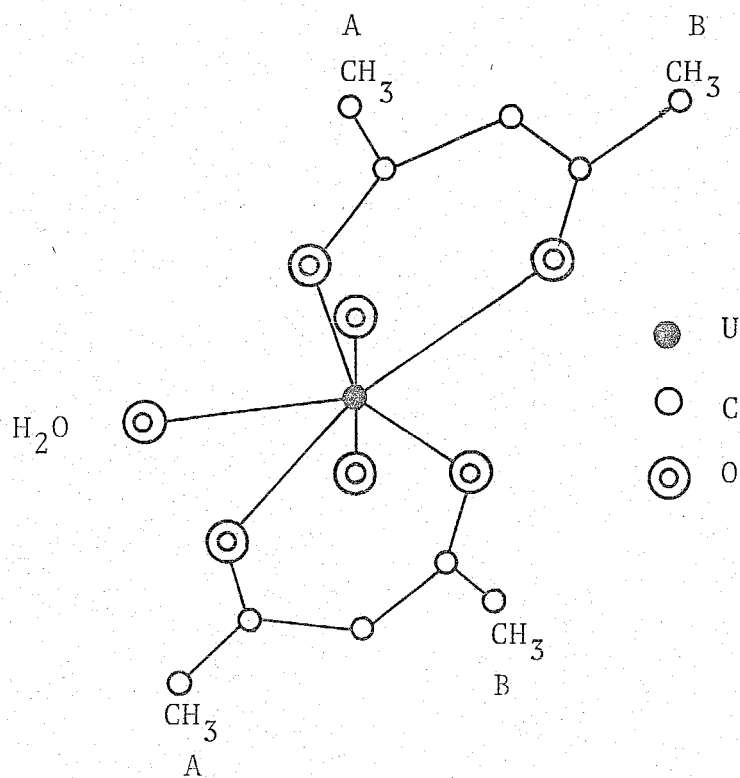
Fig. 1. The perspective veiw of the structure of

$UO_2(acac)_2H_2O$ complex. The U-O bond lengths

are 2.51 ± 0.07 Å for the oxygen atoms in the

rings, 2.48 ± 0.07 Å for water oxygen and

1.60 ± 0.07 Å for the oxygen atoms in the

uranyl group. E. Frasson, G. Bombieri and

C. Panattoni, Coord. Chem. Rev., 1, 145(1966).

ii . EXPERIMENTAL

A. Synthesis of Complexes

Preparation of $UO_2(acac)_2DMSO$ complex was made by dissolving $UO_2(acac)_2H_2O$, which was prepared acording to the procedure of Comyns et al.[10], in warm DMSO. The solution was cooled and the resultant orange crystals were filtered off and dried in vacuo for 1 day. Anal. Calcd for $UO_2(acac)_2DMSO$: C, 26.38; H, 3.69. Found: C, 26.49; H, 3.66.

Preparation of $UO_2(dbm)_2DMSO$ complex was performed by mixing DMSO with a solution of $UO_2(dbm)_2H_2O$, which was prepared by mixing an aqueous solution of uranylacetate dihydrate(1 mol) with an alcoholic solution of dibenzoylmethane(2 mol)[11], in andydrous ethyl ether. Anal. Calcd for $UO_2(dbm)_2DMSO$: C, 48.37; H, 3.55; S, 4.03. Found: C, 48.32; H, 3.52; S, 4.08.

The $UO_2(acac)_2DMF$ complex was prepared by the same method as the synthesis of $UO_2(acac)_2DMSO$. Anal. Calcd for $UO_2(acac)_2$-DMF: C, 28.84; H, 4.28; N, 2.59. Found: C, 28.79; H, 3.89; N, 2.55.

B. Other Materials

Acetone-d_6, dichloromethane-d_2, dimethyl sulfoxide, and N,N-dimethylformamide were purified and dried by the same method as described in Chapter III. Acetylacetone(Wako Pure Chemical Ind. Ltd.) and dibenzoylmethane(Tokyo Kasei Kogyo Co. Ltd.) were used without further purification.

C. Kinetic Analysis

Kinetic analysis were done by the same method as described

in Chapter II. For the DMSO exchange in $UO_2(acac)_2DMSO$ and $UO_2(dbm)_2DMSO$, the methyl proton signals of coordianted and free DMSO measured. The formyl proton signals of coordinated and free DMF were measured for the exchange of DMF in $UO_2(acac)_2DMF$.

The values of P_C and P_F were obtained from the following equation.

$$P_C = 1 - P_F = \frac{[UO_2(\beta\text{-diketonato})_2L]}{[UO_2(\beta\text{-diketonato})_2L] + [L]}$$

For the values of T_{2C} and T_{2F}, the linewidths of methyl proton signals of DMSO in CD_3COCD_3 and CD_2Cl_2 and of formyl proton signals of DMF in CD_3COCD_3 and CD_2Cl_2 were used. The chemical shifts of methyl proton signals of coordinated and free DMSO at -50 °C were used as the value of ω_{0C} and ω_{0F}, respectively. The chemical shifts of formyl proton signals of coordinated and free DMF at -50 °C were also used as the value of ω_{0C} and ω_{0F}, respectively.

iii. RESULTS AND DISCUSSION

1. KINETIC STUDY OF THE EXCHANGE REACTION OF DIMETHYL SULFOXIDE
   IN BIS(ACETYLACETONATO)DIOXO(DIMETHYL SULFOXIDE)URANIUM(VI)

A. Structure of $UO_2(acac)_2DMSO$ in Solutions

The ^1H NMR spectra of solution containing $UO_2(acac)_2DMSO$,

DMSO and CD_3COCD_3 at -25 and 40 °C are shown in Fig. 2. In the

spectrum at -25 °C, the signals of (a) and (d) can be assigned

to the methyl protons and 3-H protons of the coordinated acac, re-

spectively. The signals of (b) and (c) are the methyl protons

of free and coordinated DMSO, respectively. A comparison of

the integrated areas for (b) and (c) indicates that one DMSO

molecule is coordinated to each uranyl ion. The area ratio of

(a) to (c) to (d) was 6 : 3 : 1 from the low field, where the

signal of (d) was used as a standard and this ratio was kept

constant in solutions of various compositions.

These facts indicate that two acetylacetonate ions and one DMSO

molecule coordinate to uranyl ion. The doublet of the methyl

protons of coordinated acac means that two coordinated acac are

bidentate ligand, because if the structure of this complex is

similar to that of $UO_2(acac)_2H_2O$ (Fig. 1), the methyl protons of

coordinated acac will have two different positions i.e. near

one(A) to and far one(B) from the coordinated DMSO. This is

supported by the fact that the 3-H proton signal of coordinated

acac is a singlet. Similar phenomena were also observed in the

^1H NMR spectra of a solution containing $UO_2(acac)_2DMSO$, DMSO and
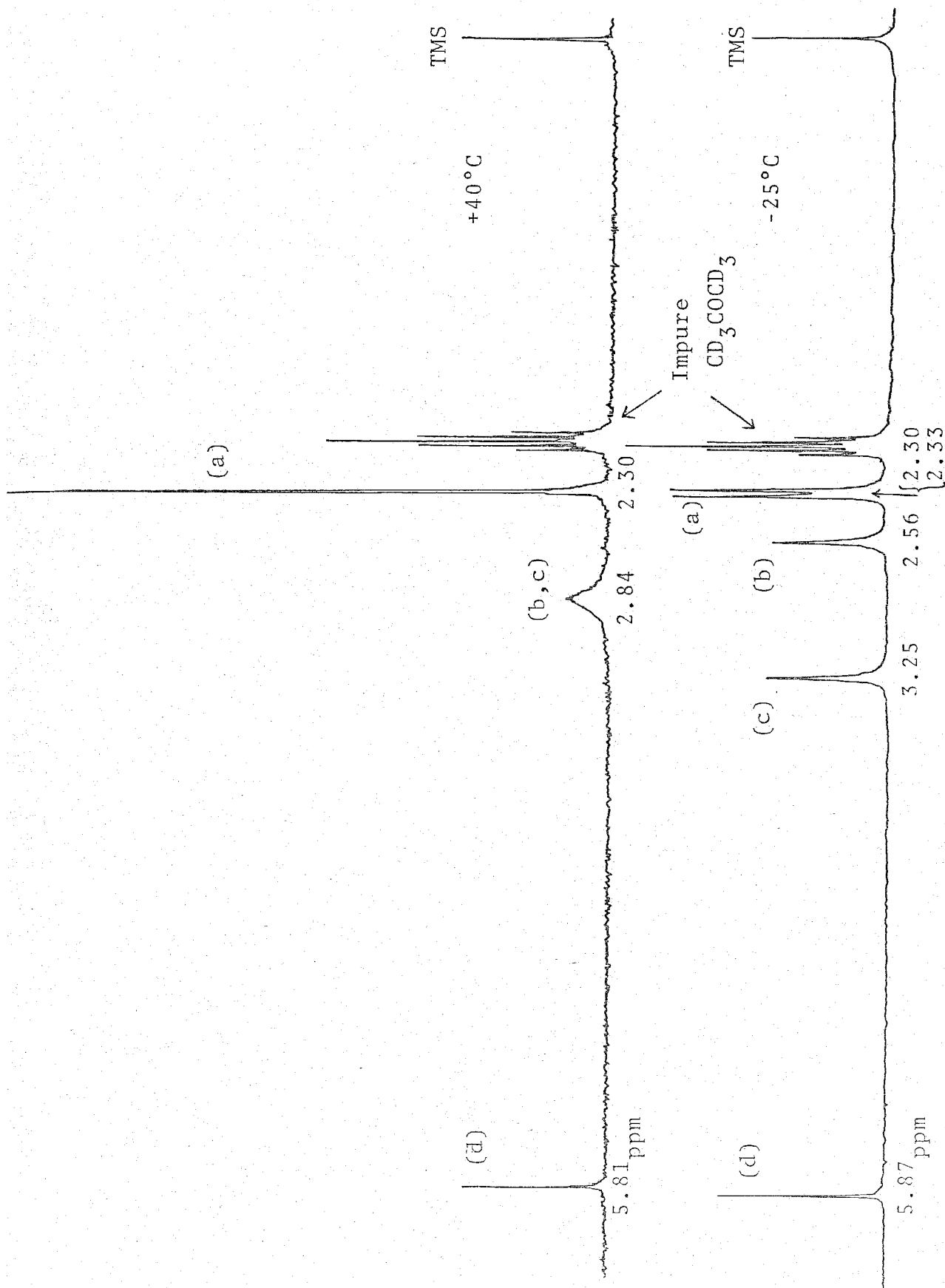
Fig. 2. The ^{1}H NMR spectra of a solution consisting of $UO_2(acac)_2DMSO(0.0298 \, M)$
DMSO(0.0294 M), and $CD_3COCD_3(13.6 \, M)$ at -25 and +40 °C, respectively.
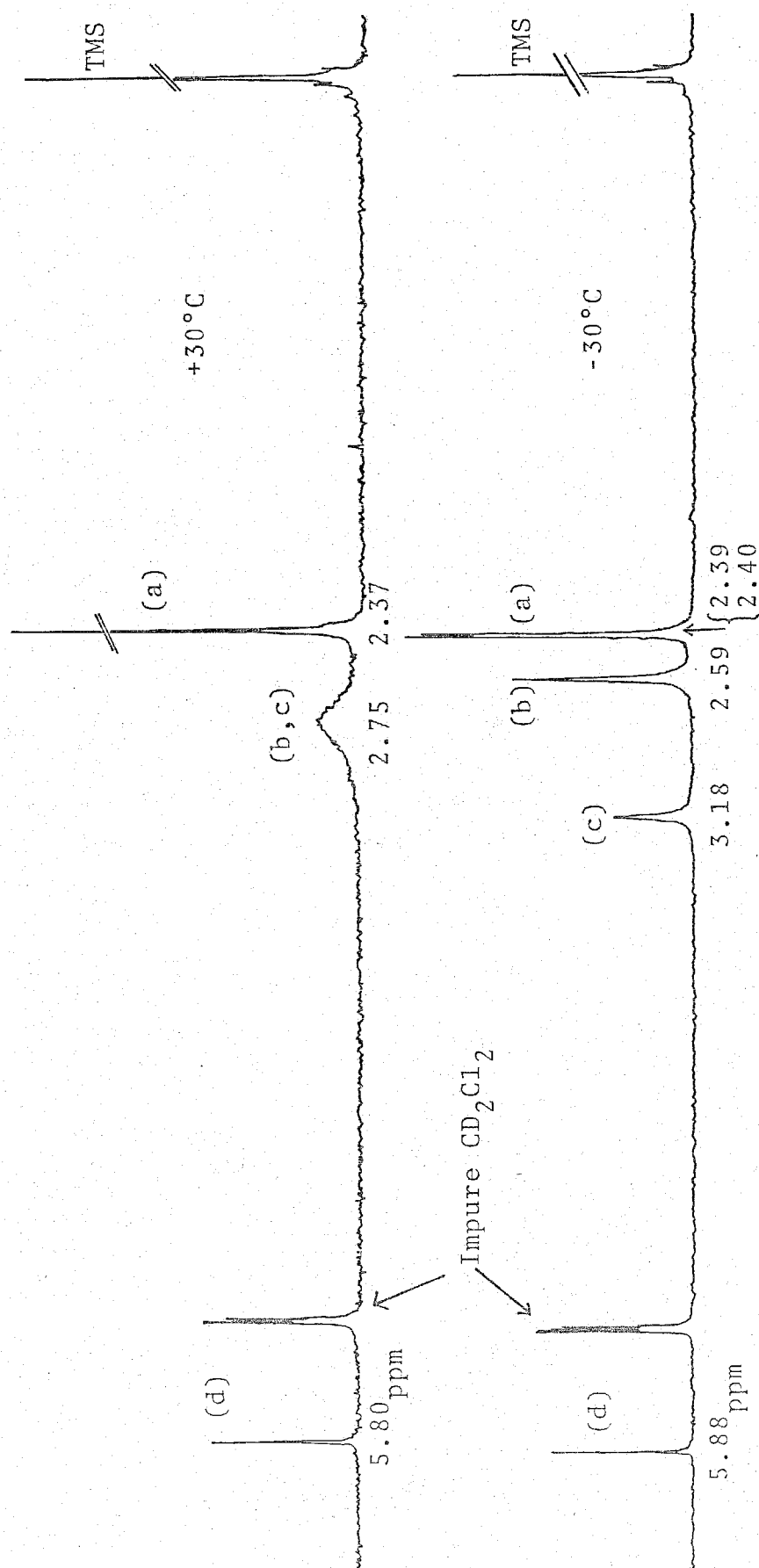
Fig. 3. The ^{1}H NMR spectra of a solution consisting of $UO_2(acac)_2$DMSO(0.0179 M), DMSO(0.0282 M), and CD_2Cl_2(15.8 M) at -30 and + 30 °C, respectively.

CD_2Cl_2 as shown in Fig. 3, in which the symbols of (a), (b), (c), and (d) correspond to those in Fig. 2.

The measurements of IR spectra of $UO_2(acac)_2DMSO$ in CD_3COCD_3 and CD_2Cl_2 may support the results of the NMR studies. The results are given in Table 1. The S=O stretching of this uranyl complex in CD_3COCD_3 and CD_2Cl_2 is observed at 1010 cm^{-1}, which is 45 cm^{-1} lower than 1055 cm^{-1} observed in pure DMSO. Cotton et al.[12] have shown that the S=O stretching frequency of sulfoxide in complexes decreases when coordination occurs through oxygen. Therefore, it was concluded that one DMSO molecule was coordinated through oxygen in this complex. In addition, it was found that two acetylacetonate ions were coordinated as bidentate ligands, because only one band corresponding to the carbonyl vibration was observed at frequencies less than 1600 cm^{-1}, which is the characteristic frequency of the carbonyl vibration of chelated metal β-diketone complexes[13].

Therefore, it is concluded that the structure of $UO_2(acac)_2$-DMSO in CD_3COCD_3 and CD_2Cl_2 is pentagonal bipyramidal as shown in Fig. 1.

Table 1. Characteristic IR stretching frequencies (cm^{-1}) for $UO_2(acac)_2DMSO$ in solutions

Solvent	$\nu_3(O=U=O)$	$\nu(S=O)$	$\nu(C-O)$
CD_3COCD_3	905	1010	1517
CD_2Cl_2	908	1010	1570

B. Exchange Reaction of DMSO in $UO_2(acac)_2DMSO$

B-1. Measurements in CD_3COCD_3 diluent

From Fig. 2. it is expected that the DMSO exchange reacion occurs between coordinated and free sites because both the methyl proton signals of coordinated and free DMSO are observed at -25 °C, while the only singlet methyl proton resonance of DMSO is observed at 40 °C. Measurements of the change of lineshape for the methyl proton of DMSO were carried out by varying temperature and the results are shown at the left side of Fig. 4. This spectral change is consistent with the DMSO exchange between coordinated and free sites. The best-fit τ-values at each temperature were obtained by the method described in Chapter II. The calculated lineshapes are shown together with the best-fit τ-values at the right side of Fig. 4.

The first-order rate constants, k_{ex}, of the DMSO exchange in $UO_2(DMSO)_5^{2+}$ were calculated by the following equation:

$$\tau = \tau_c P_F = \tau_F P_c \tag{1}$$

$$k_{ex} = 1/\tau_c = rate/[UO_2(acac)_2DMSO]$$

$$= (kT/h)\exp(-\Delta H^{\ddagger}/RT)\exp(\Delta S^{\ddagger}/R) \tag{2}$$

Similar measurements were carried out on the solutions given in Table 2. The plots of log k_{ex} agaist the reciprocal temperature are shown in Fig. 5. The activation parameters obtained from Fig. 5 are listed also in Table 2, together with the values
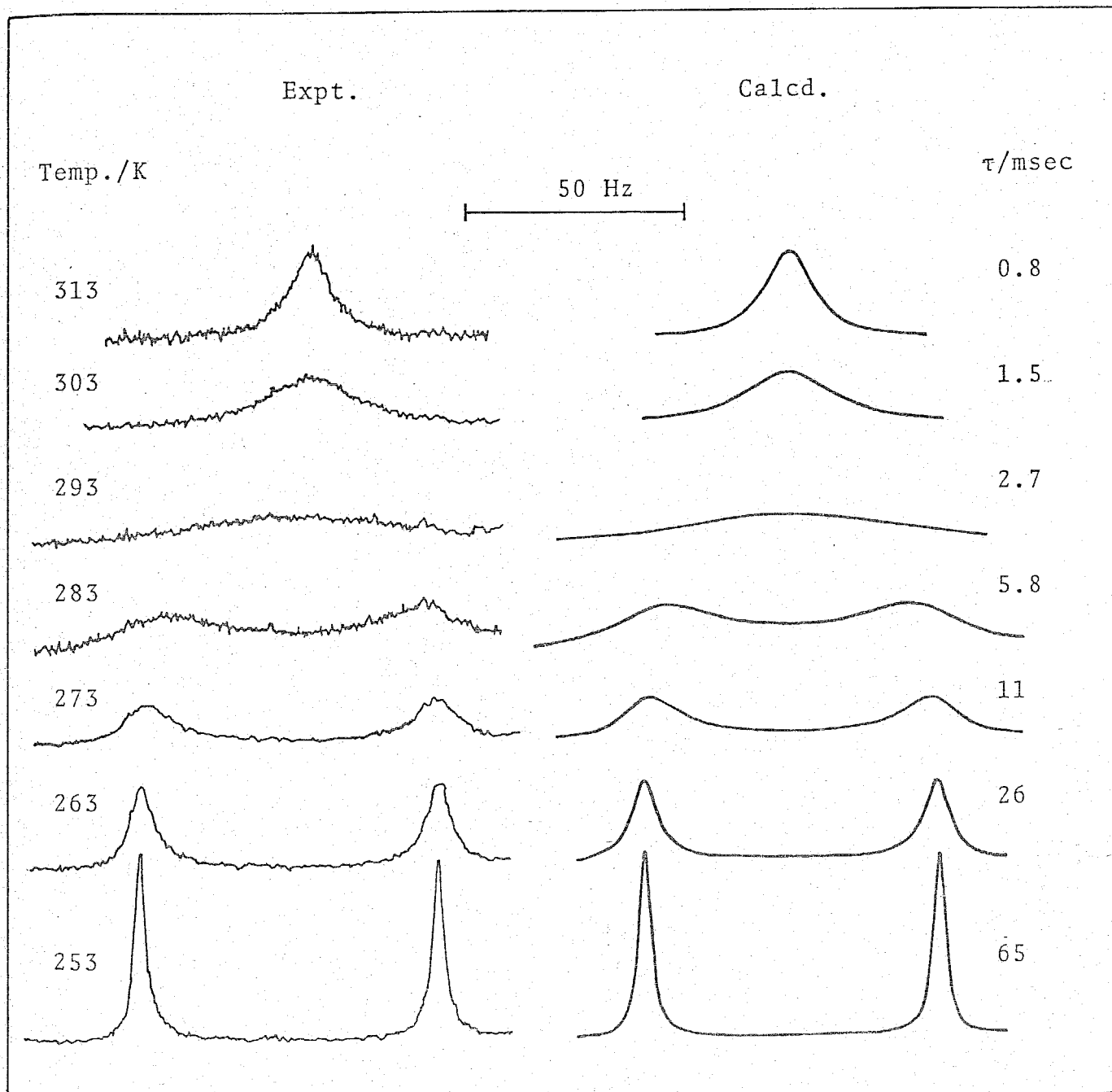
g. 4. Experimental(left-hand side) and best-fit calculated ^{1}H NMR lineshapes of a solution consisting of $UO_2(acac)_2DMSO(0.0298\ M)$, DMSO(0.0294 M), and CD_3COCD_3(13. 6 M). Temperatures and best-
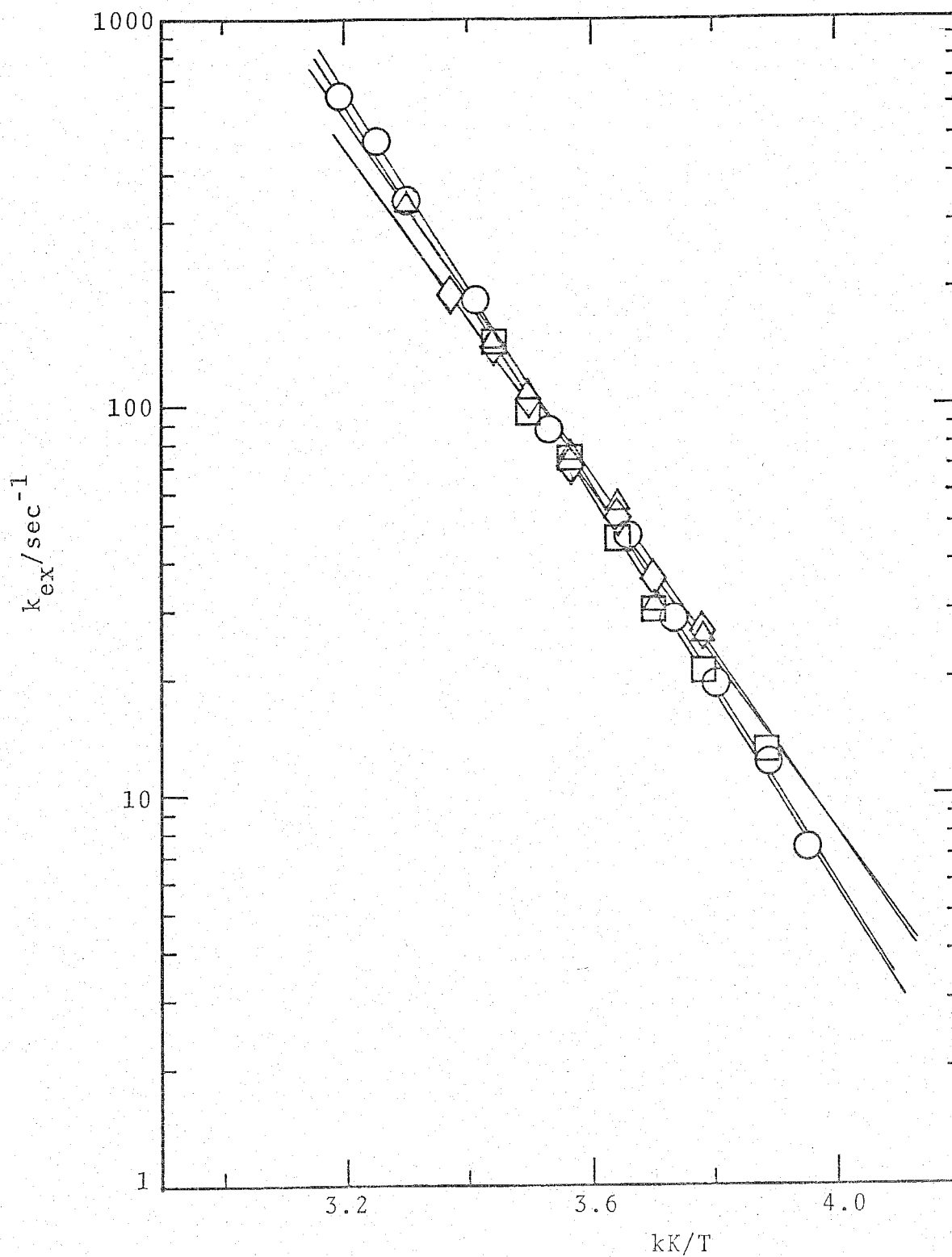
Fig. 5. Semilogarithmic plots of k_{ex} against the reciprocal temperature for the exchange of DMSO in $UO_2(acac)_2DMSO$ in CD_3COCD_3. The symbols of ◯ , △ , ☐ , and ◇ correspond to (i), (ii), (iii), and (iv) in Table 1.

Table 2. Solution compositions and kinetic parameters for the exchange of DMSO in $UO_2(acac)_2DMSO$ in CD_3COCD_3

Solution	$[UO_2(acac)_2DMSO]$ 10^{-2} M	$[DMSO]^a$ M	$[CD_3COCD_3]$ M	$\Delta H^{\ddagger}$ kJ mol^{-1}	$\Delta S^{\ddagger}$ JK^{-1}mol^{-1}	$k_{ex}(25°C)^b$ 10^2 sec^{-1}
i	2.98	0.0294	13.4	45.8 ± 0.4	-44.9 ± 1.7	2.89
ii	4.65	0.151	13.2	45.8 ± 0.8	-46.6 ± 2.9	2.36
iii	4.58	0.243	13.2	39.5 ± 0.8	-68.9 ± 2.9	2.07
iv	4.70	0.321	13.0	41.6 ± 1.7	-60.5 ± 5.9	2.43

a Added as DMSO.   b Calculated values from $\Delta H^{\ddagger}$ and $\Delta S^{\ddagger}$ at 25 °C.

of k_{ex} at 25 °C. It is obvious from Table 2 and Fig. 5 that the rate of DMSO exchange is independent of the DMSO concentrations.

B-2. Measurements in CD_2Cl_2 diluent

The DMSO exchange in CD_2Cl_2 was also measured in a similar way. Figure 6 shows the change of lineshape of DMSO methyl proton signals with temperature. Coalescence of the coordinated and free DMSO signals occurs as the temperature is raised. This phenomenon indicates that the DMSO exchange occurs between the coordinated and free sites. The best-fit τ-values for the exchange reaction and the corresponding computed lineshapes are shown at the right side of Fig. 6.

Figure 7 shows the semilogarithmic plots of k_{ex} against the reciprocal temperature for the solutions in Table 3. From this figure it is found that the first-order rate constants depend on the DMSO concentrations. The plots of k_{ex} against the DMSO concentrations are shown in Fig. 8 and this figure indicates that k_{ex} does not obey a simple linear relationship with the DMSO concentrations.

C. Mechanism

C-1. Exchange reaction in CD_3COCD_3 diluent

The rate of the DMSO exchange reaction in CD_3COCD_3 is independent of the DMSO concentrations, which indicates that the DMSO exchange proceeds through either D or I_d mechanism[14].
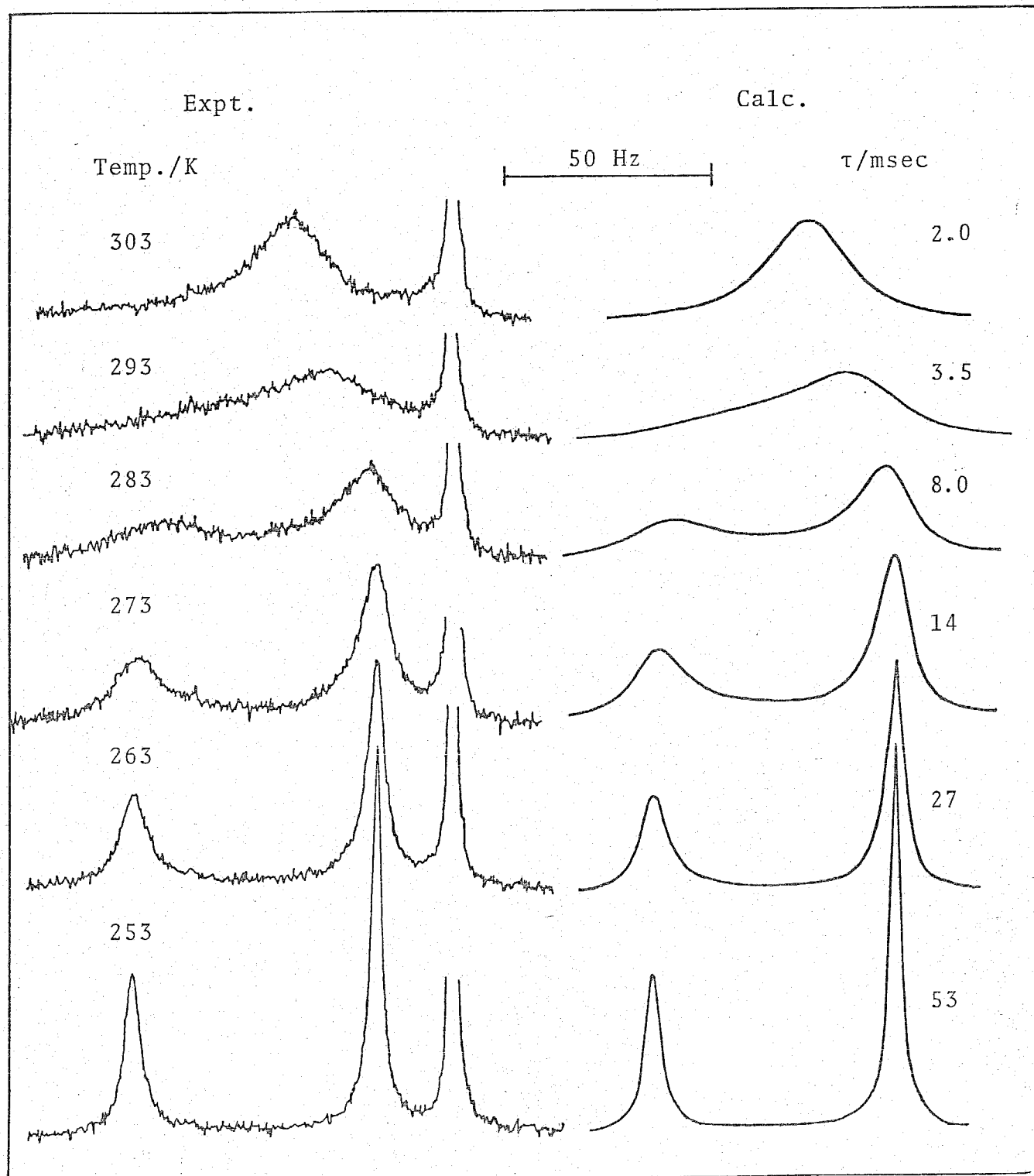
6. Experimental(left-hand side) and best-fit calculated ^{1}H NMR lineshapes of a solution consisting of $UO_2(acac)_2DMSO(0.0179$ M), DMSO(0.0282 M), and $CD_2Cl_2(15.8$ M). Temperatures and best-fit τ-values are shown at left- and right-hand sides of the figure,

Table 3. Solution compositions for the exchange of DMSO in $UO_2(acac)_2DMSO$ in CD_2Cl_2

Solution	$[UO_2(acac)_2DMSO]$ 10^{-2} M	$[DMSO]^a$ 10^{-2} M	$[CD_2Cl_2]$ M
i	1.79	2.82	15.7
ii	3.53	3.20	15.6
iii	4.05	5.63	15.4
iv	7.78	8.70	15.4
v	10.5	23.9	14.5

a Added as DMSO.
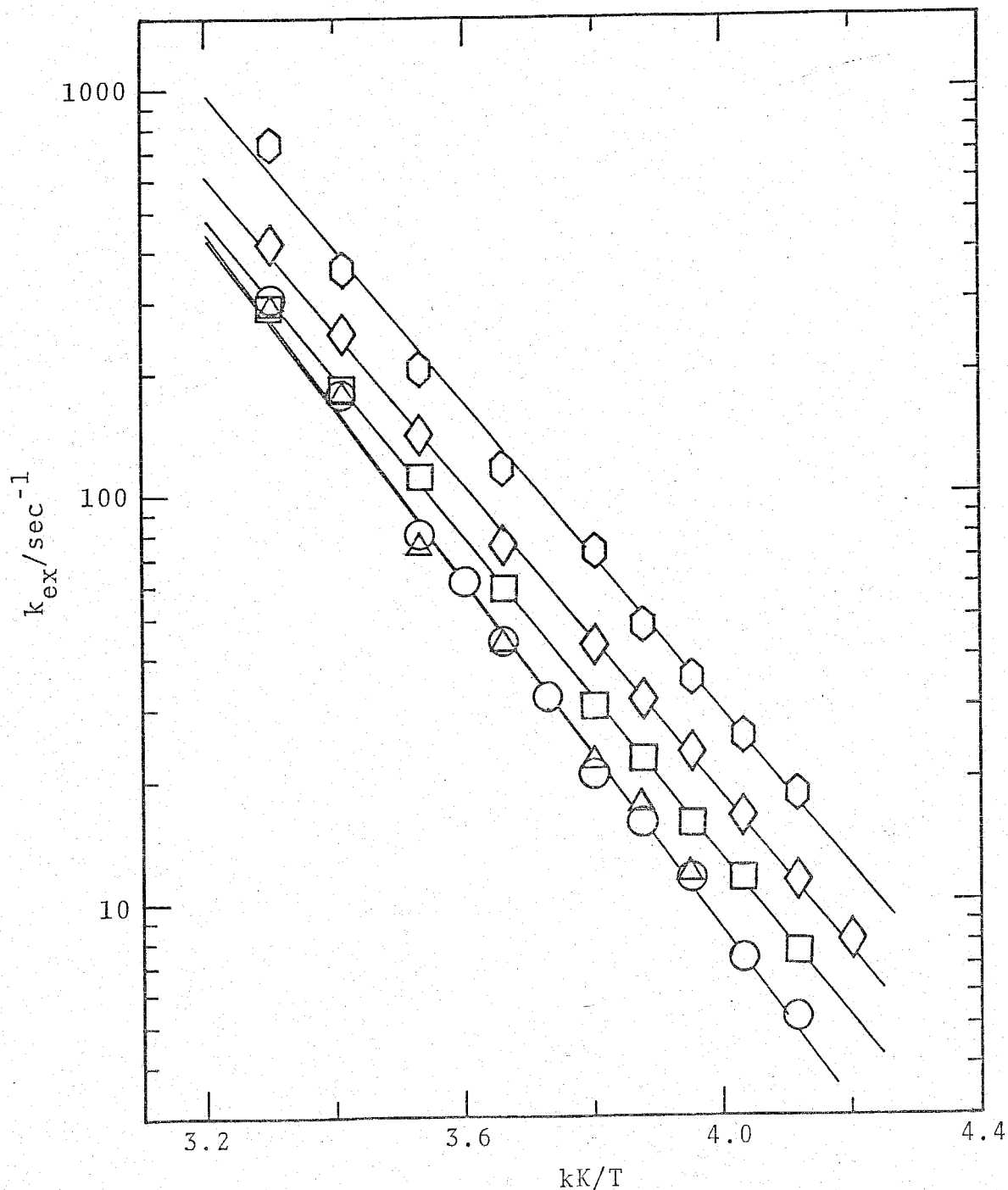
Fig. 7. Semilogarithmic plots of k_{ex} against the reciprocal temperature for the exchange of DMSO in $UO_2(acac)_2DMSO$ in CD_2Cl_2. The symbols of ○ , △ , □ , ◇ , and ⬡ correspond to (i), (ii), (iii), (iv), and (v) in Table 3.
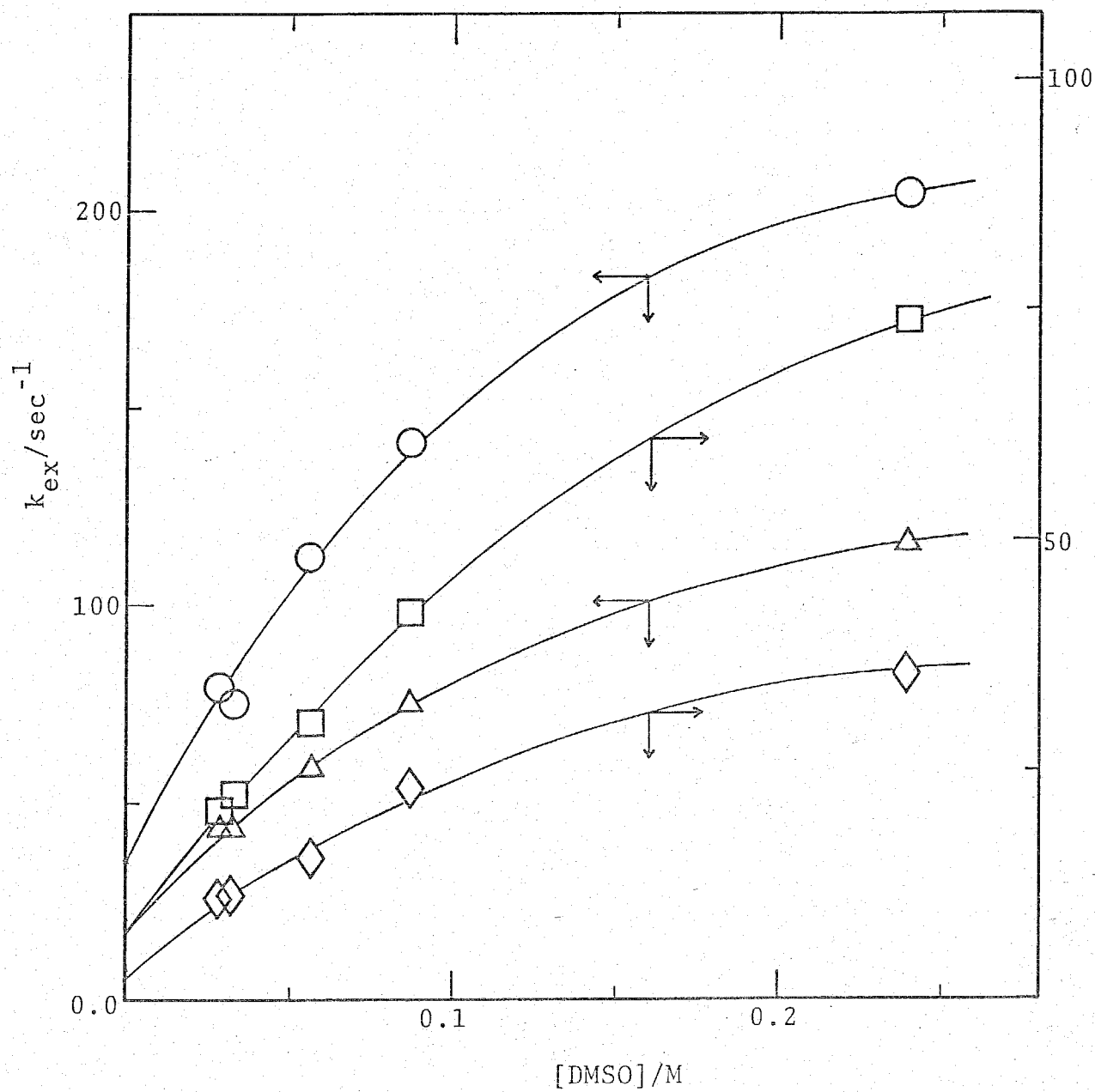
Fig. 8. Plots of k_{ex} vs. [DMSO] for the exchange of DMSO in $UO_2(acac)_2$DMSO in CD_2Cl_2. $\bigcirc$: 10 °C; $\triangle$: 0 °C; $\square$: -10 °C; $\diamondsuit$: -20 °C.

The D mechanism is expressed by Eq. (3)

$$UO_2(acac)_2DMSO + DMSO^* \xrightarrow[\text{slow}]{k_d} UO_2(acac)_2 + DMSO + DMSO^*$$

(3)

$$\xrightarrow{\text{fast}} UO_2(acac)_2DMSO^* + DMSO$$
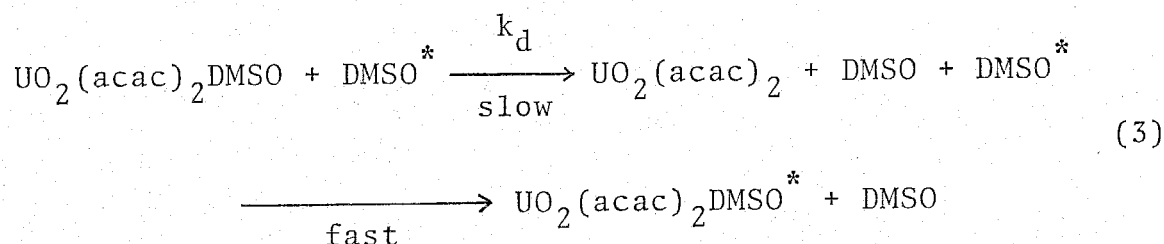
In this case, the rate-determining step is the dissociation of DMSO from $UO_2(acac)_2DMSO$ and an intermediate $UO_2(acac)$ having reduced coordination number is formed. Thus, the observed first-order rate constant, k_{ex}, is given by Eq. (4)

$$k_{ex} = k_d \tag{4}$$

In the I_d mechanism, overall processes are represented by Eq. (5)

$$UO_2(acac)_2DMSO + DMSO^* \underset{\text{fast}}{\overset{K_{os}}{\rightleftharpoons}} UO_2(acac)_2DMSO\text{---}DMSO^*$$

(5)

$$\xrightarrow[\text{slow}]{k_I} UO_2(acac)_2DMSO^*\text{---}DMSO \xrightarrow{\text{fast}} UO_2(acac)_2DMSO^* + DMSO$$
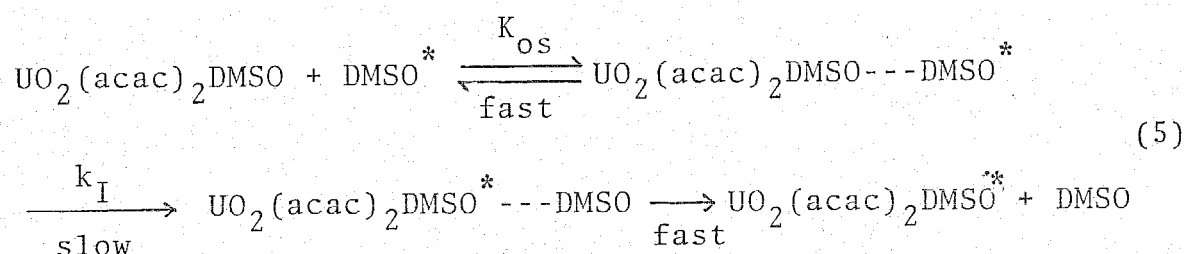
where K_{os} is the formation constant of the outer-sphere complex, $UO_2(acac)_2DMSO\text{---}DMSO^*$, and k_I is the rate constant for the inter-change of DMSO within the outer-sphere in which the incoming $DMSO^*$ is in the second coordination sphere. The rate-determining step is still governed by the dissociation of the coordinated DMSO and the observed first-order rate constant, k_{ex}, is given by Eq. (6)

$$k_{ex} = k_I K_{os} [DMSO]/(1 + K_{os}[DMSO]) \qquad (6)$$

which can be simplified to $k_{ex} = k_I$ when $K_{os}[DMSO] \gg 1$, and the exchange rate of DMSO becomes independent of DMSO concentrations. This appeared to compatible with the results of the DMSO exchnage reaction in CD_3COCD_3.

As mentioned before, the D mechanism should proceed via the four-coordinated intermediate in the equatorial plane, and is understandable from the fact that the four-coordinated uranyl complexes in equatorial plane exist. On the other hand, the condition of $K_{os}[DMSO] \gg 1$ should be satisfied in the I_d mechanism. This means a rather high value (> 100 M^{-1}) for K_{os} all over the concentration range employed in the experiments. However, it is not reasonable to assume such a large value of K_{os} because neither $UO_2(acac)_2DMSO$ nor DMSO is charged.

Therefore, it may be reasonable to assume that the DMSO exchange in CD_3COCD_3 proceeds through the D mechanism.

C-2. Exchange reaction in CD_2Cl_2 diluent

In CD_2Cl_2 diluent, the observed first-order rate constants depend on the DMSO concentrations but not linearly as shown in Fig. 8. Since the plots have the intercepts and the limiting values at high DMSO concentrations, it may be suggested that the DMSO exchange proceeds through both the D and I_d mechanisms which are given by Eqs. (3) and (5). From these mechanisms, the first-order rate constant, k_{ex}, can be expressed by Eq. (7)

$$k_{ex} = \frac{k_d + k_I K_{os}[DMSO]}{1 + K_{os}[DMSO]}$$

which can be simplified to $k_{ex} = k_d + k_I K_{os}[DMSO]$ when $K_{os}[DMSO] \ll 1$. This corresponds to the dependence of k_{ex} on the DMSO concentrations at the low concentration range. Equation (7) becomes $k_{ex} \approx k_I$ when $K_{os}[DMSO] \gg 1$ and this corresponds to the limiting values at the high concentration range. The values of k_d, k_I, and K_{os} were calculated by using the non-linear least-squares method and the results are listed in Table 4. The solid lines in Fig. 8 show the best-fit lines obtained from the calculated values of k_d, k_I, and K_{os}. The experimental data are in close agreement with the calculated values. Therefore, it is suggested that the DMSO exchange in CD_2Cl_2 occurs through both the D and I_d mechanisms. The activation parameters for k_d and k_I were obtained from the plots of $\log k_d$ and $\log k_I$ against the reciprocal temperature in Fig. 9 and are listed in Table 5.

Table 4. The values of k_d, k_I, and K_{os} at various temperatures for the exchange of DMSO in $UO_2(acac)_2$DMSO in CD_2Cl_2

Temp.	k_d	k_I	K_{os}
°C	sec^{-1}	$10^2\ sec^{-1}$	M^{-1}
10	35.5 ± 6.1	4.47 ± 1.17	4.6 ± 2.1
0	18.5 ± 0.8	1.86 ± 0.45	5.9 ± 0.4
-10	8.38 ± 0.44	1.65 ± 0.08	3.1 ± 0.2
-20	2.85 ± 0.67	0.57 ± 0.01	6.2 ± 0.5

Table 5. Kinetic parameters for k_d and k_I paths in the exchange of DMSO in $UO_2(acac)_2$DMSO in CD_2Cl_2

	$\Delta H^{\ddagger}$	$\Delta S^{\ddagger}$	$k(25\ °C)$[*]
	$kJ\ mol^{-1}$	$JK^{-1}mol^{-1}$	$10^2\ sec^{-1}$
k_d path	47.9 ± 5.2	-46.6 ± 11.2	1.02
k_I path	35.4 ± 12.4	-69.7 ± 20.5	10.1

[*] Calculated values from $\Delta H^{\ddagger}$ and $\Delta S^{\ddagger}$ at 25 °C.
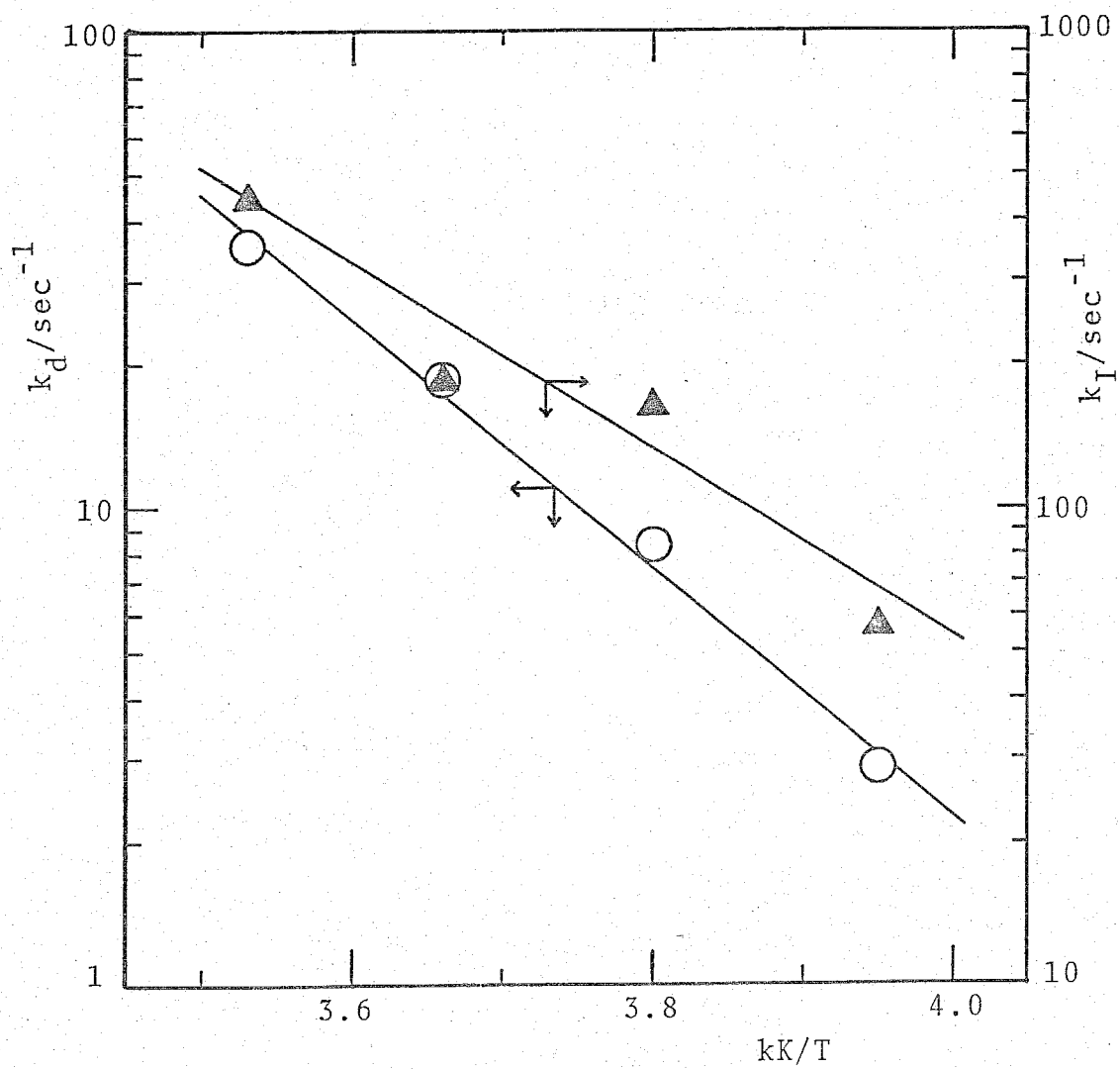
Fig. 9. Semilogarithmic plots of k_d and k_I against the
reciprocal temperature for the exchange of
DMSO in $UO_2(dbm)_2DMSO$ in CD_2Cl_2.

2. KINETIC STUDY OF THE EXCHANGE REACTION OF DIMETHYL SULFOXIDE
IN BIS(DIBENZOYLMETHANATO)DIOXO(DIMETHYL SULFOXIDE)URANIUM(VI)

A. Strucure of $UO_2(dbm)_2DMSO$ in Solutions

Figure 10 shows the ^1H NMR spectra of a solution containing $UO_2(dbm)_2DMSO$, DMSO, and CD_3COCD_3 at -30 and +30 °C. In the spectrum at -30 °C, (a) and (b) signals can be assigned to the methyl protons of free and coordinated DMSO, respectively. The signals (c) and (d) can be assigned to the 3-H protons and the protons on benzene rings of coordinated dbm, respectively.

The area ratio of (d) to (c) to (b) was 10 : 1 : 3 and this ratio was constant in solutions of various compositions. The signal for the 3-H protons of coordinated dbm is a singlet as seen in Fig. 10. These facts indicate that the two di-benzoylmethanate ions and one DMSO molecule coordinate to the uranyl ion, where dbm acts as a bidentate ligand and DMSO bonds though oxygen.

Similar spectra were observed in solutions containing $UO_2(dbm)_2DMSO$, DMSO, and CD_2Cl_2 as shown in Fig. 11. The symbols of (a), (b), (c), and (d) correspond to those in Fig. 10. Consequently, $UO_2(dbm)_2DMSO$ in CD_3COCD_3 and CD_2Cl_2 appeares to have a pentagonal bipyramidal structure.
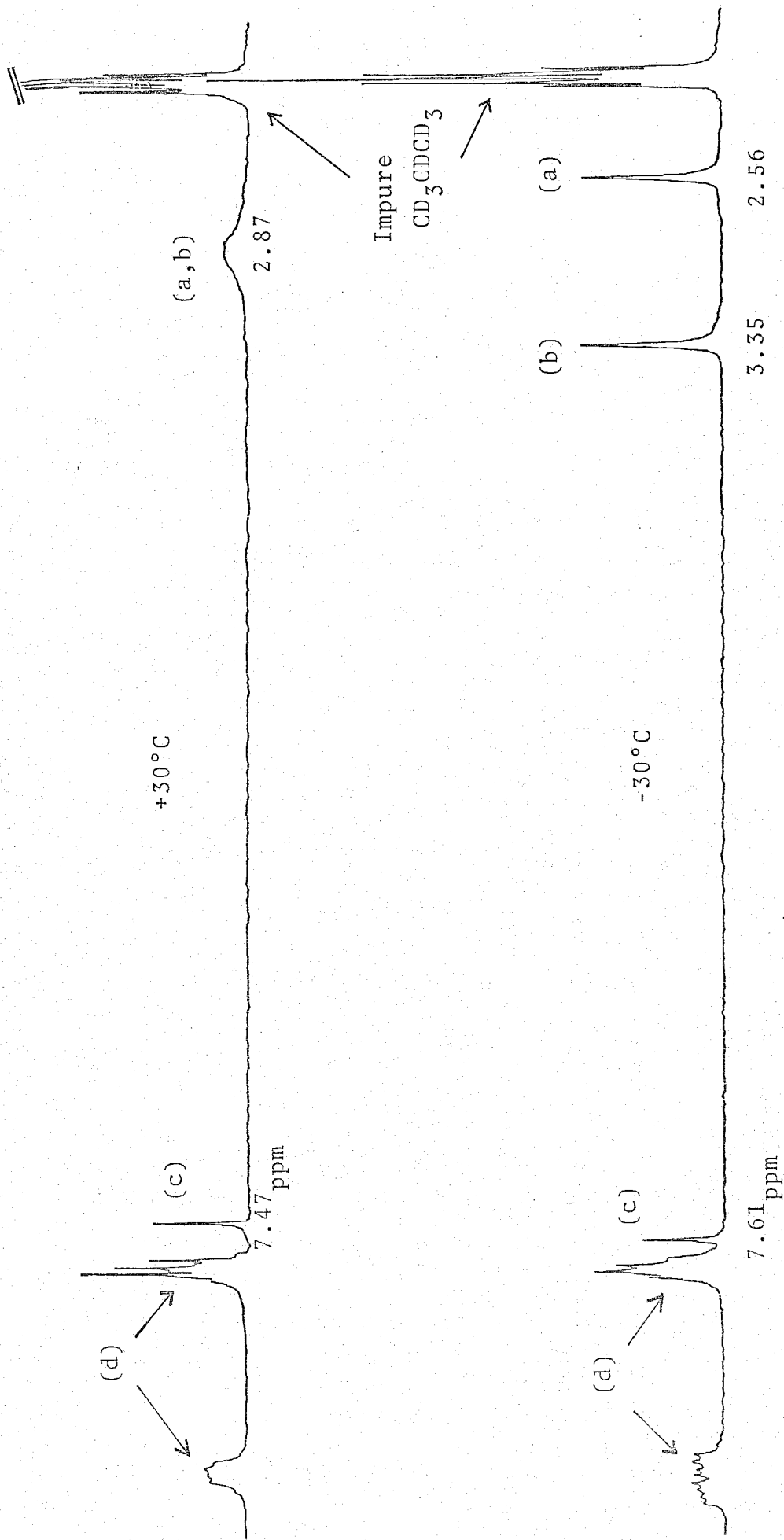
Fig. 10. The ^1H NMR spectra of a solution consisting of $UO_2(dbm)_2DMSO(0.0117 \text{ M})$, $DMSO(0.0115 \text{ M})$, $CD_3COCD_3(13.5 \text{ M})$ at -30 °C and +30 °C, respectively.
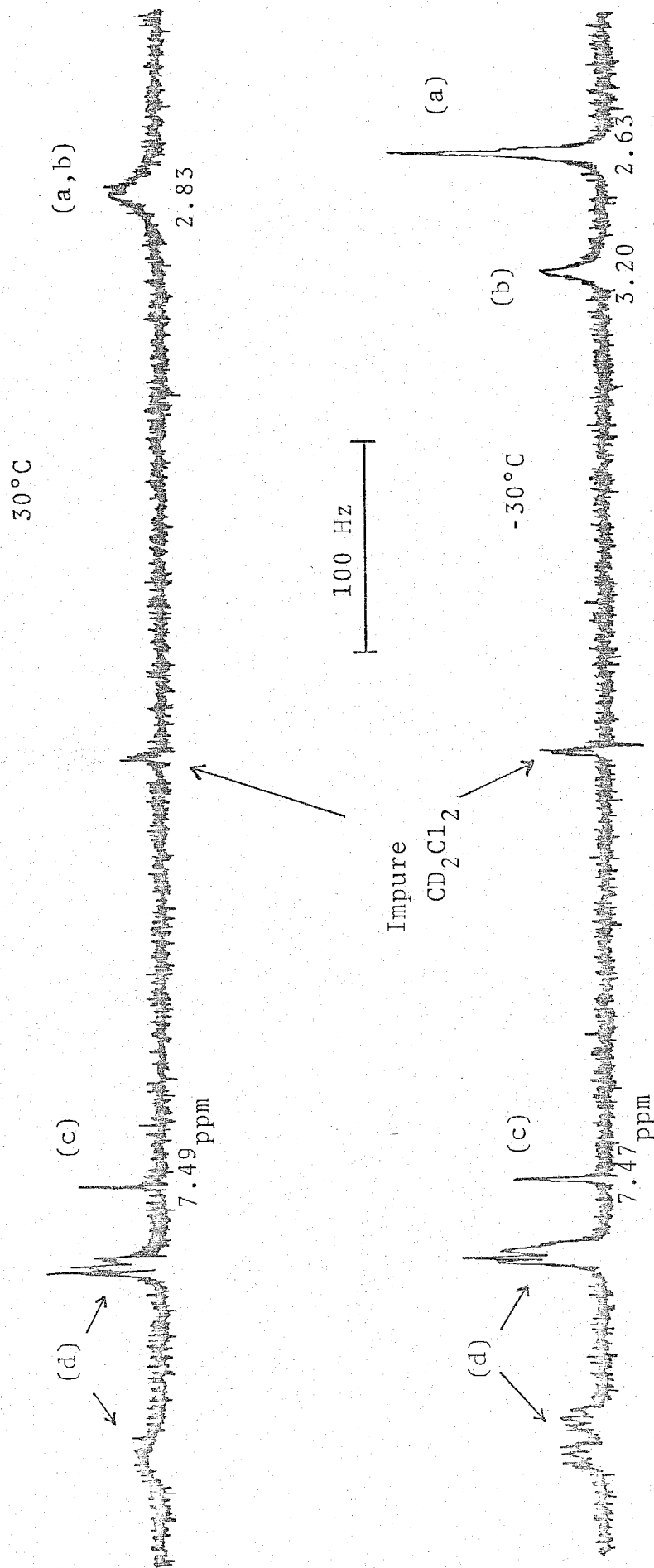
Fig. 11. The ^1H NMR spectra of a solution consisting of $UO_2(dbm)_2DMSO(0.0639$ M), DMSO(0.124 M), $CD_2Cl_2(14.8$ M) at -30 °C and +30 °C, respectively.

B. Exchange Reaction of DMSO in $UO_2(dbm)_2DMSO$

B-1. Measurements in CD_3COCD_3 diluent

From Fig. 10, it is expected that the exchange reaction of DMSO in $UO_2(dbm)_2DMSO$ complex occurs between the coordinated and free sites because two methyl proton signals of free and coordinated DMSO are observed at -30 °C, while the only one signal of the DMSO methyl protons is observed at +30 °C. The measurements of the change of lineshape were conducted at various temperatures, and the results are shown at the left side of Fig. 12, which show that the prediction is justified. The best-fit τ-values at each temperature were determined by the method described in Chapter II and are shown together with the corresponding lineshapes at the right side of Fig. 12. The first-order exchange rate constant, k_{ex}, was calculated by Eq. (21) in Chapter II, which is expressed by Eq. (8).

$$k_{ex} = rate/[UO_2(dbm)_2DMSO]$$

$$= (kT/h)\exp(-\Delta H^{\ddagger}/RT)\exp(\Delta S^{\ddagger}/R) \qquad (8)$$

The same measurements were carried out for other solutions listed in Table 6. The obtained k_{ex} values are semilogarithmically plotted against the reciprocal temperature as shown in Fig. 13. The values of activation parameters are given in Table 6 together with the values of k_{ex} at -15 and 25 °C. Table 6 and Fig. 13 indicate that the rate of DMSO exchange in $UO_2(dbm)_2$-DMSO is independent of the free DMSO concentrations.
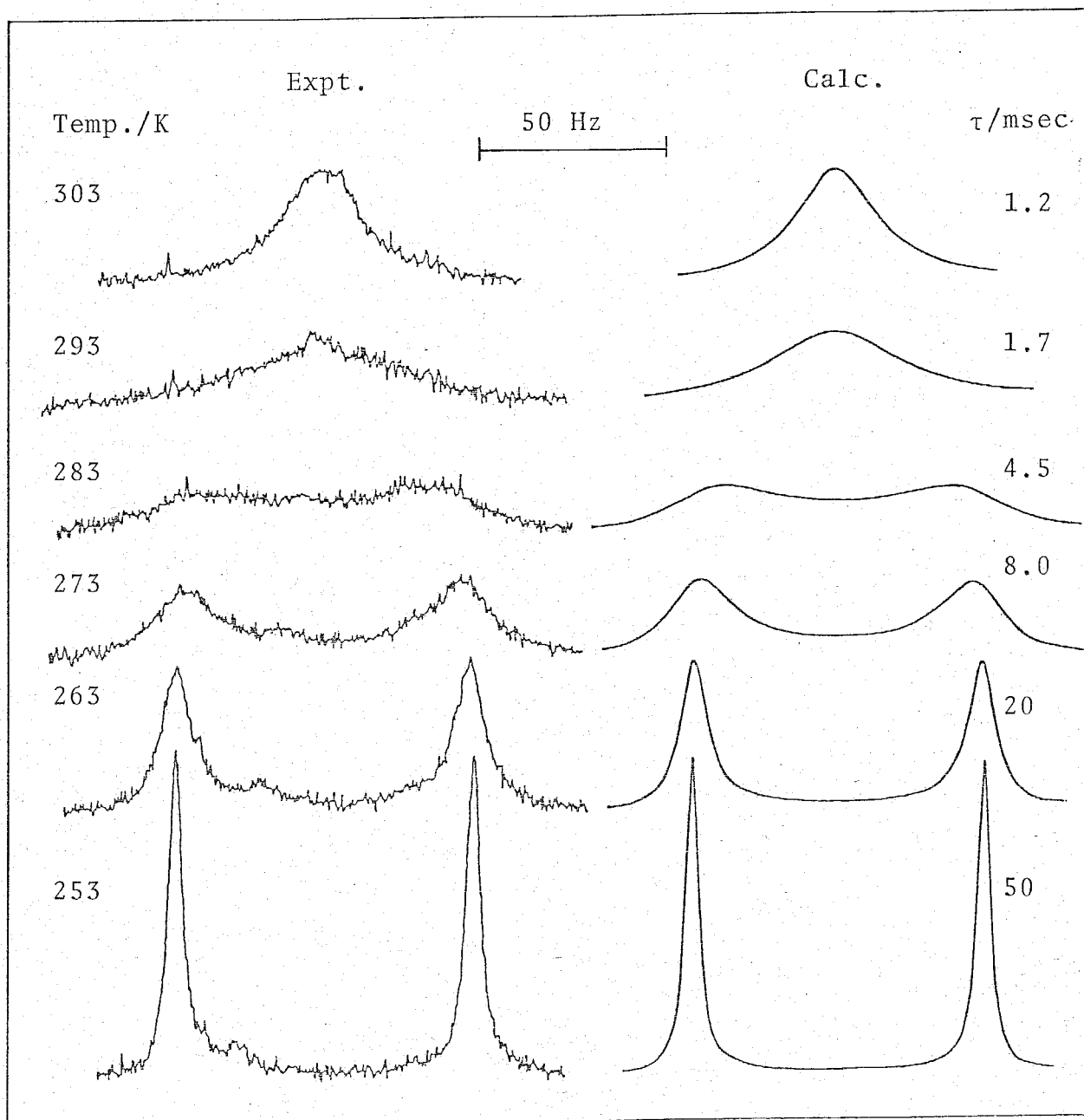
Fig. 12. Experimental(left-hand side) and best-fit calculated ^{1}H NMR lineshapes of a slution consisting of $UO_2(dbm)_2DMSO$ (0.0117 M), DMSO(0.0115 M), and CD_3COCD_3(13.5 M). Temperatures and best-fit τ-values are shown at left- and right-hand sides of the figure, respectively.

Table 6. Solution compositions and kinetic parameters for the exchange of DMSO in $UO_2(dbm)_2DMSO$ in CD_3COCD_3

Solution	$[UO_2(dbm)_2DMSO]$ 10^{-2} M	$[DMSO]^a$ 10^{-2} M	$[CD_3COCD_3]$ M	$\Delta H^{\ddagger}$ kJ mol^{-1}	$\Delta S^{\ddagger}$ JK^{-1}mol^{-1}	$k_{ex}(-15°C)$ 10 sec^{-1}	$k_{ex}(25°C)^b$ 10^2 sec^{-1}
i	1.17	1.15	13.5	44.5 ± 0.8	-47.9 ± 2.5	1.87 ± 0.10	3.37
ii	2.64	3.84	13.3	44.5 ± 0.4	-46.2 ± 2.1	2.13 ± 0.05	3.92
iii	3.10	6.78	13.1	43.3 ± 0.4	-50.8 ± 2.1	2.03 ± 0.21	3.68

a Added as DMSO.   b Calculated values from $\Delta H^{\ddagger}$ and $\Delta S^{\ddagger}$ at 25 °C.
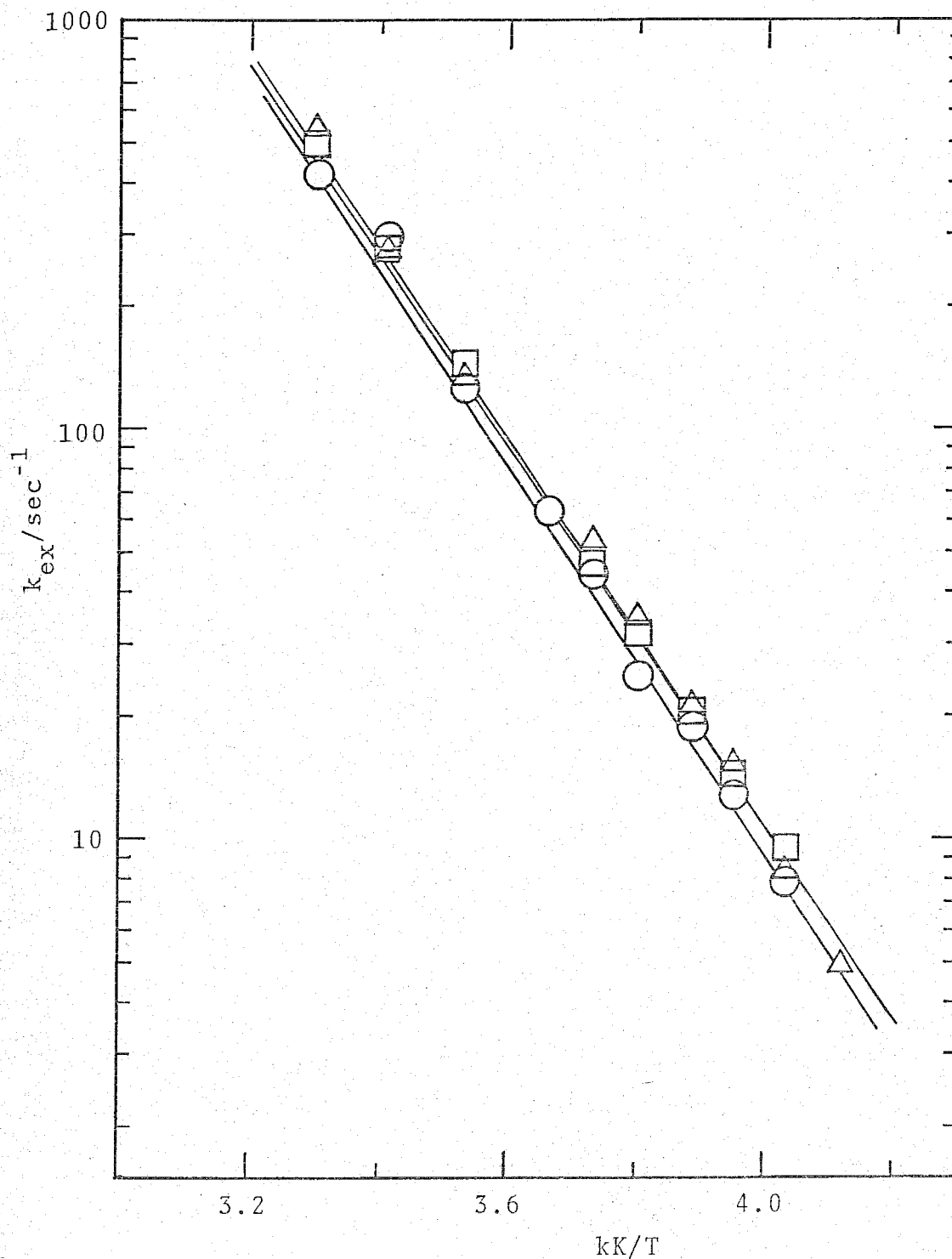
Fig. 13. Semilogarithmic plots of k_{ex} against the reciprocal temperature for the exchange of DMSO in $UO_2(dbm)_2DMSO$ in CD_3COCD_3. The symbols of $\bigcirc$, $\triangle$, and $\square$ correspond to (i), (ii), and (iii) in Table 6.

B-2. Measurements in CD_2Cl_2 diluent

In Fig. 11, ^{1}H NMR spectra of a solution containing $UO_2(dbm)_2DMSO$, DMSO, and CD_2Cl_2 are shown and suggest a similar exchange reaction to that in CD_3COCD_3. The changes of lineshape with temperature are given at the left side of Fig. 14, and it is noted that the DMSO exchange occurs between the coordinated and free sites. The best-fit τ-values at each temperature were obtained by the same method as mentioned before and are shown at the right side of Fig. 14 with the corresponding lineshapes. The same measurements were made for other solutions listed in Table 7. The logarithms of k_{ex} were plotted against the reciprocal temperature as shown in Fig. 15. It is seen that the value of k_{ex} increases as the free DMSO concentration increases. This DMSO dependence is more clearly seen in Fig. 16, where k_{ex} value was plotted against the free DMSO concentration. Figure 16 indicates that k_{ex} can be expressed by Eq. (9).

$$k_{ex} = k_1 + k_2[DMSO] \tag{9}$$

The values of k_1 and k_2 obtained from the intercepts and the slopes of the plots in Fig. 16, respectively, are listed in Table 8. The activation parameters for k_1 and k_2 paths were obtained from the plots of log k_1 and log k_2 against the reciprocal temperature in Fig. 17 and are listed in Table 9.
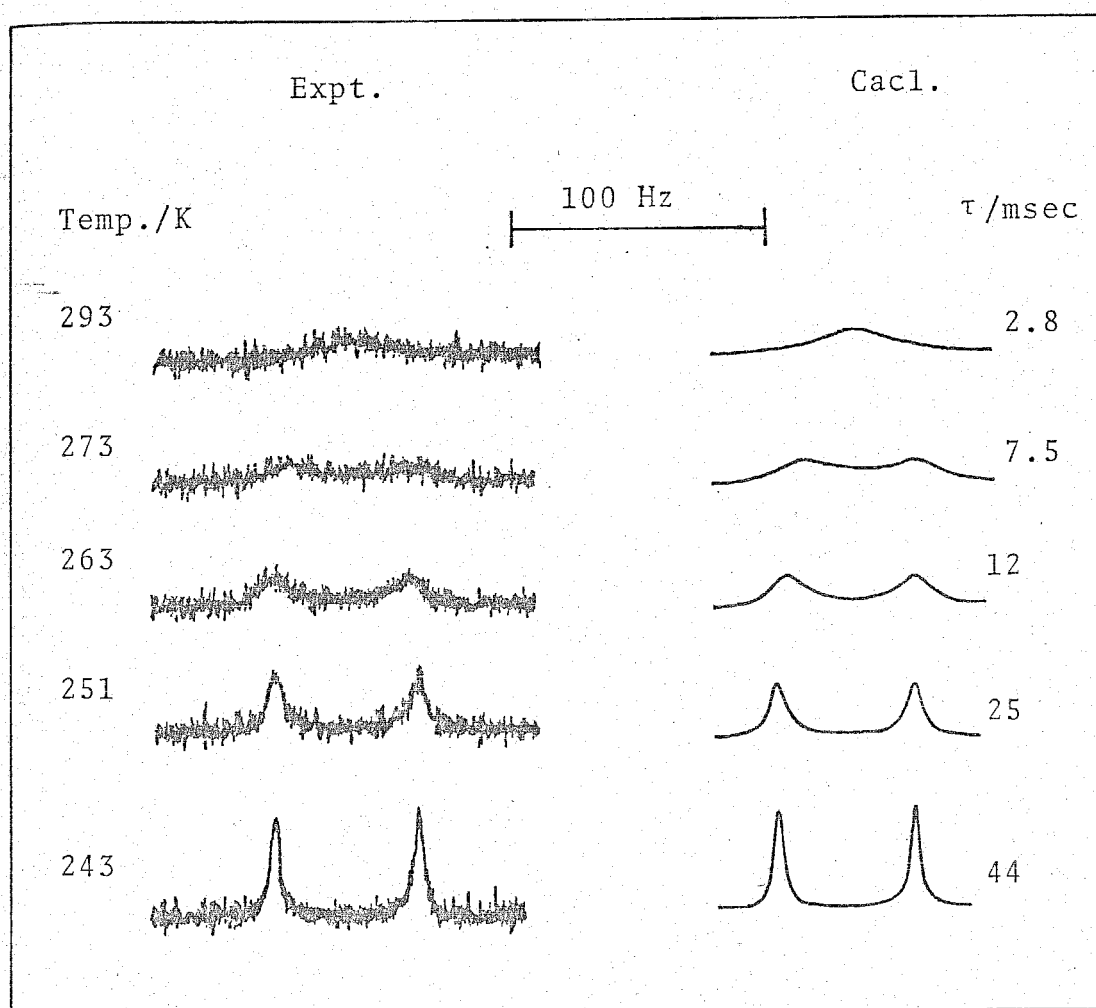
3. 14. Experimental(left-hand side) and best-fit calculated ^1H NMR lineshapes of a solution consisting of $UO_2(dbm)_2DMSO(0.0637$ M$)$, DMSO(0.0627 M), and $CD_2Cl_2(14.8$ M$)$. Temperatures and best-fit τ-values are shown at left- and right-hand sides of the figure, respectively.
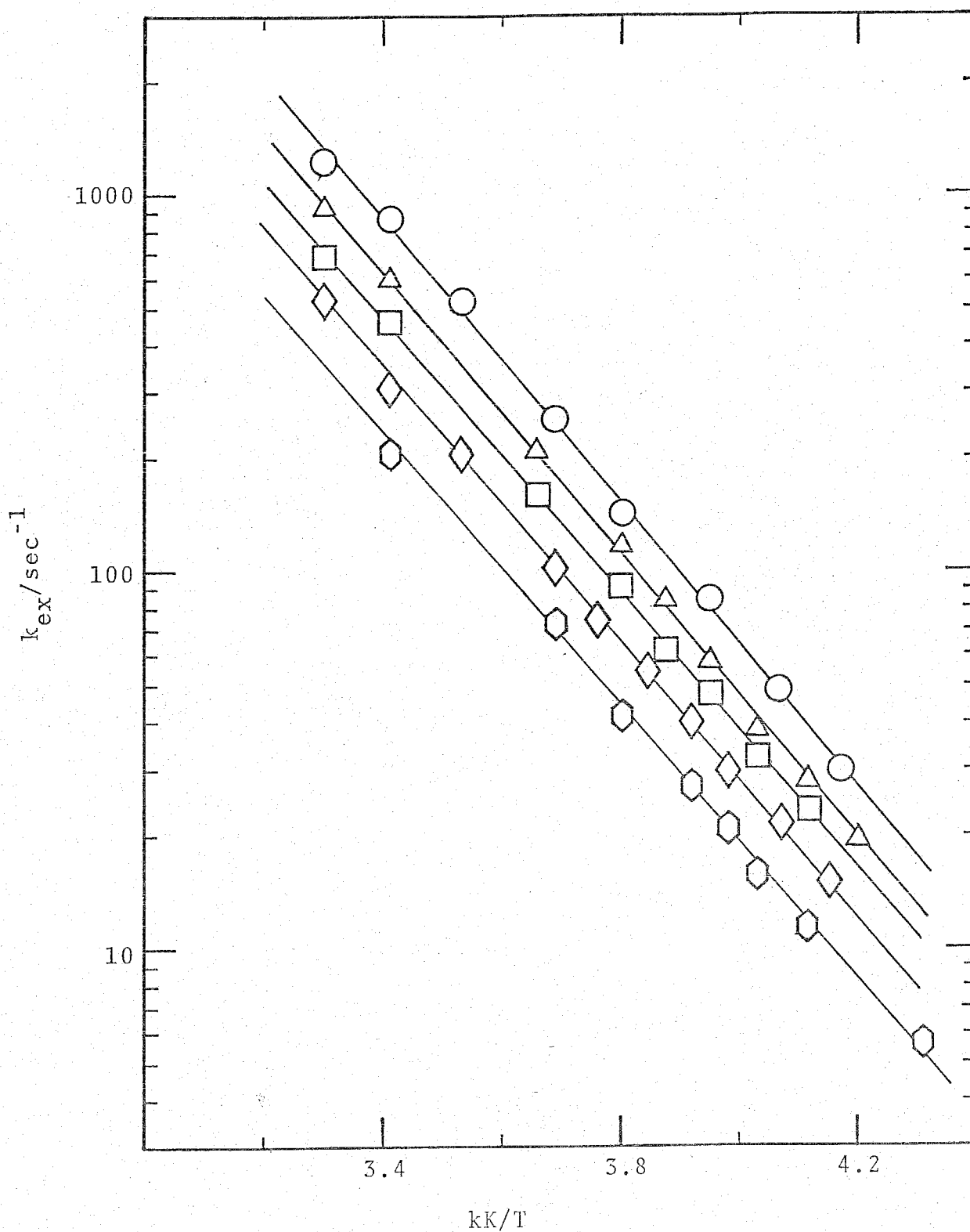
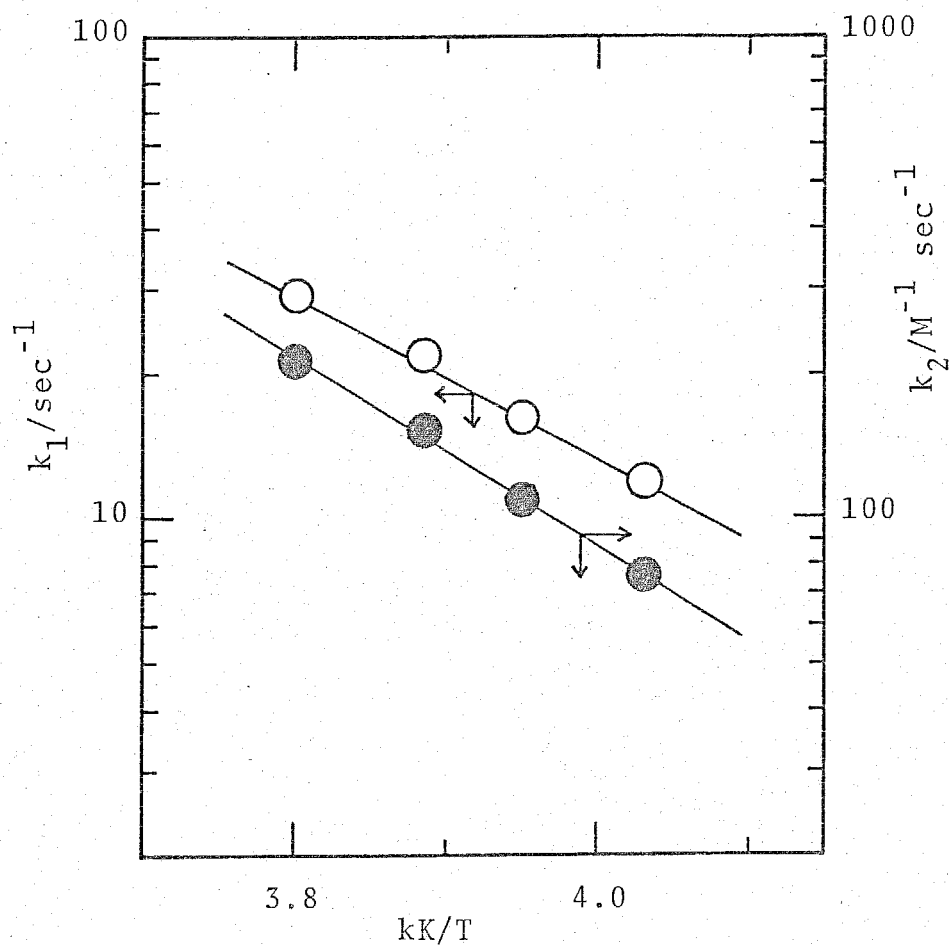Fig. 15. Semilogarithmic plots of k_{ex} against the reciprocal temperature for the exchange of DMSO in $UO_2(dbm)_2DMSO$ in CD_2Cl_2. The symbols of ⬡ , ◇ , □ , △ , and ◯ correspond to (i), (ii), (iii), (iv), and (v) in

Table 7.

Table 7. Solution compositions for the exchange of

DMSO in $UO_2(dbm)_2DMSO$ in CD_2Cl_2

Solution	$\dfrac{[UO_2(dbm)_2DMSO]}{10^{-2} \; M}$	$\dfrac{[DMSO]^a}{M}$	$\dfrac{[CD_2Cl_2]}{M}$
i	6.37	0.0627	14.8
ii	6.39	0.124	14.8
iii	6.37	0.266	14.8
iv	6.36	0.376	14.7
v	6.31	0.499	14.7

[a] Added as DMSO.

Table 8. The values of k_1 and k_2 at various

temperatures for the exchange of DMSO

in $UO_2(dbm)_2DMSO$ in CD_2Cl_2

$\dfrac{Temp.}{°C}$	$\dfrac{k_1}{10 \; sec^{-1}}$	$\dfrac{k_2}{10^2 \; M^{-1}sec^{-1}}$
-10	2.91 ± 0.44	2.12 ± 0.14
-15	2.18 ± 0.33	1.53 ± 0.11
-20	1.62 ± 0.25	1.09 ± 0.08
-25	1.19 ± 0.18	0.76 ± 0.06
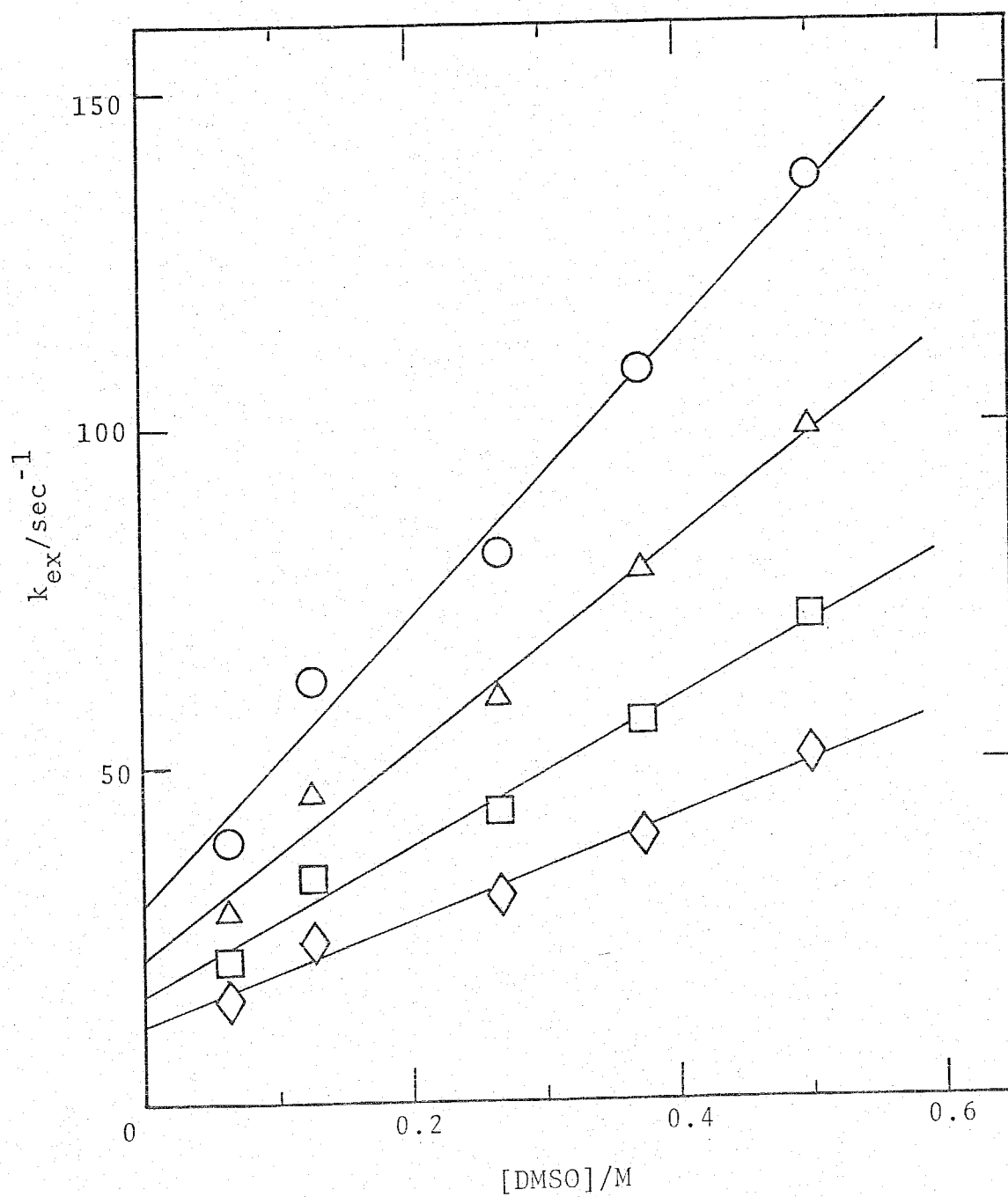
Fig. 16. Plots of k_{ex} vs. [DMSO] for the exchange of DMSO in $UO_2(dbm)_2$DMSO in CD_2Cl_2. ◯ : -10 °C; △ : -15 °C; □ : -20 °C; ◇ : -25 °C.

Fig. 17. Semilogarithmic plots of k_1 and k_2 against the reciprocal temperature for the exchange of DMSO in $UO_2(dbm)_2DMSO$ in CD_2Cl_2.

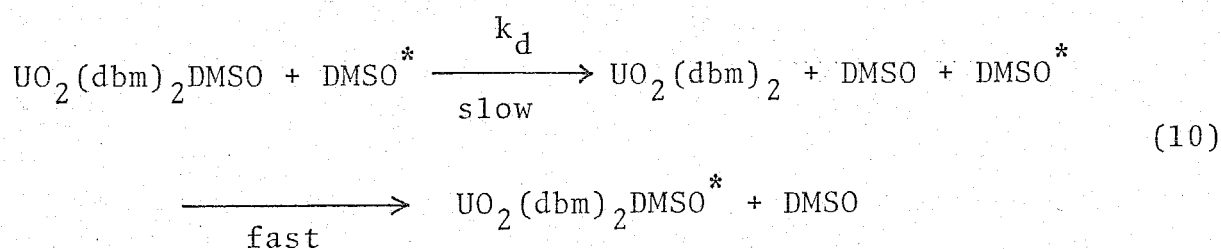Table 9. Kinetic parameters for the k_1 and k_2 paths in the exchange of DMSO in $UO_2(dbm)_2DMSO$ in CD_2Cl_2

	$\Delta H^{\ddagger}$	$\Delta S^{\ddagger}$	$k(25\ °C)^{*}$
	$kJ\ mol^{-1}$	$JK^{-1}mol^{-1}$	sec^{-1}
k_1 path	29.6 ± 2.2	-104.2 ± 8.6	1.74×10^{2}
k_2 path	34.9 ± 0.6	-67.2 ± 2.4	$1.62 \times 10^{3}/M^{-1}$

*Calculated values from $\Delta H^{\ddagger}$ and $\Delta S^{\ddagger}$ at 25 °C.

C. Mechanism

C-1. Exchange reaction in CD_3COCD_3 diluent

The rate of DMSO exchange reaction is independent of the free DMSO concentration, which indicates that the DMSO exchange takes place through either D or I_d mechanism[14]. The D and I_d mechanisms are represented by Eqs. (10) and (11), respectively.

$$UO_2(dbm)_2DMSO + DMSO^* \xrightarrow[slow]{k_d} UO_2(dbm)_2 + DMSO + DMSO^* \tag{10}$$

$$\xrightarrow{fast} UO_2(dbm)_2DMSO^* + DMSO$$

and

$$UO_2(dbm)_2DMSO + DMSO^* \underset{fast}{\overset{K_{os}}{\rightleftharpoons}} UO_2(dbm)_2DMSO---DMSO^* \tag{11}$$

$$\xrightarrow[slow]{k_I} UO_2(dbm)_2DMSO^*---DMSO \xrightarrow{fast} UO_2(dbm)_2DMSO^* + DMSO$$
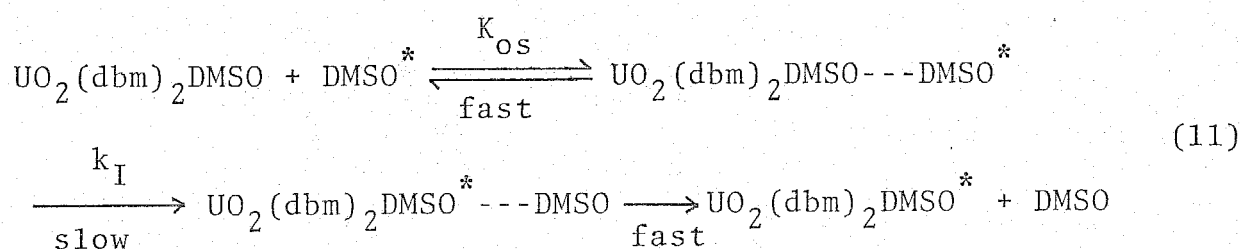
From these mechanisms, the following equations for k_{ex} can be derived. For the D mechanism,

$$k_{ex} = k_d \tag{12}$$

and for the I_d mechanism,

$$k_{ex} = k_I K_{os}[DMSO]/(1 + K_{os}[DMSO]) \tag{13}$$

which is simplified to $k_{ex} = k_I$ when $K_{os}[DMSO] \gg 1$.

Thus, the exchange rate of DMSO becomes independent of the free DMSO concentration, and this is compatible with the results of the DMSO exchange reaction in CD_3COCD_3.

However, it might not be reasonable to assume that the condition, $K_{os}[DMSO] \gg 1$, since the value of K_{os} should be larger than $200 \ M^{-1}$ to satisfy this condition over the present concentration range. Such a large value of K_{os} is unrealistic by considering that both of $UO_2(dbm)_2DMSO$ and DMSO are uncharged. On the contrary, it is most likely that the DMSO exchange proceeds through the D mechanism because the four-coordinated uranyl complexes in equatorial plane are well known[15-18].

C-2. Exchange reaction in CD_2Cl_2 diluent

In this diluent system, the DMSO exchange occurs through two paths, k_1 and k_2 paths. The k_1 path, where the excahnge rate is independent of the free DMSO concentration, is concluded to be the D mechanism as that of the DMSO exchange in CD_3COCD_3. The k_2 path exhibits a first-order dependence on the free DMSO concentration and seems to proceed through either I_d or A mechanism[14]. The A mechanism is expressed by Eq. (14).

$$UO_2(dbm)_2DMSO + DMSO^* \xrightarrow[slow]{k_a} UO_2(dbm)_2DMSO \cdot DMSO^*$$

$$\xrightarrow[fast]{} UO_2(dbm)_2DMSO^* + DMSO \tag{14}$$
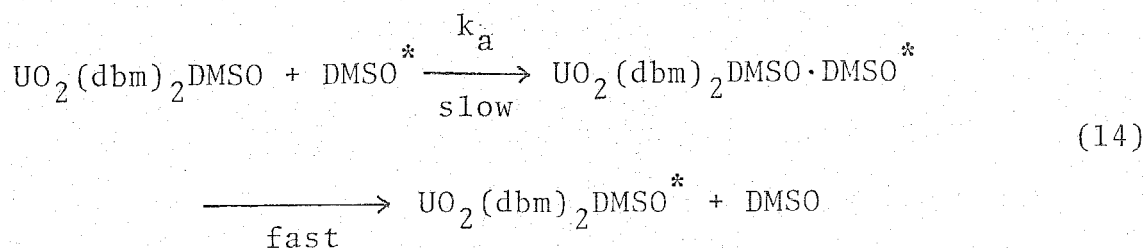
In this mechanism, the rate-determining step is the coordination of DMSO to the first coordination sphere of $UO_2(dbm)_2DMSO$ and

hence the six-coordinated intermediate in the equatorial plane should be formed. If the DMSO exchange proceeds through the D and A mechanisms indicated by Eqs. (10) and (14), the first-order rate constant, k_{ex}, can be expressed by Eq. (15).

$$k_{ex} = k_d + k_a[DMSO] \tag{15}$$

where k_d and k_a correspond to k_1 and k_2 in Eq. (9), respectively. On the other hand, if the DMSO exchange reaction takes place through the D and I_d mechanisms, k_{ex} is given by Eq. (16).

$$k_{ex} = \frac{k_d + k_I K_{os}[DMSO]}{1 + K_{os}[DMSO]} \tag{16}$$

When $K_{os}[DMSO] \ll 1$, Eq. (16) is reduced to Eq. (17).

$$k_{ex} = k_d + k_I K_{os}[DMSO] \tag{17}$$

where k_d and $k_I K_{os}$ correspond to k_1 and k_2 in Eq. (9), respectively. Both of Eqs. (15) and (17) are consistent with the experimental results.

It has been known that the uranyl ion forms the six-coordinated complexes in the equatorial plane with small ligands[19] as shown in Chapter III, but the A mechanism seems to be unlikely, because the coordinated dbm is a bulky chelating ligand and may hinder the approach of free DMSO to the first coordiantion

sphere of $UO_2(dbm)_2DMSO$. Moreover, DMSO also seems to be too bulky to form the six-coordinated intermediate in the equatorial plane.

The I_d mechanism requires the condition $K_{os}[DMSO] \ll 1$, which can be held in the exchange reaction because both DMSO and $UO_2(dbm)_2DMSO$ are uncharged and the value of K_{os} is considered to be smaller than 1 M^{-1} on the basis of the Fuoss equation[20]. Therefore, it is suggested that the DMSO exchange in CD_2Cl_2 proceeds through both the D and I_d mechanisms. If the value of K_{os} in the present reaction is larger than that in the DMSO exchange reaction in $UO_2(acac)_2DMSO$ in CD_2Cl_2, which was estimated about 5.0 M^{-1}, the exchange rate should become constant with the increase of the DMSO concentration in the present DMSO concentration range (0.0627-0.499 M) because the exchange rate of DMSO in $UO_2(acac)_2DMSO$ in CD_2Cl_2 becomes constant as the DMSO concentration incrases, where the DMSO concentration range is 0.0282 to 0.239 M. However, this tendency was not observed as shown in Fig. 16. This means that the value of K_{os} for the DMSO exchange reaction in $UO_2(dbm)_2DMSO$ is smaller than 5 M^{-1}, and may be due to the fact that dbm is a large chelating ligand than acac and make more difficult to form the outer-sphere complex.

D. Comparison with DMSO Exchange Reactions in Other Uranyl
   Complexes

The results of the DMSO exchange reactions in $UO_2(DMSO)_5^{2+}$,
$UO_2(acac)_2DMSO$, and $UO_2(dbm)_2DMSO$ in CD_3COCD_3 are summerized
in Table 10. The DMSO exchange reaction in $UO_2(DMSO)_5^{2+}$ proceeds
through two paths, k_1 and k_2 path, whose mechanisms were supposed
to be D and A mechanism, respectively, while the DMSO exchange
reaction in $UO_2(acac)_2DMSO$ and $UO_2(dbm)_2DMSO$ proceed through
only the D mechanism. This difference may be attributed to the
steric effect of bulky chelating ligands, acac and dbm, which
may hinder the approach of free DMSO to the first coordination
sphere of uranyl complexes. These results may support that the
k_2 path for the DMSO exchange reaction in $UO_2(DMSO)_5^{2+}$ proceeds
through the A mechanism.

The activation enthalpy for the DMSO exchange reaction
in $UO_2(DMSO)_5^{2+}$ is larger than those of the DMSO exchange reactions
in $UO_2(acac)_2DMSO$ and $UO_2(dbm)_2DMSO$. This fact can be inter-
preted by considering that the over-all positive charge on uranyl
ion decreases by the coordination of acetylacetonate and dibenzoyl-
methanate, and hence the bond-strength of U-DMSO in $UO_2(acac)_2-$
DMSO and $UO_2(dbm)_2DMSO$. This will make easier the dissociation
of DMSO from $UO_2(acac)_2DMSO$ and $UO_2(dbm)_2DMSO$ than from $UO_2(DMSO)_5^{2+}$.
The activation entropies for $UO_2(acac)_2DMSO$ and $UO_2(dbm)_2DMSO$
have large negative values, while that for $UO_2(DMSO)_5^{2+}$ is nearly
zero. This fact might suggest that the intermediate, $UO_2(DMSO)_4^{2+}$,
which should be formed in the D mechanism, would be formed more

easily and more stable than the respective intermediates, i.e.
$UO_2(acac)_2$ and $UO_2(dbm)_2$, formed in the DMSO exchange reactions
in $UO_2(acac)_2DMSO$ and $UO_2(dbm)_2DMSO$ in CD_3COCD_3, because the
bidentate ligands, acac and dbm, make difficult the formation
of the symmetrical intermediates in the equatorial plane.
Therefore, $\Delta S^{\ddagger}$ values for the exchange of DMSO in $UO_2(acac)_2DMSO$
and $UO_2(dbm)_2DMSO$ are much smaller than that of the DMSO exchange
reaction in $UO_2(DMSO)_5^{2+}$. As a result, the DMSO exchange rate
constants for $UO_2(acac)_2DMSO$ and $UO_2(dbm)_2DMSO$ are smaller than
that of the DMSO exchange in $UO_2(DMSO)_5^{2+}$ in spite of their small
values for $\Delta H^{\ddagger}$.

Table 10. Kinetic parameters for the exchange of DMSO
in various uranyl complexes

Complex	Mechanism	$\Delta H^{\ddagger}$ kJ mol^{-1}	$\Delta S^{\ddagger}$ $JK^{-1}mol^{-1}$	$k_{ex}(25°C)$ sec^{-1}
$UO_2(DMSO)_5^{2+}$	D	53.8 ± 2.4	6.3 ± 14.5	5.53×10^3
	A	39.1 ± 1.7	-28.1 ± 5.0	$3.22 \times 10^4 /M^{-1}$
$UO_2(acac)_2DMSO$	D	45.8 ± 0.8	-46.6 ± 2.9	2.36×10^2
$UO_2(dbm)_2DMSO$	D	44.5 ± 0.4	-46.2 ± 2.1	3.92×10^2

3. KINETIC STUDY OF THE EXCHANGE REACTION OF N,N-DIMETHYL-
   FORMAMIDE IN BIS(ACETYLACETONATO)DIOXO(N,N-DIMETHYLFORM-
   AMIDE)URANIUM(VI)

A. Structure of $UO_2(acac)_2DMF$ in Solutions

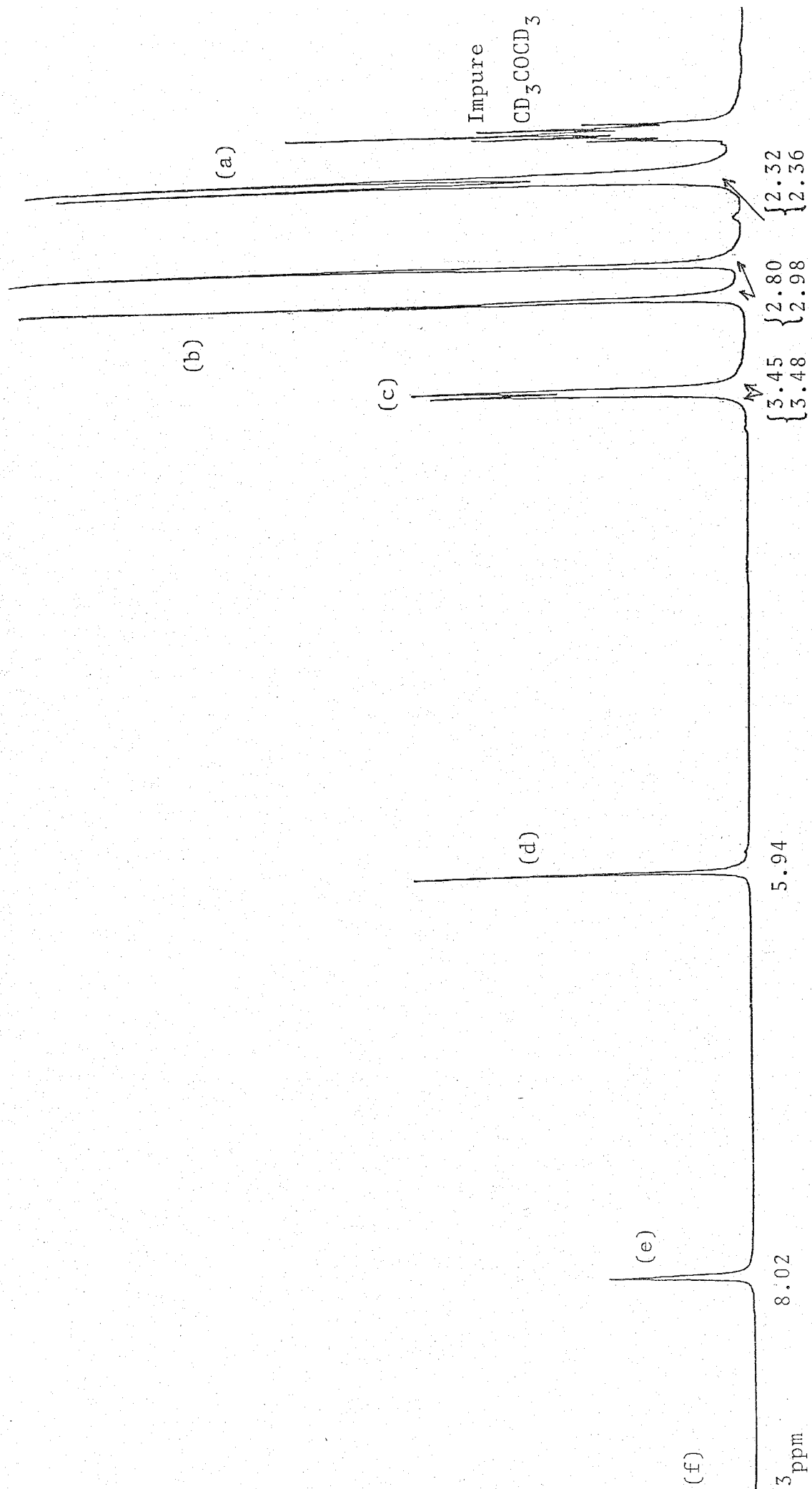 Figure 18 shows the ^1H NMR spectrum of a solution containing $UO_2(acac)_2DMF$, DMF, and CD_3COCD_3 at -50 °C. In the spectrum, the doublet of (a) and the singlet of (d) are assigned to the signals of methyl protons and of 3-H protons of coordinated acac, respectively, and the doublets of (b) and (c) and the singlets of (e) and (f) are the methyl protons and the formyl protons of free and coordinated DMF, respectively.

 The area ratio of (f) to (d) to (c) to (a) was 1 : 2 : 6 : 12, and this ratio remained constant in solutions of various compositions listed in Table 11. This fact indicates that the two acetylacetonate ions and one DMF molecule are coordinated to the uranyl ion. The doublet of the methyl protons of coordinated acac means that two acac are bidentates from the same reason as described before in the structure of $UO_2(acac)_2DMSO$. Furthermore, the singlet (d) supports that the coordinated acac is a bidentate. Comparison between the integrated areas for the doublet of (b) and (c), and those for the singlet of (e) and (f) shows that one DMF molecule is coordinated to a uranyl ion. Therefore, it is suggested that the structure of this complex in CD_3COCD_3 is pentagonal bipyramidal similar to the structure of $UO_2(acac)_2DMSO$ and $UO_2(acac)_2H_2O$.

The same results were also obtained from the ^{1}H NMR spectrum of a solution containing $UO_2(acac)_2DMF$, DMF, and CD_2Cl_2 as shown in Fig. 19, in which the symbols of (a), (b), (c), (d), (e), and (f) correspond to those in Fig. 19, and indicate that the structure of this complex in CD_2Cl_2 is also pentagonal bipyramidal.

The measurements of IR spectra support the results of the NMR studies. The IR spectra of $UO_2(acac)_2DMF$ were measured in CD_2Cl_2. The C-O stretching for DMF in the complex was observed at 1652 cm^{-1}, which is 27 cm^{-1} lower than that observed in pure DMF(1675 cm^{-1}). It has been known that the C-O stretching, so called Amide I, will shift to a lower side when DMF is coordinated through oxygen[21-23]. Therefore, the band of C-O stretching observed here indicates that DMF in the $UO_2(acac)_2DMF$ complex coordinates through oxygen. In addition, only one band corresponding to the carbonyl vibration of coordinated acac was observed at 1574 cm^{-1}. This indicates that both of acac in $UO_2(acac)_2DMF$ are coordinated as bidentates from the same reason as mentioned in the structure of $UO_2(acac)_2DMSO$[13].

On the basis of these findings, it is concluded that $UO_2(acac)_2DMF$ has a pentagonal bipyramidal structure in CD_3COCD_3 and CD_2Cl_2.

(a)

(b)

(c)

(d)

(e)

(f)

Impure
CD_3COCD_3

$\begin{cases} 2.32 \\ 2.36 \end{cases}$

$\begin{cases} 2.80 \\ 2.98 \end{cases}$

$\begin{cases} 3.45 \\ 3.48 \end{cases}$

5.94

8.02

3 ppm

18. The ^1H NMR spectrum of a solution consisting of $UO_2(acac)_2DMF(0.0661\ M)$, $DMF(0.112\ M)$, and $CD_3COCD_3\ (13.3\ M)$ at $-75\ °C$.
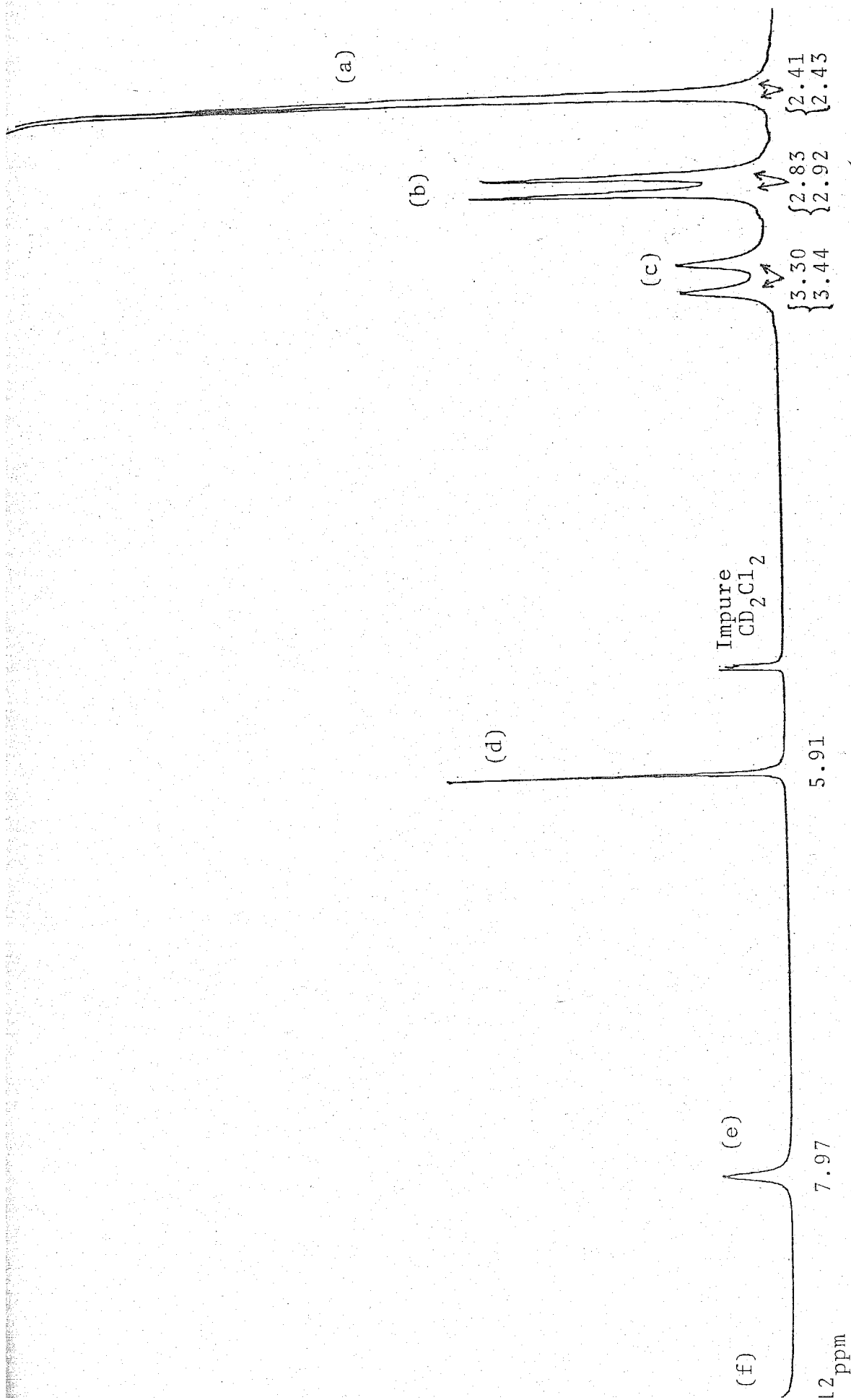
Fig. 19. The ^1H NMR spectrum of a solution consisting of $UO_2(acac)_2DMF(0.116$ M), $DMF(0.215$ M), and $CD_2Cl_2(14.7$ M) at -50 °C.

B. Exchange Reaction of DMF in $UO_2(acac)_2DMF$

B-1. Measurements in CD_3COCD_3 diluent

The measurements of the change of lineshape for formyl protons of DMF were made at various temperatures. The results are shown at the left side of Fig. 20 and found to be consistent with the DMF exchange between coordinated and free sites. The best-fit τ-values at each temperature were determined by the method described in Chapter II. The calculated lineshapes are shown with the best-fit τ-values at the right side of Fig. 20. The first-order exchange rate constant, k_{ex}, was calculated by Eq. (21) in Chapter II. In this case, k_{ex} is represented by Eq. (18).

$$k_{ex} = rate/[UO_2(acac)_2DMF]$$

$$= (kT/h)\exp(-\Delta H^{\ddagger}/RT)\exp(\Delta S^{\ddagger}/R) \qquad (18)$$

Similar measurements were performed on other solutions listed in Table 11. Figure 21 shows the plots of log k_{ex} against the reciprocal temperature for the exchange of DMF in $UO_2(acac)_2DMF$. The activation parameters obtained are listed in Table 11 together with the values of k_{ex} at 25 °C. From these results, it is found that the rate of DMF exchange is independent of the solution compositions.
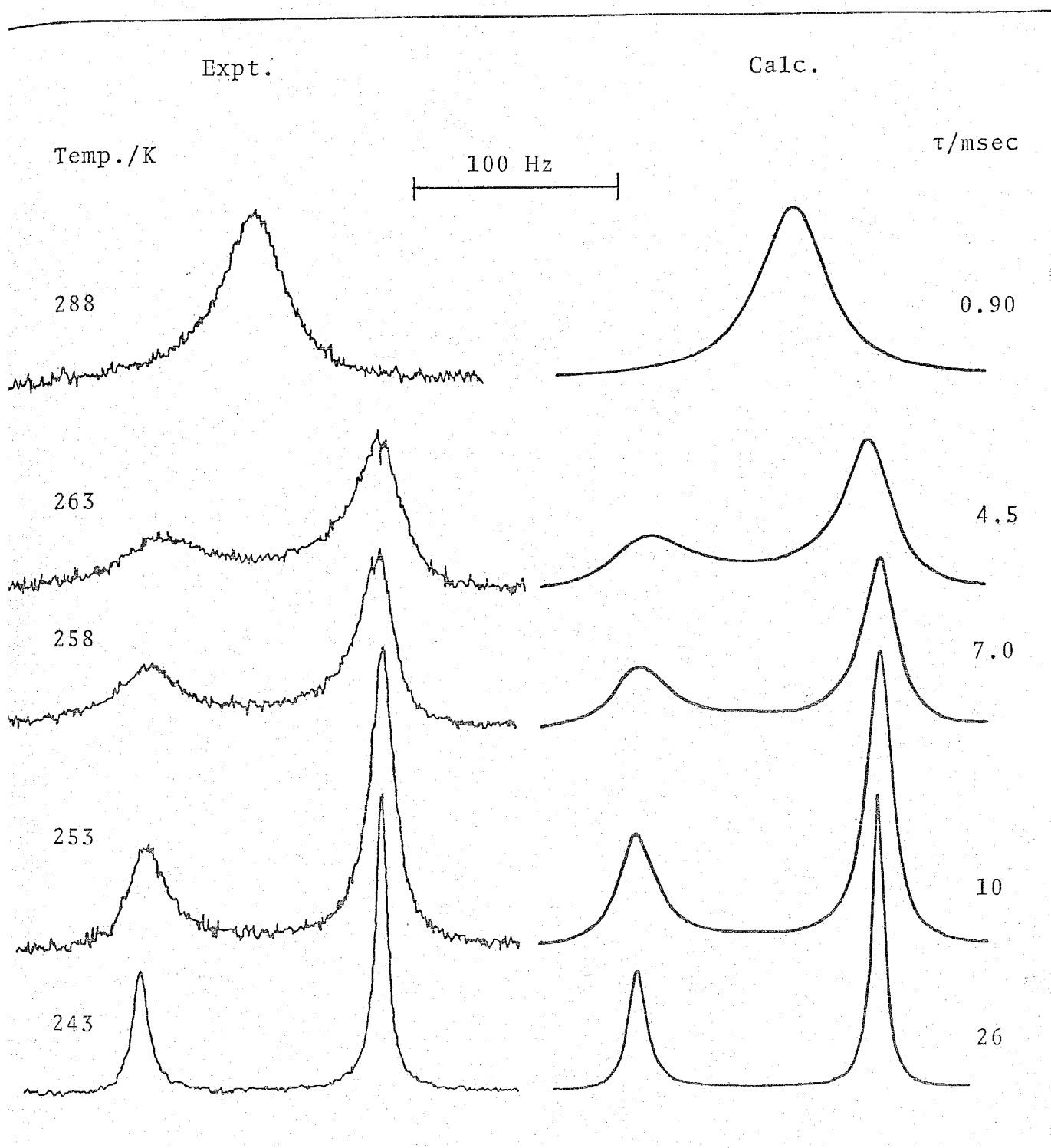
ig. 20. Experimental(left-hand side) and best-fit calculated ^{1}H NMR lineshapes of a solution consisting of $UO_2(acac)_2DMF(0.0661$ M), DMF(0.112 M), and $CD_3COCD_3(13.3$ M) . Temperatures and best-fit τ-values are shown at the left- and right-hand sides of the figure respectively

Table 11. Solution compositions and kinetic parameters for the exchange of DMF in $UO_2(acac)_2DMF$ in CD_3COCD_3

Solution	$[UO_2(acac)_2DMF]$ 10^{-2} M	$[DMF]^a$ 10^{-2} M	$[CD_3COCD_3]$ M	$\Delta H^{\ddagger}$ kJ mol^{-1}	$\Delta S^{\ddagger}$ J mol^{-1}K^{-1}	$k_{ex}(25 \ ^\circ C)^b$ 10^3sec^{-1}
i	3.25	3.83	13.6	42.0 ± 1.3	-45.8 ± 5.5	1.19
ii	6.45	6.57	13.4	42.0 ± 1.3	-46.2 ± 5.5	1.14
iii	6.61	11.2	13.3	43.7 ± 1.1	-38.6 ± 5.0	1.44

a Added as DMF. b Calculated values from $\Delta H^{\ddagger}$ and $\Delta S^{\ddagger}$ at 25 °C.
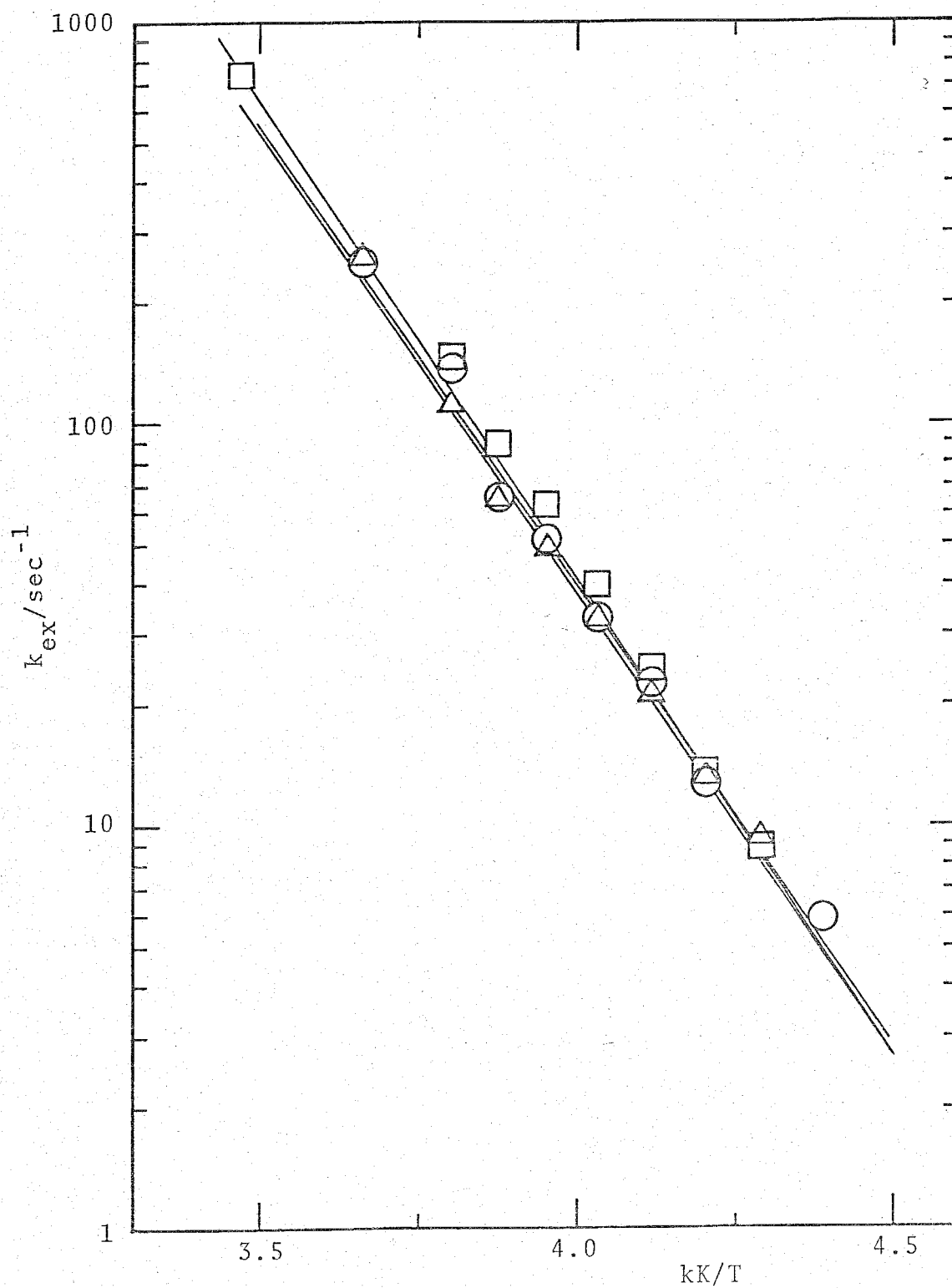
Fig. 21. Semilogarithmic plots of k_{ex} against the reciprocal temperature for the exchange of DMF in $UO_2(acac)_2DMF$ in CD_3COCD_3. The symbols of $\bigcirc$, $\triangle$, and $\square$ correspond to (i), (ii), and (iii) in Table 11.

B-2. Measurements in CD_2Cl_2 diluent

The measurements of the change of lineshape for formyl protons of DMF were done by varying temperature in soluions containing $UO_2(acac)_2DMF$, DMF, and CD_2Cl_2. The results are shown at the left-hand side of Fig. 22, which indicates that the DMF molecules exchange between the coordinated and free sites. The best-fit τ-values at each temperature are indicated at the right-hand side of Fig. 22. The first-order exchange rate constants are calculated from these τ-values and expressed by Eq. (18).

Similar measurements were carried out for the solutions listed in Table 12. The obtained k_{ex} are plotted semilogarithmically against the reciprocal temperature in Fig. 23. As seen in Fig. 23, the rate of DMF exchange seems to depend on the free DMF concentration. Figure 24 shows the plots of k_{ex} against the free DMF concentration and indicates that the DMF exchange proceeds through two paths, i.e. one is independent of the DMF concentration and another is a first-order dependence on DMF concentration. Thus k_{ex} can be expressed by Eq. (19).

$$k_{ex} = k_1 + k_2[DMF] \qquad (19)$$

The values of k_1 and k_2 are obtained from the intercepts and slopes in Fig. 24, respectively and listed in Table 13. The plots of $\log k_1$ and $\log k_2$ against the reciprocal temperature
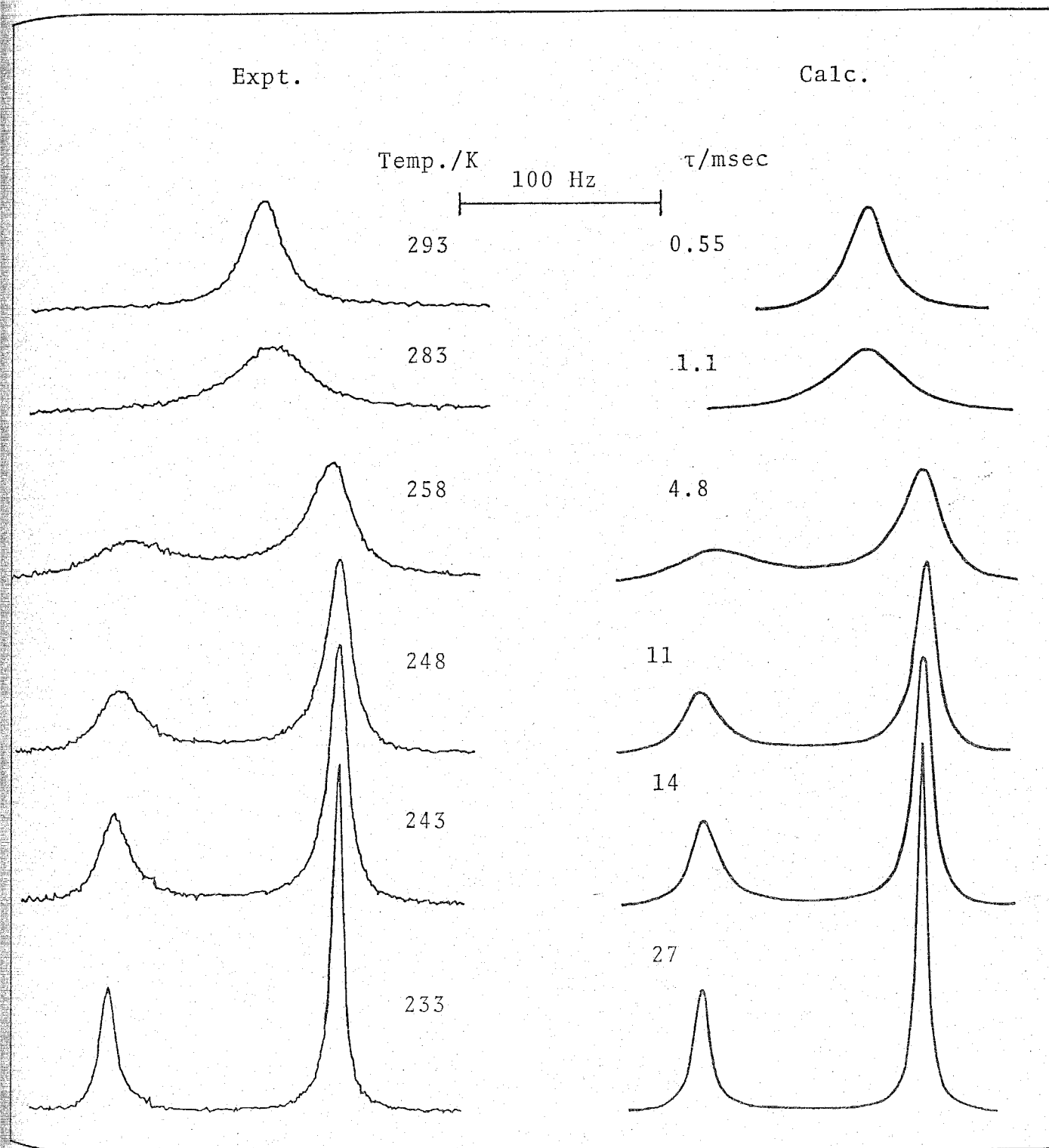
Fig. 22. Experimental(left-hand side) and best-fit calculated ^{1}H NMR lineshapes of a solution consisting of $UO_2(acac)_2DMF(0.116$ M), DMF(0.215 M), and $CD_2Cl_2(14.7$ M). Temperatures and best-fit τ-values are shown at the center of the figure.
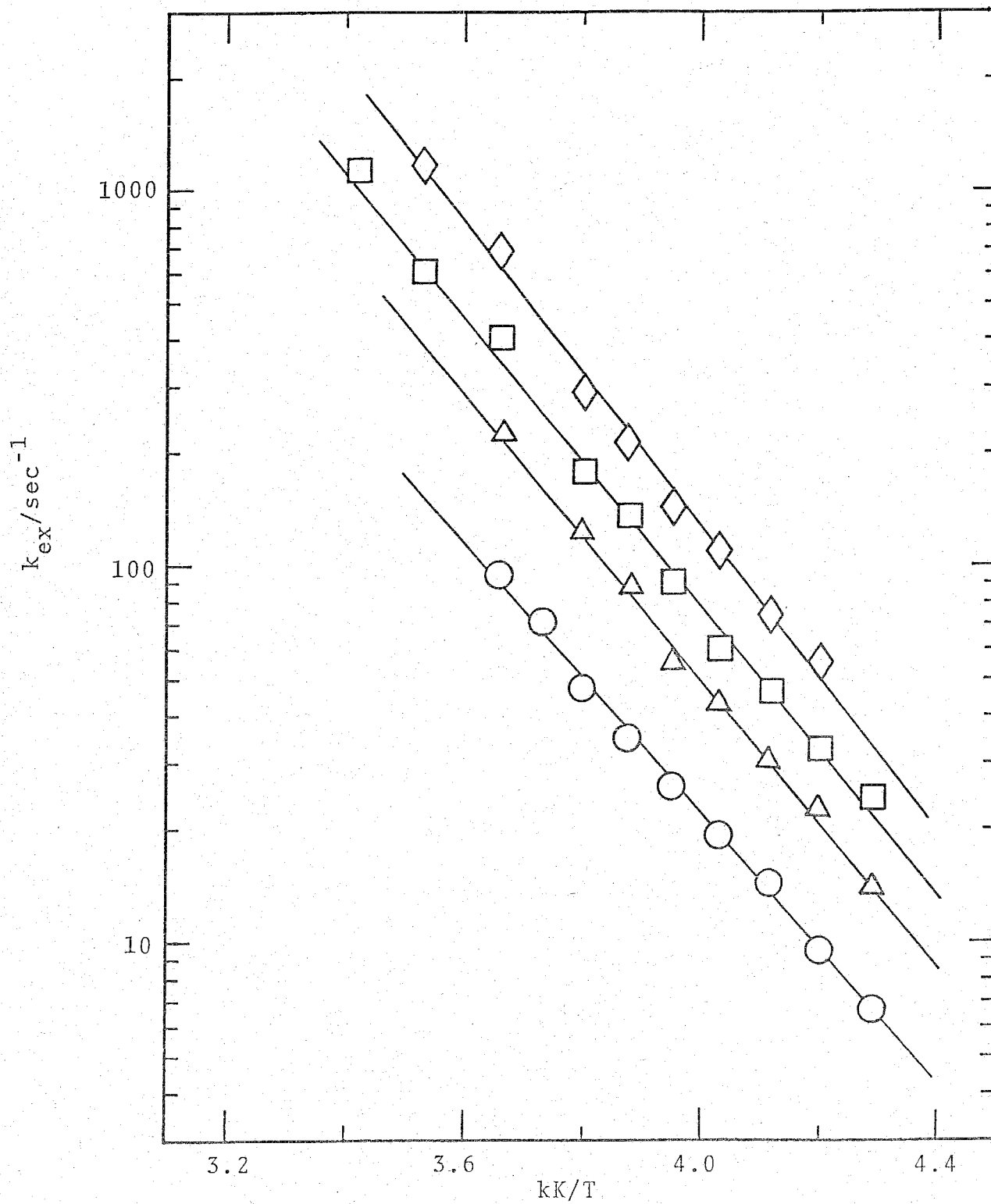
Fig. 23. Semilogarithmic plots of k_{ex} against the reciprocal temperature for the exchange of DMF in $UO_2(acac)_2DMF$

are shown in Fig. 25. From Fig. 25, the activation parameters
are calculated for k_1 and k_2 paths and listed in Table 14.

Table 12. Solution compositions for the exchange of DMF
in $UO_2(acac)_2DMF$ in CD_2Cl_2

Solution	$[UO_2(acac)_2DMF]$	$[DMF]^a$	$[CD_2Cl_2]$
	10^{-2} M	10^{-2} M	M
i	2.73	2.87	15.2
ii	11.0	12.0	14.8
iii	11.6	21.5	14.7
iv	14.6	35.7	14.7

^{a} Added as DMF.

Table 13. The values of k_1 and k_2 at various
temperatures for the exchange of DMF in
$UO_2(acac)_2DMF$ in CD_2Cl_2

Temp.	k_1	k_2
°C	10 sec^{-1}	10^2 M^{-1}sec^{-1}
-10	2.82 ± 0.72	7.26 ± 0.33
-15	2.01 ± 0.24	5.45 ± 0.11
-20	1.44 ± 0.13	3.56 ± 0.58
-25	1.08 ± 0.38	2.54 ± 0.18
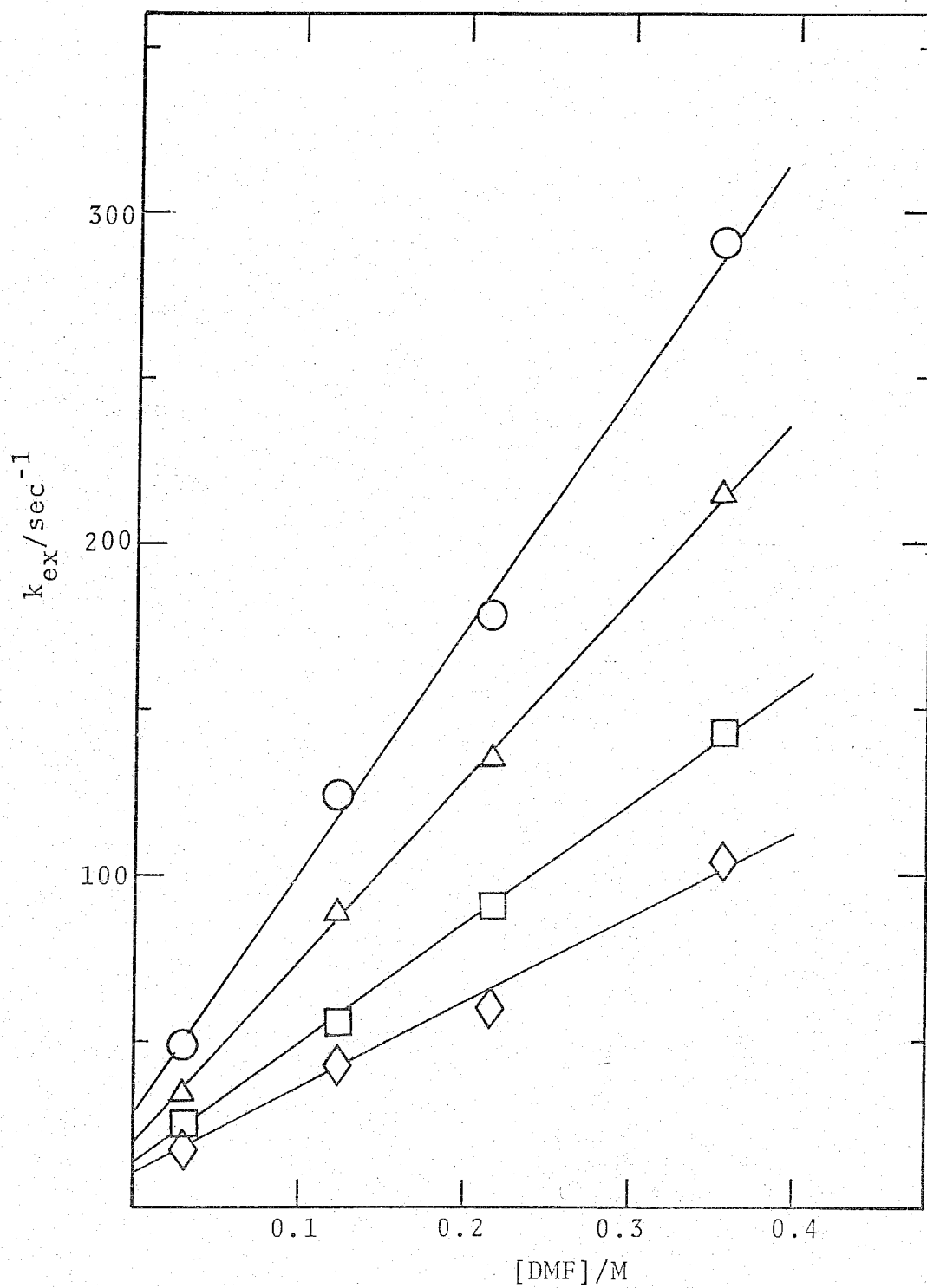
Fig. 24. Plots of k_{ex} vs. [DMF] for the exchange of DMF in $UO_2(acac)_2DMF$ in CD_2Cl_2. $\bigcirc$: -10 °C; $\triangle$: -15 °C; $\diamondsuit$: -25 °C.
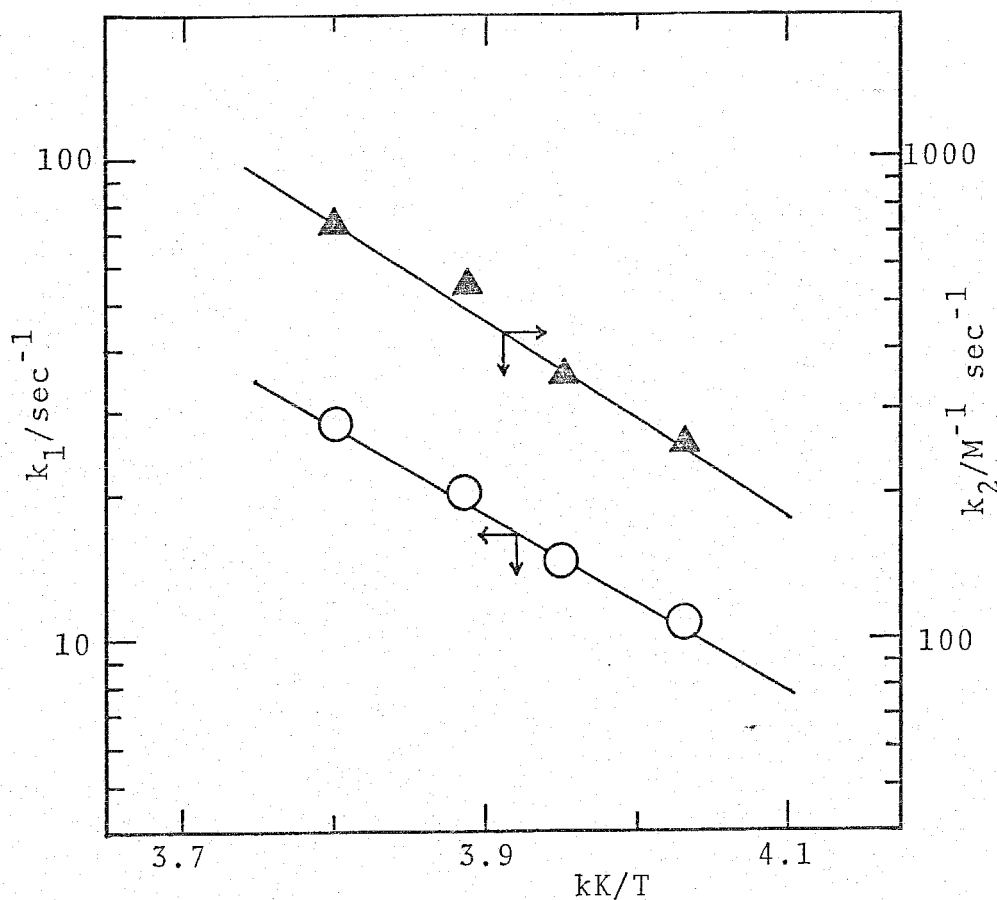
Fig. 25. Semilogarithmic plots of k_1 and k_2 against the reciprocal temperature for the exchange of DMF in $UO_2(acac)_2DMF$ in CD_2Cl_2.

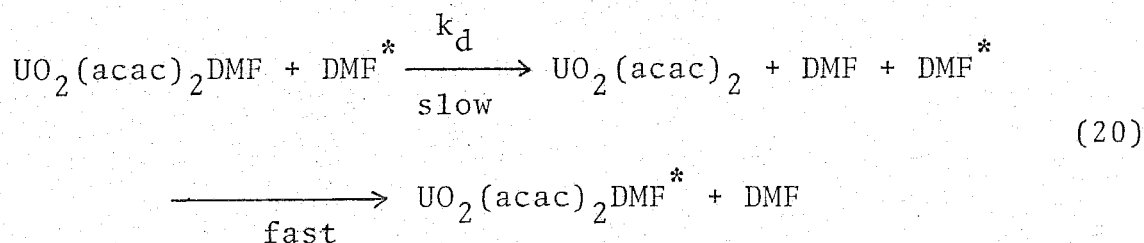Table 14. Kinetic parameters for the k_1 and k_2 paths in the exchange of DMF in $UO_2(acac)_2DMF$ in CD_2Cl_2

	$\Delta H^{\ddagger}$	$\Delta S^{\ddagger}$	$k(25\ ^{\circ}C)^{*}$
	$kJ\ mol^{-1}$	$JK^{-1}mol^{-1}$	$10^2\ sec^{-1}$
k_1 path	32.8 ± 1.7	-92.0 ± 5.9	1.90
k_2 path	37.0 ± 2.1	-49.6 ± 8.8	$56.6\ /M^{-1}$

* Calculated values from $\Delta H^{\ddagger}$ and $\Delta S^{\ddagger}$ at 25 °C.
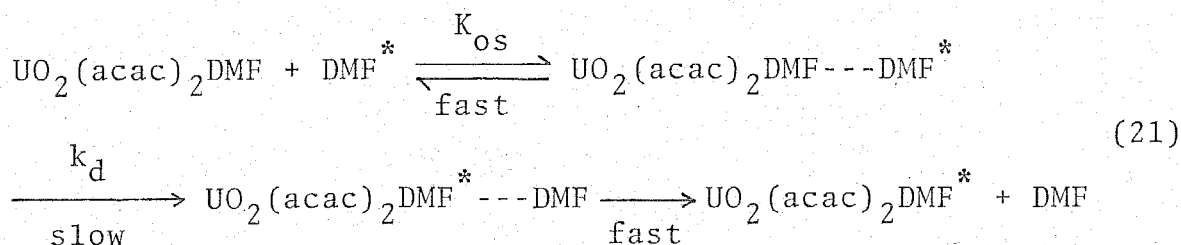
C. Mechanism

C-1. Exchange reaction in CD_3COCD_3 diluent

The rate of DMF exchange reaction in CD_3COCD_3 is independent of the free DMF concentration. This fact indicates that DMF exchange in $UO_2(acac)_2DMF$ in CD_3COCD_3 proceeds through either the D or the I_d mechanism. The D mechanism is expressed by Eq. (20)

$$UO_2(acac)_2DMF + DMF^* \xrightarrow[\text{slow}]{k_d} UO_2(acac)_2 + DMF + DMF^*$$

$$\xrightarrow[\text{fast}]{} UO_2(acac)_2DMF^* + DMF \tag{20}$$

and the I_d mechanism is represented by Eq. (21)

$$UO_2(acac)_2DMF + DMF^* \underset{\text{fast}}{\overset{K_{os}}{\rightleftharpoons}} UO_2(acac)_2DMF\text{---}DMF^*$$

$$\xrightarrow[\text{slow}]{k_d} UO_2(acac)_2DMF^*\text{---}DMF \xrightarrow{\text{fast}} UO_2(acac)_2DMF^* + DMF \tag{21}$$

Following these mechanisms, the first-order exchange rate constants are given by Eqs. (22) and (23), respectively. For the D mechanism

$$k_{ex} = k_d \tag{22}$$

and for the I_d mechanism

$$k_{ex} = k_I K_{os}[DMF]/(1 + K_{os}[DMF]) \tag{23}$$

which simplifies to $k_{ex} = k_I$ when $K_{os}[DMF] \gg 1$, and the rate of DMF exchange becomes independent of the free DMF concentration.

It seems unlikely that the condition, $K_{os}[DMF] \gg 1$, is satisfied in the range of the DMF concentration in the present experiments because both the $UO_2(acac)_2DMF$ complex and DMF molecule are uncharged and hence the value of K_{os} is thought to be smaller than 1 M^{-1}. A bulky chelating ligand, acac, may hinder the approach of free DMF to the interchange sites. On the other hand, the requirement for the D mechanism, i.e. the formation of four-coordinated intermediate, $UO_2(acac)_2$, in the equatorial plane seems reasonable as mentioned in Chapter III. These results lead to the conclusion that the DMF exchange reaction in $UO_2(acac)_2DMF$ in CD_3COCD_3 proceeds through the D mechanism.

C-2. Exchange reaction in CD_2Cl_2 diluent

In CD_2Cl_2, it is found that the DMF exchange occurs through two paths, k_1 and k_2 paths. The k_1 path, where the exchange rate is independent of the DMF concentration, is concluded to be the same D mechanism as the DMF exchange in CD_3COCD_3. The k_2 path exhibits a first-order dependence with respect to the DMF concentration and seems to proceed through either the I_d or the A mechanism. Equation (24) expresses the A mechanism

$$UO_2(acac)_2DMF + DMF^* \xrightarrow[slow]{k_a} UO_2(acac)_2DMF \cdot DMF^*$$

$$\xrightarrow[fast]{} UO_2(acac)_2DMF^* + DMF$$

(24)
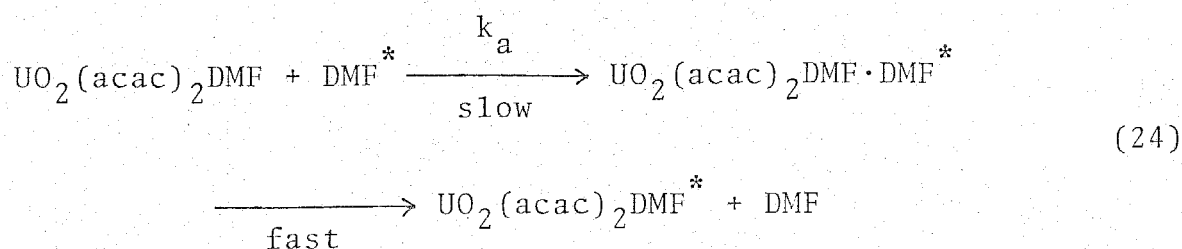
In this mechanism, the rate-determining step is the coordination of DMF to the first coordination sphere of $UO_2(acac)_2DMF$ followed by the formation of six-coordianted intermediate in the equatorial plane.

If k_1 and k_2 paths proceed through the D and A mechanisms, respectively, the frst-order rate constant, k_{ex} is expressed by Eq. (25)

$$k_{ex} = k_d + k_a[DMF] \tag{25}$$

If the DMF exchange in CD_2Cl_2 proceeds through both the D and I_d mechanisms, k_{ex} is given by Eq. (26)

$$k_{ex} = \frac{k_d + k_I K_{os}[DMF]}{1 + K_{os}[DMF]} \tag{26}$$

When $K_{os}[DMF] \ll 1$, Eq. (26) reduces to Eq. (27)

$$k_{ex} = k_d + k_I K_{os}[DMF] \tag{27}$$

where k_d and $k_I K_{os}$ correspond to k_1 and k_2 in Eq. (19), respectively. Both of Eqs. (25) and (27) are compatible with the experimental results.

Although it has been known that the uranyl ion forms the six-coordinated complexes in the equatorial plane with small ligands as stated in Chapter III, the A mechanism seems to be

unlikely, because the coordinated acac is a bulky chelating

ligand and may block access of free DMF to the first coordination

sphere of $UO_2(acac)_2DMF$. N,N-dimethylformamide itself is a

relatively bulky ligand, and it appears difficult to form

a six-coordinated intermediate in the crowded equatorial plane.

On the contrary, the I_d mechanism should satisfy the condition,

$K_{os}[DMF] \ll 1$, but nevertheless the condition seems to be reason-

able in this system since both $UO_2(acac)_2DMF$ and DMF are uncharged

and the value of K_{os} should be smaller than $1 \ M^{-1}$ on the basis

of the Fuoss equation[20]. Therefore, it is suggested that

the DMF excahange in CD_2Cl_2 proceeds through both the D and

I_d mechanisms.

D. Comparison with the DMF Exchange Reaction in $UO_2(DMF)_5^{2+}$

The results of DMF exchange in $UO_2(DMF)_5^{2+}$ and $UO_2(acac)_2^-$ DMF in CD_2Cl_2 are summerized in Table 15. It was suggested that both DMF exchange reactions proceeded through the same mechanisms, the D and I_d mechanism. However, the rate of DMF exchange reaction in $UO_2(DMF)_5^{2+}$ approaches to the constant value as the free DMF concentration increases from 0.0123 to 0.588 M as shown in Fig. 16 in Chapter III, while that in $UO_2(acac)_2DMF$ depends linearly on the free DMF concentration ranging from 0.0287 to 0.357 M as shown in Fig. 24. This difference may be attributed to the fact that the reactants are uncharged in the case of the DMF exchange reaction in $UO_2(acac)_2DMF$ and hence the outer-sphere complex formation constant becomes smaller than that in the DMF exchange in $UO_2(DMF)_5^{2+}$ (1.15-1.36 M^{-1}).

Since the diluent and ligand are the same in both reactions, the differences of the kinetic parameters in both reactions may be due to the bond-strength between uranyl ion and DMF, and to the structural difference in the equatorial plane. The $\Delta H^{\ddagger}$ values for the DMF exchange in $UO_2(DMF)_5^{2+}$ are larger than those of the DMF exchange in $UO_2(acac)_2DMF$. These results suggest that the bond-strength between uranyl ion and DMF in $UO_2(acac)_2^-$ DMF is weaker than that in $UO_2(DMF)_5^{2+}$ and the coordinated DMF may dissociate more easily in $UO_2(acac)_2DMF$ than in $UO_2(DMF)_5^{2+}$. However, a stable intermediate cannot be formed in $UO_2(acac)_2DMF$ because the two bidentate ligands will make it difficult to reform the structure in the equatorial plane. This is consistent with

the observations that the $\Delta S^{\ddagger}$ values for the DMF exchange in $UO_2(acac)_2DMF$ are more negative than those in $UO_2(DMF)_5^{2+}$. As a result, the rate constants of the DMF exchange in $UO_2(acac)_2$-DMF become smaller than those of the DMF exchange reaction in $UO_2(DMF)_5^{2+}$ in spite of small $\Delta H^{\ddagger}$ values.

Table 15. Kinetic parameters for the exchange of DMF in various uranyl complexes

Complex	Mechanism	$\Delta H^{\ddagger}$ kJ mol^{-1}	$\Delta S^{\ddagger}$ JK^{-1}mol^{-1}	$k_{ex}(25°C)$[b] sec^{-1}
$UO_2(DMF)_5^{2+}$	D	42.0 ± 2.1	-15.1 ± 3.3	4.70 x 10^4
	I_d	48.3 ± 0.9	38.6 ± 2.6	2.34 x 10^6
$UO_2(acac)_2DMF$	D	32.8 ± 1.7	-92.0 ± 5.9	1.90 x 10^2
	I_d	37.0 ± 2.1[a]	-49.6 ± 8.8[a]	5.66 x 10^3/M^{-1}[a]

[a] The values of kinetic parameters for $k_I K_{os}$.

[b] Calculated values from $\Delta H^{\ddagger}$ and $\Delta S^{\ddagger}$ at 25 °C.

iv. SUMMARY

It was found that the uranyl β-diketonato complexes studied in this chapter have a pentagonal bipyramidal structure in solution. It was supported that the k_2 path of the DMSO exchange reaction in $UO_2(DMSO)_5^{2+}$ proceeded through the A mechanism.

Table 16 shows the kinetic parameters for the DMSO and DMF exchange reactions in $UO_2(acac)_2DMSO$, $UO_2(dbm)_2DMSO$, and UO_2-$(acac)_2DMF$. From this table it is found that the mechanisms of the DMSO and DMF exhange reactions in these complexes in CD_3COCD_3 are different from those in CD_2Cl_2. This difference may be primarily due to the diluent properties because the complexes and ligands in each reaction system are the same in both diluents, which means the acidity of complex and the basicity of ligand are constant. The dielectric constant of acetone(20.7) is larger than that of dichloromethane(8.93) and these values may be almost identical with those of respective deuterated compounds, CD_3COCD_3 and CD_2Cl_2. Thus it may be expected that the outer-sphere complex formation constant, K_{os}, in CD_3COCD_3 is smaller than that in CD_2Cl_2. Moreover, acetone has a relatively large basicity, DN = 17.0 [24,25], and tends to solvate to the second coordination spheres of these complexes. This solvation may block access of DMSO molecules to the second coordination spheres of these complexes in CD_3COCD_3. This may lead to the observations that the DMSO exchange in CD_3COCD_3 proceeds through the only D mechanism, while that in CD_2Cl_2 occurs through both the D and I_d mechanisms.

It is also infered that the differences of kinetic parameters may be due to the diluent effect, e.g. the stabilization of the transition state by the bulk diluents or the rearrangement of bulk diluents, which occur simultaneously with the formation of the transition state. This is supported by the following facts. The values of $\Delta H^{\ddagger}$ for the ligand exchange reactions in CD_2Cl_2, except for the DMSO exchange in $UO_2(acac)_2DMSO$, are smaller than those in CD_3COCD_3, while $\Delta S^{\ddagger}$ in CD_2Cl_2 has more negative values than those in CD_3COCD_3. As a result, the values of k_{ex} in CD_2Cl_2 becomes smaller than those in CD_3COCD_3.

Table 16. Kinetic parameters for the exchange reactions of L in $UO_2(\beta\text{-diketonato})_2L$ (L = DMSO and DMF)

Complex	Solvent	Mechanism	$\Delta H^{\ddagger}$ kJ mol^{-1}	$\Delta S^{\ddagger}$ JK^{-1}mol^{-1}	$k_{ex}(25\ °C)$[a] sec^{-1}
$UO_2(acac)_2$DMSO	CD_3COCD_3	D	45.8 ± 0.8	-46.6 ± 2.9	2.36 × 10^2
	CD_2Cl_2	D	47.9 ± 5.2	-46.6 ± 11.2	1.02 × 10^2
		I_d	35.4 ± 12.4	-69.7 ± 20.5	1.01 × 10^3
$UO_2(dbm)_2$DMSO	CD_3COCD_3	D	44.5 ± 0.4	-46.2 ± 2.1	3.92 × 10^2
	CD_2Cl_2	D	29.6 ± 2.2	-104.2 ± 8.6	1.74 × 10^2
		I_d	34.9 ± 0.6[b]	-67.2 ± 2.4[b]	1.62 × 10^3/M^{-1}[b]
$UO_2(acac)_2$DMF	CD_3COCD_3	D	42.0 ± 1.3	-46.2 ± 5.5	1.14 × 10^3
	CD_2Cl_2	D	32.8 ± 1.7	-92.0 ± 5.9	1.90 × 10^2
		I_d	37.0 ± 2.1[b]	-49.6 ± 8.8[b]	5.66 × 10^3/M^{-1}[b]

a Calculated values from $H^{\ddagger}$ and $S^{\ddagger}$ at 25 °C. b The values of kinetic parameters for $k_I K_{os}$.

REFERENCES

1. J.R. Ferraro and T.V. Healy, J. Inorg. Nucl. Chem., $\underline{24}$, 1463(1962).

2. M.S. Subramanian and A. Viswanatha, J. Inorg. Nucl. Chem., $\underline{31}$, 2575(1969).

3. M.S. Subramanian and A. Viswanatha, J. Inorg. Nucl. Chem., $\underline{33}$, 3001(1971).

4. T.V. Healy and J.R. Ferraro, J. Inorg. Nucl. Chem., $\underline{24}$, 1449(1962).

5. T.V. Healy, D.F. Peppard, and G.W. Mason, J. Inorg. Nucl. Chem., $\underline{24}$, 1429(1962).

6. Y. Baskin and J.R. Ferraro, J. Inorg. Nucl. Chem., $\underline{30}$, 241 (1968).

7. J.M. Haigh and D.A. Thornton, J. Inorg. Nucl. Chem., $\underline{33}$, 1787(1971).

8. E. Frasson, G. Bombieri, and C. Panattoni, Nature, $\underline{202}$, 1325 (1964).

9. E. Frasson, G. Bombieri, and C. Panattoni, Coord. Chem. Rev., $\underline{1}$, 145(1966).

10. A.E. Comyns, B.M. Gatehouse, and E. Wait, J. Chem. Soc., 4655(1958).

11. L. Sacconi and G. Giannoni, J. Chem. Soc., 2368(1954).

12. F.A. Cotton and R. Francis, J. Am. Chem. Soc., $\underline{82}$, 2986(1960).

13. K. Nakamoto, Infrared and Raman Spectra of Inorganic and Coordination Compounds, John Wiley, New York(1971).

14. G.H. Langford and H.B. Gray, Ligand Substitution Processes, Benjamin, London(1974).

15. A. Fratiello, V. Kubo, R.E. Lee, and R.E. Schuster, J. Phys. Chem., 74, 3726(1970).

16. A. Fratiello, G.A. Vidlich, C. Cheng, and V. Kubo, J. Solution Chem., 1, 433(1972).

17. L.R. Nassimbeni and A.L. Rodgers, Cryst. Struct. Commun., 5, 301(1976).

18. G. Bombieri, J.P. Day, and W.I. Azeez, J.C.S. Dalton, 1978 (1978).

19. I.I. Chernyaev, Complex Compounds of Uranium(Translated from Russian), Israel Program for Scientific Translations, Jerusalem(1966).

20. R.M. Fuoss, J. Am. Chem. Soc., 80, 5059(1958).

21. W. Gerrard, M.F. Lappert, H. Pyszora, and J.W. Wallis, J. Chem. Soc., 2144(1960).

22. C.D. Schmulbach and R.S. Drago., J. Am. Che. Soc., 82, 4484 (1960).

23. S.J. Kuhn and J.S. McIntyre, Can. J. Chem., 43, 375(1965).

24. V. Gutmann, Coordination Chemistry in Non-Aqueous Solvents, Springer-Verlag, Wien-New York(1968)

25. V. Gutmann and R. Schmid, Coord. Chem. Rev., 12, 263(1974).

CHAPTER V

KINETIC STUDY OF THE INTRAMOLECULAR EXCHANGE

REACTION OF METHYL GROUPS IN URANYL ACETYL-

ACETONATO COMPLEXES BY NMR

i . INTRODUCTION

In Chapter IV, the results were reported in detail for the ligand exchange reactions in $UO_2(acac)_2L$ (L = DMSO and DMF). In these experiments, it was found that the methyl proton signals of coordinated acac were a doublet at low temperature and became a singlet as temperature increased. These phenomena indicate that the exchange takes place between two methyl groups of coordinated acac, i.e. near one to and far one from the coordinated DMSO and DMF.

Similar phenomena have been observed in various β-diketonato complexes, e.g. the intramolecular rearrngement process in the β-diketonato complexes of Ti(IV)[1,2], Al(III)[3-5], Ga(III)[3,6], Mo(VI)[7], Zr(IV), Hf(IV), Ce(IV), and Th(IV)[8], and the twist or bond rupture mechanism has been proposed for these intramolecular reactions.

In this chapter, the intramolecular exchange reaction in $UO_2(acac)_2L$ is dealt with and a new type of mechanism will be proposed.

ii. EXPERIMENTAL

A. Synthesis of Complexes

The $UO_2(acac)_2DMSO$ and $UO_2(acac)_2DMF$ complexes were the same reagents which were used in the study of the exchange reactions of DMSO and DMF in these complexes. Preparation of $UO_2(acac)_2DEF$ (DEF = N,N-diethylformamide) was made by the same method as shown in Chapter IV. Anal. Calcd for $UO_2(acac)_2DEF$: C, 31.64; H, 4.78; N, 2.46. Found: C, 31.43; H, 4.41, N, 2.58.

B. Solvents

Acetone-d_6(CD_3COCD_3), dichloromethane-d_2(CD_2Cl_2), nitro-methane-d_3(CD_3NO_2), and ortho-dichlorobenzene($o-C_6H_4Cl_2$) were used as solvents. The solvents CD_3COCD_3, CD_3NO_2, and CD_2Cl_2 were dried over 3A and 4A molecular sieves and $o-C_6H_4Cl_2$ was distilled twice in vacuo and stored over 3A molecular sieves.

C. Kinetic Analysis

Kinetic analysis was done by the same method as described in Chapter II. In the present study, the values of P_C and P_F are taken to be equal to 0.5, since the exchange reaction takes place between the two methyl groups of coordinated acac. The linewidths of methyl proton signal of enol isomer of acetylacetone in each solvent were used as the values of $1/T_{2C}$ and $1/T_{2F}$. The chemical shifts of low and high field signals of the methyl protons of coordianted acac were used as the values of ω_{0C} and ω_{0F}.

iii. RESULTS AND DISCUSSION

A. Exchange Reaction of Methyl Groups of acac in $UO_2(acac)_2DMSO$

The ^{1}H NMR spectra of $UO_2(acac)_2DMSO$ in $o\text{-}C_6H_4Cl_2$ at -20 and +30 °C are shown in Fig. 1, in which the signals of (a) and (c) are due to the methyl protons and 3-H protons of coordinated acac, respectively, and (b) is the methyl proton signal of coordinated DMSO. (I-a) represents the expanded signal of (a). It is found that the methyl proton signal of coordinated acac has two equivalent peaks at -20 °C, while the corresponding peak is a singlet at 30 °C. The chemical shifts of (a), (b), and (c) were not changed. These facts suggest that the complex is present in the pentagonal bipyramidal structure in $o\text{-}C_6H_4Cl_2$ over the present temperature range and that the exchange takes place between the two methyl groups of coordinated acac, i.e. near one to and far one from the coordianted DMSO. Similar phenomena were observed in the ^{1}H NMR spectra of $UO_2(acac)_2DMSO$ in CD_3NO_2, CD_2Cl_2, and CD_3COCD_3 as shown in Figs. 2, 3, and 4, respectively. The symbols of (a), (b), and (c) in these figures correspond to those in Fig. 1. The results of the change of lineshape for the methyl proton signal of coordinated acac with temperature are shown at the left sides of Figs. 5, 6, 7, and 8 and indicate the typical two-site exchange. The best-fit τ-values at each temperature were determined by using the method described in Chapter II. The obtained τ-values are shown together with the calculated lineshapes at the right sides of Figs. 5, 6, 7, and 8.
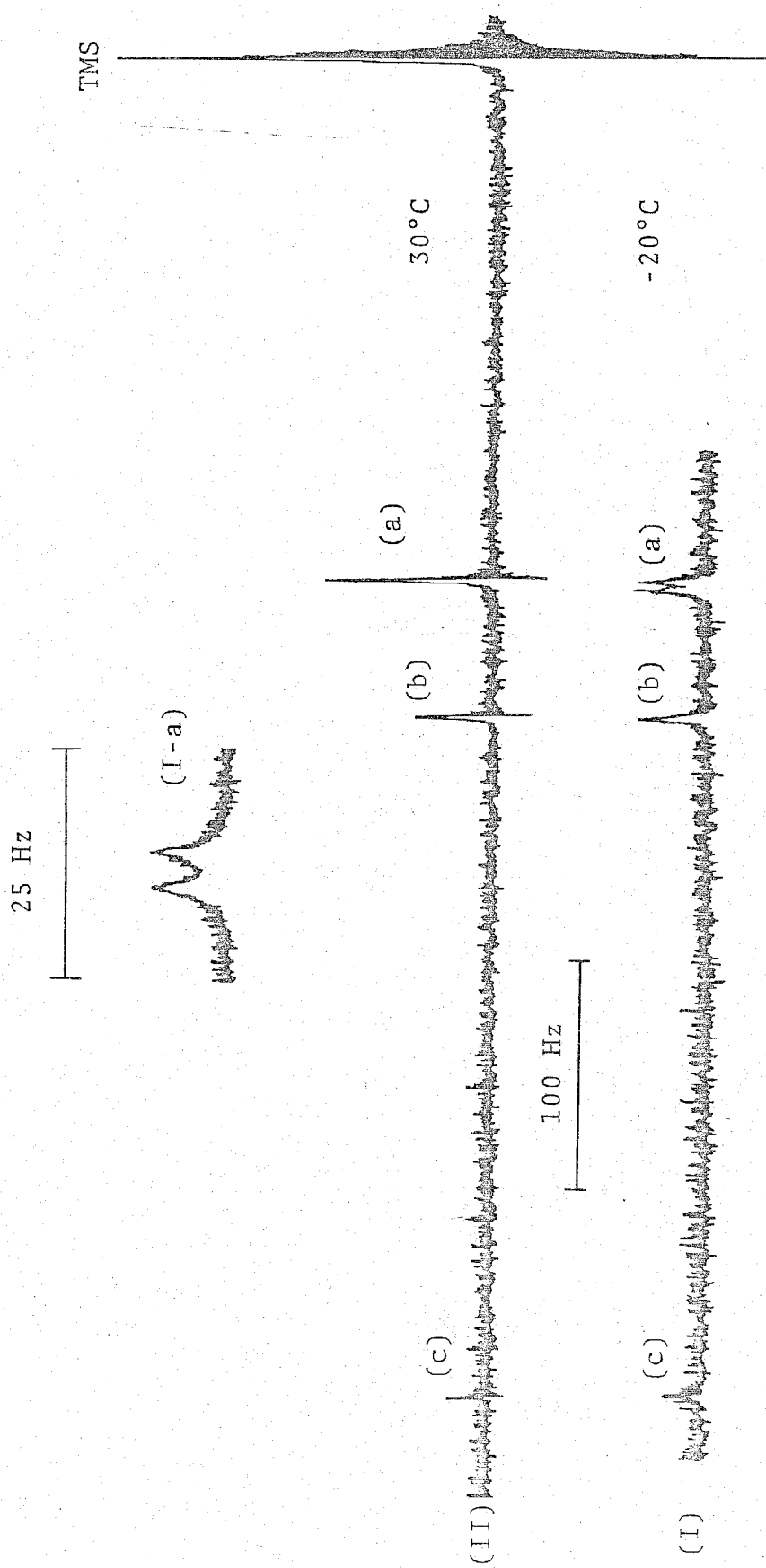
Fig. 1. The ^1H NMR spectra of $UO_2(acac)_2DMSO(0.0349\ m)$ in $o\text{-}C_6H_4Cl_2$ at -30 and +30 °C, respectively.

161

TMS

(I-a)

25 Hz

(a)

(a)

(b)

(b)

100 Hz

Impure
CD_3NO_2

+30 °C

−20 °C

(c)

(c)

(II)

(I)
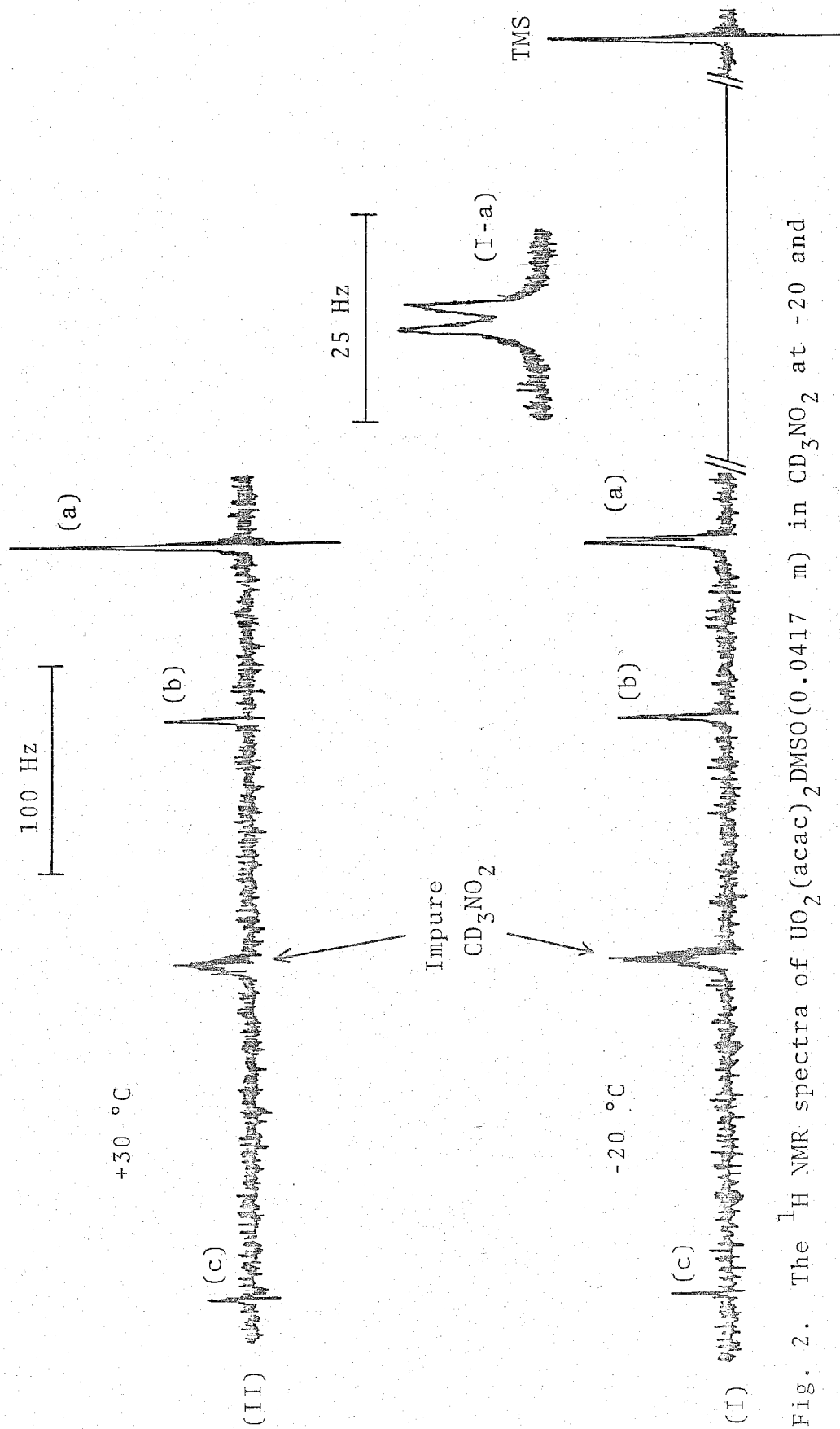
Fig. 2. The ^1H NMR spectra of $UO_2(acac)_2DMSO(0.0417\ m)$ in CD_3NO_2 at −20 and

+30 °C, respectively.
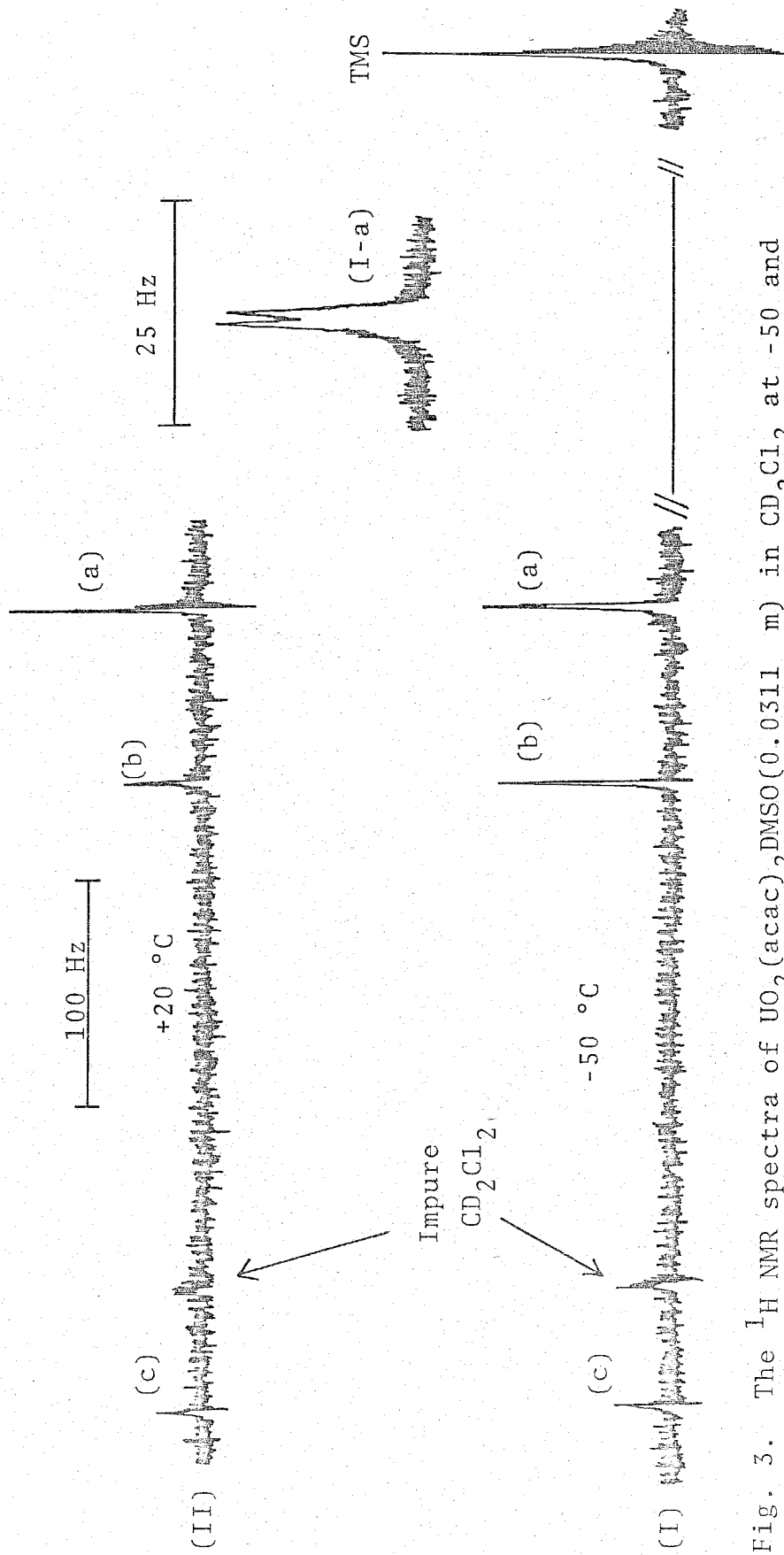
Fig. 3. The ^{1}H NMR spectra of $UO_2(acac)_2DMSO(0.0311$ m) in CD_2Cl_2 at -50 and $+20$ °C, respectively.
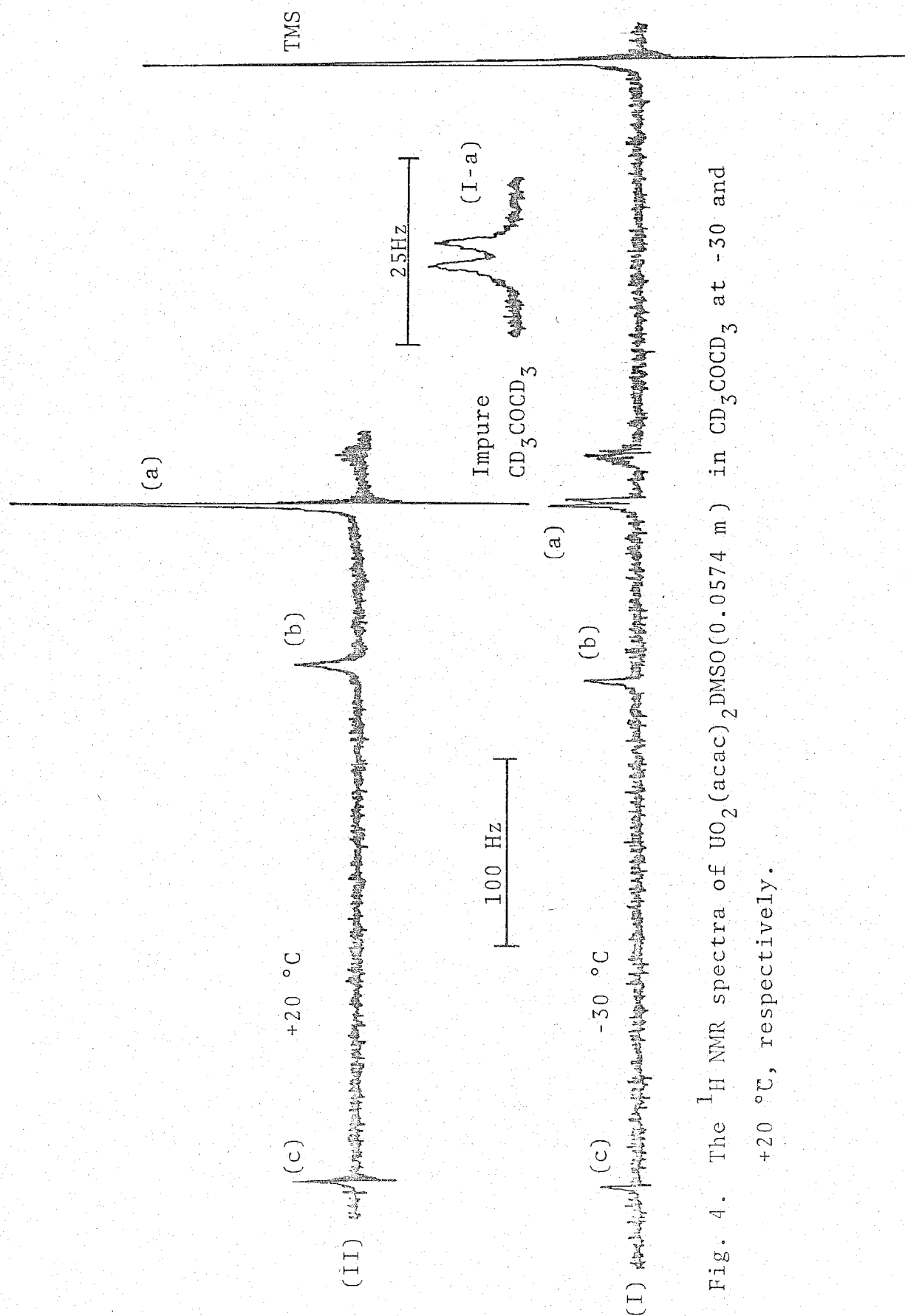
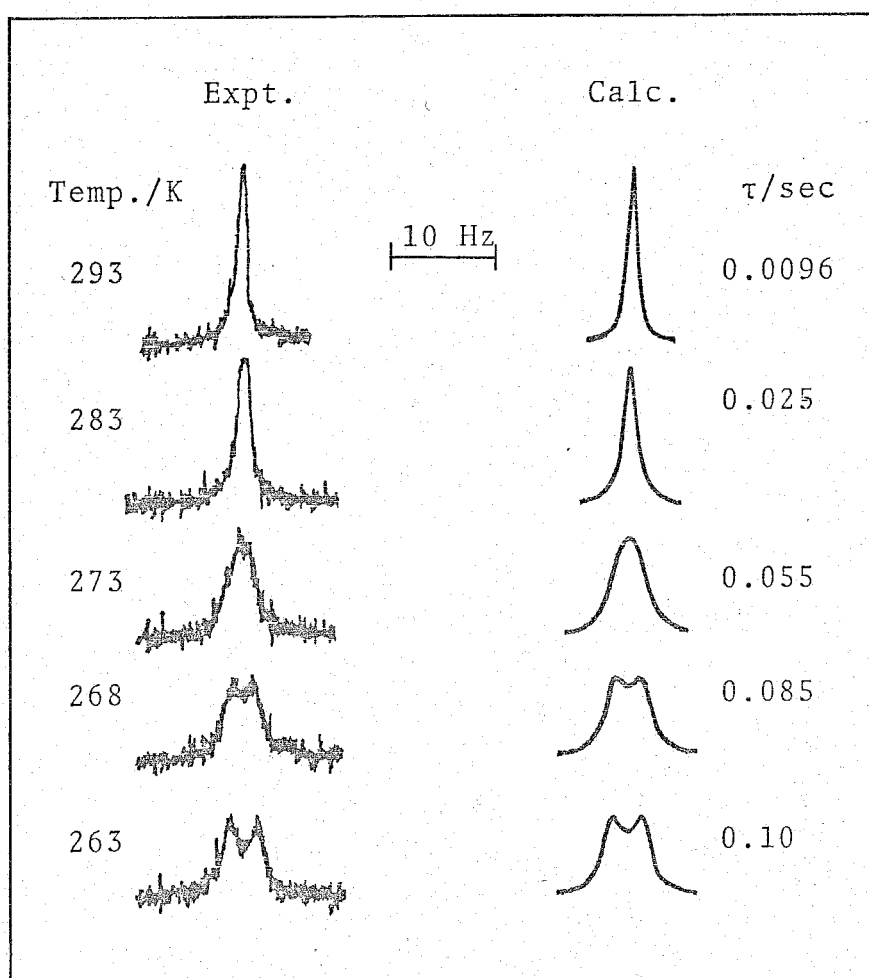Fig. 4. The ^{1}H NMR spectra of $UO_2(acac)_2DMSO(0.0574 \text{ m})$ in CD_3COCD_3 at -30 and $+20$ °C, respectively.

Fig. 5. Experimental (left-hand side) and best-fit
calculated ^{1}H NMR lineshapes of $UO_2(acac)_2DMSO$
(0.0349 m) in $o\text{-}C_6H_4Cl_2$. Temperatures and
best-fit τ-values are shown at the left- and
right-hand sides of the figure, respectively.

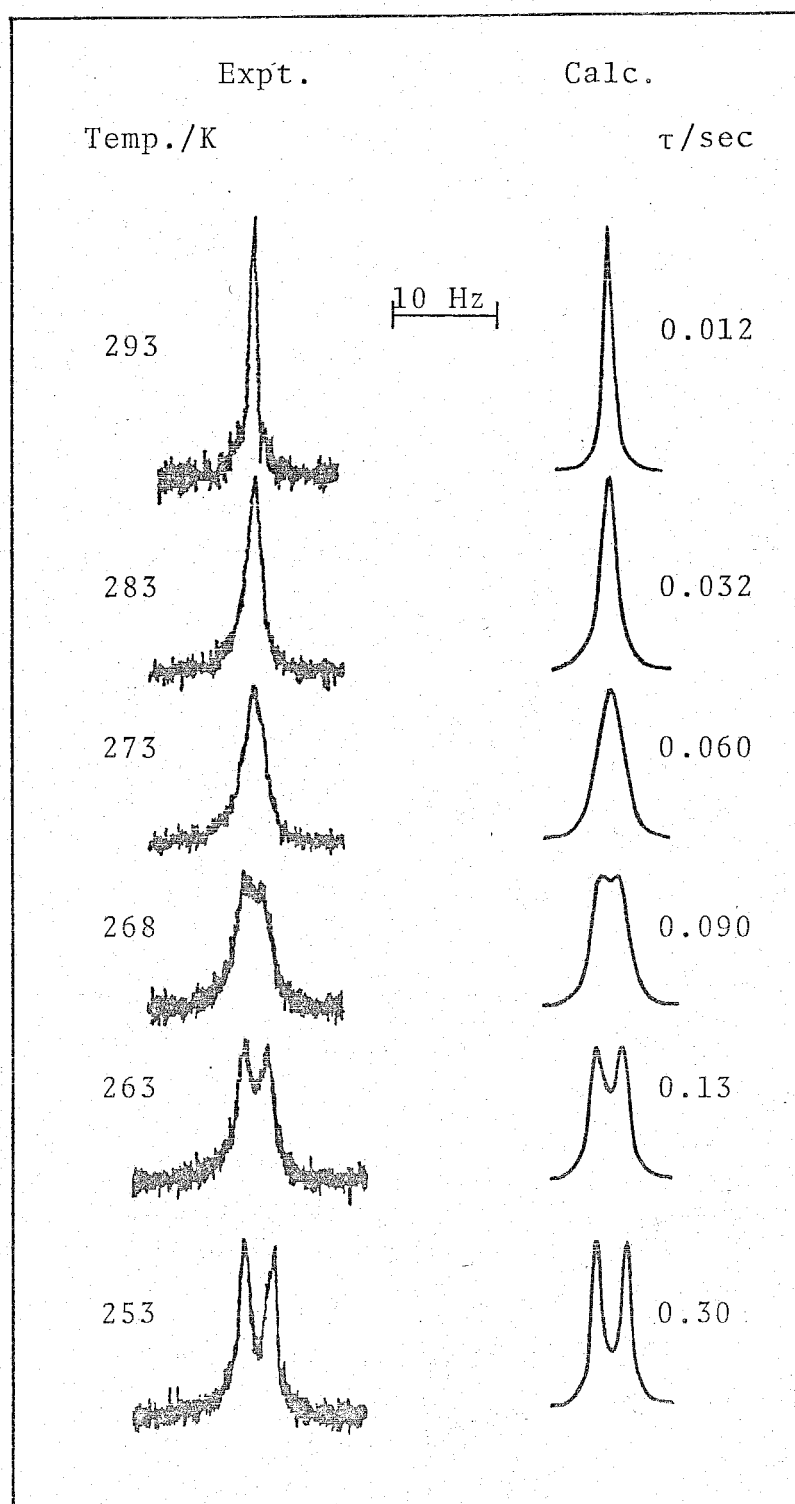Fig. 6. Experimental(left-hand side) and best-fit
calculated ^{1}H NMR lineshapes of $UO_2(acac)_2$-
$DMSO(0.0417 \ m)$ in CD_3NO_2. Temperatures
and best-fit τ-values are shown at the
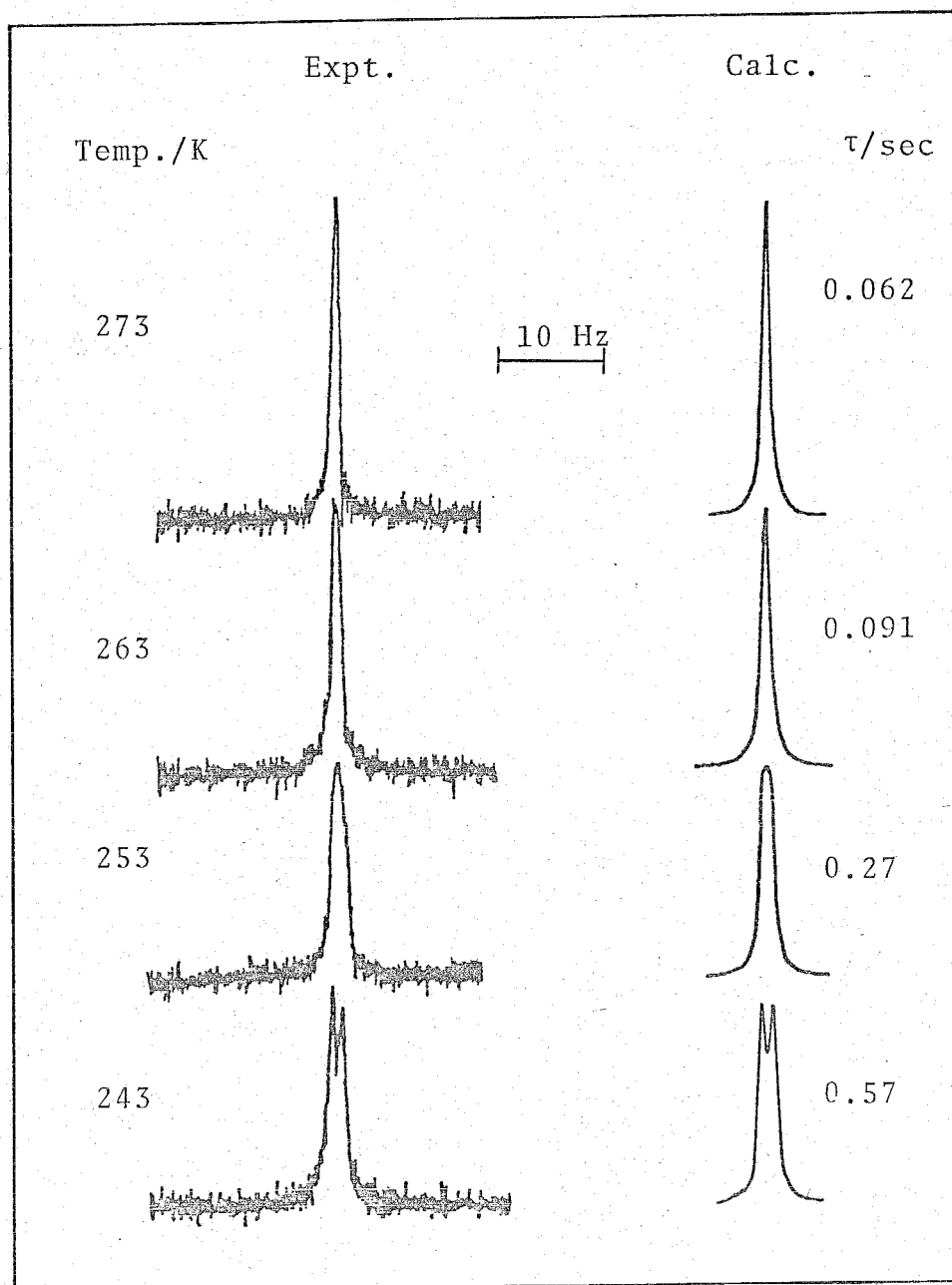
Fig. 7. Experimental(left-hand side) and best-fit calculated ^1H NMR lineshapes of $UO_2(acac)_2DMSO(0.0311 \ m)$ in CD_2Cl_2. Temperatures and best-fit τ-values are shown at the left- and right-hand sides of the
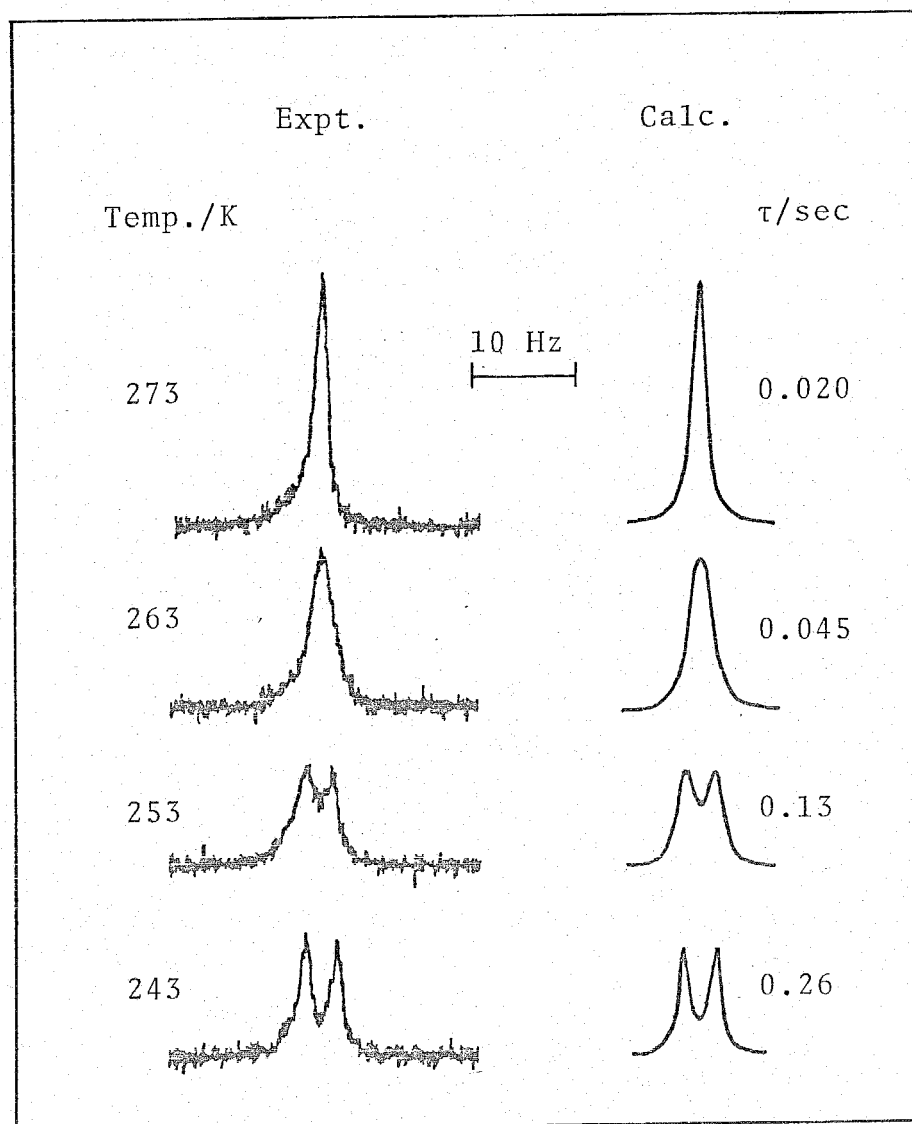
Fig. 8. Experimental(left-hand side) and best-fit calculated ^{1}H NMR lineshapes of $UO_2(acac)_2DMSO$ (0.0574 m) in CD_3COCD_3. Temperatures and best-fit τ-values are shown at the left-and right-hand sides of the figure, respectively.

In the present exchange reaction, the exchange reaction occurs between the two methyl groups of coordinated acac. Hence $\tau_C = \tau_F$, and $P_C = P_F = 0.5$. The first-order exchange rate constant, k_{intra}, is given by Eq. (1)

$$k_{intra} = 1/(2\tau) = (kT/h)\exp(-\Delta H^{\ddagger}/RT)\exp(\Delta S^{\ddagger}/R) \qquad (1)$$

The k_{intra} values were calculated from the best-fit τ-values by using Eq. (1). The logarithms of k_{intra} obtained in each solvent were plotted against the reciprocal temperature as shown in Fig. 9. The activation parameters obtained from these plots are listed in Table 1.

The exchange rate consatnts in solutions of various concentrations of $UO_2(acac)_2DMSO$ were measured in CD_2Cl_2. The results are shown in Table 2 and indicate that the exchange rate is first-order with respect to the complex concentration.
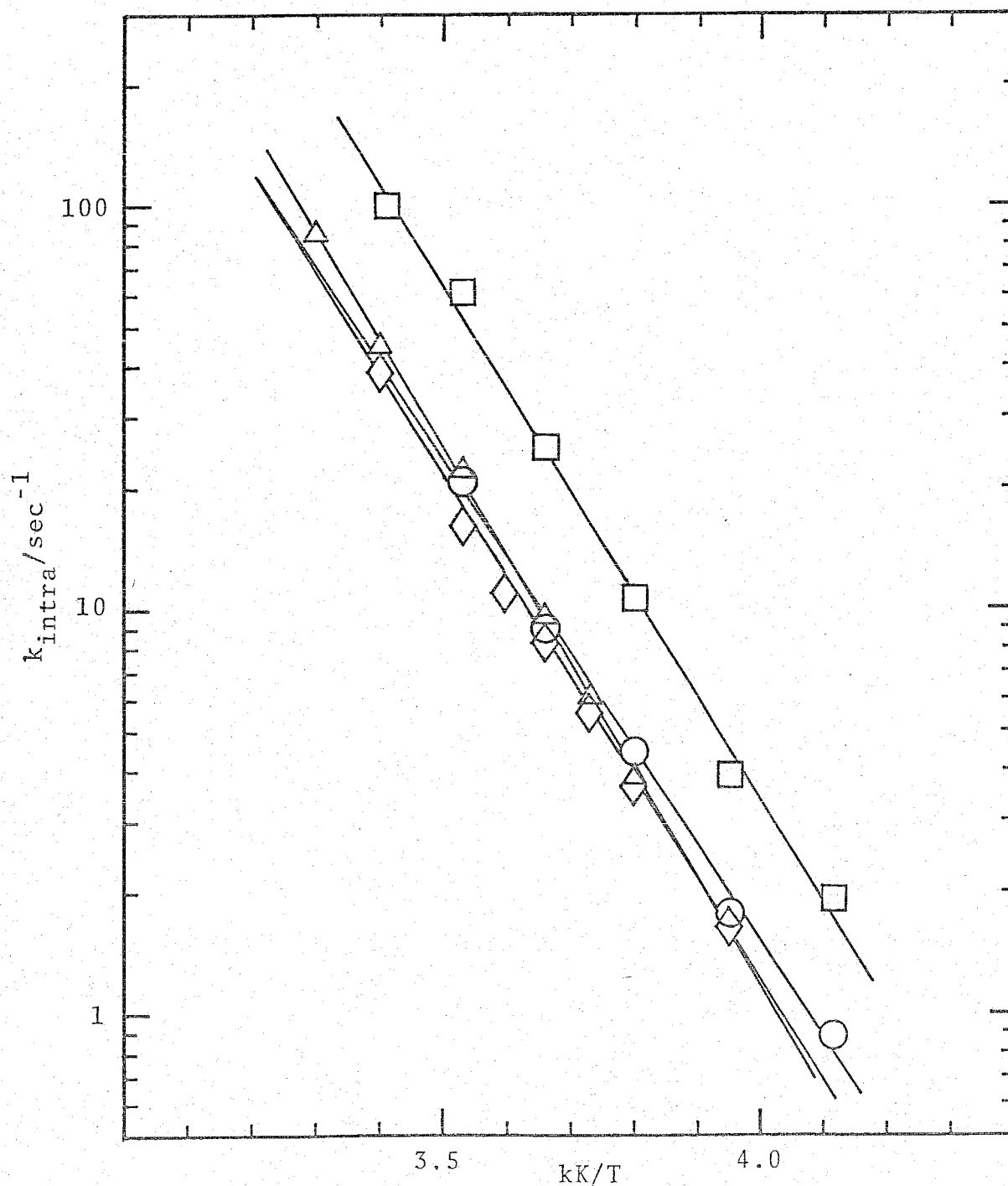
Fig. 9. Semilogarithmic plots of k_{intra} against the reciprocal temperature for the exchange of methyl groups of acac in $UO_2(acac)_2DMSO$. $\bigcirc$: CD_2Cl_2; $\triangle$: $o\text{-}C_6H_4Cl_2$; $\square$: CD_3COCD_3; $\diamondsuit$: CD_3NO_2.

Table 1. Kinetic parameters for the exchange of methyl groups of acac in

$UO_2(acac)_2L$ (L = DMSO, DMF, and DEF)

Complex	[Complex] 10^{-2} m	Solvent	$\Delta H^{\ddagger}$ kJ mol^{-1}	$\Delta S^{\ddagger}$ JK^{-1}mol^{-1}	$k_{intra}(25°C)^{a}$ 10 sec^{-1}
$UO_2(acac)_2DMSO$	3.11	CD_2Cl_2	42.4 ± 2.9	-70.1 ± 10.9	5.45
	5.74	CD_3COCD_3	46.6 ± 1.7	-47.5 ± 6.7	15.2
	3.49	$o\text{-}C_6H_4Cl_2$	49.6 ± 0.8	-44.9 ± 2.5	6.32
	4.17	CD_3NO_2	45.8 ± 1.3	-60.5 ± 5.0	4.49
$UO_2(acac)_2DMF$	3.64	CD_2Cl_2	35.3 ± 1.3	-94.5 ± 4.2	5.19
	5.98	CD_3COCD_3	39.1 ± 1.5	-63.4 ± 3.4	47.0
$UO_2(acac)_2DEF$	4.72	CD_2Cl_2	34.0 ± 1.3	-100.4 ± 5.0	4.26

a   Calculated values from $\Delta H^{\ddagger}$ and $\Delta S^{\ddagger}$ at 25 °C.

Table 2. Dependence of k_{intra} on the concentration of $UO_2(acac)_2L$ (L = DMSO, DMF, and DEF)[a]

Temp. °C	$\dfrac{k_{intra}}{sec^{-1}}$	
	$\dfrac{[UO_2(acac)_2DMSO]}{10^{-2}\ m}$	
	1.74	3.11
10	18.0 ± 1.5	20.8 ± 1.0
0	9.36 ± 0.48	8.84 ± 0.72
-10	5.00 ± 0.92	4.41 ± 1.08
-20	2.20 ± 0.52	1.76 ± 0.19
	$\dfrac{[UO_2(acac)_2DMF]}{10^{-2}\ m}$	
	1.76	3.64
10	25.8 ± 2.1	22.8 ± 1.1
0	12.8 ± 0.5	14.5 ± 1.7
-10	6.09 ± 0.64	6.70 ± 0.22
-20	3.75 ± 0.48	3.26 ± 0.15
	$\dfrac{[UO_2(acac)_2DEF]}{10^{-2}\ m}$	
	1.83	4.72
10	20.9 ± 2.9	22.5 ± 2.5
0	12.1 ± 1.8	11.5 ± 0.4
-10	5.31 ± 0.61	6.85 ± 0.29
-20	4.63 ± 1.15	3.14 ± 0.19

[a] In CD_2Cl_2 solutions

B. Exchange Reaction of Methyl Groups of acac in $UO_2(acac)_2DMF$

and $UO_2(acac)_2DEF$

Similar phenomena were observed in the ^{1}H NMR spectra of

$UO_2(acac)_2DMF$ and $UO_2(acac)_2DEF$ in CD_2Cl_2 as shown in Figs. 10

and 11, respectively.

In Fig. 10, the doublet of (a) and the singlet of (c) are

the signals of methyl protons and of 3-H protons of coordinated

acac, respectively. The doublet of (b) and the singlet of (d)

are assigned to the methyl protons and the formyl protons of

coordinated DMF, respectively. The area ratio of these signals

indicates that the structure of $UO_2(acac)_2DMF$ is pentagonal

bipyramidal described in Chapter IV.

In Fig. 11, the signals of (b) and (d) are the methyl

protons and the 3-H protons of coordinated acac, respectively.

The signals of (a) and (c) can be assigned to the methyl and

methylene protons of the ethyl groups of coordinated DEF,

respectively. The signal of (e) is the formyl protons of coordi-

nated DEF. From the comparison of the integrated areas for

these signals, it is assumed that the structure of $UO_2(acac)_2DEF$

in solution is a pentagonal bipyramidal similar to those of UO_2-

$(acac)_2DMSO$ and $UO_2(acac)_2DMF$.

The change of lineshapes of the methyl proton signal of

coordinated acac were observed at various temperatures. The

results, which are shown at the left sides of Figs. 12 and 13,

indicate that the exchange reactions between the

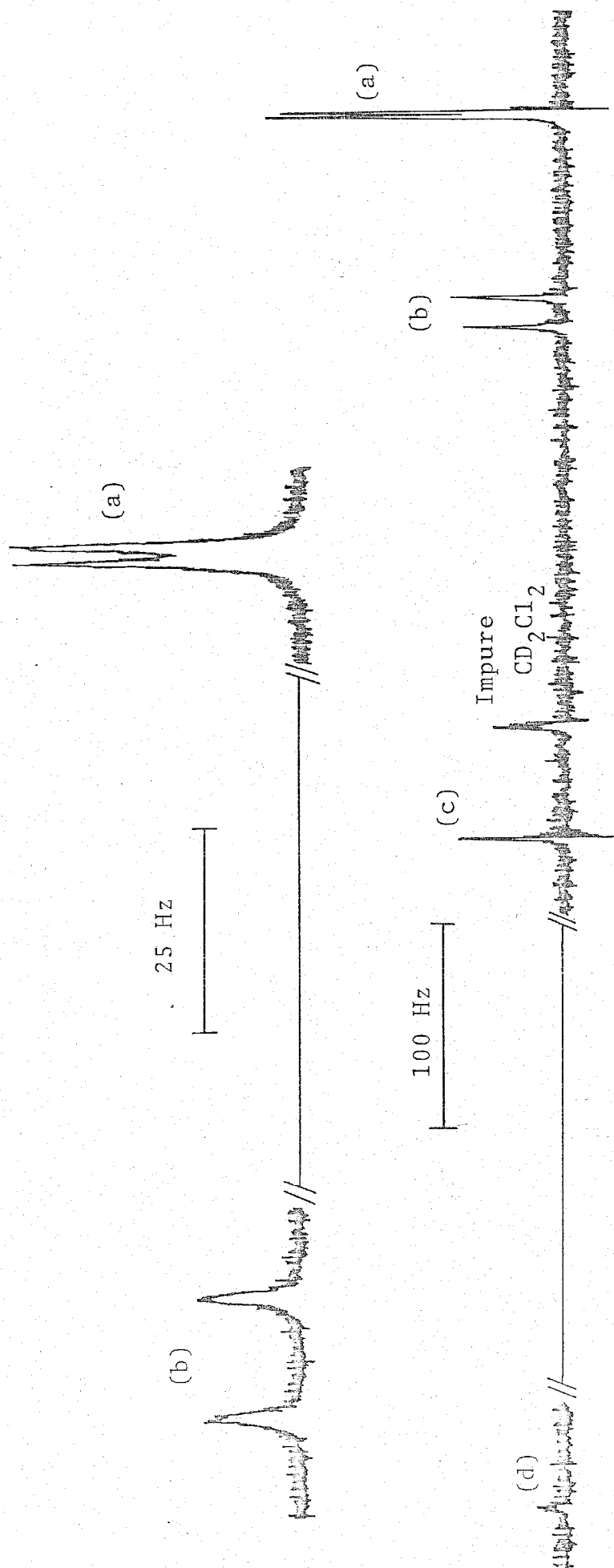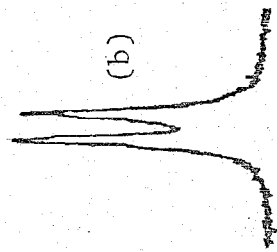two methyl groups of coordinated acac, i.e. near one to and far

Fig. 10. The ^{1}H NMR spectrum of $UO_2(acac)_2DMF(0.0364\ m)$ in CD_2Cl_2 at $-40\ °C$.

Fig. 11. The ^{1}H NMR spectrum of $UO_2(acac)_2DEF(0.0472\ m)$ in CD_2Cl_2 at -60 °C.

one from the coordinated DMF or DEF, occur in these complexes. The computed best-fit τ-values are given together with the corresponding lineshapes at the right side of Figs. 12 and 13. For $UO_2(acac)_2DMF$, the exchange reaction of methyl groups was also measured in CD_3COCD_3. The logarithms of k_{intra} obtained from best-fit τ-values are plotted against the reciprocal temperature(Fig. 14) and the activation parameters are listed in Table 1.

The exchange rate constants for various concentrations of complexes were measured in a similar manner as in the $UO_2(acac)_2DMSO$ system, and the results are listed in Table 2. It is found that the exchange rate is first-order with respect to the concetration of complexes.

Fig. 12. Experimental(left-hand side) and best-fit calculated ^{1}H NMR lineshapes of $UO_2(acac)_2DMF$ (0.0364 m) in CD_2Cl_2. Temperatures and best-fit τ-values are shown at the left- and right-hand sides of the figure, respectively.
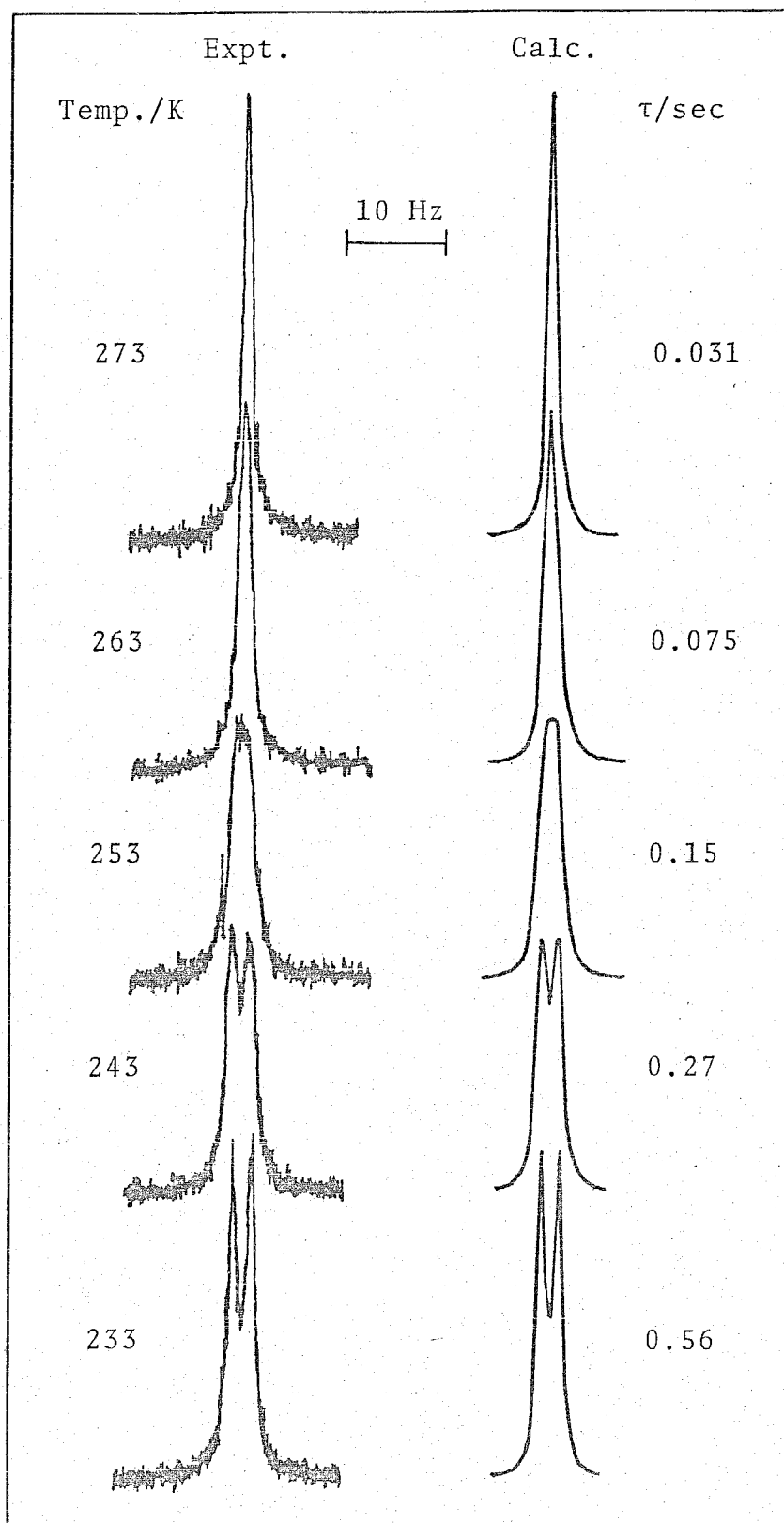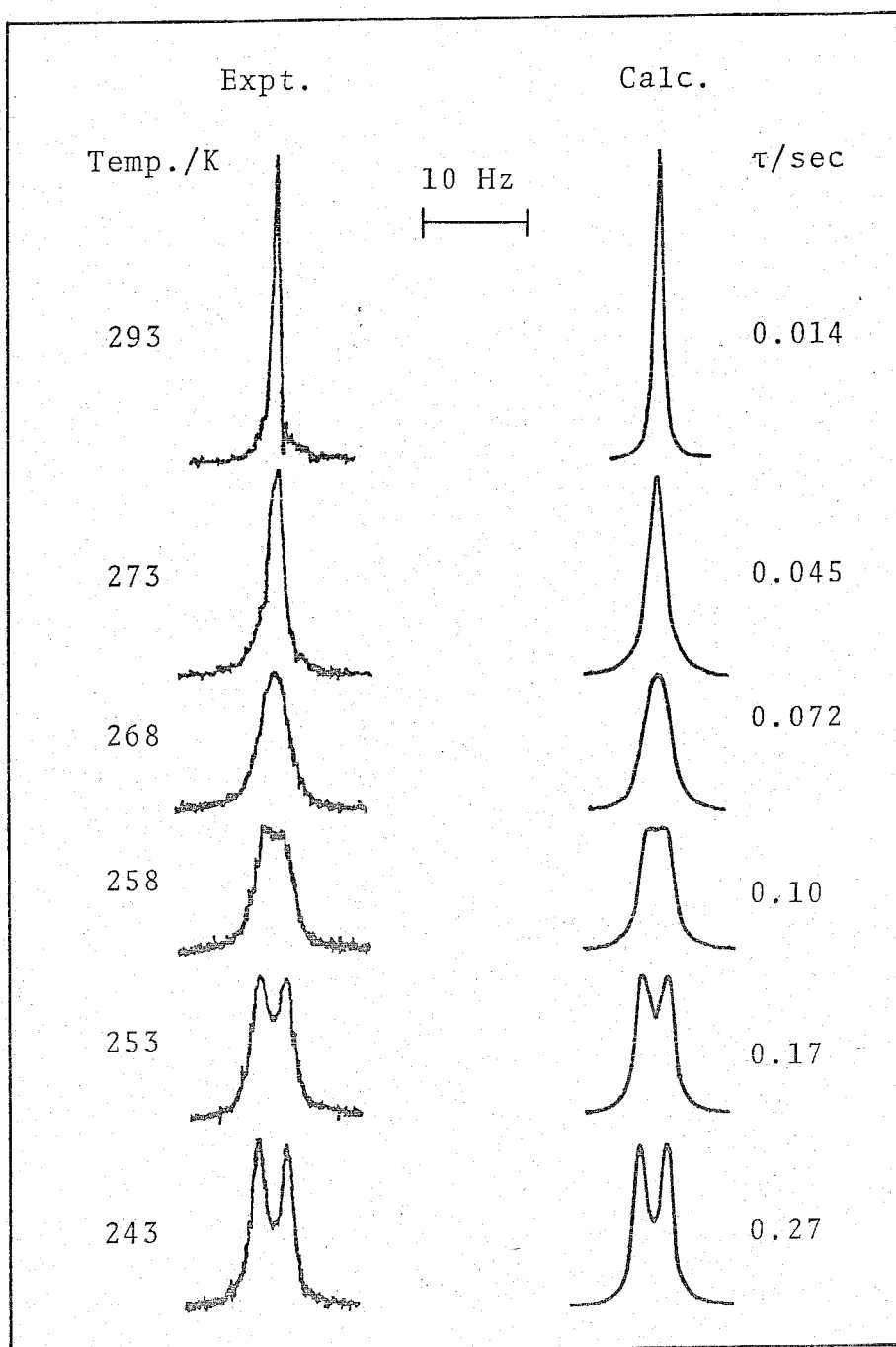
Fig. 13. Experimental (left-hand side) and best-fit
calculated ^{1}H NMR lineshapes of $UO_2(acac)_2DEF$
(0.0472 m) in CD_2Cl_2. Temperatures and best-fit
τ-values are shown at the left- and right-hand
sides of the figure, respectively.

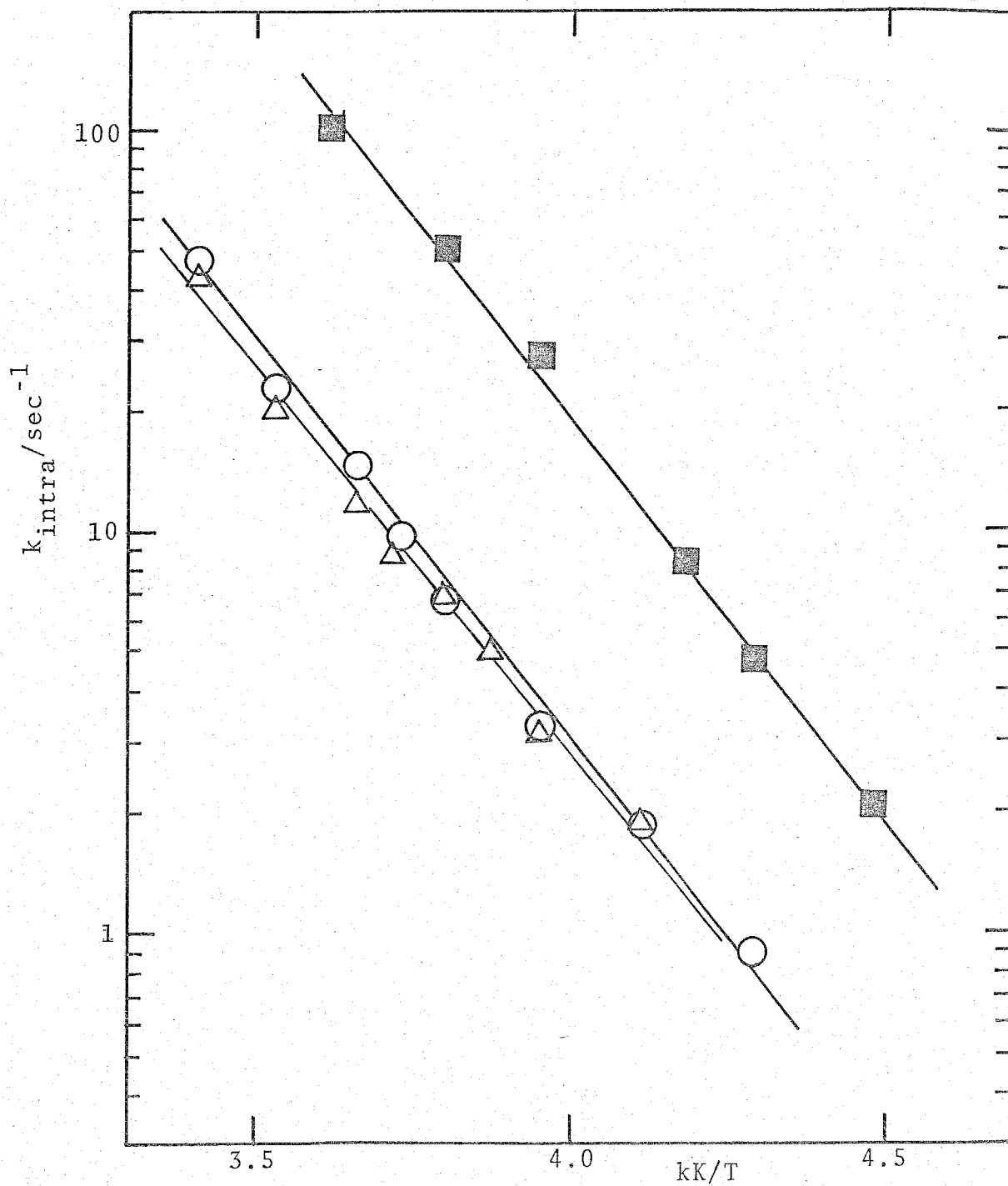Fig. 14. Semilogarithmic plots of k_{intra} against the reciprocal temperature for the exchange of methyl groups of acac in $UO_2(acac)_2L$ (L= DMF and DEF). $\bigcirc$: $UO_2(acac)_2DMF$ in CD_2Cl_2; $\blacksquare$: $UO_2(acac)_2DMF$ in CD_3COCD_3; $\triangle$: $UO_2(acac)_2DEF$ in CD_2Cl_2.

C. Mechanism

The data listed in Table 2 indicate that the exchange rate of the methyl groups depends on the concentration of $UO_2(acac)_2L$ in the first-order and it is unlikely that the exchange proceeds through the binulear complex formed by collision of $UO_2(acac)_2L$ complexes. Therefore, it can be considered that one of the following four mechanisms is responsible for the operative mechanism which may elucidate the intramolecular exchange of methyl groups of coordinated acac in $UO_2(acac)_2L$ complexes:

(i) Complete dissociation of one of two coordinated acetyl-acetonate ions;

(ii) Rupture of one U-O bond to give a four-coordinated inter-mediate in the equatorial plane which has one unidentate and one bidentate acetylacetonate and L;

(iii) A twist mechanism in which the methyl groups exchange without dissociation of coordinated acetylacetonate ion;

(iv) Dissociation of L to give a four-coordinated intermediate in the equatorial plane.

In these mechanisms, mechanism (i) is eliminated because the exchange between the coordinated acac and the free acetylacetonate ion is not observed in the present temperature range where the exchange of methyl groups occurs rapidly. Figure 15 shows the ^1H NMR spectra of $UO_2(acac)_2DMSO$ in $o\text{-}C_6H_4Cl_2$ at 30 °C and of a solution containing $UO_2(acac)_2DMSO$, free acetylacetone, and $o\text{-}C_6H_4Cl_2$ at 40 °C. Symbols (a), (b), and (c) are identical with those in Fig. 1. The methyl proton signal of the coordinated acac at 30 °C

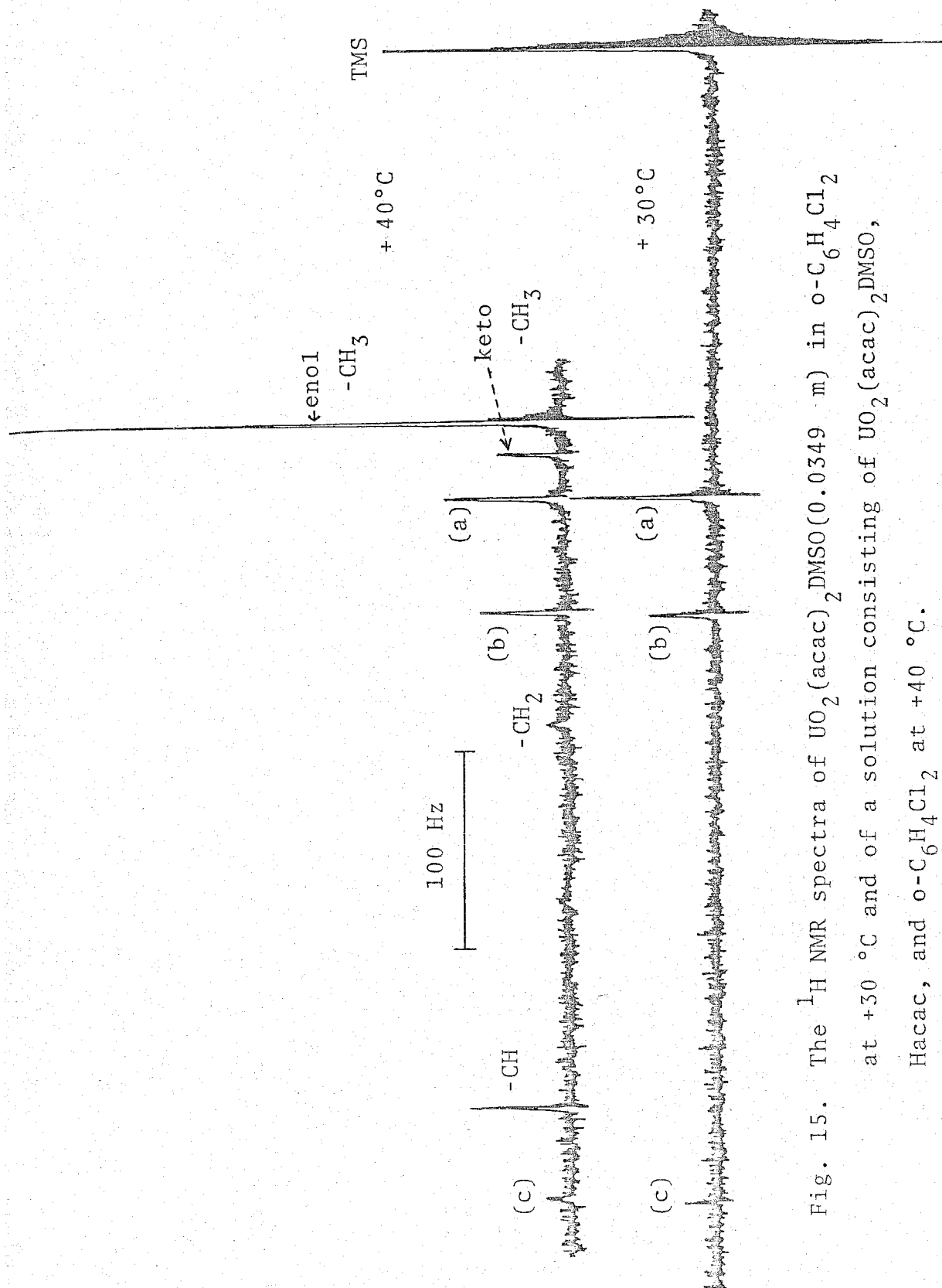Fig. 15. The ^{1}H NMR spectra of $UO_2(acac)_2DMSO(0.0349 \cdot m)$ in $o\text{-}C_6H_4Cl_2$ at +30 °C and of a solution consisting of $UO_2(acac)_2DMSO$, Hacac, and $o\text{-}C_6H_4Cl_2$ at +40 °C.

is a singlet. This means that the exchange rate of methyl groups of the coordinated acac is fast at this temperature. At 40 °C, the methyl proton signals of keto and enol isomers of free acetyl-acetone were observed at higher field than that of the coordinated acac. This indicates that the rate of exchange between the coordinated acac and the free acetylacetone is very slow. Similar phenomena were also observed in the exchange reaction of methyl groups in $UO_2(acac)_2DMSO$ in other solvents and in those in $UO_2(acac)_2DMF$ and $UO_2(acac)_2DEF$.

Mechanism (ii) also may not be applied to this reaction because the rate constant for the dissociation of one-end of coordinated acac has been estimated to be 2.04 sec^{-1} at 25 °C in $o\text{-}C_6H_4Cl_2$ as shown in the next chapter. This value is much smaller than 63.2 sec^{-1} of the present reaction at 25 °C in $o\text{-}C_6H_4Cl_2$.

Mechanism (iii) also may be unlikely since the uranyl ion has a stable linear structure, O=U=O. This structure may hinder the formation of the twisted intermediate.

It is found from Table 1 that the activation enthalpies for the exchange of methyl groups in $UO_2(acac)_2L$ in CD_2Cl_2 and CD_3COCD_3 decrease in the order L = DMSO > DMF > DEF. This fact suggests that the exchange of methyl groups in these complexes proceeds through the mechanism(iv), in which the properties of L may reflect directly in the value of the activation enthalpy. This mechanism is also supported by the fact that the exchange of L is fast enough in the present temperature range(-30 - +20 °C)

and takes place through the D mechanism as shown in chapter IV.

The mechanism (iv) is represented by Scheme I.
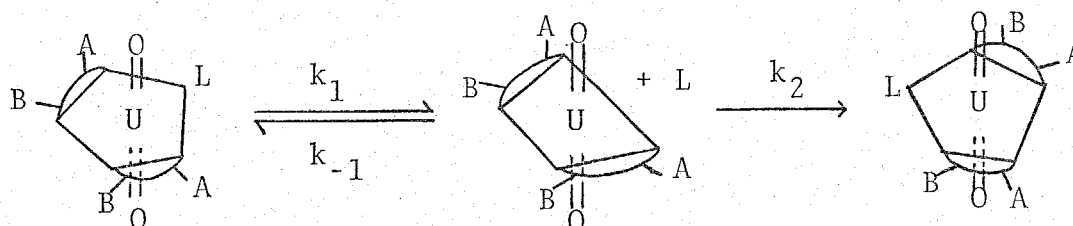
Scheme I

where the symbols of A and B represent the two kinds of methyl groups of coordinated acac. The rate-determining step is the dissociation of L from $UO_2(acac)_2L$. It is assumed that the resulting intermediate, $UO_2(acac)_2$, has an unsymmetrical tetragonal bipyramidal structure and the exchange of methyl groups occurs in only the k_2 path.

From this mechanism, the observed first-order exchange rate constant, k_{intra}, is given by Eq. (2)

$$k_{intra} = k_1 k_2 / (k_{-1} + k_2) \qquad (2)$$

Two limiting forms of Eq. (2) are:

(i) $k_{intra} = k_1 = k_{inter}$ when $k_2 \gg k_{-1}$

(ii) $k_{intra} = k_1 k_2 / k_{-1}$ when $k_2 \ll k_{-1}$

where k_{inter} denotes the rate constant for the exchange between the free and coordianted L in $UO_2(acac)_2L$ (Chapter IV). If the exchange of methyl groups proceeds through this mechanism, the rate constant should not exceed the value of k_{inter}, and the activation enthalpy for k_{intra} should be equal to that for k_{inter}. The kinetic parameters for the exchange of methyl groups and of L in $UO_2(acac)_2L$ are shown in Table 3. It is seen that $\Delta H^{\ddagger}$ values for both reactions are equal within experimental error and the values of k_{intra} do not exceed those of k_{inter}. These facts indicate that the exchange of methyl groups proceeds through the mechanism (iv) and that the intermediate, $UO_2(acac)_2$, has an unsymmetrical tetragonal bipyramidal structure. If the symmetrical intermediate is formed, the values of k_{intra} become equal to those of k_{inter}.

Table 1 shows that the values of k_{intra} in CD_3COCD_3 are larger than those in other solvents for both of $UO_2(acac)_2DMSO$ and $UO_2(acac)_2DMF$. This may be chiefly attributable to the basicity of solvents. Acetone has the largest basicity among four solvents used and solvates to the intermediate more strongly than other solvents do. This solvation makes the intermediate more stable in acetone than in the other solvents. Hence the activation entropy in acetone becomes larger than in the others, and the rate of the exchange of methyl groups in acetone becomes faster than those in the other solvents in spite of large activation enthalpies.

It has been suggested generally[3,5] in the intramolecular

exchange reaction that the activation free energy decreases with increasing dielectric constant of the solvent owing to a lowering of the activation enthalpy as a result of greater charge separation and greater solvation in the transition state. The greater solvation in the transition state better meets the bond rupture mechanism (ii) than the twist mechanism (iii), because in the mechanism (ii) the charge separation in the transition state is greater than that in the ground state due to the presence of a partially charged uncoordinated carbonyl group. In the present study, the activation free energy decreases in the order $CD_3NO_2 > CD_2Cl_2 > o\text{-}C_6H_4Cl_2 > CD_3COCD_3$ (see Table 1). This tendency is different from the order, $CD_2Cl_2 > o\text{-}C_6H_4Cl_2 > CD_3COCD_3 > CD_3NO_2$, which is expected from that of the dielectric constants[9], i.e. CH_3NO_2 (33.94) $> CH_3COCH_3$ (20.7) $> o\text{-}C_6H_4Cl_2$ (9.93) $> CH_2Cl_2$ (8.93). This fact indicates that the difference in k_{intra} is not attributable to the contribution of only the activation enthalpy and that both mechanism (ii) and (iii) are not responsible to the exchange of methyl groups of coordinated acac in $UO_2(acac)_2L$.

Table 3. Kinetic parameters for the exchanges of methyl groups of acac and of L in $UO_2(acac)_2L$ (L = DMSO and DMF)

Complex	Solvent	Reaction [a]	$\Delta H^{\ddagger}$ kJ mol^{-1}	$\Delta S^{\ddagger}$ JK^{-1}mol^{-1}	$k(25\ ^{\circ}C)$[b] 10 sec^{-1}
$UO_2(acac)_2DMSO$	CD_3COCD_3	intra	46.6 ± 1.7	-47.5 ± 6.7	15.2
		inter	45.8 ± 0.8	-46.6 ± 2.9	23.6
	CD_2Cl_2	intra	42.4 ± 2.9	-70.1 ± 10.9	5.45
		inter	47.9 ± 5.2	-46.6 ± 11.2	10.2
$UO_2(acac)_2DMF$	CD_3COCD_3	intra	39.1 ± 1.5	-63.4 ± 3.4	47.0
		inter	42.0 ± 1.3	-46.2 ± 5.5	114
	CD_2Cl_2	intra	35.3 ± 1.3	-94.5 ± 4.2	5.19
		inter	32.8 ± 1.7	-92.0 ± 5.9	19.0

[a] intra and inter represent the exchange reactions of methyl groups of acac and of L in $UO_2(acac)_2L$ (L = DMSO and DMF), respectively. [b] Calculated values from $\Delta H^{\ddagger}$ and $\Delta S^{\ddagger}$ at 25 °C.

iv. SUMMARY

It is concluded that the exchange reaction of the methyl groups of coordinated acac in $UO_2(acac)_2L$ (L = DMSO, DMF, and DEF) takes place through the mechanism (iv) and that the intermediate, $UO_2(acac)_2$, formed in this mechanism has an unsymmetrical structure in the equatorial plane. The mechanism (iv) is different from that found in most of β-diketonato complexes[1-7], where the exchange reaction proceeds through the mechanism (ii) or (iii). This difference is attributed to the fact that most of β-diketonato complexes are octahedral and, as a whole, can easily change their structures in the transition state, whereas a uranyl ion has a stable linear structure, O=U=O, and the structure change is restricted within the equatorial plane.

REFERENCES

1. R.C. Fay and R.N. Lowry, Inorg. Chem., $\underline{6}$, 1512(1967).

2. N. Serpone and R.C. Fay. Inorg. Chem., $\underline{6}$, 1835(1967).

3. R,C. Fay and T.S. Piper, Inorg. Chem., $\underline{3}$, 348(1964).

4. J.J. Fortman and R.E. Sievers., Inorg. Chem., $\underline{6}$, 2022(1967)

5. D.A. Case and T.J. Pinnavaia., Inorg. Chem., $\underline{10}$, 482(1971).

6. T.J. Pinnavaia, J.M. Sebeson, II, and D.A. Case, Inorg. Chem., $\underline{8}$, 644(1069).

7. T.J. Pinnavaia and W.R. Clements, Inorg. Nucl. Chem. Letters, $\underline{7}$, 1127(1971).

8. R.C. Fay and J.K. Howie, J. Am. Chem. Soc., $\underline{101}$, 1115(1979).

9. T.R. Griffiths and D.C. Pugh, Coord. Chem. Rev., $\underline{29}$, 129(1979).

CHAPTER VI

KINETIC STUDY OF THE EXCHANGE REACTION

OF ACETYLACETONATE IN BIS(ACETYLACETONATO)

DIOXO(DIMETHYL SULFOXIDE)URANIUM(VI) BY NMR

i. INTRODUCTION

The ligand exchange reactions in various β-diketonato complexes have been studied by the labelling method[1-13] or NMR method[14-18], and the mechanism and the reactivity of various metal ions have been discussed.

Little information is available, however, concerning the ligand exchange reactions in uranyl β-diketonato complexes in spite of a large number of studies on the ligand exchange reactions in the uranyl complexes with unidentate ligands.

In this chapter, hence, the exchange reaction between the free acetylacetone(Hacac) and the coordinated acetylacetonate (acac) in bis(acetylacetonato)dioxo(dimethyl sulfoxide)uranium (VI), $UO_2(acac)_2DMSO$, is dealt with and the reaction mechanism will be discussed in detail and compared with the ligand exchange reactions in other β-diketonato complexes.

In the previous chapter, the results of the exchange reaction of methyl groups in the coordinated acac in $UO_2(acac)_2L$ (L = DMSO, DMF, and DEF) were reported and proposed that this exchange reaction proceeds through the dissociation of L. This mechsnism was proposed on the basis of the results that the acac exchange rate in $UO_2(acac)_2DMSO$ was much slower than that of DMSO. However, if the dissociation rate of one-end of coordinated acac is faster than that of DMSO, the mechanism which proceeds through the dissociation of L becomes groundless. The present study was undertaken to solve this difficulty.

ii. EXPERIMENTAL

A. Materials

The complex $UO_2(acac)_2DMSO$ was the same one as used as in previous chapter. Acetylacetone(Wako Pure Chemical Ind. Ltd.) was stored over K_2CO_3 and then distilled twice under vacuum. ortho-Dichlorobenzene($o-C_6H_4Cl_2$) was distilled twice in vacuo and stored over 3-A molecular sieves. This solvent was used because of its high boiling point(180.5 °C)

B. Measurements of NMR, UV, and IR Spectra

^1H NMR spectra were measured by using the same instruments as described in Chapter III. The ^1H NMR spectra were recorded at least twice, and particulaly the methyl proton signals of the coordianted acac and the free Hacac were observed more than three times. Ultraviolet and infrared spectra of $UO_2(acac)_2DMSO$ in $o-C_6H_4Cl_2$ and of $UO_2(acac)_2DMSO$ in $o-C_6H_4Cl_2$ containing free Hacac were measured by using Jasco UVIDEC-505 spectrophotometer and Jasco DS-701 G IR spectrometer, respectively. The samples for these measurements were prepared by the same method as that described in Chapter IV.

C. Measurement of Keto-Enol Equiliblium of Acetylacetone

Acetylacetone exists in keto and enol isomers. The fraction of the keto and enol forms of acetylacetone in $o-C_6H_4Cl_2$ has been measured from the areas of the methyl proton signals of the keto and enol isomers. The measurement was done for 0.131 and 1.00 M solutions of acetylacetone in $o-C_6H_4Cl_2$.

Equiliblium constant, $K = [\text{Hacac}]_{\text{Keto}}/[\text{Hacac}]_{\text{Enol}}$, where $[\text{Hacac}]_{\text{Keto}}$ and $[\text{Hacac}]_{\text{Enol}}$ denote the concentrations of the keto and enol isomers of acetylacetone, respectively, was calculated from these fractions.

D. Kinetic Analysis

Kinetic analysis was done by the same method as described in Chapter II. In the present system, the keto isomer does not contribute to the ligand exchange reaction and hence P_c and P_F are given by the following equation

$$P_c^{'} = \frac{2[\text{UO}_2(\text{acac})_2\text{DMSO}]}{2[\text{UO}_2(\text{acac})_2\text{DMSO}] + [\text{Hacac}]_{\text{Enol}}}$$

$$P_F = 1 - P_c$$

The values of T_{2c} and T_{2F} were obtained from the linewiths of the methyl proton signal of the coordinated acac in $\text{UO}_2(\text{acac})_2$-DMSO and of the methyl proton signal of the enol isomer of acetylacetone in $\text{o-C}_6\text{H}_4\text{Cl}_2$, respectively. The chemical shifts of the coordinated acac and of enol methyl proton signal were used as the values of ω_{0c} and ω_{0F}. The best-fit τ-values were obtained by using these parameters.

iii. RESULTS AND DISCUSSION

A. Structure of $UO_2(acac)_2DMSO$ in Solution containing

$UO_2(acac)_2DMSO$, Hacac, and $o-C_6H_4Cl_2$

As shown in Chapter V, the structure of $UO_2(acac)_2DMSO$

in $o-C_6H_4Cl_2$ has been found to be pentagonal bipyramidal.
In order to examine the structure of $UO_2(acac)_2DMSO$ in $o-C_6H_4Cl_2$
containing free Hacac, the spectra of NMR, UV, and IR for this
solution were measured.

^1H NMR spectra are shown in Fig. 1. The signals of (a)
and (b) correspond to the methyl protons of enol and keto isomers
of Hacac, respectively. The (c) and (d) signals are the methyl
protons of the coordinated acac and the coordinated DMSO, respec-
tively. In the spectrum at 60 °C in Fig. 1, the area ratio of
(d) to (c) was 1 : 2. It was found from the area ratios of
(a) to (b) to (c) and of (d) to (c) that two acetylacetonate ions
and one DMSO molecule coordinate to uranyl ion.

The measurements of UV and visible spectra were carried out
for two solutions containing $UO_2(acac)_2DMSO$, Hacac, and $o-C_6H_4Cl_2$,
and $UO_2(acac)_2DMSO$ and $o-C_6H_4Cl_2$. These spectra were consistent
with each other. This fact may indicate that the following
equilibrium does not exist.

$$UO_2(acac)_2DMSO + Hacac \rightleftharpoons UO_2(acac)_2acacH + DMSO \qquad (1)$$
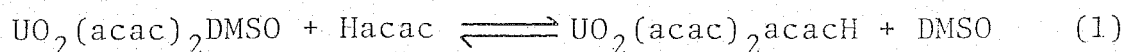
The IR spectra of two solutions mentioned above were also
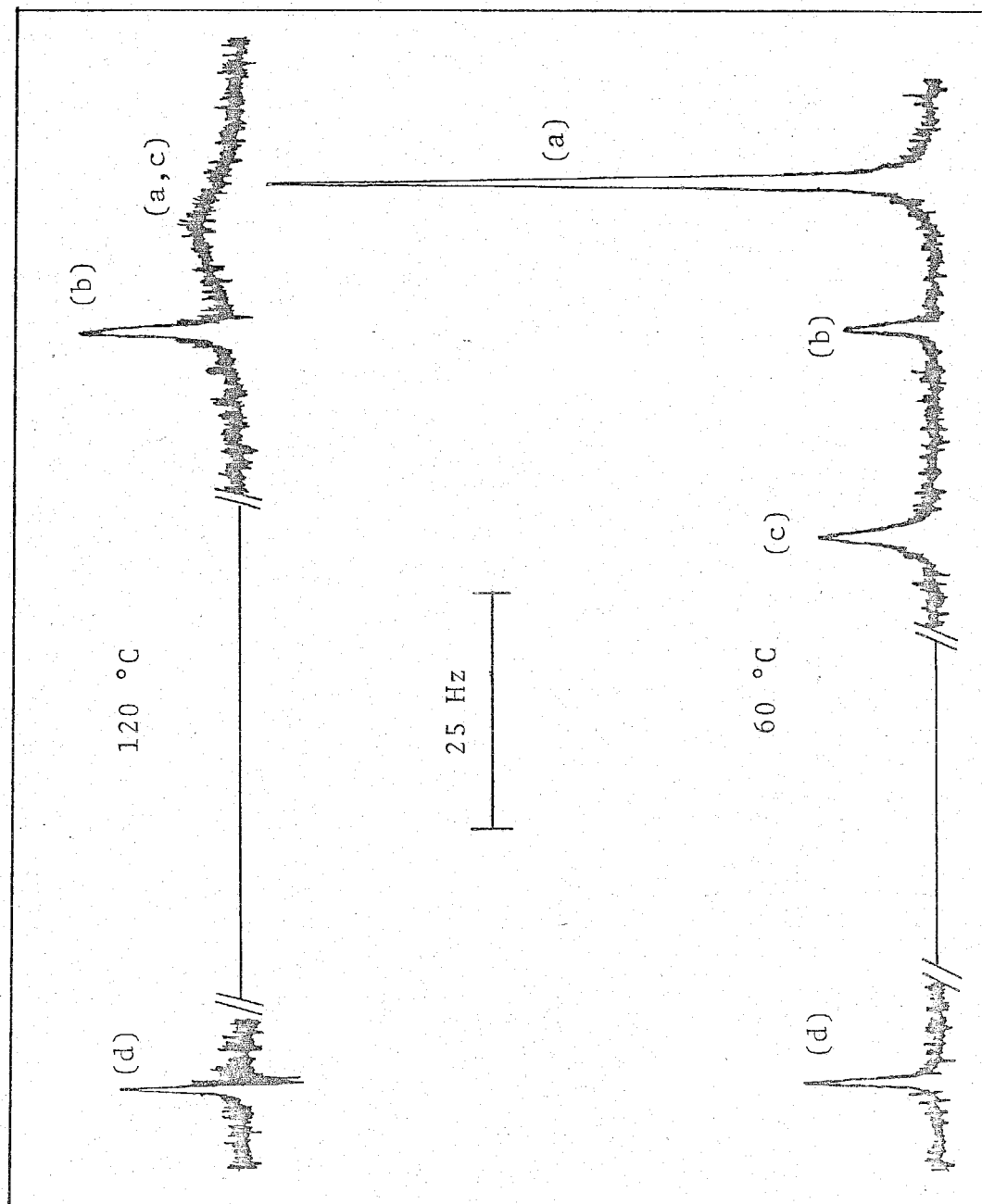
Fig. 1. The ^{1}H NMR spectra of a solution consisting of UO$_2$(acac)$_2$DMSO (0.0679 M), Hacac(0.487 M), and o-C$_6$H$_4$Cl$_2$(8.62 M) at 60 and 120 °C, respectively.

measured. The S=O stretching of $UO_2(acac)_2DMSO$ in $o-C_6H_4Cl_2$
and of $UO_2(acac)_2DMSO$ in $o-C_6H_4Cl_2$ containing free Hacac was
observed at 998 and 994 cm^{-1}, respectively, which is 57 and 61
cm^{-1} lower than that observed in pure DMSO(1055 cm^{-1}), These
results indicates that the DMSO molecule coordinate to the uranyl
ion through oxygen, because it has been known[19] that the S=O
stretching frequency decrease when DMSO coordinates through
oxygen in DMSO complexes.

Therefore, it can be concluded that even if the free Hacac
is present in solvent, the equiliblium as shown in Eq. (1) does
not exist.

B. Keto-Enol Equiliblium of Acetylacetone in $o-C_6H_4Cl_2$

It is apparent from Fig. 1 that the keto isomer does not
exchange with the coordinated acac in $UO_2(acac)_2DMSO$ in this
temperature region(60-120 °C). If the keto isomer exchange with
the coordinated acac, the chemical shift and lineshape of the
keto methyl proton signal should be changed with increasing
temperature, but this phenomenon was not observed. Consequently,
it is concluded that the exchange of the keto isomer is very
slow.

It is necessary for kinetic analysis to measure the fraction
of keto and enol isomers of Hacac in $o-C_6H_4Cl_2$ at each temp-
erature. The fraction of keto and enol isomers has been measured
from the areas of the methyl proton signals of the each isomer
and the equiliblium constant, $K = [Hacac]_{Keto}/[Hacac]_{Enol}$, was

Fig. 2. A plot of -ln K agaist the reciprocal temperature

for the keto-enol equilibrium of acetylacetone

in $o\text{-}C_6H_4Cl_2$.
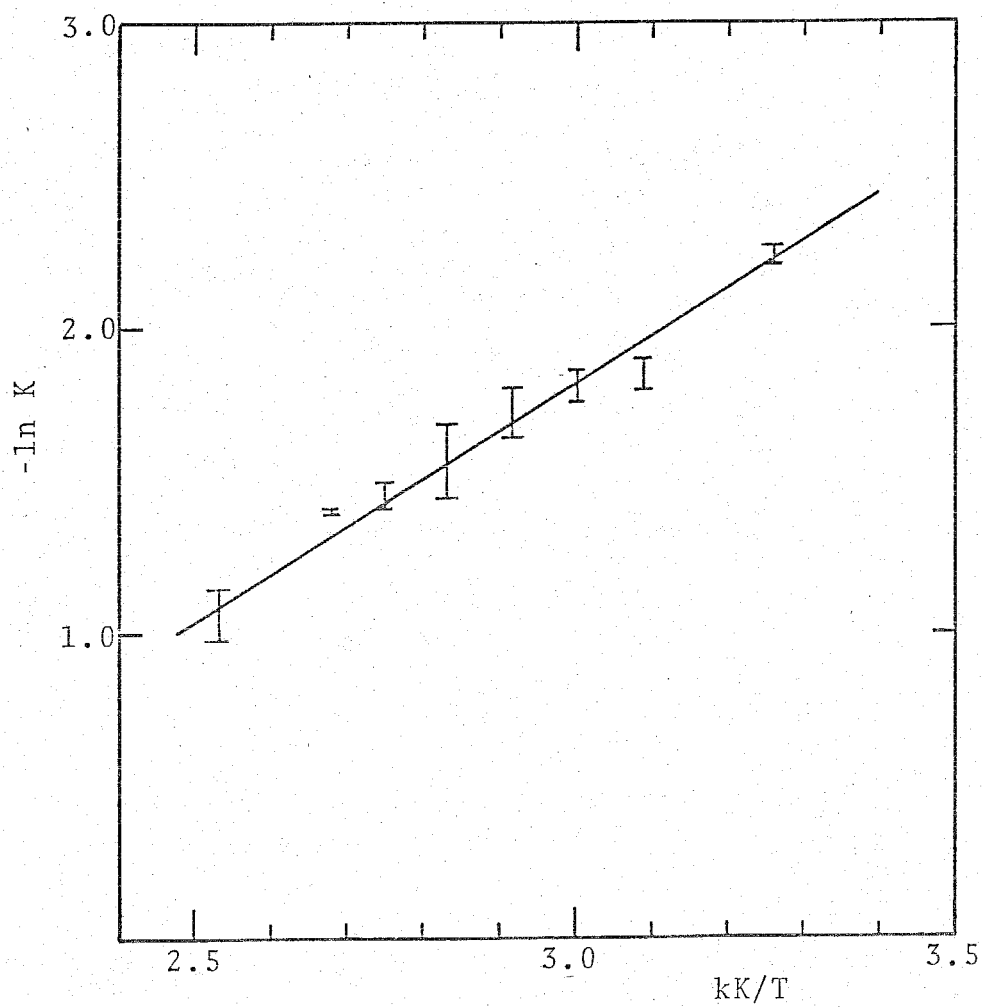
calculated from these fractions. Figure 2 shows the plot of $-\ln K$ against the reciprocal temperature, and the values of enthalpy and entropy obtained are $\Delta H = 12.2$ kJ mol^{-1} and $\Delta S = 21.4$ JK^{-1} mol^{-1}. The fraction of enol isomer of Hacac at each temperature was calculated by using these values.

C. Exchange Reaction of acac in $UO_2(acac)_2DMSO$

C-1. Measurements in $o\text{-}C_6H_4Cl_2$

Figure 3 shows the lineshape change of the methyl proton signals of coordinated acac and free Hacac with temperature. The best-fit τ-value at each temperature was determined by the method described in Chapter II and is shown at the right side of Fig. 3 together with the calculated lineshapes. The first-order rate constant, k_{ex}, was obtained from these τ-values and is expressed by Eq. (2).

$$k_{ex} = rate/2[UO_2(acac)_2DMSO]$$

$$= (kT/h)\exp(-\Delta H^{\ddagger}/RT)\exp(\Delta S^{\ddagger}/R) \qquad (2)$$

Similar measurements were done for solutions listed in Table 1. The logarithms of k_{ex} were plotted against the reciprocal temperature(Fig. 4). It is apparent that the exchange rate depends on the enol isomer concentration and the values of k_{ex} were plotted against $[Hacac]_{Enol}$(Fig. 5). Figure 5 shows that k_{ex} approaches a constant value as the $[Hacac]_{Enol}$ increases. This
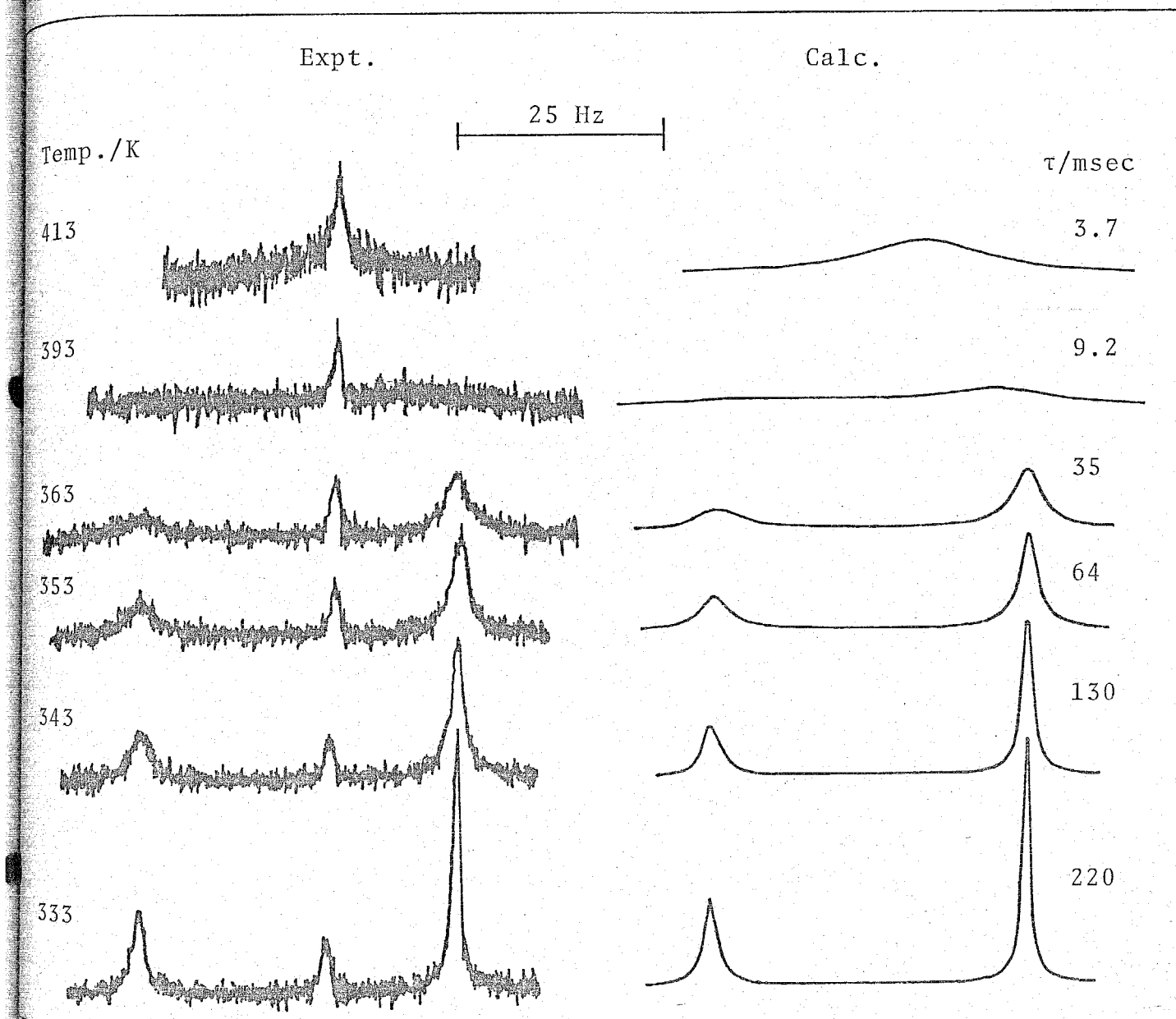
Fig. 3. Experimental (left-hand side) and best-fit calculated ^{1}H NMR lineshapes of a solution consisting of $UO_2(acac)_2DMSO(0.0600$ M) Hacac(0.256 M) and o-$C_6H_4Cl_2$(8.71 M). Temperatures and best-fit τ-values are shown at left- and right-hand sides of the figure, respectively.
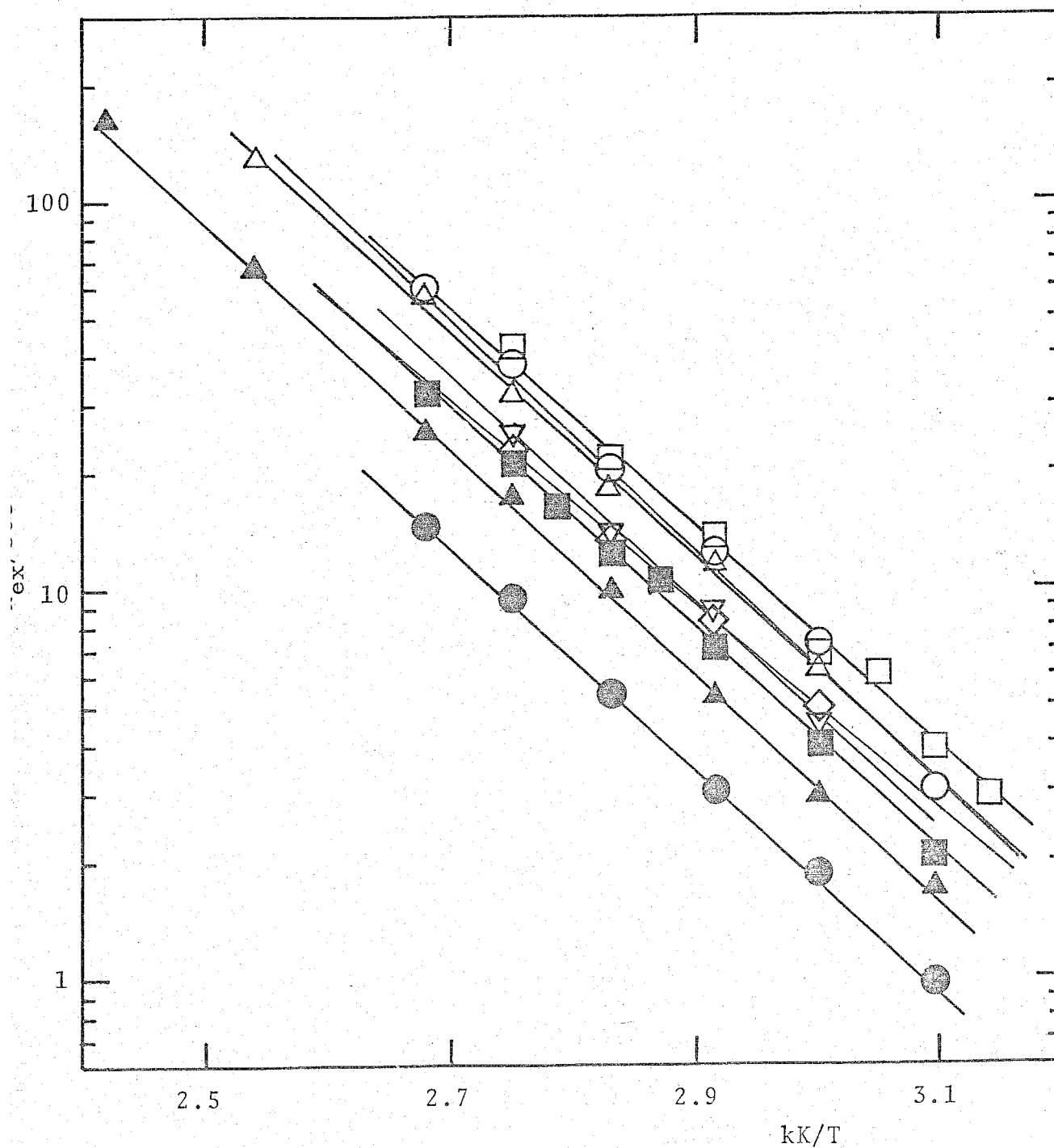
g. 4. Semilogarithmic plots of k_{ex} against the reciprocal temperature for the exchange of acac in $UO_2(acac)_2DMSO$. The symbols of ⊙, △, ▣, ○, △, □, ◇, and ▽ correspond to (i), (ii), (iii), (iv), (v), (vi), (vii), and (viii) in Table 1, respectively.

Table 1. Solution compositions and kinetic parameters for the exchange of acac in $UO_2(acac)_2DMSO$ in $o\text{-}C_6H_4Cl_2$

Solution	$[UO_2(acac)_2DMSO]$ 10^{-2} M	[Hacac] M	$[o\text{-}C_6H_4Cl_2]$ M	$\Delta H^{\ddagger}$ kJ mol^{-1}	$\Delta S^{\ddagger}$ JK^{-1}mol^{-1}	k_{ex}(80 °C) sec^{-1}
i	6.17	0.147	8.85	51.7 ± 0.8	-86.9 ± 2.5	5.35 ± 0.28
ii	6.00	0.256	8.71	53.3 ± 1.3	-77.3 ± 3.8	9.91 ± 1.32
iii	6.02	0.301	8.64	52.1 ± 1.3	-78.5 ± 2.9	12.2 ± 1.25
iv	6.28	0.580	8.56	55.9 ± 1.7	-63.8 ± 4.6	17.6 ± 0.8
v	6.04	0.605	8.52	52.9 ± 2.5	-72.7 ± 7.1	18.0 ± 1.1
vi	6.15	0.703	7.96	51.2 ± 1.7	-76.0 ± 5.0	21.5 ± 0.8
vii	1.56	0.300	8.84	48.3 ± 1.7	-88.8 ± 5.1	13.6 ± 1.9
viii	3.59	0.305	8.72	54.3 ± 1.3	-71.2 ± 3.2	14.4 ± 1.3
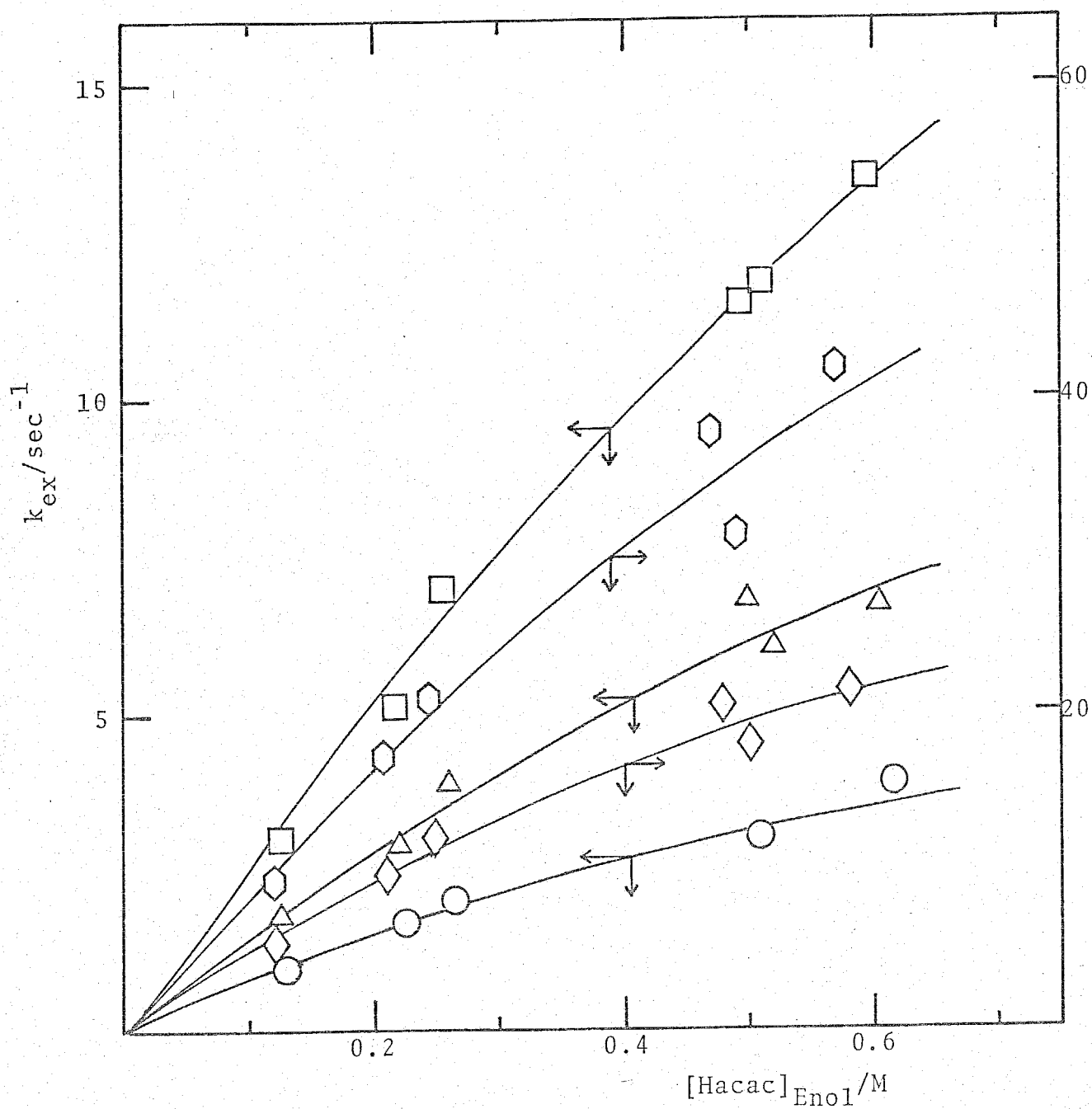
Fig. 5. Plots of k_{ex} vs. $[Hacac]_{Enol}$ for the exchange of acac in $UO_2(acac)_2DMSO$. ○ : 50 °C; △ : 60 °C; □ : 70 °C; ◇ : 80 °C; ⬡ : 90 °C.
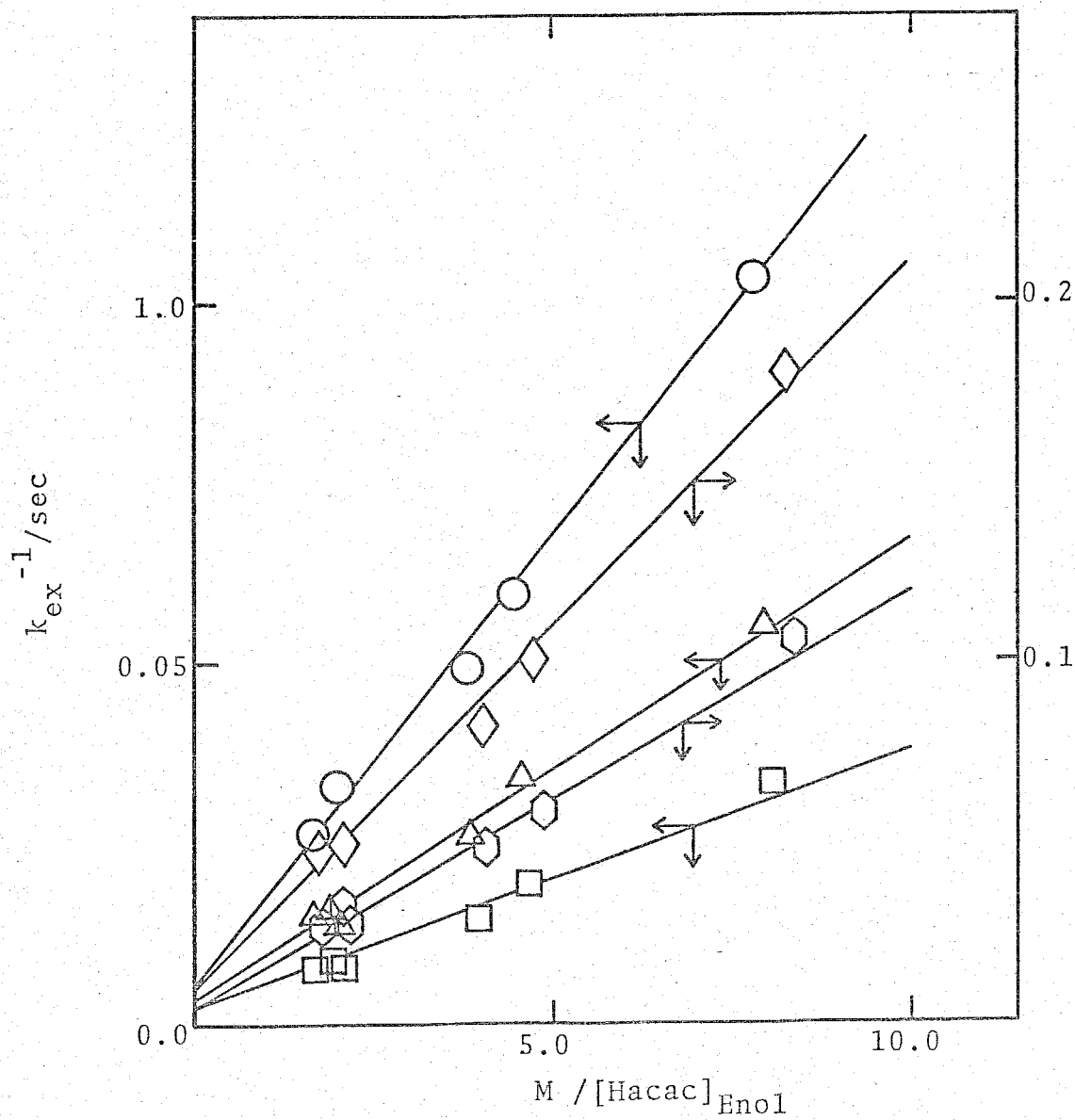
Fig. 6. Plots of $1/k_{ex}$ vs. $1/[Hacac]_{Enol}$ for the exchange of acac in $UO_2(acac)_2DMSO$. ◯ : 50 °C; △ : 60 °C; ☐ : 70 °C; ◇ : 80 °C; ⬡ : 90 °C.

Table 2. The values of k_a, k_b, k_1, k_I, k_2/k_{-1}, and K_{ac} at various temperatures and kinetic parameters for k_1 or k_I path

Temp. °C	k_a* 10^{-3} sec	k_b** 10^{-2} M sec	k_1 or k_I 10 sec^{-1}	k_2/k_{-1} or K_{ac} M^{-1}
50	59.5 ± 26.3	12.3 ± 0.6	1.68 ± 0.74	0.48 ± 0.21
60	24.5 ± 14.0	6.61 ± 0.03	3.92 ± 2.24	0.39 ± 0.22
70	11.7 ± 10.5	3.62 ± 0.02	8.58 ± 7.70	0.32 ± 0.29
80	6.83 ± 7.49	2.14 ± 0.02	14.6 ± 16.0	0.32 ± 0.35
90	3.27 ± 3.08	1.19 ± 0.07	30.6 ± 28.8	0.27 ± 0.25

The kinetic parameters for the k_1 or k_I path

$\Delta H^{\ddagger}$/kJ mol^{-1} = 66.4 ± 8.4

$\Delta S^{\ddagger}$/JK^{-1}mol^{-1} = -17.1 ± 26.8

k_1 or k_I(25°C)/sec^{-1} = 2.04

* k_a = 1/k_1 = 1/k_I. ** k_b = k_{-1}/$k_1 k_2$ = 1/($k_I K_{ac}$).

relation is represented by the following Eq. (3)

$$k_{ex} = [Hacac]_{Enol}/(k_b + k_a[Hacac]_{Enol}) \qquad (3)$$

because the plots of $1/k_{ex}$ vs. $1/[Hacac]_{Enol}$ yield a straight line with an intercept(Fig. 6) and are expressed by Eq. (4).

$$1/k_{ex} = k_a + k_b([Hacac]_{Enol})^{-1} \qquad (4)$$

The values of k_a and k_b were obtained from the intercepts and slopes in Fig. 6, respectively, and are listed in Table 2.

C-2. Dependence of the exchange rate of acac on the complex concentration

It is found from Table 1 that k_{ex} values are constant regardless of the change in the complex concentration (Solutions iii, vii, viii). This indicates that the exchange rate depends on in the first-order with respect to the complex concentration.

C-3. Effect of the added DMSO on the exchange rate of acac

In Chapter IV, the DMSO exchange in $UO_2(acac)_2DMSO$ has been studied. The DMSO exchange proceeds through the D and I_d mechanisms and the exchange rate constant is more than 10^3 sec^{-1} in the present temperature range(50 - 140 °C). In order to examine the effect of this fast exchange of DMSO, the exchange rate of acac were measured for the solutions listed in Table 3. The plots of log k_{ex} against the reciprocal temperature are shown in Fig. 7. The activation parameters were obtained from these plots and

Table 3.   Solution compositions and kinetic parameters for the exchange of acac

in $UO_2(acac)_2DMSO$ in $o\text{-}C_6H_4Cl_2$ containing free DMSO

Solution	$[UO_2(acac)_2DMSO]$ 10^{-2} M	[Hacac] M	[DMSO] 10^{-2} M	$[o\text{-}C_6H_4Cl_2]$ M	$\Delta H^{\ddagger}$ kJ mol^{-1}	$\Delta S^{\ddagger}$ JK^{-1}mol^{-1}
i	6.02	0.301	0.0	8.64	52.1 ± 1.3	-78.5 ± 2.9
ii	5.97	0.314	1.15	8.56	54.4 ± 1.0	-74.3 ± 2.7
iii	5.95	0.300	2.82	8.55	55.3 ± 0.8	-73.2 ± 2.2
iv	5.88	0.304	4.61	8.50	53.6 ± 1.8	-80.0 ± 5.2
v	5.84	0.299	6.40	8.46	52.6 ± 1.1	-83.6 ± 3.2
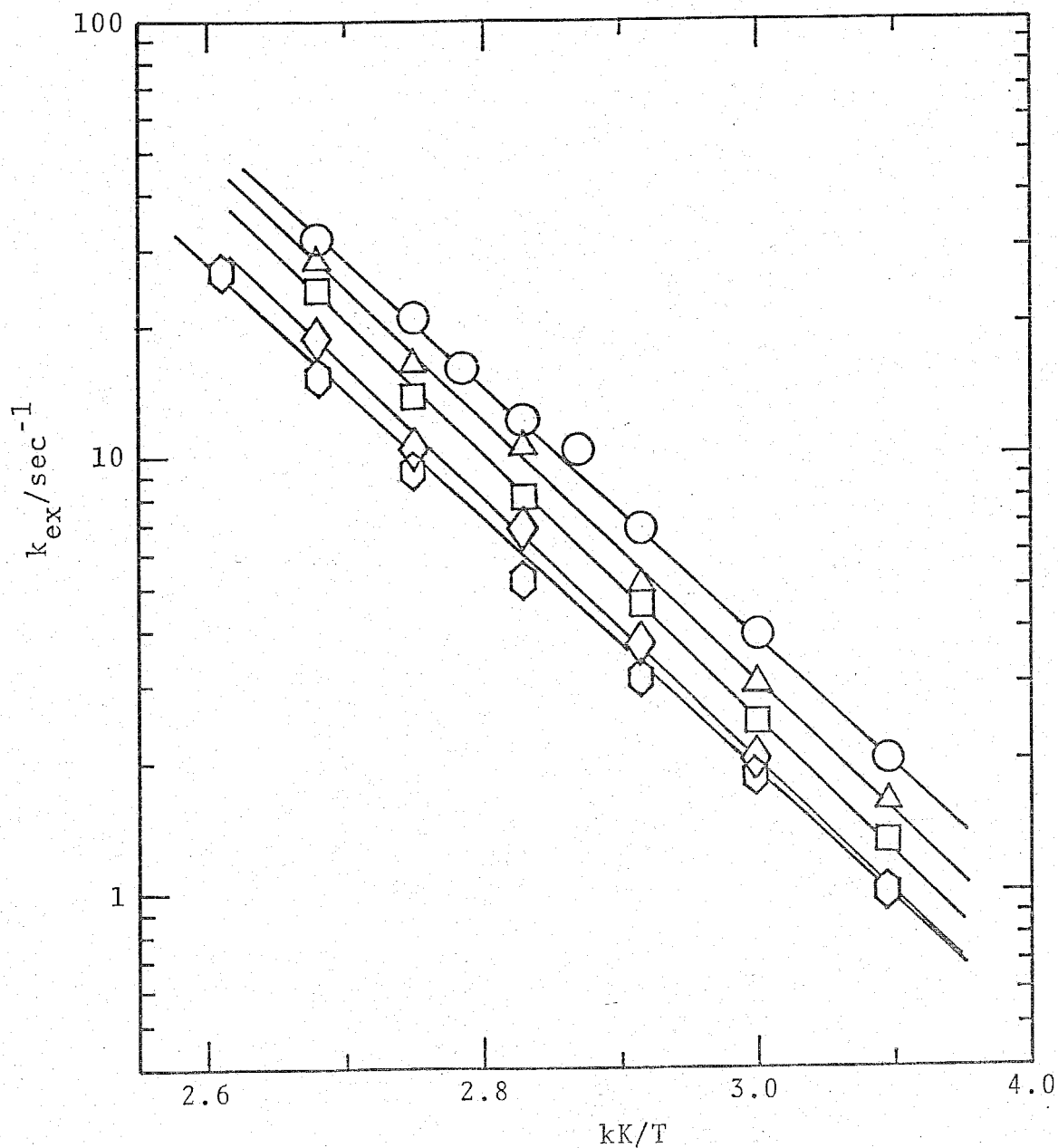
Fig. 7. Semilogarithmic plots of k_{ex} agaist the reciprocal temperature for the exchange of acac in $UO_2(acac)_2DMSO$ in $o\text{-}C_6H_4Cl_2$ containing the free DMSO.

The symbols of $\bigcirc$, $\triangle$, $\square$, $\diamondsuit$, and $\hexagon$ correspond to (i), (ii), (iii), (iv) and (v) in Table 4, respectively.

the results are listed in Table 3. The values of activation parameters are consistent with those in Table 1. These results indicate that the rate-determining step is the same in both reaction systems.

The exchange rate becomes slow as the added DMSO concentration increases(Fig. 8). The plots of $1/k_{ex}$ vs. [DMSO] give the straight lines with the intercepts(Fig. 9) and may be expressed as

$$1/k_{ex} = k_a' + k_b' [DMSO]$$

or

$$k_{ex} = 1/(k_a' + k_b' [DMSO]) \tag{5}$$

The values of k_a' and k_b' were obtained from the intercepts and slopes in Fig. 9 and are listed in Table 4.
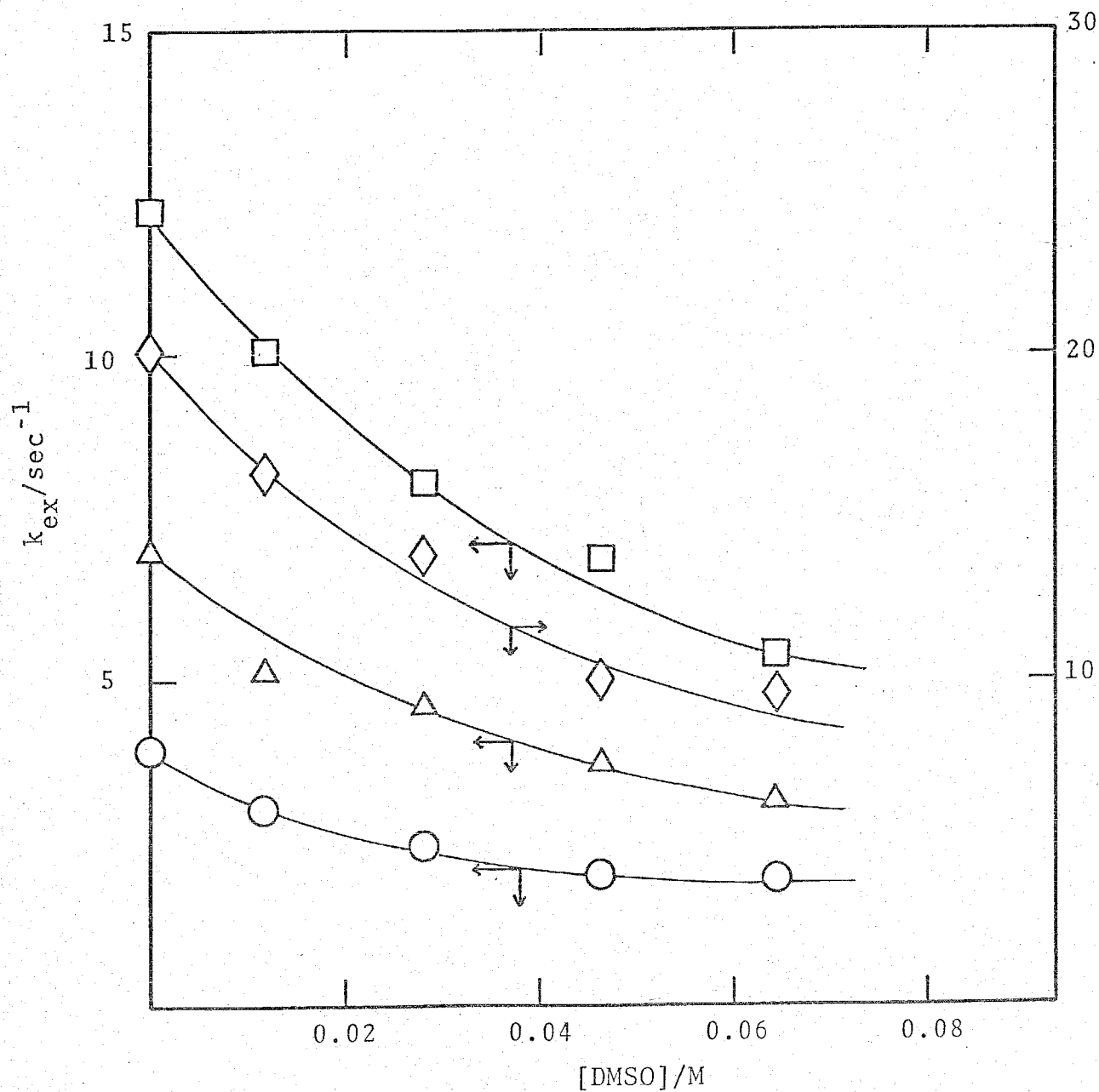
Fig. 8. Plots of k_{ex} vs. [DMSO] for the effect of added DMSO on the exchange of acac in $UO_2(acac)_2DMSO$.
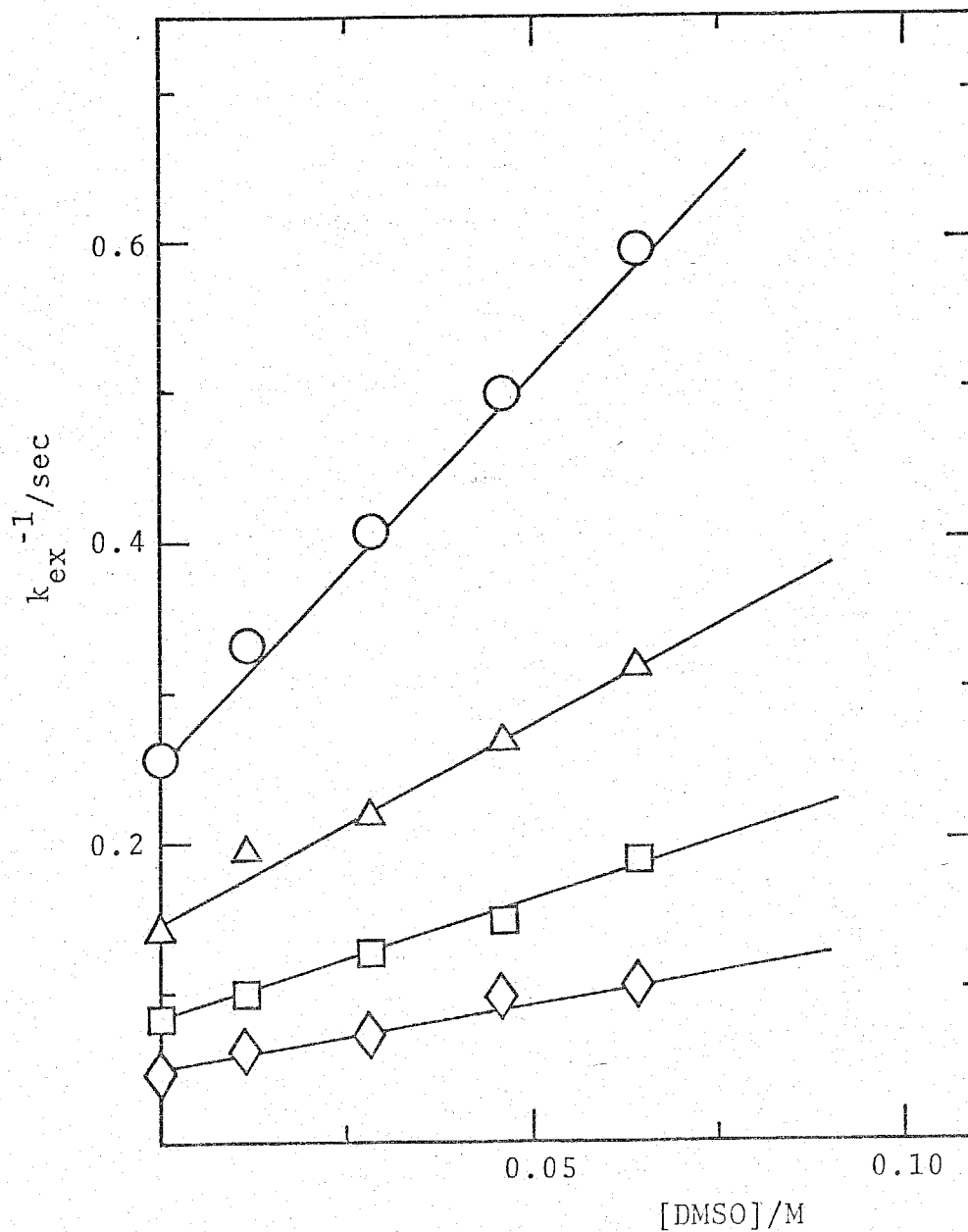
○ : 60 °C; △ : 70 °C; □ : 80 °C; ◇ : 90 °C.

Fig. 9. Plots of $1/k_{ex}$ vs. [DMSO] for the effect of added DMSO on the exchange of acac in $UO_2(acac)_2DMSO$. $\bigcirc$: 60 °C; $\triangle$: 70 °C; $\square$: 80 °C; $\diamondsuit$: 90 °C.

Table 4. The values of k_a' and k_b', k_3/k_2 and K_{ds}
at various temperatures

Temp.	k_a' *	k_b' **	k_3/k_2	K_{ds}
°C	10^{-2} sec	M^{-1} sec		M^{-1}
60	26.2 ± 0.6	5.13 ± 0.15	51.9	20.2
70	15.1 ± 0.7	2.57 ± 0.20	56.9	18.2
80	8.04 ± 0.39	1.58 ± 0.10	57.4	18.4
90	4.91 ± 0.28	0.902 ± 0.073	67.3	18.2

$$* \quad k_a' = \frac{k_{-1} + k_2 [Hacac]_{Enol}}{k_1 k_2 [Hacac]_{Enol}} \quad or \quad \frac{1 + K_{ac}[Hacac]_{Enol}}{k_1 K_{ac}[Hacac]_{Enol}}$$

$$** \quad k_b' = \frac{k_3}{k_1 k_2 [Hacac]_{Enol}} \quad or \quad \frac{K_{ds}}{k_I K_{ac}[Hacac]_{Enol}}$$

D. Mechanism

D-1. Exchange reaction in o-$C_6H_4Cl_2$

In general, it is necessary that two M-O bonds should be broken in order to exchange the coordianted acac, and the proton transfer should occur between coordinated acac and free Hacac. Hence the possible mechanisms for the exchange of acac in UO_2-$(acac)_2$DMSO may be represented as shown in Scheme (I).

In this scheme, (II) is the four-coordinated intermediate in the equatorial plane which has one unidentate acetylacetonate. (III) is the outer-sphere complex which consists of $UO_2(acac)_2$-DMSO and Hacac which is still in the second coordination sphere immediately adjacent to $UO_2(acac)_2$DMSO. The intermediates (IV) and (V) are the six- and three-coordinated complexes in the equatorial plane, respectively. The proton transfer takes place in the path of (IV) $\longrightarrow$ (IV') or between the dissociated acac and free Hacac. The symbols of O-O and O-OH represent acac⁻ and enol isomer of Hacac, respectively.

Some reaction routes are proposed as possible mechanisms. If the exchange reaction proceeds through the route (I) $\longrightarrow$ (IV) $\longrightarrow$ (IV') $\longrightarrow$ (I'), where the path of (I) $\longrightarrow$ (IV) is the rate-determining step, the exchange rate should be proportional to the concentration of the enol isomer, and the activation entropy should be a large negative value. If the exchange reaction takes place through the route (I) $\longrightarrow$ (II) $\longrightarrow$ (V) $\longrightarrow$ (I'), where the rate-determining step is the (I) $\longrightarrow$ (II) path, the exchange rate should not depend on the concentration of the enol isomer, and the activation

DMSO(acac)UO$_2$$\overset{O}{\underset{O}{\diagup}}$)---acacH*

(III)

Hacac*

DMSO(acac)UO$_2$$\overset{O-O}{\underset{O-OH}{\diagup}}$*

(IV)

Proton transfer

DMSO(acac)UO$_2$$\overset{O-OH}{\underset{O-O}{\diagup}}$*

(IV')

DMSO(acac)UO$_2$$\overset{O}{\underset{O}{\diagup}}$)*

(I')

acac^{-}*

Hacac*

DMSO(acac)UO$_2$$\overset{O}{\underset{O}{\diagup}}$)

(I)

Hacac*

DMSO(acac)UO$_2$$\overset{O-O}{}$

(II)

Hacac*

DMSO(acac)UO$_2$ + acac^{-}

acacH*

}---Proton transfer

(V)
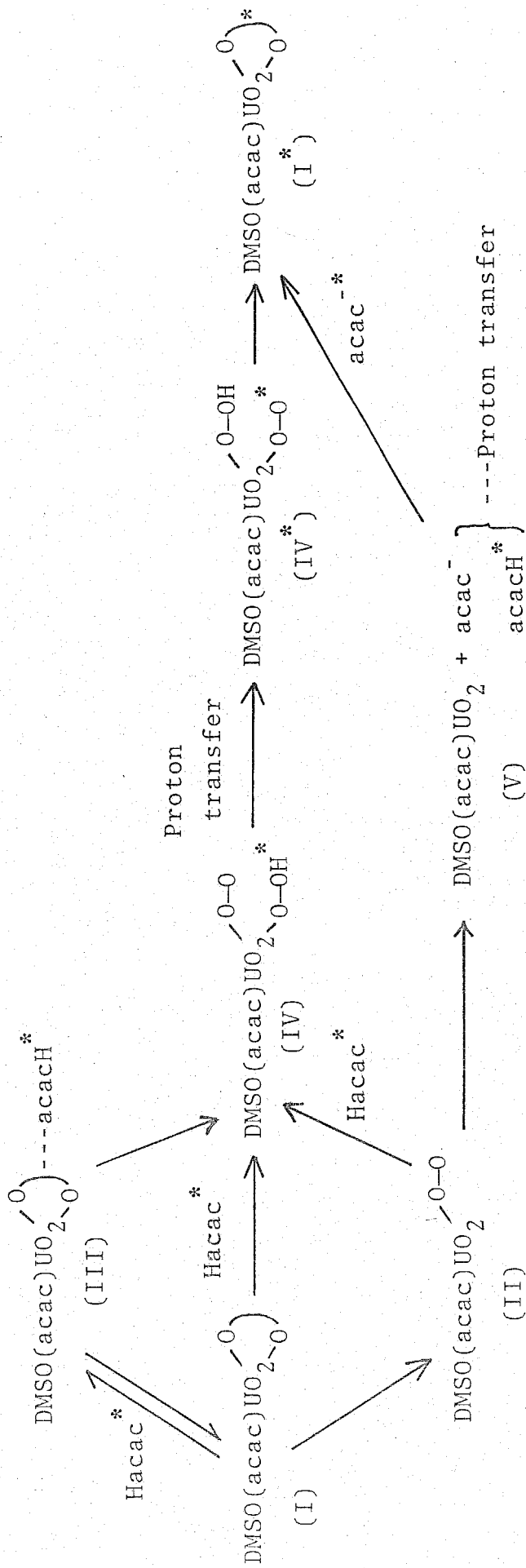
Scheme I

entropy should be a large positive value. Finally, if the proton transfer is the rate-determining step, the exchange rate should not depend on the enol isomer concentration. These three mechanisms are not compatible with the results of the acac exchange reaction, because the exchange rate increases and approaches the limiting value as the concentration of the enol isomer increases as is seen in Fig. 5.

Other than three mechanisms as mentioned above, the following routes, $(I) \longrightarrow (II) \longrightarrow (IV) \longrightarrow (IV') \longrightarrow (I')$ [mechanism 1] and $(I) \longrightarrow (III) \longrightarrow (IV) \longrightarrow (IV') \longrightarrow (I')$ [mechanism 2], are considered to be possible mechanisms. In both mechanisms, the intermediate (IV) is formed. This is in agreement with the fact that the activation entropies for the first-order rate constants are large negative values. Mechanism 1 is represented by Eq. (6)

$$
\text{DMSO(acac)UO}_2\underset{O}{\overset{O}{\diagdown}}\Big) \quad \underset{k_{-1}}{\overset{k_1}{\rightleftharpoons}} \quad \text{DMSO(acac)UO}_2\diagup^{O-O} \tag{6}
$$

$$
\begin{array}{c}
(I) \qquad\qquad\qquad\qquad\qquad\qquad (II) \\[4pt]
\xrightarrow[\text{Hacac}^*]{k_2} \text{DMSO(acac)UO}_2\underset{O-OH}{\overset{O-O}{\diagdown}}{}^* \longrightarrow (IV') \longrightarrow (I') \\[4pt]
(IV)
\end{array}
$$
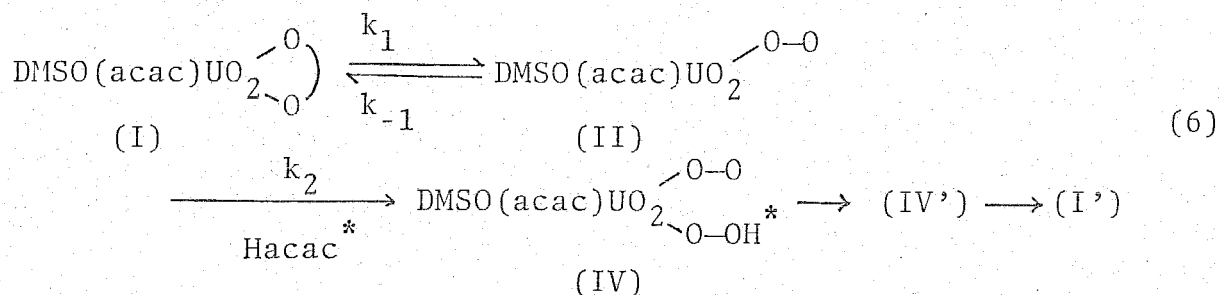
where the rate-determining step is the path of $(I) \longrightarrow (II)$. By applying the steady state approximation to the intermediate (II), the first-order exchange rate constant, k_{ex}, is derived from Eq. (6) as follows,

$$
k_{ex} = \frac{k_1 k_2 [\text{Hacac}]_{\text{Enol}}}{k_{-1} + k_2 [\text{Hacac}]_{\text{Enol}}} \tag{7-a}
$$

or

$$\frac{1}{k_{ex}} = \frac{1}{k_1} + \frac{k_{-1}}{k_1 k_2 [Hacac]_{Enol}} \qquad (7-b)$$

Mechanism 2 is represented by Eq. (8)

$$DMSO(acac)UO_2\binom{O}{O} \underset{Hacac^*}{\overset{K_{ac}}{\rightleftharpoons}} DMSO(acac)UO_2\binom{O}{O} ---acacH^*$$

(I)   (III)   (8)

$$\xrightarrow{k_I} DMSO(acac)UO_2\binom{O-O}{O-OH}^* \longrightarrow (IV') \longrightarrow (I')$$

(IV)
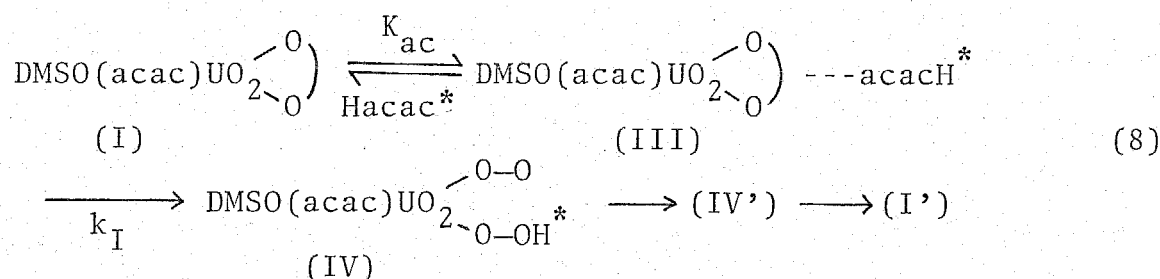
where K_{ac} is the outer-sphere complex formation constant.
In the path, (III) $\longrightarrow$ (IV), the dissociation of one-end of the co-
ordinated acac occurs, followed by the coordination of the
incoming enol isomer. In this mechanism, k_{ex} is given by Eq.
(9-a)

$$k_{ex} = \frac{k_I K_{ac} [Hacac]_{Enol}}{1 + K_{ac} [Hacac]_{Enol}} \qquad (9-a)$$

or

$$\frac{1}{k_{ex}} = \frac{1}{k_I} + \frac{1}{k_I K_{ac} [Hacac]_{Enol}} \qquad (9-b)$$

Both of Eqs. (7-b) and (9-b) are in accord with Eq. (4).
This indicates that the acac exchange reaction may proceed
through either mechanism 1 or 2. The k_a and k_b in Eq. (4)
correspond to the coefficients of Eqs. (7-b) and (9-b) as follows:

for Eq. (7-b)

$$k_a = 1/k_1 \quad \text{and} \quad k_b = k_{-1}/k_1 k_2 \tag{10}$$

and for Eq. (9-b)

$$k_a = 1/k_I \quad \text{and} \quad k_b = 1/k_I K_{ac} \tag{11}$$

It is found from Eqs. (10) and (11) that $k_1 = k_I$ and $k_2/k_{-1} = K_{ac}$. These values obtained from k_a and k_b are listed in Table 2. The logarithm of k_1 or k_I was plotted against the reciprocal temperature (Fig. 10). From this plot, the activation parameters were obtained and listed in Table 2. The $\Delta S^{\ddagger}$ value is not largely negative and may be agreeable with the view that the path (I) $\longrightarrow$ (II) or (III) (IV) is dissiciative. When the value of k_2/k_{-1} (Table 2) are extrapolated to 25 °C, we find $k_2/k_{-1} = K_{ac} = 0.89\ M^{-1}$. The K_{ac} value of $0.89\ M^{-1}$ is equal to that estimated from Fuoss equation, $4\pi Na^3/3000$, for an interaction distance (a) of 7 Å and is much smaller than the value ($4.9 \pm 1.8\ M^{-1}$) which was obtained from the DMSO exchange reaction in $UO_2(acac)_2 DMSO$ in $CD_2 Cl_2$. By considering that the basicity of Hacac (DN = 17.0)[9] is smaller than that of DMSO (DN = 29.8)[21], the value of K_{ac} for Hacac is expected to be smaller than that for DMSO. Accordingly, the K_{ac} value seems to be reasonable.

The reaction of uranyl ion with acetylacetone has been reported[22], and the formation rate constant of the mono acac complex
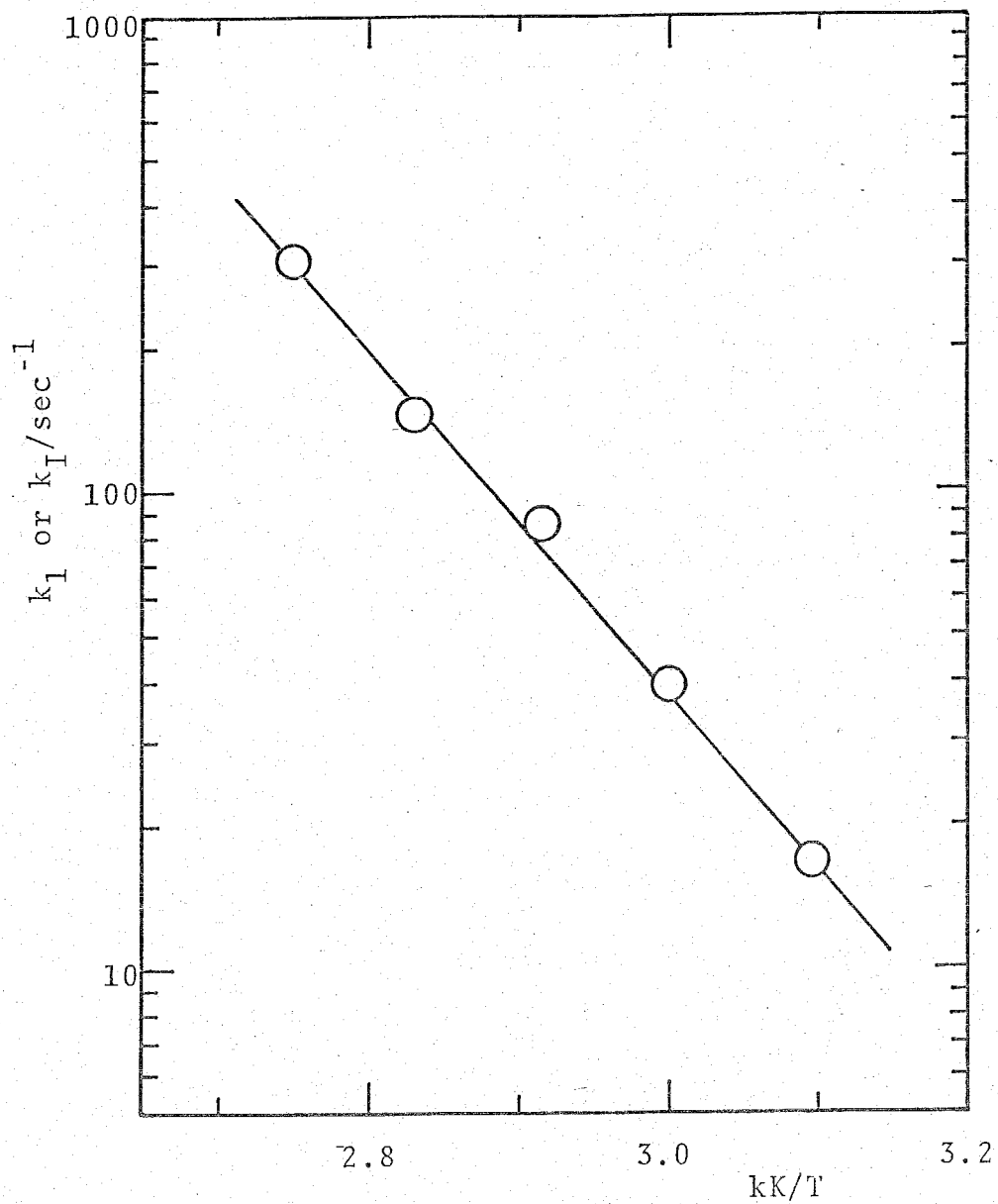
Fig. 10. A semilogarithmic plot of k_1 or k_I against the reciprocal temperature for the exchange of acac in $UO_2(acac)_2DMSO$.

in a methanol-water mixed solvent was 4930 sec^{-1} at 25 °C.

If the value of k_2 is assumed to be equal to or less than 4930 $M^{-1} sec^{-1}$, the value of k_{-1} is estimated to be less than 5.6×10^3 sec^{-1} at 25 °C. This value may be reasonable because k_{-1} is considered to be larger than the exchange rate constant of uni-dentate ligand in uranyl complexes. The rate constants of the DMSO exchange in $UO_2(DMSO)_5^{2+}$ and $UO_2(acac)_2DMSO$ are 2.25×10^3 sec^{-1} and 2.23×10^2 sec^{-1}, respectively, as shown in Chapters III and IV.

Although it is difficult to distinguish between mechanism 1 and 2 from the present results, it may be considered that the rate-determining step is the dissociation of one-end of the coordinated acac and the resulting formation of intermediate (IV).

D-2. Exchange reaction in $o-C_6H_4Cl_2$ containing free DMSO

The exchange rate of acac becomes slow by the addition of DMSO to the reaction system as seen in Fig. 8. The activation parameters for the first-order rate constant in this reaction are very similar to those for the reaction in $o-C_6H_4Cl_2$. This indicates that the mechanism may be the same as that for the exchange reaction of acac in $o-C_6H_4Cl_2$.

If the acac exchange reaction proceeds through the same mechanism 1 or 2, and the DMSO molecule behaves as a competitor to free Hacac in the coordination site, mechanisms 1 and 2 are modified as Eqs. (12) and (13), respectively.

For mechanism 1,

$$\text{DMSO (acac) UO}_2\!\!\diagdown_{O}^{O} \quad \underset{k_{-1}}{\overset{k_1}{\rightleftharpoons}} \quad \text{DMSO (acac) UO}_2^{O-O}$$

(I)   (II)

k_3 / DMSO^* $\text{Hacac}^* \quad k_2$ (12)

$$\text{DMSO (acac) UO}_2\!\!\diagdown_{\text{DMSO}^*}^{O-O} \quad \xrightarrow{\text{Hacac}^*} \quad (IV) \rightarrow (IV') \rightarrow (I')$$

where DMSO molecule competes with the free Hacac for the coordination to the vacant site in the intermediate (II).

For mechanism 2,

$$\text{DNSO (acac) UO}_2\!\!\diagdown_{O}^{O} \quad \underset{\text{Hacac}^*}{\overset{K_{ac}}{\rightleftharpoons}} \quad \text{DMSO (acac) UO}_2\!\!\diagdown_{O}^{O} ---\text{acacH}^*$$

(I)   (III)

$K_{ds} \Big\updownarrow \text{DMSO}^*$ $\Big\downarrow k_I$ (13)

$$\text{DMSO (acac) UO}_2\!\!\diagdown_{O}^{O} ---\text{DMSO}^* \qquad\qquad (IV) \rightarrow (IV') \rightarrow (I')$$

$$\text{DMSO}^* \text{(acac) UO}_2\!\!\diagdown_{O}^{O}$$

where the DMSO molecule forms an outer-sphere complex with $UO_2(acac)_2DMSO$ and this formation results in a decrease in the concentration of the outer-sphere complex (III) and the exchange rate.

From Eq. (12), k_{ex} is derived as in Eq. (14)

$$k_{ex} = \frac{k_1 k_2 [\text{Hacac}]_{Enol}}{k_{-1} + k_2 [\text{Hacac}]_{Enol} + k_3 [\text{DMSO}]} \qquad (14\text{-a})$$

or

$$\frac{1}{k_{ex}} = \frac{k_{-1} + k_2 [Hacac]_{Enol}}{k_1 k_2 [Hacac]_{Enol}} + \frac{k_3 [DMSO]}{k_1 k_2 [Hacac]_{Enol}} \qquad (14\text{-}b)$$

and from Eq. (13), the following equation is derived,

$$k_{ex} = \frac{k_I K_{ac} [Hacac]_{Enol}}{1 + K_{ac} [Hacac]_{Enol} + K_{ds} [DMSO]} \qquad (15\text{-}a)$$

or

$$\frac{1}{k_{ex}} = \frac{1 + K_{ac} [Hacac]_{Enol}}{k_I K_{ac} [Hacac]_{Enol}} + \frac{K_{ds} [DMSO]}{k_I K_{ac} [Hacac]_{Enol}} \qquad (15\text{-}b)$$

If these assumptions are valid, the plots of $1/k_{ex}$ vs. [DMSO] should give a straight line with an intercept (Fig. 9). Figure 9 indicates that these mechanisms are reasonable. The values of k'_a and k'_b in Eq. (5) correspond to the coefficients of Eqs. (14-b) and (15-b) as follows. For Eq. (14-b),

$$k_{ex} = \frac{k_{-1} + k_2 [Hacac]_{Enol}}{k_1 k_2 [Hacac]_{Enol}}$$

$$k'_b = \frac{k_3}{k_1 k_2 [Hacac]_{Enol}}$$

and for Eq. (15-b),

$$k'_a = \frac{1 + K_{ac} [Hacac]_{Enol}}{k_I K_{ac} [Hacac]_{Enol}}$$

$$k_b' = \frac{K_{ds}}{k_I K_{ac} [\text{Hacac}]_{\text{Enol}}}$$

In the present reaction system, [Hacac] is constant as shown in Table 3 and $[\text{Hacac}]_{\text{Enol}}$ at each temperature was calculated from the equilibrium constant. By using the values $[\text{Hacac}]_{\text{Enol}}$, k_1, k_I, and K_{ac} (see Table 2), the values of k_3/k_2 and K_{ds} at each temperature were calculated from the k_b' values and are listed in Table 4. Moreover, the values of k_3/k_2 and K_{ds} at 25 °C are estimated to be about 32 and 60 M^{-1}, respectively by using the values of k_b' (120 M^{-1} sec^{-1}), k_1 (2.04 sec^{-1}), k_I (2.04 sec^{-1}), and K_{ac} (0.89 M^{-1}) at 25 ° C. The calculated K_{ds} is much larger than that expected from the Fuoss equation (0.86 M^{-1})[20] and that obtained from the study of the DMSO exchange reaction in $UO_2(\text{acac})_2\text{DMSO}$ in CD_2Cl_2 (4.9 ± 1.8 M^{-1}). If the value of k_2 is assumed to equal to or less than 4930 M^{-1} sec^{-1} [22] which is the formation rate constant of mono acac complex of uranyl ion, k_3 is estimated to be less than 1.6 x 10^5 M^{-1} sec^{-1} at 25 °C from the value of k_3/k_2 = 32. This value is larger than those of the DMSO exchange in $UO_2(\text{DMSO})_5^{2+}$ and $UO_2(\text{acac})_2\text{DMSO}$. However, by considering that the k_3 path indicates the coordination of DMSO to the vacant site of the intermediate (II), it may not an absurd value.

If these considerations are resonable, it is more likely that the acac exchange reaction in $UO_2(\text{acac})_2\text{DMSO}$ proceeds through the mechanism 1 [(I) $\longrightarrow$ (II) $\longrightarrow$ (IV) $\longrightarrow$ (IV') $\longrightarrow$ (I')].

C. Comparison with Related Reactions

Kinetic parameters for the present exchange reaction and other ligand exchange reactions in uranyl complexes with oxygen donor ligands are summerized in Table 5. The value of k_{ex} for the present reaction is widely different from those of other ligand exchange reactions, where the the ratios of rate constants are ranging from 30 to 10^4. Such marked inertness in the exchange of bidentate ligands has been reported in many metal complexes[9,12,13]. Most of the ligand exchange reactions in Table 5 proceed through the D mechanism. The values of $\Delta H^{\ddagger}$ and $\Delta S^{\ddagger}$ of the present exchange reaction are larger than those of other exchange reactions in $UO_2(acac)_2DMSO$. The dissociation of one-end of the coordinated acac should reduce the steric tension in the equatorial plane. This effect may reflect in the $\Delta S^{\ddagger}$ value of present exchange reaction, which seems to be not so negative value as compared with those of other exchange reactions. However, the $\Delta H^{\ddagger}$ value is larger than others. As a result, the present exchange rate becomes slower than other exchange reactions.

Furthermore, the kinetic parameters of the present exchange reaction are different from the methyl group exchange reaction in $UO_2(acac)_2DMSO$. These differences indicate that the methyl group exchange of the coordinated acac in $UO_2(acac)_2DMSO$ does not proceed through the bond rupture of one-end of the coordinated acac [mechanism(ii) in Chapter V] and support the proposal that the methyl group exchange proceeds through the dissociation of the DMSO molecule.

Table 5. Kinetic paramters for the exchange reactions in some uranyl complexes

System	Solvent	Mechanism	$\Delta H^{\ddagger}$ kJ mol^{-1}	$\Delta S^{\ddagger}$ JK^{-1}mol^{-1}	$k_{ex}(25\ °C)^{a}$ sec^{-1}	Ref.
$UO_2(acac)_2DMSO$ — acac exchange	$o\text{-}C_6H_4Cl_2$	f	66.4 ± 8.4	-17.1 ± 26.8	2.04	h
$UO_2(acac)_2DMSO$ — intra^b	$o\text{-}C_6H_4Cl_2$	g	49.6 ± 0.8	-44.9 ± 2.5	6.32×10	i
$UO_2(acac)_2DMSO$ — inter^c	CD_3COCD_3	D	45.8 ± 0.8	-46.6 ± 2.9	2.36×10^2	j
	CD_2Cl_2	D	47.9 ± 5.2	-46.6 ± 11.2	1.02×10^2	j
		I_d	35.4 ± 12.4	-69.7 ± 20.5	1.01×10^3	j
$UO_2(DMSO)_5^{2+}$ — DMSO exchange	CD_3COCD_3	D	53.8 ± 2.4	6.3 ± 14.5	5.53×10^3	k
		A	39.1 ± 1.7	-28.1 ± 5.0	$3.22 \times 10^4 /M^{-1}$	k
$UO_2(DMF)_5^{2+d}$ — DMF exchange	CD_2Cl_2	D	42.0 ± 2.1	-15.1 ± 3.3	4.70×10^4	k
		I_d	48.3 ± 0.9	38.6 ± 2.6	2.34×10^6	k
$UO_2(DMA)_5^{2+e}$ — DMA exchange	CD_2Cl_2	D	42.8 ± 0.8	-43.7 ± 2.9	1.10×10^3	l

a Calculated values from $\Delta H^{\ddagger}$ and $\Delta S^{\ddagger}$ at 25 °C.   b intra: the exchange of methyl groups of the coordinated acac.   c inter: the exchange of DMSO.   d DMF = N,N-dimethylformamide.
e DMA = N,N-dimethylacetamide.   f the dissociation of the one-end of coordinated acac.   g the dissociation of coordinated DMSO.   h This work.   i Chapter V.   j Chapter IV.   k Chapter III.   l Ref.24

iv. SUMMARY

It is suggested that the exchange reaction of acac in

$UO_2(acac)_2DMSO$ proceeds through either mechanism 1 [(I) $\rightarrow$ (II) $\rightarrow$

(IV) $\rightarrow$ (IV') $\rightarrow$ (I')] or mechanism 2 [(I) $\rightarrow$ (III) $\rightarrow$ (IV) $\rightarrow$ (IV')

$\rightarrow$ (I')]. These mechanisms are identical in some respects

that they have the intermediate (IV), and the rate-determining

step is the dissociation of one-end of the coordinated acac, while

the intermediate (IV) is formed via (II) in mechanism 1 and via

(III) in mechanism 2.

It is well known that in many acetylacetonato complexes

the ligand exchange reaction proceed through the intermediate

$(acac)_nM\overset{\displaystyle O-O}{\underset{\displaystyle O-OH}{\Big\langle}}$ (n = 1 or 2, M = V(III), V(IV), Cr(III), Fe(III),

Ru(III), and Rh(III))[9,12,13,23], which is directly formed from

$M(acac)_{n+1}$. In this mechanism the rate-determining step is the

coordination of free Hacac to $M(acac)_{n+1}$.

The difference in mechanisms can be attributed to the

structure of $UO_2(acac)_2DMSO$. Since the reaction site of UO_2-

$(acac)_2DMSO$ is restricted in the equatorial plane which was

occupied by bulky DMSO and acac molecules, the entering Hacac can not

approach the first coordiantion sphere of $UO_2(acac)_2DMSO$,

while the dissociation of one-end of the coordinated acac will make

it easy to form the intermediate (IV).

REFERENCES

1. K. Saito and K. Masuda, Bull. Chem. Soc. Jpn., 41, 384(1968).

2. K. Saito and K. Masuda, Bull. Chem. Soc. Jpn., 43, 119(1970).

3. T. Inoue and K.Saito, Bull. Chem. Soc. Jpn., 46, 2417(1973).

4. K. Matsuzawa and K. Saito, Bull. Chem. Soc. Jpn., 46, 2777 (1973).

5. C. Chatteriee, K. Matsuzawa, H. Kido, and K. Saito, Bull. Chem. Soc. Jpn., 47, 2808(1974).

6. M. Nishizawa, H. Kido, I. Kinishita, Y. Soma, and K. Saito, Bull. Chem. Soc. Jpn., 49, 819(1976).

7. A. Nagasawa and K. Saito, Bull. Chem. Soc. Jpn., 49, 3079 (1976).

8. H. Kido and K. Saito., Inorg. Chem., 16, 397(1977).

9. M. Nishizawa and K. Saito, Bull. Chem. Soc. Jpn., 51, 483(1978).

10. A. Nagasawa and K. Saito., Bull. Chem. Soc. Jpn., 51, 2015 (1978).

11. H. Kido and K. Saito, Bull. Chem. Soc. Jpn., 52, 3545(1979).

12. H. Kido, Bull. Chem. Soc. Jpn., 53, 82(1980).

13. H. Kido and K. Saito, Bull. Chem. Soc., 53, 424(1980).

14. A.C. Adams and E.M. Larsen, Inorg. Chem., 5, 814(1966).

15. A.J.C. Nixon and D.R. Eaton, Can. J. Chem., 56, 1012(1968).

16. G.E. Glass and R.S. Tobias, J. Organometal. Chem., 15, 481 (1968).

17. G.M. Tanner, D.G. Tuck, and E.J. Wells, Can. J. Chem., 50, 3950(1972).

18. N. Serpone and R. Ishayek, Inorg. Chem., 13, 52(1974).

19. F.A. Cotton and R. Francis, J. Am. Chem. Soc., 82, 2986(1960).

20. R.M. Fuoss, J. Am. Chem. Soc., 80, 5059(1958).

21. V. Gutmann and R. Schmid, Coord. Chem. Rev., 12, 263(1974).

22. M.J. Hynes and B.D. O Regan, J.C.S. Dalton, 1502(1980).

23. A. Watanabe, private communication.

24. R.P. Bowen, S.F. Lincoln, and E.H. Williams, Inorg. Chem., 15, 2126(1976).

CHAPTER VII

CONCLUSION

The main conclusion to be drawn from the present work is as follows.

[i] In the uranyl complexes with unidentate ligands which coordiante through oxygen, most of the complexes except $UO_2(H_2O)_4^{2+}$ and $UO_2(HMPA)_4^{2+}$ have the pentagonal bipyramidal structure, i.e. $UO_2L_5^{2+}$ (L = DMSO, DMF, DMA, TMP, TEP, NMA, and TMU). It appears well established that the difference in the coordination number of uranyl complexes is attributed to the basicity and size of ligands. The ligand having large basicity can strongly coordinate to the uranyl ion and the ligand size relates with the bulkiness in the equatorial plane. It is concluded that the most stable structure of uranyl complexes is the pentagonal bipyramidal one which has the coordination number of 5 in the equatorial plane.

[ii] It has not been determined so far whether the rate constant of water exchange in the equatorial plane of uranyl ion is the order of 10^2 sec^{-1} or of 10^5 sec^{-1}. It was found from the present study that the rate constant of water exchange in the equatorial plane of uranyl ion is 9.8×10^5 sec^{-1}, which is in good agreement with the value expected from the complex formation reactions of uranyl ion with 4-(2-pyridylazo) resorcinol and acetylacetone, and that the water exchange reaction proceeds through the I_d mechanism. The rate of water exchange in uranyl ion is much faster than that in uranium(IV) (U^{4+}), where the rate constant of water exchange lies between 1 and 100 sec^{-1}. This difference may be explained

by considering that the surface charge density of UO_2^{2+} is smaller than that of U^{4+} and that the ionic radius of UO_2^{2+} (> 1.7 Å) is larger than that of U^{4+} (0.96 Å).
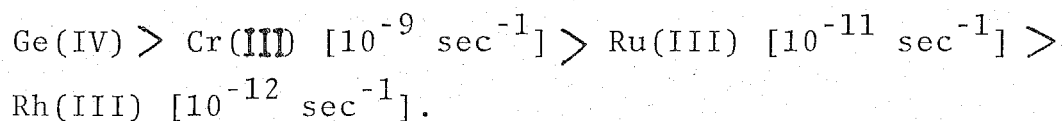
[iii] The rate constants of ligand exchange reactions in most of the uranyl complexes range from 10^2 sec^{-1} to 10^6 sec^{-1} and are independent of free ligand concentrations. Among the ligand exchange reactions studied so far, only three ligand exchange reactions in $UO_2(HMPA)_4^{2+}$, $UO_2(DMSO)_5^{2+}$, and $UO_2(DMF)_5^{2+}$ proceed through not only the ligand concentration dependent path but also the independent path. It is concluded that the ligand exchange reactions in equatorial plane of uranyl complexes proceed through the D mechanism fundamentally, while three reactions mentioned above take place even through the A or the I_d mechanism depending on the conditions.

[iv] The plots of the activation enthalpies against the activation entropies for the ligand exchange reactions in $UO_2L_5^{2+}$ show a linear relationship, i.e. an isokinetic relationship and lie between the similar plots for AlL_6^{3+} and ML_6^{2+} (M = V, Mn, Fe, Co, Ni, and Mg). This means that the surface charge density of the $UO_2L_5^{2+}$ complexes lies between those AlL_6^{3+} and ML_6^{2+}. Furthermore, the isokinetic plot of $UO_2L_5^{2+}$ are consistent with that for the solvent exchange reactions in VOL_5^{2+} (L = H_2O, CH_3OH, CH_3CN, DMF, DMA, and DMSO). This indicates that the surface charge density of VOL_5^{2+} complexes is the same as that of $UO_2L_5^{2+}$ complexes and that the mechanism of the solvent exchange reactions in VOL_5^{2+} may be similar

to that of the ligand exchange reactions in $UO_2L_5^{2+}$, i.e. the D mechanism.

[v] From the results of the intramolecular exchange reactions of methyl groups of the coordinated acac in $UO_2(acac)_2L$ (L = DMSO, DMF, and DEF), it was found that the structural change of uranyl complexes was restricted only within the equatorial plane, and the linear structure, O=U=O, was kept even in the transition state. This property is different from that of dioxomolibdenum(VI) ion, MoO_2^{2+}, which is a d^0 oxocation similar to a uranyl ion, but O=Mo=O is bent rather than linear. It has been known that the intramolecular exchange reaction of tert-$C(CH_3)_3$ groups of the coordianted dpm in $MoO_2(dpm)_2$ (dpm = dipivaloylmethanate) proceeds through the twist mechanism. It seems that the bent structure is less rigid than the linear structure in the standpoint of stereochemistry.

[vi] It was found that the exchange reaction of acac in $UO_2(acac)_2$-DMSO proceeded through the mechanism where the rate-determining step is the dissociation of one-end of the coordinated acac. The rate constant of the corresponding step was found to be 2.04 sec^{-1} at 25 °C. Comparison of the exchange rate constants of bidentate ligand in various metal complexes gives the following order of the reactivity.
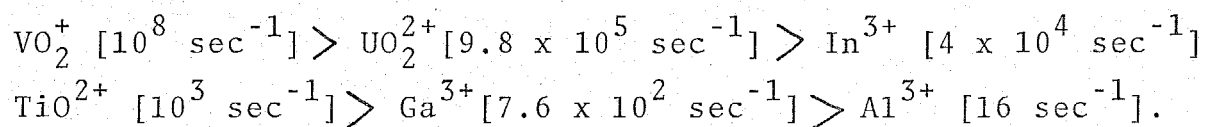
Th(IV) $\approx$ U(IV) $[10^2 \; sec^{-1}]$ > Zr(IV) $\approx$ Hf(IV) $[10^1 \; sec^{-1}]$ >
U(VI), UO_2^{2+} $[10^0 \; sec^{-1}]$ > V(IV), VO^{2+} > Ti(IV) $\approx$ In(III) >
Fe(III) $[10^{-3} \; sec^{-1}]$ > Ga(III) > V(III) $[10^{-4} \; sec^{-1}]$ >
Al(III) > Be(II) > Pd(II) > Co(III) $[10^{-8} \; sec^{-1}]$ > Si(IV) >

Ge(IV) $>$ Cr(III) $[10^{-9}$ sec$^{-1}]$ $>$ Ru(III) $[10^{-11}$ sec$^{-1}]$ $>$ Rh(III) $[10^{-12}$ sec$^{-1}]$.

An additional comparison of the exchange rate constants of bidentate ligands in various d^0 and d^{10} metal complexes lead to the following order.

Th(IV) $>$ Zr(IV) $>$ U(VI),UO_2^{2+} $>$ Ti(IV) $\approx$ In(III) $>$ Ga(III) $>$ Al(III) $>$ Ge(IV).
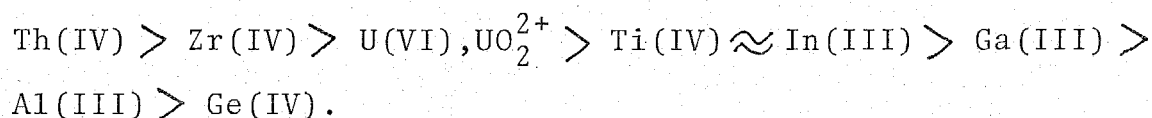
This order is consistent with that for the water exchange rate constants in various d^0 and d^{10} metal ions, i.e.

VO_2^+ $[10^8$ sec$^{-1}]$ $>$ UO_2^{2+} $[9.8 \times 10^5$ sec$^{-1}]$ $>$ In^{3+} $[4 \times 10^4$ sec$^{-1}]$ TiO^{2+} $[10^3$ sec$^{-1}]$ $>$ Ga^{3+} $[7.6 \times 10^2$ sec$^{-1}]$ $>$ Al^{3+} $[16$ sec$^{-1}]$.

From the results mentioned above, it is concluded that a uranyl ion can be classified as a labile ion.

ACKNOWLEDGMENT